## A Sheffield Hallam University thesis

101 441 987 5

**Fines are charged at 50p per hour**

1 5 OCT 2002
08.55pm

ProQuest Number: 10697434

ProQuest 10697434

# THE DEPENDENCE OF ULTRASOUND VELOCITY

# AND ATTENUATION ON THE MATERIAL

# PROPERTIES OF CANCELLOUS BONE

Christopher  Forti  Njeh

*Sheffield Hallam University*
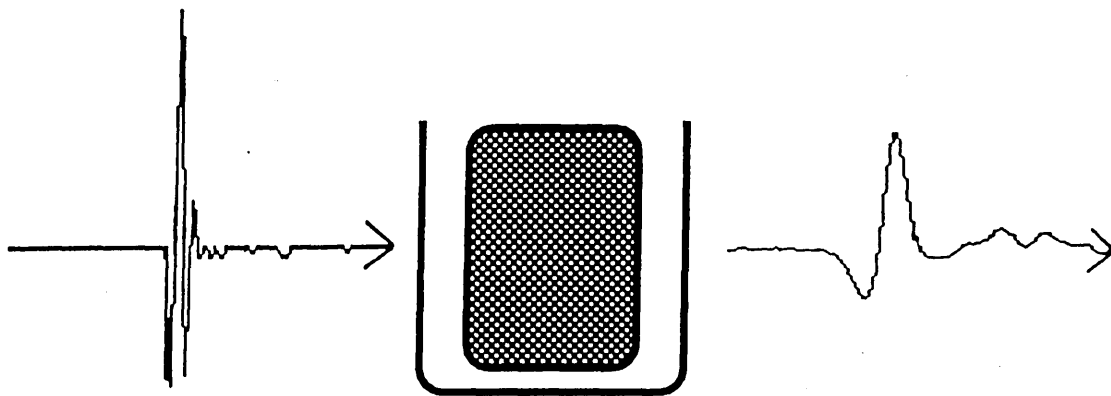
# The Dependence of Ultrasound Velocity and Attenuation on the Material Properties of Cancellous Bone

Christopher  Forti  Njeh

A thesis submitted in partial fulfilment of

the requirement of  Sheffield Hallam University

for the degree of  Doctor of  Philosophy

*Division of Applied Physics*

*School of Science*

January 1995

# I. Abstract

There is an increasing interest in evaluating the role of ultrasound in the identification and management of osteoporosis. We may measure the velocity of ultrasound through bone and the frequency-dependent attenuation, generally referred to as broadband ultrasound attenuation(BUA). The dependence of these parameters upon osteoporotic changes in density and architecture(total loss or thinning of trabeculae width) is still not well defined.

A physical model for cancellous bone was developed by introducing an array of cylindrical voids of defined diameter and configuration into polymethylmethacrylate (Perspex). Experimental studies on the cancellous bone model demonstrated that the relationship between BUA and porosity is approximately parabolic, with low BUA values obtained at both low (cortical bone) and high (bone marrow) porosities. This explains the discrepancies in the correlation between BUA and density for different bone structures reported in the literature. BUA was also found to be dependent on the number of pores and the pore distribution(structure). Velocity was found to be dependent on pore size only. BUA and velocity were also found to be temperature dependent. Permeability provides quantitative information related to structure, validated using the perspex model.

In vitro studies were carried out on bovine and human cancellous bone (calcaneus and vertebrae). The relationship between Young's modulus, strength and density followed the power law predicted by theoretical models. Measurements on bovine and vertebrae samples were carried out in three orthogonal directions. Young's modulus, strength, BUA, velocity and permeability were shown to be direction dependent and hence dependent upon structure. The relationship between BUA and density followed the parabolic trend observed in the physical model, with the human samples on the rising phase and the bovine on the falling phase of the parabola. BUA in the calcaneus was found to follow a power law relationship with density ($BUA = \rho^{1.99}$). BUA was a good predictor of strength in both the bovine ($R^2 = 74\%$) and calcaneus ($R^2 = 75\%$) samples. Velocity was a good predictor of both Young's modulus and strength when applied to the bar wave equation ($E = V^2\rho$) with an $R^2$ of 94% and 88% respectively for the calcaneus and 91% and 92% respectively for the bovine samples. For the calcaneus samples an $R^2$ of 83% and 80% for Young's modulus and strength were obtained when density in the bar wave equation was substituted by BUA. The cortical end plates have a significant offset effect on BUA in the calcaneus. Permeability was highly correlated to strength. BUA and velocity were shown to be good predictors of cancellous bone strength in vitro.

Future work should concentrate upon the investigation of controlled structural models of cancellous bone and also on the extrapolation of this study to the in vivo prediction of bone strength.

# II. Aim of Project

Osteoporosis may be defined as a deficiency of the protein matrix of bone with loss of the hard calcium-rich mineral hydroxapatite, resulting in an increased risk of fracture from non-traumatic fall [National Osteoporosis Society, 1990]. It is now known that 50% of all Caucasian women can expect an osteoporosis - related fracture at some time. 1 in 5 of hip fracture patients die and more than half become dependent on others [National Osteoporosis Society, 1990; Law et al., 1991]. Recent reports from a variety of international communities reveal that the prevalence of osteoporosis is increasing, along with an increasing incidence of vertebral fractures [Avioli, 1991].

Bone density measurement have been shown to be a predictor of fracture risk [Cummings et al., 1993], but density may not be the only determinant of bone strength. Other properties of bone such as fatigue damage, trabecular architecture, mineralization and elasticity may be important in determining fracture risk [Kleerekoper et al., 1993; Goldstein et al., 1993]. Current radiological techniques such as quantitative computed tomography, single or dual - photon absorptiometry and dual-energy x-ray absorptiometry provide only density measurement. These methods only measure the amount and distribution of minerals in bone [Tothill, 1989]. Therefore a technique which provides structure information in addition to density is required.

Since the pioneering work of Langton [Langton et al., 1984], a great incentive has developed into the possibility of using ultrasound in diagnosis of bone diseases, especially osteoporosis. The attractiveness of ultrasound in clinical application lies in its low radiation risk and its sensitivity to structural changes [Langton et al., 1990a]. Its low radiation risk has pushed forward the idea of using ultrasound as a screening tool for osteoporotic risk group women. The need for screening is vital because all prophylactic and therapeutic procedures in relation to osteoporosis are based on modifying either bone formation or resorption or both. A bone framework must exist. No extra bone can be created where bone trabeculae have been replaced by fat.

A few questions still haunt researchers in this field which include:

* What is ultrasound measuring ?: can empirical formulae be derived to correlate the structural and density changes to velocity and BUA ?

* What is the role of ultrasound measurements of bone at the calcaneus in osteoporosis management ?

* How does ultrasound at the calcaneus compare to other established modalities such as DXA ?

The first question constitutes my research theme and therefore the objectives of the project are:

♦ Develop the understanding of ultrasound transmission through cancellous bone

♦ Determine the relationship between ultrasound, mechanical and structural properties of cancellous bone

♦ Identify the structural dependence of broadband ultrasound attenuation (BUA)

Before trying to answer the above questions, fundamental descriptions of the structure and functions of bone must be discussed. Thus, the first part of this thesis presents a clinical background and literature review and the second part presents the experimental investigation.

# III. Acknowledgement

I am especially grateful to my supervisor Dr C.M Langton whose initial work in 1984 put ultrasound as a diagnostic tool in osteoporosis management. I will like to thank him for his persistent encouragement, support, advice and help throughout the project and for ensuring that the project was completed.

I would like to acknowledge SERC and Sheffield Hallam University for sponsoring the project.

The mechanical measurements were achieved with the assistance of Prof. J.D Currey and Dr R Hodgskinson of Biology Dept in York University, to whom I am eternally grateful. I would like to thank Dr E.B Fosam for his support throughout the duration of the project and for statistical advice.

Life would have been unbearable if not for the support of my wife Janet who provided moral support, encouragement and also proof read part of the document. I am grateful to my in-laws for being around especially Dr L.J Stewart for proof reading part of the document.

I am also grateful to the head of department Dr J Young under whose canopy various projects including mine are successfully carried out, my colleagues at the department especially R.X Boutinaud and the technicians who provided the technical expertise.

My sincere appreciation goes to Mrs K.E Goldstone (Addenbrooke's Hospital, Cambridge) who allowed me to use the Radiation Protection Service's computing facilities during the writing up phase and also for her encouragement.

One is no island and thus constantly lean on family and friends for support and advise. To my whole family and friends who I will not list I express my sincere gratitude. I am also grateful to everyone else who has helped me in one way or the other to accomplish this work.

# IV. Dedication

Dedicated to the memories of my

Late father *Samuel Tamanji Njeh* and mother *Martha Angeck Njeh*

who passed away while I was in the pursue of knowledge

# TABLE OF CONTENT

# LIST OF FIGURES

# LIST OF TABLES

# PART I

# CLINICAL AND EXPERIMENTAL BACKGROUND

---

# CHAPTER

# 1. THE STRUCTURE OF BONE AND OSTEOPOROSIS

---

## *1.1 Bone Structure*

### 1.1.1 Introduction

Bone is a very highly specialised form of connective tissue. Its extreme hardness distinguishes it from other forms of connective tissue. It makes up the skeleton on which the human body is built, constituting about 18% of total adult body components. The adult human skeleton usually consist of 206 named bones . In addition to contributing to body shape and form, bones provide the body with some fundamental functions such as :- stability, locomotion, ion exchange, protection of various organ and storage of chemicals [Spencer and Mason,1979].

Bone tissue can be considered to be a composite material consisting of a fibrous, organic matrix protein (collagen) which is permeated by large stores of inorganic salts. The organic components include the cells (osteoblast and osteoclast) and approximately one third of the matrix are proteoglycans, glycoprotein and collagen fibres, all of which are secreted by osteoblasts. Collagen fibres provide bone with great tensile strength, that is, its ability to resist stretch and twisting [Spencer and Mason, 1979]

On the other hand, the inorganic salts of bone are principally calcium and phosphate. The precise nature of the mineral composition of bone, both its chemistry and morphology is still a matter of some dispute [Currey, 1984]. However there is

agreement that some of the bone mineral is the version of calcium phosphate called hydroxyapatite whose unit cell contains $Ca_{10}(PO_4)_6OH)_2$. The presence of this mineral salts is responsible for the most notable characteristic of bone - its exceptional hardness, which allows it to resist compression [Marieb, 1989]. The right combination of fibre (organic) and salts (inorganic) makes bone exceptionally strong without being brittle. Water accounts for about 20% of the wet weight of mature cortical bone, bone salts make up approximately 45% and organic substances account for the remaining 35% [ Carter and Spengler, 1978].

Bones come in many shapes and sizes. So, at a macroscopic level bone can be classified according to shape. Four principal types can be identified namely ; long bones (e.g. humerus, femur, radius), short bones (wrist), flat bones (ribs) and irregular bones (vertebrae). The various shapes and sizes of bones have evolved through the process of natural selection. This implies that natural selection will favour structures which will enable the organism to execute its locomotory function with the greatest efficiency [Currey, 1984]. Bones of different shapes contain different proportions of the two basic types of osseous tissue; compact (cortical) and spongy (cancellous, trabeculae) bone.

## 1.1.2  The Structure of Cortical Bone

Cortical(compact) bone tissue forms the diaphyses of long bones and the thin shell of the bone ends. It appears dense to the unaided eyes, however, a microscope reveals that it is composed of many organised systems of interconnecting  canals and passageways serving as conduits for nerves, blood vessels and  lymphatic vessels. The structural unit of compact bone is called the osteon  or haversian system [Spencer and Mason, 1979]. Each haversian system has  a  central haversian canal that is surrounded by a series of concentric  layers (lamellae) of bony matrix. Located between adjacent lamellae are small cavities called lacunae, each of which contains  one bone cell or osteocyte. The lacunae within each haversian system are interconnected by  tiny canals called canaliculi (see Figure 1.1).  Insterstitial lamellae fill in the spaces between the closely packed cylindrical systems. Nutrient supply  and  waste  disposal  from  the

osteocytes within the lacunae are accomplished by blood capillaries in the haversian canal. Haversian canals are interconnected by Volkmann's canals.
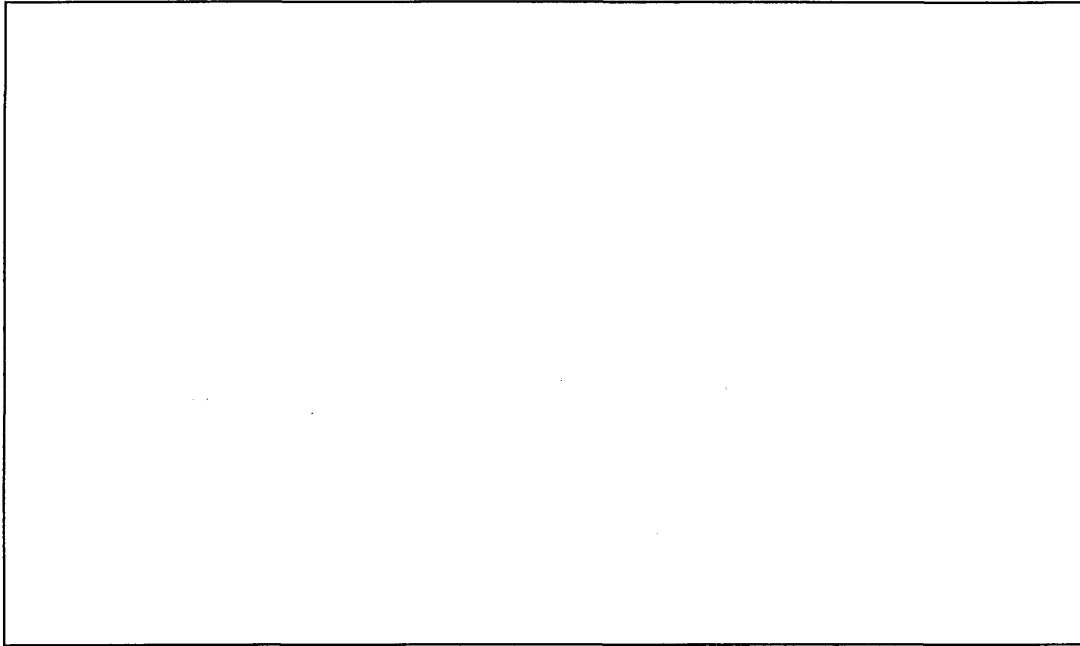
*Figure 1-1: Typical Harversian System (Courtesy of Spencer and Mason, 1979)*

## 1.1.3 The Structure of Cancellous Bone

Unlike compact bone, cancellous (trabecular) bone exists as a 3-dimensional network of bony plates and columns filled with bone marrow and fat. The structural component is the trabeculae(struts) which is only a few cell layers thick and contain irregularly arranged lamellae and osteocytes interconnected by canaliculi. No osteons are present. Nutrients reach the osteocytes of cancellous bone by diffusion through from the marrow spaces between the bony spicules [Marieb, 1989]. Cancellous bone is found in many places and Currey [1984] distinguishes four major locations:

• At the end of long bones, under synovial joints

• Where it completely fills short bones

- Where it acts as a filling in flattened bones

- Under protuberances to which tendons attach.


It is apparent from the above that, the location of cancellous bone are in places where stresses are applied over large areas. This indicates that cancellous bone plays an important role in the transmission and distribution of stresses in the human skeletal system. This occurs in places where the stresses if the bone were solid would be extremely low (and the weight of the bone correspondingly high); also, the morphology does not allow a mere thinning of the cortex of the bone, for this would produce a too fragile shell.

There has been extensive microscopic studies to reveal the network structure of cancellous bone or the arrangement of the struts (trabeculae) in space. These include the work of Whitehouse [Whitehouse et al., 1971, Whitehouse, 1975] and Singh [1978]. These work revealed various aspects of the structure. At low relative densities (real density[1]/apparent density[2]) the simplest kind of cancellous bone occurs, consisting of randomly oriented cylindrical struts(rods), about 0.05-0.14 mm in diameter, each extending for about 1 mm before making a connection with one or more struts [Singh, 1978]. As the relative density increases more material accumulates in the cell wall, the cylindrical struts are replaced by small plates (0.1-0.2 mm thick). The variation ranges from the just occasional plates among the struts to occasional struts among the plates. At the other extreme exists cancellous bone consisting wholly of plates forming long tubular cavities which interconnect by means of fenestae in the walls [Singh, 1978].

Bone re-models in response to the loads applied to it [Wolff's law]. The density of bone in a particular location depends on the magnitude of the applied loads. The work of Whitehouse and Dyson[1974] have supported this claim. The direction of the

---

[1]Real density = the ratio of bone tissue mass and volume occupied by the tissue.

[2]Apparent density = the ratio of bone tissue mass and bulk volume of the test specimen

applied loads dictates the symmetry of the structure in cancellous bone. So, if the stress pattern in cancellous bone is complex, then the structure of the network of trabeculae is also complex and highly asymmetric. But in bones where the loading is largely uniaxial, such as the vertebrae, the trabeculae often develop a columnar structure with cylindrical symmetry [Gibson, 1985]. The observations of Whitehouse [1971] led Gibson [1985] to suggest four basic types of structure for cancellous bone:

♦ The asymmetric, open cell, rod like structure,

♦ The asymmetric, closed cell, plate like structure,

♦ The columnar, open cell, rod like structure,

♦ The columnar, closed cell, plate like structure.
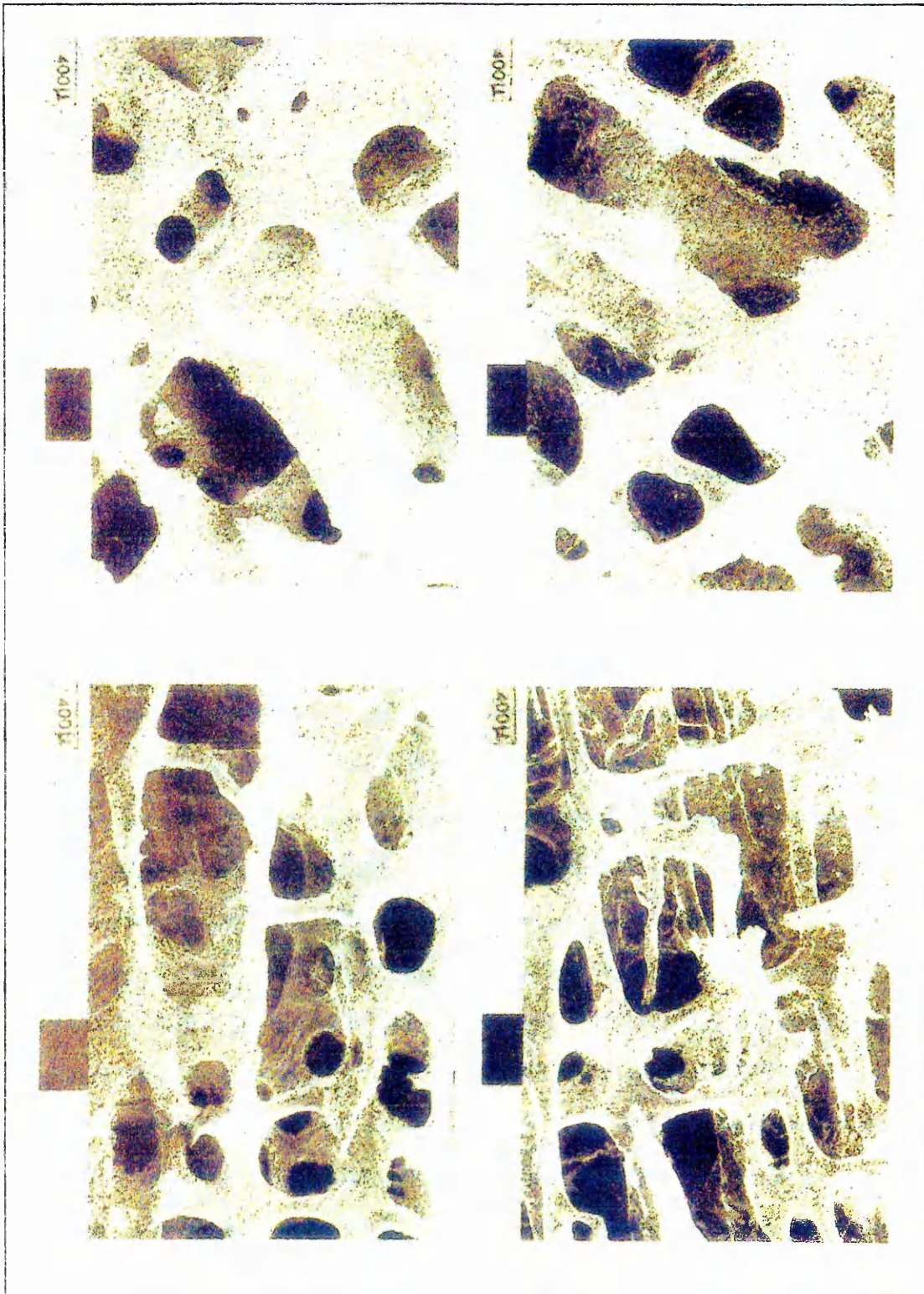
*Figure 1-2: Scanning Electron Micrograph Showing the Structure of Cancellous Bone(Courtesy of Gibson and Ashby, 1988)*

Evidently the different versions of cancellous bone are found in characteristically different places. Roughly, the type made of asymmetric, open cell rod like structure are

7

found deep in bones, well away from any loaded surface, while the more oriented types made of many plates or completely of plates are found just underneath loaded surfaces, particularly where the pattern of stress is reasonably constant [Currey, 1984].

The structural characteristic of the trabeculae change according to their thickness. The thinner trabeculae (less than 100-120μm thick) are completely devoid of vascular canals and consist of bony lamellae parallel to one another, while the thicker ones enclose secondary osteons- either extending throughout the trabeculae or limited to discrete segments of it. they consistently contain harversian systems when they are thicker than 450 μm. Most of the concentric lamellar systems found in the trabeculae of the calcaneus are secondary. [Lozupone, 1985].

### 1.1.4 Calcaneus

The calcaneus (os calcis) is the largest of the tarsal bones and forms the posterior leg of the subtalar stool. Thus it is one of the limbs of both the medial and lateral longitudinal arches. The calcaneus is mostly (>90%) cancellous with a thin cortical shell and multiple ligamentous and tendonous attachments. There are three articulating facets that form the subtalar joints; the posterior which is the largest, the middle and the anterior. The remaining joint with which the calcaneum articulates is the calcaneocuboid [Ross and Sowerby, 1985].

## *1.2 Osteoporosis:*

### 1.2.1 Introduction

Osteoporosis is the world's most common bone disease (others bone diseases include osteomalacia, osteomyelitis, rickets, Paget's disease). It can be defined as a reduction in the amount of bone tissue per unit volume of bone or simply as a reduction with age [Stevenson and Whitehead, 1982]. Other schools of thought tend to restrict the definition to describe the fracture syndrome that results after bone mineral has been

reduced to a level at which structural integrity of the skeleton is impaired. The general condition of low bone mineral density without fracture is then given the generic name osteopenia [Schapira and Schapira, 1992], this later definition is confusing and unhelpful because diagnosis then depends on one incident which results in fracture, while the precipitation events are ignored.

There are two common forms of osteoporosis - involutional and secondary. Involutional osteoporosis describes the progressive loss of bone mineral that occurs naturally with age. Secondary osteoporosis is due to predisposing medical condition such as rheumatoid arthritis and life style. Involutional could be further subdivided into Type I and Type II. Type I occurs in women in the 10 - 20 years after menopause, it is related to oestrogen deficiency and involves mainly trabecular bone. Type II osteoporosis or senile osteoporosis results in steady bone loss from the peak bone mass. It affects both females and males and involves trabecular and cortical bone [ Riggs and Melton, 1983, National Osteoporosis Society, 1990]. Type I osteoporosis is thought to be primarily responsible for wrist and vertebral crush fractures, while Type II for hip, humeral, pelvic and multiple asymptomatic vertebral wedge fractures seen in old age.

## 1.2.2 Pathogenesis of Osteoporosis

There are many causes of osteoporosis, the most common causes are old age, immobility and menopause, and the less common causes are complications of a predisposing medical condition (such as rheumatoid arthritis, chronic renal disease, endocrine disorder, malabsorption syndromes or drug therapy) and life style ( smoking, no physical exercise, diet and body habitus). Osteoporosis occurring from these less common causes is called secondary osteoporosis [ Stevenson and Whitehead, 1982; Ostlere and Gold, 1991].

Bone is involved in three fundamental activities namely: modelling, repair and remodelling. Modelling refers to the process by which the characteristic shape of the bone is achieved. Repair is the regenerative response to fracture. Remodelling is a

continuous cycle of destruction (resorption) by the osteoclast cells and renewal (bone formation) by the osteoblast cells that is carried out by individual independent bone remodelling units [Marcus, 1991]. Osteoclasts increase in number and in activity in response to parathyroid hormone and 1, 25-dihydroxy vitamin D, and their number and activity is decreased by calcitonin. Bone renewal is most rapid in the young thus growth, reaching a peak bone mass in the mid thirties [Smith, 1987]. After that, in men there is a steady decline in bone mass of less than 1% per year. This steady loss occurs in women too, but is accelerated at menopause and for 10 - 15 years after that to between 3 and 5% each year [ Newton-John and Morgan, 1970]. Bone loss is more rapid in trabecular bone than in cortical. This is because trabecular surface area is greater and the turnover rate is eight times that of cortical bone. Hence fracture tend to occur at sites where there are relatively large amounts of trabecular bone.
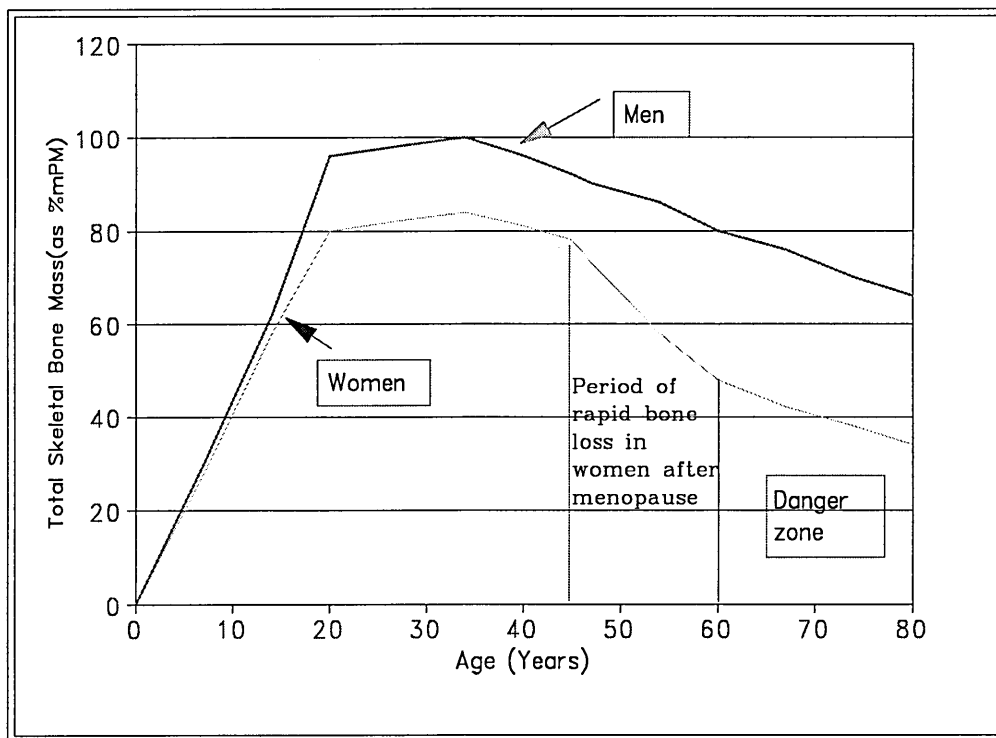


*Figure 1-3: Total Skeletal Mass as a function of Age (where %mPM represents male peak mass), courtesy of the National Osteoporosis Society*

The age-related bone loss probably results from a combination of remodelling imbalance and an age-related increase in blood parathyroid hormone concentration [Eastel and Riggs, 1987]. Remodelling imbalance refers to an inequality between bone formation and bone resorption at the level of the bone remodelling unit [Parfit, 1984]. In men, bone loss appears to result from decreased bone formation and thus thinning of trabecular, whereas in women, bone loss appears to result from an increase in bone resorption and thus perforation of trabecular plate [ Aaron et al., 1987].

The cause of post-menopausal bone loss is still controversial. Recent studies have led to the belief that postmenopausal increase in bone resorption is not primarily attributable to an increase in bone-resorbing hormones. The current concept therefore of the pathogenesis of bone resorption is that loss of ovarian function accelerates the decline in the secretion of calcitonin (calcitonin is a hormone which acts directly on bone to reduce resorption, its secretion is increased by oestrogen) which occurs with age, and as a result the actions of the bone resorbing-hormones are unopposed [Stevenson and Whitehead, 1982].

Immobility in a younger person is source of low bone mass due to lack of applied mechanical forces. Bone mass is in part determined by genetic factors, mechanical forces and hormones then act on this genetic background to determine eventual bone mass. Some races and families have smaller, lighter and more fragile bones than others. For example Negroid have higher peak bone mass than Caucasians [Cohn et al., 1977] and men have higher peak bone mass than women. Epidemiologically, the most important risk factors are age, gender and race. Other risk factors include a positive family history, premature menopause, inadequate calcium intake, petite frame, smoking, alcohol and sedentary life style [Ostlere and Gold, 1991].

## 1.2.3 Osteoporosis and Fracture

The most important consequence of bone loss is an increase of fractures which might occur either spontaneously or after minimal trauma when the bone mass has gone

below the fracture threshold (Fig 1.4). The fracture threshold is defined as a bone mass level above which fracture does not usually occur without severe trauma.

The mortality, morbidity and financial significance of osteoporosis are reviewed by Avioli L V, [1991]. The classic sites for fractures in postmenopausal osteoporosis are distal forearm, the vertebral bodies and the neck of the femur (hip). These three fracture have a combined incidence of 35 - 40% in women age 65 and over [Stevenson and Whitehead, 1982]. Although vertebral fractures are extremely common, they are often asymptomatic and are not associated with high morbidity [Gershon-Cohen et al., 1953]. Fractures of the wrist are readily treatable in an outpatient setting and long term complications are rare. Hip fractures, on the other hand are associated with significant morbidity and mortality [Riggs and Melton, 1986]. In England in 1985, 37600 people aged 65 and over fractured a hip and nearly a quarter of all orthopaedic beds were committed to people over 65 with hip fracture [Law et al., 1991]. From this data and other there is a consensus that almost one woman in four living to the age of 90 in England can expect to have a hip fracture [Law et al., 1991]. Compared to age-matched controls, mortality in patients with hip fractures is 12% to 21% higher during the four to eight months following fracture. Only 25% - 50% of patients with hip fractures maintained their level of function when daily living activities and walking ability are considered. The financial cost is vast, in the UK approximately 500 million pounds each year. With an ever increasing elderly population, these cost are expected to at least double by the year 2000.

The incidence of femoral neck fracture in the United States appears to be increasing by about 40% per decade, with an increase in age-dependent incidence among the at risk population, from 1.8% per annum to 2.05% per annum between the years 1970 and 1980 [Melton et al., 1987].

## 1.2.4 Prevention, Treatment and Diagnosis of Osteoporosis

### *1.2.4.1 Prevention of Osteoporosis*

The primary aim in the prevention of osteoporosis will be to build or achieve a high bone peak mass. This is because all prophylactic and therapeutic procedures in relation to osteoporosis are based on modifying either bone formation or resorption or both. A bone framework must exist. No extra bone can be created where bone trabeculae have been replaced by fat. High peak bone mass can be achieved by regular physical exercises, adequate attention to dietary calcium and non-smoking [Law et al., 1991; Marcus, 1991]. For women at menopause, the timely administration of oestrogen is the most powerful intervention for preserving bone mass, but the benefit of general calcium supplementation is still debatable.

### *1.2.4.2 Treatment of Osteoporosis*

Having made the diagnosis of osteoporosis the course of treatment is dependent upon whether it is to provide symptomatic treatment or whether treatment is to prevent further loss of bone mass. Symptomatic treatment will concentrate on relieving pain and restoring and then maintaining mobility. No treatment available can restore bone mass to normal, but further bone loss could be prevented. Pharmacologic approaches to preventing further bone loss falls into two categories namely: agents that constrain the rate of bone loss (such as oestrogen, calcitonin, and bisphosphates) and bone forming agents such as fluoride [Marcus, 1991]. Oestrogen replacement at menopause has been shown to protect bone mass and provides significant protection against osteoporotic fractures [Stevenson and Whitehead, 1982]. Injectable calcitonin is not used in Britain mainly because of its side effects and expense [Stevenson and Whitehead, 1981] also calcitonin has not been shown to decrease the risk for osteoporotic fracture [Marcus, 1991].

### *1.2.4.3 Diagnosis of osteoporosis*

There is a relationship between bone density and skeletal strength [Weaver and Chalmers, 1966]. Population studies have shown that the incidence of vertebral and hip fractures is inversely related to bone mass. In most studies a decrease of 1 standard

deviation in bone mass is associated with an increase of 50-100% in the incidence of fracture [Johnston Jr et al., 1991] . This is the reason why diagnosis of osteoporosis has concentrated on measurement of bone density. Several technique have been developed to measure bone mineral density (BMD). These methods indicate the potential for future fractures, as well as the seriousness of underlying bone loss in those who already have fractured. Also, changes over time are monitored either to assess the course of a disease or its therapy.

The various methods in current clinical application have been reviewed by P. Tothill[1989], Mazess [1990], Alhava [1991], Lang et al.[1991] and Ostlere and Gold [1991]. The methods include:- radiogrammetry, photodensitometry, single energy gamma photon absorptiometry (SPA), dual-energy gamma photon absorptiometry (DPA), single energy x-ray absorptiometry (SXA), dual-energy X-ray absorptiometry (DXA), quantitative computed tomography (QCT), peripheral quantitative computed tomography (PQCT), ultrasound, neutron activation analysis, compton and coherent scattering, magnetic resonance imaging and biochemical markers. The most common methods are discussed briefly below , with comparative performance described in Table 1.1.

♦ **SPA:-** The total BMC in the scan path is calculated from the difference in photon absorption between bone and soft tissue. The monoenergetic photon is provided by sources such as 125 Iodine ($^{125}$I, 28 keV) or 241 americium ($^{241}$Am, 60 kev) which are linked to a scintillation detector. The use of a rectilinear scanner allows measurement of area several centimetres long on anatomically variable regions. SPA is frequently used for measuring the forearm (radius and ulna) and the calcaneus

♦ **DPA:-** This is a modification of SPA using a radioisotope that emits photons of two energy levels. In DPA measurements no condition is placed on the soft tissue thickness as opposed to SPA where a constant tissue thickness is required. In the DPA technique, a high purity, high activity gadolinium ($^{123}$Gd) source, which has photons of predominantly 44 and 100 keV, is used as the transmission source and the scans performed on a whole body rectilinear scanner. After measuring the absorption of the photons for each of the energies, simultaneous equations can be used to calculate the

attenuation due to bone and to cancel out the effect of the soft tissue. The BMD is expressed in $gcm^{-2}$ an area-density rather than a volumetric density measurement. The principal advantages of DPA are low radiation dose, clinically sufficient accuracy and a large number of accessible measurement sites [Lang et al., 1991]. Short comings include long scanning time, gradual decay of the gadolinium source necessitating costly replacement every 18 months [Ostlere and Gold, 1991]

♦ **DXA:-**The gamma rays are replaced by high flux X-rays (50 - 1000 times greater than DPA). This offers several advantages over DPA including better spatial resolution, precision and much lower scanning time. However, errors related to source instability and beam hardening must be reduced. The necessary pairs of effective energies can be obtained either by K-edge filtering (e.g. Lunar) or by rapidly switching the generator potential (e.g. Hologic QDR).

♦ **QCT :-** In QCT either a contiguous transverse slices or a single slice are imaged. Under appropriate circumstances, the image can be quantified to obtain a distribution of attenuation coefficients and thus some measure of bone mineral density. The method offers the possibility of measuring trabecualar bone independently of surrounding cortical bone in practically any part of the skeleton [Alhava, 1991] . The major disadvantage of QCT is its relatively inferior accuracy mainly because of variations in the composition of the vertebral marrow. An attempt to solve this problem has been in the development of dual-energy QCT, which however, has less precision, higher patient dose, and longer scanning time. Hence dual-energy QCT is not widely available.

♦ **Ultrasound:-** Ultrasound is a non-invasive methods of osteoporosis diagnosis which does not involves ionising radiation. Ultrasonic velocity and attenuation through bone is related to both bone density and some other factors affecting bone fragility (See Chapter 3). Ultrasound equipment are cheaper and the scan fast, making ultrasound a very attractive tool for population screening.

*Table 1.1 : Comparative Performance of Common Physical Techniques for the Assessment of Osteoporosis*

| Technique | Site | Precision[3] % | Accuracy[4] % | Exam time min | Absorbed dose($\mu$Sv) | Cost Dollars |
|---|---|---|---|---|---|---|
| SPA | p and d radius Calcaneus | 1-3 | 5 | 15 | 100-200 | 75 |
| DPA | spine, hip total body | 2-4 | 4-10 | 20-40 | 50 | 1-150 |
| DXA | spine , hip, total body | 0.5-2 | 3-5 | 3-7 | 10-30 | 75-150 |
| QCT | spine, hip, Peripheral bones | 2-5 | 5-20 | 10-15 | 1000- 10000 | 100 - 200 |

Although new technology has now provided the clinician with accurate and precise methods of measuring BMD, there is still no consensus on how these methods should be applied in clinical practice [Ostlere and Gold, 1991]. Measurements of BMD is not a useful screening test for future hip fractures or for most vertebral fractures because differences in bone density between people who subsequently have fracture and those who do not are to small to discriminate between them (The average difference between cases and control was 0.3 standard deviations in a survey by Law et al., [1991] ). However, there is a general agreement that densitometry is useful in monitoring the response to therapy of specific disorders of bone metabolism including osteoporosis

---

[3]Precision is a measure of reproducibility, usually of multiple measurements over a short time period

[4]Accuracy is a measure of the ability of any technique to produce results that reflect the actual values

and in confirming or disputing reontgenographically suspected osteoporosis [Ostlere and Gold, 1991].

---

*Two fields of endeavours are involved in trying to answer the theme of this project. These are mechanical properties of bone and ultrasound. The next two Chapters will attempt to put them in perspective.*

<table>
<tr><td>

# Chapter

# 2. PHYSICAL AND MECHANICAL PROPERTIES OF CANCELLOUS BONE

</td></tr>
</table>

## 2.1 Introduction

### 2.1.1 Basic Theory of Mechanical Measurements of Bone

In normal day to day activities, a complex pattern of forces are imposed on the skeletal system. Like any other material, when forces act on them they alter in size and shape. Solids unlike liquids completely recover to their original form if the deformation was not above a certain limit known as the elastic limit. Within the elastic range, the deformation is linearly proportional to the magnitude and direction of the applied force. This relationship is known as Hooke's law. The direction and magnitude of the deformations are dependent upon the direction and magnitude of the imposed loads, the geometry of the bone being loaded and the material properties of the bone tissues.

When a load is applied to a bar rod, the proportional changes in length $\Delta l/l$ and width $\Delta b/b$ are called normal strains, denoted by $\varepsilon$. A shearing deformation produces a shear strain. Shear strain is usually quantified as the change in angle undergone by two lines originally at right angles. The relationship between load applied to a structure and deformation in response to the load is called a load-deformation curve. On the other hand, stress is defined as force per unit area and may be classified as tensile, compressive or shear depending upon how the load is applied. The normal or tensile stress ($\sigma$) is applied when equal and opposite forces act away from each other. Compressive stress can also be applied when the forces act toward each other. A shearing stress denoted by $\tau$ is applied when equal and opposite forces have different lines of action which tend to alter the shape of the object without changing its

volume. Stress is reported in units of Pascals (1 Pa = 1 $Nm^{-2}$). The relationship between stress and strain can be represented on a stress-strain curve. The slope of the stress-strain curve within the elastic region is called the elastic modulus E (expressed in Pascals ($Nm^{-2}$), the reciprocal of which is known as compliance.

If the material has the same properties in all directions (perfectly isotropic), then there are only two moduli- Young's modulus for extension (generally the same value for compression) and the shear rigidity modulus G for the tangential forces [Blair, 1969]. Young's modulus is defined as the ratio of the axial stress to axial strain in simple elongation. Where simple elongation is the deformation produced in a long prismatic rod by forces acting parallel to its axis, the resultant force acting at the centroid of the cross section [Hall, 1968]. Young's modulus is the elastic modulus often referred to in the literature on mechanical properties of bone because of its straight forwardness in measurement. In cortical bone it has value in the range 4 - 25 GPa [Currey, 1984] , and a value in the range 1 -18 GPa for cancellous bone. The bulk modulus (K) is defined as the modulus of volume expansion, that is, the ratio of the isotropic stress to the relative change in volume. The isotropic stress simply implies that the specimen is being stressed equally in all three planes or $P_x = P_y = P_z$ [Blair , 1969].

Balanced axial forces applied to a prismatic bar not only produce a linear strain but also give rise to a change in cross sectional area (lateral or transverse strain $\varepsilon_1$). It has been found experimentally that the ratio of lateral strain to the linear (axial) strain is a material constant. This ratio is known as the Poisson's ratio ( $\nu$ ) of the material [Sprackling, 1985]. For an isotropic linear elastic material, the elastic constants can be represented as

$$E = 3K(1-2\nu) \hspace{3cm} (2.1)$$

$$E = 2G(1+\nu) \hspace{3cm} (2.2)$$

where $E$ = Young's modulus, $G$ = shear modulus and $K$ is bulk modulus

Since E and K are both positive, Equation (2.1) indicates that the value $\nu$ cannot be greater than 1/2 [Sprackling, 1985].

The elastic theory works on the assumption of perfect elasticity. But for most materials such as polythene, perspex and bone, the elastic properties and strength are dependent upon both the rate and duration of application of the stress. This phenomenon is known as creep. Materials which exhibit creep are said to be visco-elastic. Mechanical testing has shown that bone, especially cortical bone, is a visco-elastic material [Schoenfeld et al., 1974; Carter and Spengler, 1978]. Using a Kelvin body the stress ( $\sigma$ ) in a viscoelastic material can be represented as:

$$\sigma = E\varepsilon + n\dot{\varepsilon} \qquad\qquad (2.3)$$

Where E is the elastic modulus, $\varepsilon$ is the strain and $\dot{\varepsilon}$ is the strain rate.

This implies that the true modulus of elasticity is only obtained by letting $\dot{\varepsilon} \rightarrow 0$. Thus, an infinitely low deformation rate ( quasi- static testing) is recommended for purely elastic property results [Linde and Hvid, 1987]. But, the human strain range is 0 - 0.12 with strain rates of 0.001- $0.03s^{-1}$. Carter and Hayes [1976] suggested that the longitudinal strength and stiffness of mineralised bone tissue are approximately proportional to the strain rate raised to the 0.06 power. The viscoelastic property of bone necessitates the report of the strain rate used during testing in all mechanical property investigations.

Bone like wood and other biological structures is heterogeneous (elastic properties vary from point to point) and anisotropic (elastic properties and strength are dependent upon the orientation of the bone microstructure with respect to the direction of loading) [Currey, 1984]. For cancellous bone it is dependent on the orientation of the struts. This anisotropy was demonstrated by the work of Brown and Ferguson [1980]. They obtained detailed quantitative information about the spatial and directional variations of the material properties of the cancellous bone (proximal femur).

The stress-strain curve (Figure 2.2) is typically divided into two regimes: elastic and plastic region, which are divided by the yield point. In the first region, behaviour is linear elastic (that is, it obeys Hooke's law) as the cell walls bend or compress axially. The next phase is known as the plastic region (cellular collapse phase) whereas an increase in strain results in little or no stress. This so called plastic behaviour can be

caused by a great variety of phenomena at the microscopic level, including collapse of the cells by elastic buckling, plastic yielding, crack growth or brittle fracture of the cell walls [Gibson, 1985]. The point/region where the deformation changes from being elastic to at least partially plastic is the yield point . Although a bone reaching this point still has far to go before it breaks, it is permanently damaged to some extent once it enters the plastic region. [Currey, 1984]. The amount of post yield strain that occurs in a material before fracture is a measure of the ductility of the material, the opposite of which is brittleness.

The yield strength is the stress at the yield point. The yield point is difficult to define when testing bone samples. Researchers such as Hvid and Jensen [1984] defines it as the point where the stress-strain curve begins to become non-linear. The maximum stress the bone can sustain is called the ultimate strength, and the breaking strength is the stress at which the bone actually breaks. The strength of a specimen as used in the literature refers to the maximum stress achieved before progressive trabecular tearing (in the case of tension) or collapse (in the case of compression).

The area under the stress-strain curve is a measure of the amount of energy needed to cause a fracture. This property is called energy absorption or toughness of bone and is an important property from a biomechanics point of view. A low toughness makes the bone more liable to fracture, and it is widely thought that bone toughness decreases substantially with age [Burstein et al. 1976]. On the other hand, measuring fracture toughness is not easy because samples with dimensions which meet the requirements of valid test can be cut only from large bones [Gibson and Ashby, 1988].

---

*The basic mechanical properties terminology has been established. It will now be related to bone. Bone will henceforth in this text be referring to cancellous bone, except otherwise stated. Before describing the various methods of measuring the mechanical properties a resume of the importance of these properties is given in the following section.*

## 2.1.2 Why Study the Mechanical Properties of Bone

There are many reasons why the study of the mechanical properties of bone is important, apparent from the wide ranged of fields interested in these properties. These include orthopaedic surgeons, trauma surgeons, orthodontists, prothodontist, radiologist, practitioners of general medicine and scientists.

◆ A good knowledge of these properties can help predict how bones can be expected to behave in the body. For example, the loads they can and cannot bear or the amount of energy they will absorb before fracturing [Currey, 1970]. This knowledge can also be used as a predictor of the effects of ageing, and disease on the bone behaviour.

◆ Knowledge of the material properties of cancellous bone has a twofold implication for bone implantation. Firstly, if other materials are to be substituted for bone, their mechanical properties must be compatible with those of bone to ensure a viable system. Secondly, the whole process of fracture fixation- implant design and implant insertion will all depend upon the internal distribution of the material properties [Brown and Ferguson, 1980]. This is more so, when the prosthesis are predominantly surrounded by cancellous bone and accordingly rely on cancellous bone for fixation. An example is the total hip-joint replacement, in which one part of the artificial joint occupies the medullary canal of the femur and the other part occupies the acetabular region of the pelvis [Charnley, 1970].

◆ Data on the strength characteristics and other mechanical properties of bone might also be useful in the selection of sites for obtaining bone grafts.

◆ The ability of the human body to withstand acceleration and deceleration forces of various magnitude without severe trauma is of major importance to the safety engineer who must design the automobile, airplane cockpit or space vehicle to protect the occupant as much as possible from the effect of these forces.

◆ Some knowledge of these limits of tolerance is likewise of practical significance to the designers and manufacturers of protective clothing and equipment used in sports such as football, skiing and motor vehicle racing. Other researchers like

anatomists, zoologists, physiologists, anthropologists, physicists, crystallographers and bio-engineers are also interested in the mechanical properties of bone.

---

*The importance of the mechanical properties has been discussed. The next section will review the various test methods used in measuring the mechanical properties of cancellous bone, the values obtained, and the problems associated with the various measuring modalities. A distinction is made between the methods which are aimed at measuring the structural properties of cancellous bone and those measuring the material(trabeculae) properties.*

# 2.2 Methods and Problems of Measuring Mechanical Properties of Cancellous Bone.

The porous nature of cancellous bone, with 3-dimensional arrangement of trabecular struts and marrow-filled cavities, lends itself to a mechanical description by both material and structural properties. This implies that the method of measurement of cancellous bone will depend on whether it is the structure or the material that is being measured. The subsequent paragraphs will attempt to address the methods and problems associated with the different types of measurement starting with structure related measurement.

## 2.2.1 Uniaxial Compression Tests

Test specimens are machined from the region of interest. A load is then applied by squeezing the specimen between two flat platens (see Figure 2.1 ). The validity of the test depends critically on the two ends of the tests samples being plane and parallel to each other. If the faces are not parallel, a misalignment may occur with the loading platens resulting in a non uniform distribution of the stress, causing an underestimation of both Young's modulus and strength. Porous compression platens are used in cases where the specimen were tested with marrow in situ. The specimen are not usually given shoulders. As the Poisson ratio effect tries to make them expand radially outwards, frictional forces arise at the specimen - platen interface and add to the stress

distribution pattern within the specimen. A long specimen with shoulders would help to decrease this effect. Some of the compression testing are carried out while confining the specimen in rigid cylindrical cavities [Carter and Hayes, 1976].
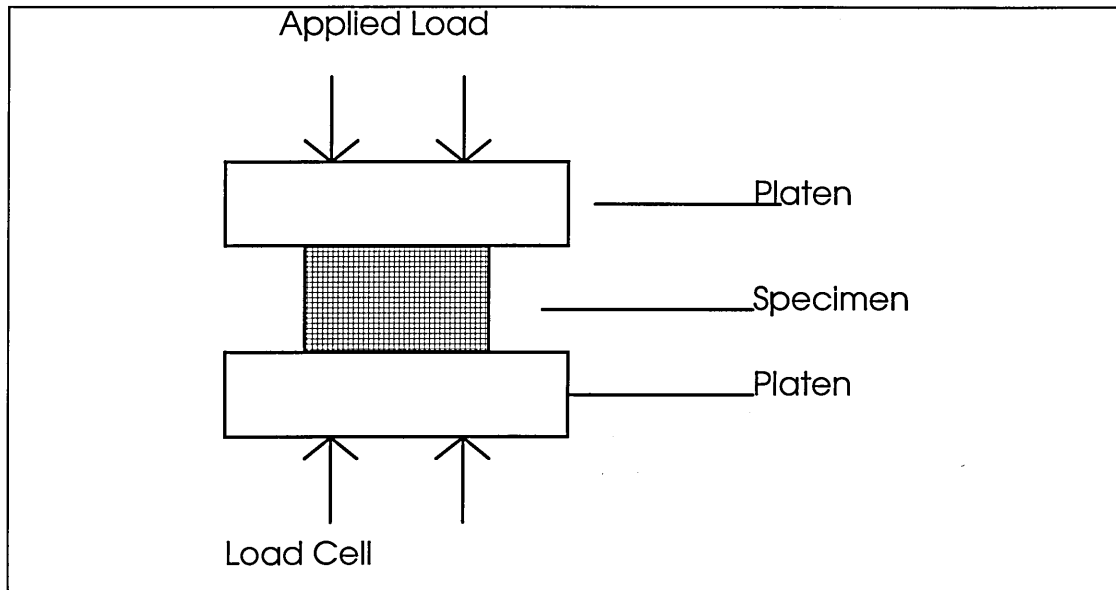


*Figure 2-1: Uniaxial Compression Test*

The stress - strain curve obtained from mechanical compression testing reveals three distinct regimes of behaviour (see Figure 2.2); linear elastic, plastic region and fracture region. The second phase of collapse progresses at roughly constant load until the cell walls meet and touch. Once this happens the resistance to load increases , giving rise to a final increasing steep portion of the stress- strain curve. This is usually called the densification phase.
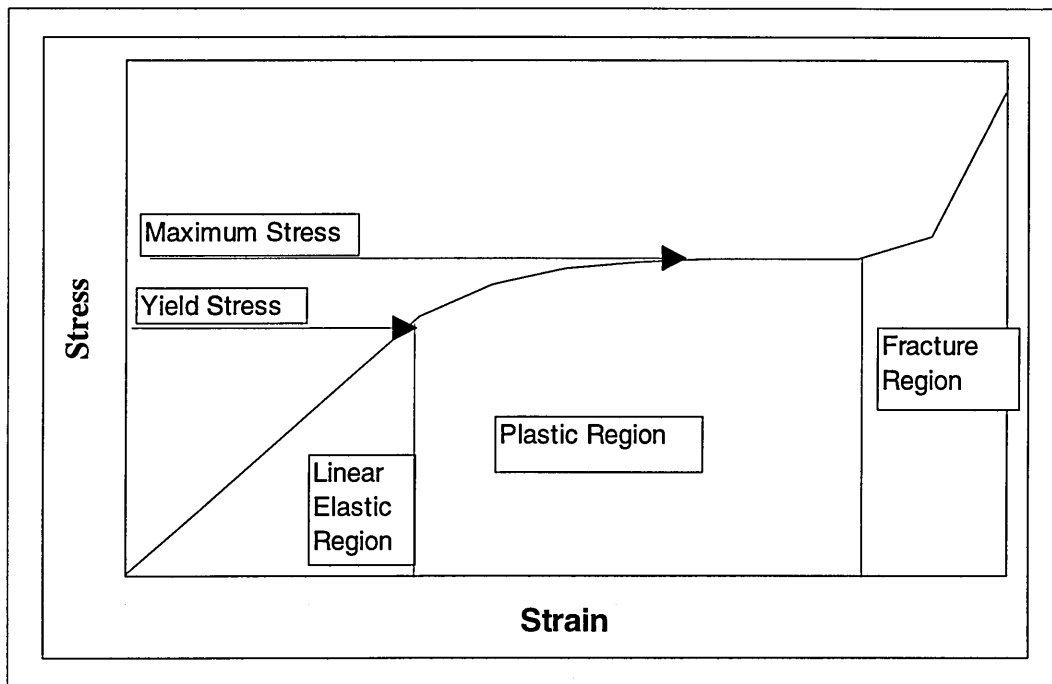
*Figure 2-2: Compressive Stress-Strain Curve*

## 2.2.2 Uniaxial Tensile Tests:

Tensile testing can be one of the most accurate methods for measuring bone properties, but bone specimens must be relatively large and carefully machined. Test pieces are machined from the region of interest. A tensile force is applied over a cross sectional area, generating both normal and shearing stresses. It is assumed that the applied force F is distributed uniformly over the cross sectional area. In order to ensure this uniformity of the load, tensile test pieces are made with shoulders and usually of circular cross section (see Figure 2.3 ) [Gilan 1969 ]. Ashman et al. [1984] used parallelipped tensile test specimens of 5mm*5mm*20mm. To strengthen the specimen ends and better distribute tensile loads, the ends of the bone specimens were potted in perspex).
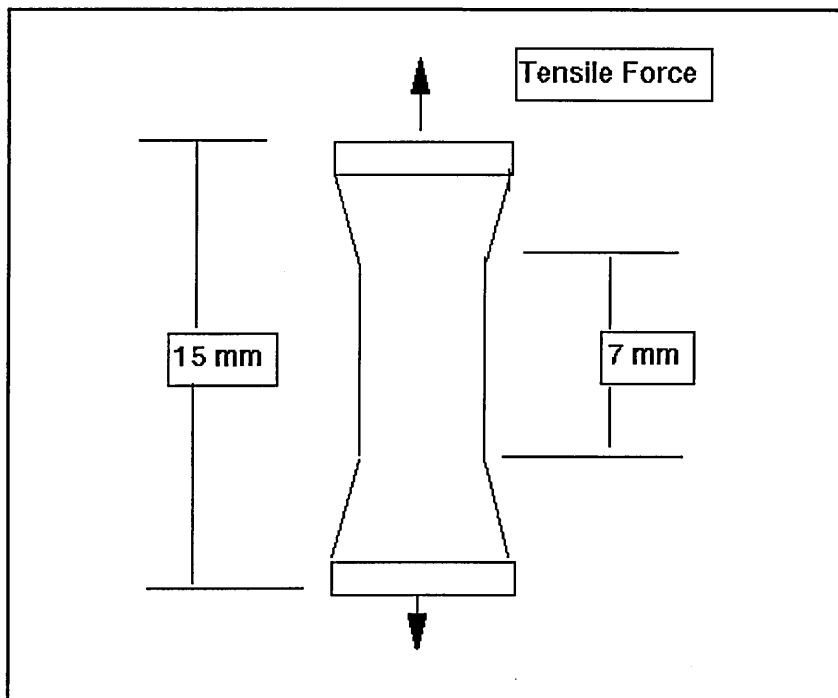
***Figure 2-3:*** *Example of Tensile Test Configuration*

The stress-strain curve recorded for tensile testing has a slight variation from compression. There is the initial linear region followed by a region which is non linear until a maximum stress is achieved. Beyond this point progressive trabecular fracture occurred, resulting in a gradual loss of stress with increasing strain until total separation of the fracture surfaces is observed (Figure 2.4) [Carter et al., 1980]. The gradual decrease in stress after the maximum is accompanied by a tearing phenomenon wherein the trabeculae of the cancellous bone progressively tear free from adjacent bone.

The graph shows Stress (y-axis) versus Strain (x-axis). The curve rises linearly labelled "Linear Elastic Region", peaks, then falls through the "Plastic Region".
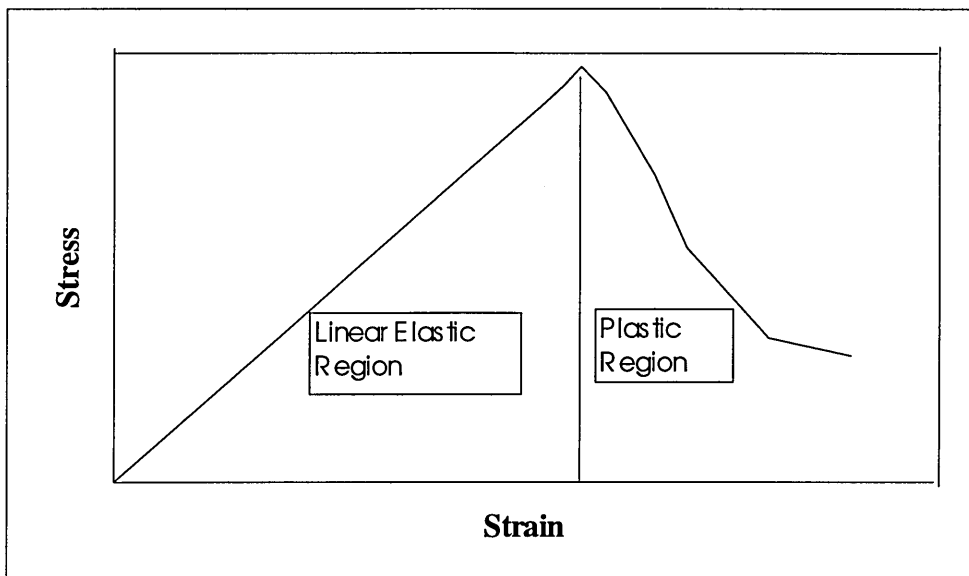
***Figure 2-4:*** *The Stress-Strain curve for tensile loading*

Studies of the mechanical properties of cancellous bone have emphasised the utilisation of compressive properties, both for reasons of experimental expediency and because compressive failure of trabecular bone is a common problem clinically. Difficulties in tensile measurement have arisen due to the porous nature of cancellous bone. This makes it difficult to grip the sample in tension measurement without crushing it [Carter et al., 1980].

The tensile behaviour of most porous materials differs significantly from the compressive behaviour. The modes of failure in the two types of loading could account for some of the differences. The struts in porous materials do not buckle under tensile loading, whereas some buckling may occur in compressive loading. In addition, since tensile fracture is associated with distraction of two fracture surfaces, no further energy is absorbed with continued loading after fracture. consequently, porous materials absorb much less energy in tension than in compression. The above arguments support the finding of Stone et al.[1983] and Kaplan et al. [1985], that the compressive strength of cancellous bone is greater than the tensile strength. The average ultimate strength recorded by Kaplan et al. [1985] was 7.6 ±2.2 MPa in tension and 12.4 ± 3.2 MPa in compression for bovine trabecular bone from the proximal humerus. These results are contrary to those of other researchers (see Table 2.1). Carter et al. [1980] found no significant difference between tensile and

compressive strength for human trabecular bone (femora), although, they noted that the energy absorption capacity was significantly lower in tension. Neil et al. [1983] and Bensusan et al. [1983] using human vertebral specimen and bovine trabecular bone respectively, supported Carter et al. [1980] findings. The source of specimen (human or bovine) and method of measurement may explain some of the discrepancies in the two schools of reasoning.

*Table 2-1: Examples of tensile and compressive strength of cancellous bone*

| Author | Specimen | Tensile Strength(MPa) | Compressive (MPa) |
|---|---|---|---|
| Evans(1973) | Human vertebrae | 1.18 | 6.27-8.62 |
| Carter et al.(1980) | Human femora | No statistical | difference |
| Stone et al.(1983) | Bovine humerus | 2.63 | 8.29 |
| Neil et al.(1983) | Human vertebral | No statistical | difference |
| Kaplan et al.(1985), | Bovine humerus | 7.6± 2.2 | 12.4 ±3.2 |

## 2.2.3 Bending

An *in situ* bone in the living body is subjected to a variety of force systems-gravitational, muscular activity, static and dynamic support and impact, which tend to bend and twist the bone. Logic will dictate that the strength and other mechanical properties of bone be determined from bending and torsion tests. However, when a specimen of any material is tested in bending, its cross sectional area is subjected to a combination of tensile, compressive and shearing force. None of these forces is uniformly distributed over the cross- sectional area. Consequently, in bending, it is difficult to determine the numerical value for the various kinds of stress and the relative importance of each in the failure mechanism. This lends itself to the assumption for example, that E is the same in tension as in compression. It also assumes that the material is homogeneous and isotropic. For the above reasons, Evans [1973] supposed bending to be a rather unsatisfactory test for determining the mechanical properties of

a material. Burstein and Frankel [1971] were also not satisfied with bending mode of testing.

On the other hand, Currey [1970], Simkin and Robin [1973] were in favour of the method. Their argument being that clamping or supporting the cortical bone is simpler when this method is used than with tension or compression tests. They also pointed out that the deflections are larger and the method is relatively insensitive to inaccuracies in the centricity of the load. Bending tests also allow testing to be done on samples which are slightly curved, without altering the value of E. Also, drying which may happen during the test, will not greatly alter the value of E obtained, whereas in the compression tests, the shrinkage is of the same order of magnitude as the strain. There is little data in the literature for bending measurements on cancellous bone. The structural nature of cancellous bone which makes test specimen difficult to machine may be the major reason.

## 2.2.4 Fatigue Test

Fatigue is a well known phenomenon occurring in engineering structures, most of which are subjected to time dependent variation in the applied loads. Such variation cause fluctuations in the stresses of different parts of a structure. If theses fluctuating stresses are sufficiently large, failure of a structure may occur, provided the stress is repeated often enough [Evans, 1973]. A failure produced by repetitive loading of a material or a structure is called a fatigue failure.

During the daily activities of life, the bones of the skeleton are repeatedly subjected to stress by gravity and muscle action. The response of the bones to this repetitive loading is important in understanding the nature of the so- called " fatigue", "stress", or " march" fracture. This type of fracture are commonly encountered in the metatarsal. Fatigue properties can be measured using either tensile, compressive, bending or torsional loading. Fatigue testing requires a test machine capable of applying cyclic loading. Fatigue tests are considerable more time consuming than the other discussed methods.

## 2.2.5 Osteopenetrometer

This method is based on the principle of recording the force necessary to advance a needle into the bone and also the depth of penetration [Hvid et al., 1984]. The strength data is reported as the average penetration strength(pa), given by the force average over 1 mm interval divided by the projected area of the measuring profile [ Hvid et al.; 1985b, Jensen et al., 1991]. Penetration tests do not reflect any well defined mechanical property of trabecular bone, but Hvid et al. [1984] have shown that the relation to the ultimate strength of bone cylinder could be expressed as average penetration strength given by $1.74\sigma\mu^{1.06}$. This method has a fundamental flaw however, which is the lack of relationship between the measured values and the mechanical properties of bone.

## 2.2.6 Problems Associated with the Measurement of Cancellous Bone Properties

The Young's modulus of cancellous bone reported in the literature ranges from 0.2 - 9800 MPa in compression. A survey of the published data is given in Table 2.2. The variations is accounted for by factors such as age of the bone, anatomical location and testing conditions. The following sections will discuss how the testing conditions affect the reported data on cancellous bone.

### 2.2.6.1 Specimen Configuration

High porosity makes complicated specimen shapes difficult to machine. Different specimen configurations have been used for different methods of testing, cubic and cylindrical specimens are commonly used in compressive testing. Generally, the specimen must be large enough that a representative section of pores and struts can be analysed, yet small enough to resolve the heterogeneity of the tissue. It has been shown that 5 mm cubic test samples is the minimum size for which the continuum

characterisation is realistic [ Brown and Ferguson, 1980; Harrigan et al., 1985,]. This minimum size is still disputed with Linde et al. [1988] advocating 7 mm.

Surface irregularities; induced bending; and difficulties associated with accurately measuring strains present a problem for compressive testing. Attempt to solve the problems is usually done by making the width to length ratio as small as possible, and making the measuring surfaces as parallel as possible. The use of a confining ring has been reported to result in the data being higher than that which would be measured in an unconfined uniaxial test by a factor of about one third [Gibson, 1985]. This may be because side bending is prevented. On the other hand, loading in tension though less susceptible to non- uniform loading requires larger more complicated shapes.

The anisotropic structure require mechanical properties to be measured in several different directions to completely characterise the anisotropy.

### 2.2.6.2 Strain Rate

The viscoelastic property of bone poses problems of reproducibility with variation in strain rate used. The resistance of bone to load varies proportionally to the rate at which the load is applied, so the mechanical properties of  wet bone vary slightly with strain rate. If strain rate is increased by an order of magnitude, measured bone strength will increase by about 15% [Carter and Hayes, 1977].

### 2.2.6.3 Preservation

A problem of great importance in studies on mechanical properties of bone is the preservation of a specimen during the time between harvest and testing. The main concern is to avoid the specimen from drying. This can be done by keeping it in water, physiological saline solution, embalming fluid, alcohol or by freezing it. The possible effect on mechanical properties will depend on the method and length of preservation. The effects of the various methods of preservation have been investigated by Sedlin and Hirsch [1966] and by Evans [1973]. Sedlin and Hirsh could not demonstrate an effect of fixation of the specimen in formalin but advised against fixation. On the other hand Evans revealed that alcohol fixation causes a significant and irreversible decrease in the deflection of human tibia tested in bending.  Freezing at $-20^{o}c$  has been shown

not to affect the physical properties of bone so long as the specimen is adequately hydrated and thawed before testing [Sedlin and Hirsch, 1966, Evans, 1973]. Most researchers have taken to freezing as a mode of storage, although at various freezing temperatures. For example, Evans et al. [1990] at -20°c, Brown and Ferguson [ 1980] at -10°c, and  Hvid et al.[ 1985a] at -30°c.

### 2.2.6.4 Miscellaneous

Cancellous bone as explained earlier, has the porous cells filled with marrow. Carter and Hayes [1976] reported that the presence of marrow during testing did not generally alter the elastic properties of cancellous bone. So, while some researchers carry out their investigations on defatted specimens [Ashman et al., 1987], others either carry out on specimens with fat *in situ* or do not bother to report [Vahey and Lewis, 1987].

In defatting of the samples, Carter et al. [1980] used two methods: jet of warm water, and methanol and chloroform on two different set of specimen. They demonstrated that the method of marrow extraction did not affect the elastic properties. They also showed that samples which were kept wet throughout the preparation procedure were generally more compliant than samples which were dried and rewetted. Sharp et al. [1990] showed that only immersion in trichloroethylene and ultrasound bath for 4 hours removed all the fat.

It worth noting that most mechanical measurements are performed *in vitro*. *In vivo* bones are more springy(elastic) and resilient, have a nerve supply (cortical bone only) and rich in blood supply. They are in a state of continual and rapid turnover as far as their inorganic material is concerned. They can adapt their shape to their function, particularly when they are young, so that faulty posture or unsuitable shoes may cause distortion of bones. Hence it is difficult to relate *in vivo*  to *in vitro* data.

## 2.2.7 Conclusion

The above are major methods used in the literature. As it is apparent from above each of the methods has inherent problems and advantages, but current sentiment favours uniaxial compression testing.

*Table 2-2: Survey of Compressive Young's Modulus Reported for Cancellous Bone*

| Author | Region | Modulus (MPa) |
|---|---|---|
| Evans and King(1961) | p. femur | 20.68-965 |
| McElhaney et al.(1970) | vertebral | 151.7 |
| Pugh et al.(1973) | d. femur | 413-1516 |
| Schoenfield et al.(1974) | p. femur | 344.7 |
| Townsend et al.(1975) | patella | 121.3-580 |
| Lindahl (1976) | p. tibia | 1.4- 79.2 |
|  | vertebral | 1.1- 139 |
| Carter and Hayes(1977) | p. tibia | 20-200 |
| Ducheyne et al.(1977) | d. femur | 58.8- 2942 |
| Brown and Ferguson(1980) | p. femur | 1000-9800 |
| William and Lewis(1982) | p. tibia | 100- 500 |
| Goldstein et al.(1983) | p. tibia | 4.2 -430 |
| Martens et al.(1983) | p. femur | 58- 2248 |
| Ashman et al.(1986) | vertebral | 158- 378 |
| Ciarelli et al.(1986) | p. tibia | 5- 552 |
|  | p. femur | 49- 572 |
|  | d. femur | 7.6- 800 |
|  | humerus | 1.1- 448 |
| Struhl et al.(1987) | vertebral | 10- 428 |
|  | iliac crest | 5- 282 |
| Ashman & Rho(1988) | d. femur | 1636 |

where p = proximal, d = distal

## 2.3 Methods and Problems of Measuring the Mechanical Properties of the Trabeculae

The trabeculae could be said to be the unit structure of the cancellous bone. The field of biomechanics has acquired a good understanding of trabeculae bone behaviour on a continuum level (macroscopic or structural level). Investigators have now begun to study trabecular bone behaviour on a microstructure level (material level). The structural properties of cancellous bone are defined using the cross-sectional area which is inclusive of both trabeculae and pores. Conversely, material properties define the intrinsic properties of the trabecular struts alone. This is the source of the two densities- apparent(bulk) density and real(material) density mentioned earlier. Material properties are generally higher than structural properties. For example the apparent density varies from 100 - 1000 kg m$^{-3}$, while material density varies from 1600 - 1900 kg m$^{-3}$.

Characterisation of the mechanical properties of human trabecular bone is a very important aspect of musculoskeletal research. The progress of the research has been hampered by the controversy over the value of the trabeculae compared to cortical bone. It all started with the speculation by Wolff(1892) that trabecular bone posses similar properties to cortical bone. This has been supported by the highly referred empirical model of Carter and Hayes [1976], where they indicated that the strength and Young's modulus were proportional to the square and cube of the apparent density respectively. In their model, they proposed that all bone should be viewed as a single material. The smallness of the struts (111- 181 $\mu$m) makes mechanical properties measurement difficult to implement. Different methods have been used by different laboratories including; microhardness, ultrasonic testing, buckling of single struts, three point bending and finite element. The results of some of the investigations are summarised in Table 2.3. The following section will discuss briefly some of the methods used.

## 2.3.1 Microhardness

Hardness is usually defined as the resistance of the material to indentation under static or dynamic loading [Davis et al., 1964]. The indentation hardness value is obtained by pressing a specially shaped diamond or hard steel ball into the polished surface of the material with a known loading for a specified time. According to Buckle[1959] if the indent is less than 30 $\mu$m made with a load of less than 200 g, then the hardness should be included within the microhardness range. If Vickers hardness tester is used then the Vickers hardness number (VHN) is calculated from the expression

$$VHN = 1854.4*P/d^2 \qquad (2.7)$$

where P = applied force(g),    d = mean of two measured diagonals ($\mu$m).

Microhardness is an attractive method of quantifying the physical effects of small scale spatial variation in the composition of bone. This is more so for material (trabeculae) measurement of cancellous bone because bone specimen can be as small as 150$\mu$m across. Weaver [1966] showed that microhardness was an accurate and reliable measure of the degree of mineralisation. Evans et al. [1990] suggested that microhardness data was a feasible way of estimating the mechanical properties of specimens that are not easily accessible by conventional testing methods.

## 2.3.2 Buckling

It has been suggested that bending and buckling are highly probable modes of deformation of trabeculae in most cancellous bone area [Pugh et al., 1973]. This has encouraged the direct use of mechanical buckling to investigate the trabeculae properties. The elastic buckling theory is based on the Euler's Equation given by

$$P_c = \frac{\pi^2 EI}{k^2 l^2} \qquad (2.8)$$

where $P_c$ is the critical applied load, E is Young's modulus, I the area moment of inertia, $k$ the end condition constant and $l$ the free length of the beam. Researchers like Runkle and Pugh[1975] and Townsend et al.[1975] have used the above method to

35

obtain 8.75 GPa and 11.46 GPa(wet), 14.1 GPa(dry ) respectively as the Young's modulus of trabeculae.

Other techniques as shown in Table 3.3 have been implemented to the study of trabeculae. The discrepancy and controversy still exist as to the value of the elastic modulus of trabeculae as compared to cortical bone. While Ku et al.(1987) showed no difference (3.8 GPa (cortical) and 3.17 GPa (trabeculae)), William and Lewis (1982) predicted an order of 10 difference (1.3 GPa (trabeculae) 16 GPa (cortical)). The small value for the Young's modulus of cortical bone obtained by Ku et al.(1987) is rather puzzling in comparison with published data for cortical bone. Rice et al.[1988] speculated that the very small specimen size may enhance surface imperfections effects on the measured value.

*Table 2-3: Estimates and Determinations of the Elastic Modulus of Individual Trabeculae of Cancellous Bone*

| Author | Type of bone | Analytical/ Test method | Estimate of trabeculae elastic modulus |
|---|---|---|---|
| Wolff (1892) | Human Bovine | * | 17 - 20 GPa (wet) 18 - 22 GPa(wet) |
| Pugh et al. (1973) | Human distal Femur | finite element method | concluded that $E_{trab} < E_{compact}$ |
| Townsend et al. (1975) | Human proximal Tibia | inelastic buckling | 11.38 GPa(wet) 14.13 GPa(dry) |
| Runkle and Pugh(1975) | Human distal Femur | buckling | 8.69 ± 3.17 GPa(dry) |
| Williams and, Lewis (1982), | Human proximal Tibia, | expt. with 2 - D, finite element method | 1.30 GPa |
| Ryan and Williams (1986) | Fresh bovine Femur | tension test, single trabeculae | 0.76±0.39 GPa |
| Mente and Lewis 1987 | Dried human Femur | experiment with finite element method | 5.3 ±2.6 GPa |
| Ku et al. (1987) | Fresh frozen Human tibia | three point bending of ultra small machined, specimen | 3.17 ±1.5 GPa |
| Ashman and Rho (1988) | Bovine femur Human femur | ultrasound test method ultrasonic test method | 10.90 ± 1.60 GPa(wet) ultrasonic test method |
| Rice et al.(1988) | Human Bovine | statistical data statistical data | 0.61 GPa 1.17 GPa |
| Hodgskinson et al. (1989) | Bovine proximal Femur | microhardness | concluded no statistical difference |

## 2.3.3  Conclusions

♦  Dissection of single trabeculae from cancellous bone is a problem of its own.

- ◆ The various measuring procedures have their own inherent problems and assumptions which contribute to the results.

- ◆ The turnover rate in cancellous tissue is eight times that in cortical bone tissue, thus making calcium content of trabeculae bone not a constant value [Rice et al., 1988].

The above factors may be wholly or partly responsible for the discrepancies in the values obtain by different researchers. On the other hand the question of the similarity of the elasticity of trabeculae and cortical bone is disputable on two accounts. Firstly it has been shown that the bone mineral content (BMC) and material density of trabeculae are less than those of cortical bone (BMC = 63%(cortical), 51%(trabecular)) [Gong et al., 1964]. The density of ash cortical bone is consistently higher than in cancellous bone tissue [Galante et al., 1970]. Secondly, the exponential influence of small changes to mineral content and density on stiffness and strength [Currey, 1969; Carter and Hayes, 1977; Currey, 1984]. Ashman and Rho[1988] using Currey[1984] equation of the dependence on BMC estimated that elastic modulus of trabecular bone would be expected to exhibit a 25% lower value than cortical bone. This argument coupled with the fact that most investigations find that the Young's modulus of the trabeculae to be less than that of compact bone will call for a rethink of the assumption made by Wolff[1892] and later by Carter and Hayes[1976]. Hopefully in the future, more refined modes of measurement will help resolve categorically the controversies.

## 2.4 Factors Affecting the Mechanical Properties of Cancellous Bone

### 2.4.1 Introduction

There is now a general consensus that the mechanical properties of cancellous bone, like any other cellular material, are affected by three intrinsic factors;

1. Apparent density (volume fraction of solids)
2. Architecture or fabric of the trabeculae

3.  Properties of the cell wall material, this relates to the mineral content of the bone material itself [ Carter and Hayes, 1976; Carter and Hayes, 1977; Carter et al., 1980; Gibson, 1985; Hodgskinson et al., 1989].

Additional variables include temperature at which the properties are being determined, whether the bone is living or dead, embalmed or fresh, the age, sex, race and species of animal from which the bone is obtained. There may be other microstructural factors such as amorphous- to crystalline calcium phosphate ratio, and mineral to non -mineral bonding [ Evans, 1973; Behrens et al., 1974] . Over the years many researchers have tried to relate the above physical properties to the mechanical properties (compressive strength, elastic modulus, tensile strength). This has stemmed from the societal need to be able to predict fracture risk and the physical factors could easily be measured in vivo. The following sections will summarise the various attempts to correlate these physical factors to mechanical properties.

## 2.4.2 Density

As mentioned earlier, two types of densities are always referred to in the literature:- apparent density (bulk density) $\rho$ and real density (material density) $\rho_m$ (see section 1.3.2). The porosity of a porous material varies approximately linearly to the apparent density of the material, but it is assumed that the matrix material density does not vary. Hence, it is assumed that the apparent density is proportional to the solid volume fraction. Therefore porosity and apparent density are reasonable measures of the amount of mineralised tissue.

Different methods of measuring the density have been used in the literature, thus making comparison of results difficult. Sharp et al. [1990] reviewed some of the methods used in the literature. They went on to suggest a protocol for measuring the density of trabecular bone: the total specimen volume and total specimen mass are measured prior to mechanical testing, the sample is then defatted in trichlorethylene in an ultrasound bath for 4 hours. The defatted specimen is then rehydrated in distilled water for 4 hours under vacuum, and then suspended on a hook, submerged in distilled

water, and the submerged weight measured using Archimedes' principle. The specimen is then centrifuged for 15 minutes at 17g on blotting paper, and finally weighed in air to obtain the hydrated tissue mass. The density of water multiplied by the difference between the hydrated tissue mass and the submerged mass gives the bone tissue volume. The densities may then be calculated.

There is a catalogue of data attempting to relate mechanical properties (Young's modulus(E), compressive strength and tensile strength) to the apparent density. The attractiveness of these correlations lies in the fact that these measures are relatively easy and may relate to similar non-invasive techniques enabling the characterisation of bone properties to be performed *in vivo* [Currey, 1969; Galante et al., 1970; Townsend et al., 1975; Carter and Hayes, 1977; Brown and Ferguson, 1980 and reviewed by Goldstein, 1987]. This has become necessary, because of the need to be able to predict fracture risk. Most of the relationships have been expressed as a function of linear regressions and power functions (see Table 2.4 ). Current sentiment among researchers tends to favour the power relation. This has been generated because of the similarity of trabecular bone to porous engineering materials.

Carter and Hayes [1976,1977] reported a power relationship between apparent density and compressive strength and Young's modulus for test on human and bovine cancellous bone. Employing data from the work of McElhaney [1966] and Galante et al. [1970], Carter and Hayes[1977] concluded that the axial Young's modulus E, depended upon the apparent density to the third power and strain rate $\dot{\varepsilon}$ to the 0.06 power, thus arriving at E in MPa as

$$E = 3790 \dot{\varepsilon}^{0.06} \rho^2 \qquad (2.9)$$

where $\rho$ is the apparent density in $gcm^{-3}$ and $\dot{\varepsilon}$ is the strain rate in $s^{-1}$. They also concluded that the axial compressive stress $\sigma$ depended upon strain rate to the 0.06 power and upon the square of apparent density thus

$$\sigma = 68 \dot{\varepsilon}^{0.06} \rho^2 \qquad (2.10)$$

where $\sigma$ is in MPa, the rest as in Equation 2.9. Two assumptions were made before empirically arriving at the above results namely:

1.  Young's modulus and strength of both human and bovine cancellous bone have exactly the same dependence on apparent density.

2.  Based on the suggestion of Wolff[1892] law that cortical bone is simply more dense cancellous. The validity of the above assumptions is debatable.

On the other hand other researchers such as Brear et al. [1988] and Hodgskinson and Currey[1990] could only demonstrate a quadratic relationship for both strength and Young's modulus. Rice et al. [1988] have conducted a comprehensive survey of the literature. By taking into consideration the factors of species (bovine/human), direction (longitudinal, anterior-posterior and medial-lateral), axial stress condition (compressive or tensile), method of testing(confined, unconfined and indentation), they carried out a rigorous statistical analysis and came to the following conclusions;

♦   Elastic modulus is proportional to the square of apparent density.

♦   Strength is proportional to the square of apparent density.

♦   Elastic modulus is directly proportional to strength.

♦   The data on mechanical properties of cancellous bone tissue from different species cannot be combined.

♦   The mechanical properties of compact bone can not be obtained by extrapolation of the mechanical properties of cancellous.

*Table 2-4: The Relationship Between Mechanical Properties and Density of Trabecular Bone*

| Author | Region | Relationship |
|---|---|---|
| Weaver and Chalmers (1966) | Human vertebral | linear[&] |
| | Human calcaneus | linear |
| Galante et al.(1970) | vertebral | linear |
| McElhaney et al.(1970) | Cranial bone | $E_c \propto \rho^3$ |
| | | $\sigma_c \propto \rho^2$ |
| Behrens et al.(1974) | Distal femur | linear |
| | proximal tibia | linear |
| Lindahl(1976) | vertebral | linear |
| Carter and Hayes(1977) | human tibia and | $\sigma_c = 68\,\dot\varepsilon^{0.06}\rho^2$ |
| | bovine tibia | $E_c = 3790\,\dot\varepsilon^{0.06}\rho^3$ |
| Carter et al.(1980) | proximal femur | as above |
| Marten et al.(1983) | proximal femur | linear |
| Stone et al.(1983) | bovine humeri | $\sigma_s = 21.6\rho^{1.65}$ |
| Kaplan et al.(1985) | bovine humeri | $\sigma_T = 14.5\rho^{1.71}$ |
| | | $\sigma_c = 32.4\rho^{1.85}$ |
| Ciarelli et al.(1986) | Distal femur | linear |
| | proximal femur | linear |
| | Proximal tibia | linear |
| | proximal humerus | linear |
| | distal radius | linear |
| Brear et al.(1988) | bovine femur | $E_c \propto \rho^{1.87}$ |
| | | $\sigma_c \propto \rho^{1.77}$ |

where $E$ is the Young's modulus, $\sigma$ is the strength and c, s, and T are compressive, shear and tensile respectively.

The results obtained by Carter and Hayes[1976, 1977] are empirically arrived. Theoretical calculation of elastic modulus and strength of very highly porous materials will depend on the state of the pores of the material, that is

a)  whether it is closed or open cell, and

b)  whether the loads applied to the cell walls deform them primarily in simple axial loading (tension, or compression) or in bending

---

[&] Linear implies that both E and $\sigma$ are linearly related to density

These are idealised models and cancellous bone is no ideal. As mentioned in Section 1.3.2 its structure ranges from open cell symmetric to closed cell columnar. So its structure will depend on the specimen in question. Most of the evidence of cancellous bone mechanics suggest that bending is the primary mode of deformation of the cell walls [Pugh et al., 1973; Gibson, 1985], although William and Lewis[1982] identified situations where deformation was primarily axial loading.

Gibson and Asby[1982], and Gibson [1985] have attempted to tie together the power relationships (quadratic and cubic) obtained by different researchers, using theoretical models. They argued that at low apparent densities, the structure of cancellous bone is one of connecting rods to form open cells. At higher apparent densities the cells fill in more, and the structure becomes one of plates forming closed cells. It was further argued that the principal mechanism of the linear elastic deformation is cell wall bending and that elastic collapse is caused by elastic bending and buckling of cell wall. The model and analysis predicts (for both compressive strength and Young's modulus) a quadratic relation for an open cell and cubic relation for a closed cell structure. This work by Gibson and Ashby [1982] has been supported by Christensen[1986]. The limitation of the above theoretical treatise is that it is based on regular repeating cells. The cell size of trabecular bone however is not uniform. Also, in some locations, the pores in the trabecular bone have a distinct orientation which induces a mechanical anisotropy.

The bone mineral content (BMC) has got the advantage that it could be measured *in vivo* either radiologically or by gamma ray or x-ray absorption techniques. Weaver and Chalmers [1966] as well as other investigators have sought a correlation between mineral content and mechanical properties. Behrens et al. [1974] reported a statistically significant but not very strong, relationship between the linear photon absorption coefficient and the compressive strength of cancellous bone using americium as a photon source. Hvid et al. [1985b] reported a linear relationship between BMC and mechanical properties. Currey [1986] using Hvid et al.[1985b]'s data demonstrated that power relationship should be favoured.

The problem and cause of the scatter in the relationship between mechanical properties and density is that the mechanical properties are influenced by many factors. For example , it must be remember that bone is anisotropic, requiring different correlations with density for different material directions. Furthermore, the degree of anisotropy varies significantly throughout most cancellous structure. Therefore one should use caution when predicting tensorial properties (moduli) from a scalar property (density) [Ashman et al. 1987]. So, a more reliable correlation will be obtained from an experiment thoroughly executed with most of the other influencing factors at minimum.

## 2.4.3 Architecture

The architecture basically refers to how the bone is arranged in space. On a broad term, the architecture of the bone will include it apparent density, its connectivity (the extent to which structural elements are connected together ) and its anisotropy. It has generally been known that the physiology of bone function directly influences the structure and strength of bone, a relationship known as Wolff's law [Wolff, 1892]. It follows that the arrangement of trabeculae in space follows the lines of stress pattern and the architecture of trabecular bone then exist as a physiological optimisation maintaining mechanical integrity while minimising bone mass. These variations in mechanical properties have been shown to be a function of anatomical position and loading direction. This has been supported by work done on cancellous bone at knee [Behren et al., 1974], proximal femur [Brown and Ferguson, 1980], ankle joint [Jensen et al., 988; Hvid et al., 1985a], and proximal tibia [Hvid and Jensen, 1984].

Early evidence of architecturals effect were recorded by Bell et al.[1967]. They pointed out that in an ageing human vertebrae, the cancellous bone loses strength more rapidly than the reduction in the amount of bone tissue. They attributed their findings to the fact that the loss is largely in transverse struts. The functions of these struts is probably to a great extent to act as lateral braces so that the longitudinal struts do not buckle. Reducing the number of points at which sideways support is provided for a slender column considerably reduces the load it can bear even though the cross-sectional area remains unchanged [Currey, 1970]. Galante et al.[1970] showed that

specimens (vertebral bone) loaded in the superior-inferior direction were more than twice as strong as those loaded in the lateral-medial direction. Behrens et al. [1974] also observed that the compressive strength of the knee varies with the location. Brown and Ferguson [1980] produced a detailed quantitative information about the spatial and directional variations of the material properties of cancellous bone (proximal femur).

The continuous process of remodelling that occurs throughout life changes the internal architecture of bone. The modelling and remodelling activity of bone is influenced by the complete loading history to which the tissue is exposed over some period of time [Cowin, 1986]. Behren et al. [1974] was able to show a strength difference between loaded and unloaded condyles of specimens taken from patients suffering from vagus.

Researchers including Brown and Ferguson [1980] have tried to link the stress pattern to the actual orientation of trabeculae. This has been thanks to advanced stereology, digital analysis algorithms and refined imaging processes. Pugh et al.[1973], Townsend et al. [1975] and Hodgskinson and Currey [1990] have attempted to correlate the architectural properties (anisotropy, fabric, and connectivity) and morphologic measures (trabecular plate thickness, trabecular plate separation) to the material properties. Due to the problems of multicollinearity it was difficult to correlate them.

## 2.4.4 Temperature

It is generally known that the elastic properties of many materials are temperature dependent. But, a great majority of tests on cancellous bone have been carried out at room temperature (21$^{\circ}$C). However, it is likely that these properties will have different values at body temperature (37$^{\circ}$C). Smith and Walmsley [1959] demonstrated that Young's modulus was approximately linear but inversely proportional to the temperature in the temperature range used (5$^{\circ}$C-37$^{\circ}$C). Recently, Brear *et al* [1988] demonstrated that loading at 37$^{\circ}$C rather than room temperature results in lower values for all the mechanical properties they tested, but the decrease is not large (2-4%).

# 2.5 Quantitative Assessment of the Structure of Cancellous Bone

## 2.5.1 Introduction

There is now the necessity to quantify the structural morphology of cancellous bone since it has been hypothesised that bone strength is linked to its structural integrity. Cancellous bone has been defined as a 3-dimensional network of struts (Section 1.1.3). A 3-dimensional characterisation of it will require a 3-dimensional analysis of structure. The structure of porous medium can be quantified by a variety of geometrical properties. The major ones being porosity (volume fraction), connectivity (degree of connection of the individual struts) and anisotropy (orientational dependence of connectivity).

The well established methods of stereology would provide 3-D parameters from random plane sections through the material. However, topological parameters (number of features and connections between these features, that is connectivity) are not accessible from the plane. Different methods can be used to determine these topological parameters. One method is the direct analysis of the material by serial sections on which the topological parameters are counted manually [Kwiecen et al., 1990]. This method is tedious and time consuming. Other methods include theoretical model to build the 3-D structure [Quiblier, 1984] and computer simulation of the structure [Jernot et al., 1992].

Different methods for measuring structural anisotropy have been developed for cancellous bone. The early works of quantifying the structural anisotropy of cancellous bone was by Whitehouse [1974], who measured the mean intercept length in cancellous bone as a function of direction on polished plane sections. It was further demonstrated that when the mean intercept lengths were plotted in a polar diagram as a function of the angle, the polar diagram produced an ellipse. Harrigan and Mann [1984] extended Whitehouse's work by showing that the mean intercept length measured on cancellous bone specimen fitted the Equation of an ellipsoid in three dimension and could be represented as a second rank tensor. The term "fabric" has

been used to describe the anisotropy of cancellous bone, with slight difference in definition with different authors [Cowin, 1986; Hodgskinson and Currey, 1990]. The structural analysis using the above method is time consuming. An alternative method using permeability (the rate of flow of fluid) is used as a structural index herein.

## 2.5.2 Permeability

It has been proposed that the rate of flow of a fluid through the porous sample will give a quantitative description of the porosity and connectivity of the sample. This follows from the dependence of rate of fluid flow on the following properties, namely:

- Number, size, shape and orientation of the pores inside the medium.
- Its dependence on density and viscosity of the fluid
- The boundary conditions.

The main advantages of permeability measurements over the other methods of quantifying porous media are :

- It is very easy and quick to carry out
- It is non-destructive.
- It could be theoretically modelled and experimental evaluated

## 2.5.3 Theory

In 1856 the French mathematician Darcy observed that the flow a fluid through a porous material is directly proportional to the pressure drop and inversely proportional to the flow path. The flow is also dependent on the viscosity and density of the fluid. This relationship is now known as the Darcy's law written as

$$Q = \frac{KA \, \Delta P}{d} \qquad (2.11)$$

where $Q$ is the flow rate ($m^3s^{-1}$), A is the cross-sectional area of the porous medium ($m^2$), P is the hydraulic pressure, K is a proportionality constant and d is the specimen thickness. The constant K is proportional to both the viscosity ($\eta$) and permeability ($\kappa$) of the porous medium. So Equation 2.11 can be written as

$$Q = \frac{\kappa A \, \Delta P}{\eta d} \qquad (2.12)$$

but $Q$ = velocity of flow($v$)*cross-sectional area of path ($A_p$), therefore Equation 2.12 can be rewritten as

$$v = \frac{\kappa A \, \Delta P}{\eta A_p d} \qquad (2.13)$$

when $A_p = A$, then

$$v = \frac{\kappa \Delta P}{\eta d} \qquad (2.14)$$

and in differential form as

$$v = \frac{\kappa \, grad P}{\eta} \qquad (2.15)$$

where $\eta$ is the viscosity of the fluid and $\kappa$ is the permeability values of the porous media and $v$ is the flow velocity.

The above Equation applies to an incompressible liquid of constant density and viscosity and porous media of homogeneous permeability. It ceases to apply at high flow rate velocities due to the emergence of inertia effects, in laminar flow and the onset of turbulence. There have been attempts to introduce a critical value above which Darcy laws ceases to apply by the introduction of Reynolds number. It is given by Equation 2.16

$$Re = \frac{\rho_l v d}{\eta} \qquad (2.16)$$

where $d$ is the diameter of the flow channel (cell size), $\rho_l$ is the density of the liquid, $\eta$ is the viscosity and $v$ is the fluid velocity. Experiment shows that the critical Reynolds number for the transition between laminar and turbulent flow depends on the tortuosity of the channel. For flow through a straight pipe the transition occurs at Reynolds number of 2100 and for flows through soils ( with large tortuosity and low porosity) it occurs at 10 [Gibson and Asby, 1988]. Different researchers have reported different values. External conditions of the porous medium also affects Equation 2.15, for example if the medium is compressible then external stresses might affect the results [Scheidegger, 1974].

# Chapter

## 3. ULTRASONIC STUDIES OF CANCELLOUS BONE

## 3.1 Basic Physics of Ultrasonic Wave Propagation

### 3.1.1 Introduction

This chapter will endeavour to define the basic physics and principles of ultrasonic application in medicine. The last two sections will examine the present method of ultrasonic interrogation of bone, and the *in vivo* and *in vitro* results obtained.

Ultrasound is generally defined as sound waves above the human audible frequency ($\geq$ 20 KHz). Ultrasonic waves may be used in medicine in preference to audible sound because they are directional and can be more easily focussed. Generally the principles of waves propagation applies to ultrasound.

### 3.1.2 Generation of Ultrasound

Waves can be generated in a stationary medium when its equilibrium is disturbed by the application of forces which vary periodically with time. This disturbance causes the particles in the medium to vibrate, with the result that sound waves are propagated in the medium.

Ultrasonic waves generation can be achieved using different types of generators such as mechanical, piezoelectric and magnestostrictive. The main component of the generator is the transducer which in general terms converts energy from one form to another. In biology and medicine, the transducers are usually made of piezoelectric materials. These materials have the property that any voltage applied across the electrodes produces a proportional change in thickness and conversely, pressure

applied across its two faces produces a potential difference between the electrode. The piezoelectric material commonly used is lead zirconate titanate (PZT), which is a synthetic ceramic.

When a transducer is vibrating in a liquid or gas the condition for resonance is fulfilled when its radius r is equal to one quarter wavelength, ie

$$r = \frac{\lambda}{4} = \frac{c}{4f} \qquad (3.1)$$

where r is the radius of the transducer, $c$ is the longitudinal wave velocity in quartz ( $\approx$ 4000ms$^{-1}$ in PZT along the x-axis) and $f$ is the resonance frequency. The characteristic acoustic impedance Z for PZT is approximately 14 times that for water and soft tissue. For detail construction principles of transducer refer to Bamber and Tristam [1988].

### 3.1.3 Ultrasonic field

The ultrasonic field of a transducer is the term used to describe the spatial distribution of its radiated energy. The configuration depends on the dimension of the transducer and also on the wavelength. The field is usually considered to consist of two regions namely, the near field (Fresnel region) and far field (Fraunhofer region). These regions are separated at the position of last axial maximum given by

$$X_{max} = \frac{4r^2 - \lambda^2}{4\lambda} \approx \frac{r^2}{\lambda} \qquad (3.2)$$

where $r$ is the radius of the source and $r^2 >> \lambda^2$ [Woodcock, 1979]. Beyond the near field the beam diverges at an angle $\theta$ where

$$\sin\theta = \frac{0.61\lambda}{r} \qquad (3.3)$$

The configuration of the far field depends on the directional characteristic of the transducer for a particular medium. The shape of an ultrasonic field in a fluid is a function of the ratio of the diameter of the transducer to the wavelength. For solids the directional characteristics are more complex than for fluids. This is especially true where the diameter of the transducer does not exceed the wavelength, because of the

appearance of transverse and surface waves as well as longitudinal waves. The directional properties will also depend upon whether it is a continuous or pulsed wave.

## 3.1.4 Ultrasonic Waves Within Matter

Ultrasonic waves can be propagated in all forms of media:- solids, gases, and liquids. In isotropic and homogeneous solids (where the wavelength << the radius(d) of the bar), both transverse(shear) $(C_s)$ and longitudinal (compression)$(C_l)$ waves can be propagated [Pain.1985], the velocities are given by:

$$C_s = \sqrt{G/\rho} = \sqrt{\frac{E}{2\rho(1+\nu)}} \qquad (3.4)$$

$$C_l = \sqrt{\frac{(K+4/3G)}{\rho}} = \sqrt{\frac{E(1-\nu)}{\rho(1-2\nu)(1+\nu)}} \qquad (3.5)$$

where $E$ = Young's modulus, $G$ = shear modulus, $K$ = bulk modulus, $\nu$ = Poisson's ratio.

In straight uniform bars with small radius (d) compared with the wavelength ($\lambda$) of the propagating longitudinal waves, the velocity is represented by

$$C_{rod} = \sqrt{E/\rho} \qquad (3.6)$$

Complications arise when the radius of the rod is nearly equal to the wavelength. Ashman et al.[1987] have shown that the density($\rho$) in Equation 3.6 is the apparent density. It may be assumed that with the exception of bone, biological tissues act for ultrasound transmission like fluids. They are unable to support transverse waves to any great extent and the longitudinal wave speed is as given in Equation 3.6, where $\rho$ is mean tissue density and E is adiabatic bulk elastic modulus. The average speed for soft tissue is about 1540 ms$^{-1}$ ± 6% . The speed of sound $(c)$ is not a strong function of frequency, except in bone and is temperature dependent [Evans and Tavakoli, 1992].

Anisotropic solids may have as many as 21 independent elastic constants. In one direction of wave propagation, three plane wave velocities could be equated to longitudinal and transverse wave velocities in isotropic solids. This implies that

Equation 3.4 to 3.6 could be applied to anisotropic cancellous bone. In this application, definition of the direction of propagation is essential.

If the solid medium is limited by a free surface another type of wave motion, a surface wave, may be propagated. The particles of the medium execute vibrations both along and perpendicular to the direction of the wave propagation. Also, in a medium which has two free parallel surfaces, situated at a distance of the order of a wavelength apart (ie a lamina or plate), lamina, plate or lamb waves can be propagated [Leszek, 1966].

## 3.1.5 Attenuation of Ultrasonic Waves in Matter

As Ultrasound beam interrogates a medium, some of its energy is lost from the beam. The phenomenon is known as attenuation. So, the intensity of a plane wave propagating in the x direction decreases exponentially with distance as

$$I_x = I_0 \exp(-\mu x) \qquad (3.7)$$

where $\mu$ is the intensity attenuation coefficient.

Factors contributing to this attenuation include beam spreading (diffraction), scattering, absorption due to various mechanisms and mode conversion resulting in partitioning of the energy among two or more wave modes each traveling at its own velocity. The beam diffraction is an extrinsic factor and the main factors depending on the media are absorption and scattering.

**Absorption** is the dissipation of ultrasonic energy in the medium via conversion to heat, due mainly to the internal friction. This process is utilised in ultrasound induced hyperthermia. There are many mechanisms by which this may occur. Depending on the medium, three classes of mechanism are used to explain absorption; classical, molecular relaxation and relative motion losses [Bamber and Tristam, 1988]. Classical mechanism which involves viscous losses, give rise to an $f^2$ frequency dependence. In molecular relaxation the temperature or pressure fluctuations associated with the wave cause reversible alterations in molecular configuration. Also, in relative motion losses, the wave induces a viscous or thermally damped movement of small-scale structural elements of tissue.

**Scattering** effects occur when particles absorb part of the ultrasound energy and reradiate it in all directions as a spherical field. Different kinds of scattering phenomena occur at different levels of structure (see Table 3.1). The types of scattering interactions have been classified according to the scale of the characteristic dimension a of the scattering structure relative to the wavelength of the ultrasound [Bamber and Tristam, 1988]

*Table 3.1: Types of Scattering Interactions*

| Scale of interaction | Frequency dependence | Scattering strength |
|---|---|---|
| $a \gg \lambda$ <br> Geometrical region | $f^0$ | strong |
| $a \approx \lambda$ <br> Stochastic region | variable | moderate |
| $a \ll \lambda$ <br> Rayleigh region | $f^4$ | weak |

Where a is characteristic dimension of the scattering structure.

♦ **Geometrical Region:** At a large scale boundary, representing the interface between two homogeneous media, the usual law of reflection and Snell's law for refraction apply to predict the direction of the reflected and refracted sound [Pain, 1985]. The intensity of the reflected sound beam, relative to the incident intensity depends on the relative acoustic impedances of the two media. Acoustic impedance (Z) is an inherent property of every material, and is the product of the density of the material ($\rho$) and the speed of propagation of sound (c) within it ( $Z = \rho c$). The acoustic impedance of air $= 4*10^2$, fat $= 1.38*10^6$, brain $= 1.58*10^6$ and bone $7.8*10^6$. The intensity reflection coefficient(R) for ultrasound encountering an interface is given by

$$R = \left\{ \frac{Z_2\cos\theta_i - Z_1\cos\theta_t}{Z_2\cos\theta_i + Z_1\cos\theta_t} \right\}^2 \qquad (3.8)$$

Where $\theta_i, \theta_t$ are the incident and transmitted angles respectively [Pain, 1985]. Hence one would expect from this equation that, the interfaces between media that are separated by the greatest difference in acoustic impedance to provide the largest reflection coefficient.

♦ **Rayleigh Region**. This is the region where the diameter of the scattering structure is much smaller than the wavelength of the ultrasound wave. The scattering strength is very weak, is proportional to the volume of the scatterer and follows $f^4$ frequency dependence [Bamber and Tristam, 1988].

♦ **Stochastic Region**. When the diameter of the scattering structure could be approximated to the wavelength of the propagating wave then the region is known as stochastic. Scattering in this region is characterized by a variable frequency dependence. Scattering is highly anisotropic

Generally, the size of the scattering particle compared to the wavelength of the interrogating wave determines the frequency dependency. Taking cancellous bone for example, scattering effects are a function of mean trabeculae length, mean pore size, and the ratio of the pore diameter to the ultrasonic wavelength.

### 3.1.6 Propagation of Ultrasound in Porous Media

The diverse type of structured matrices and inclusions in a porous media has led to numerous theories being developed. These include single scattering, the multiple scattering and the Biot theories. The single scattering theory calculates the attenuation produced by a single obstacle. It then assumes that the total attenuation is this value multiplied by the number of obstacles. This approach is therefore only valid for very low concentrations of isolated scatterers and is therefore irrelevant for the study of cancellous bone.

For more concentrated media, the multiple scattering theory has been developed. It introduces the concept of averaging the spatial distribution of a number of scatterers and summing their effect as in the single scattering theory (Waterman and Truell, 1961). The drawbacks of this model include the prerequisite of discrete scatterer and spherical pores. Athough self consistent theories have been presented [ Sayer and

Smith, 1982], they fail to encompase the high porosity and interconnectivity found in cancellous bone.

Ultrasound wave propagation in highly porous media such as cancellous bone saturated by viscous fluid is influenced in various degrees by dynamic interactions between the fluid and the frame. Biot theory [Biot,1956, 1962] analyses the relative motion of the porous structure (trabeculae framework) and the interspaced fluid ( marrow) induced by the ultrasonic wave. This approach considers the energy loss due to the frictional inter-action of the marrow flowing within a trabecular framework cell, and on the inelasticity of the trabecular bone framework. This theory has been used by Mckelvie and Palmer [1991] to predict ultrasound attenuation in cancellous bone. They found that the theory produced significant deviant results. However, Williams [1992] was able show a correlation of r = 0.78 between experimental ultrasonic velocity through bovine tibia and the velocities predicted by Biot's theory. To test the validity of this theory to cancellous bone accurate mechanical and structural properties , such as bulk modulus, permeability and tortuosity will be required.

## *3.2 Principles of Ultrasonic Measurement*

### 3.2.1 Velocity Measurement

It was discussed in Chapter 2 that the high degree of porosity, anisotropy, heterogeneity and size limitations imposed by the overall size of bones, add to the difficulty of measuring the elastic properties of cancellous bone. These problems are acute in mechanical testing (compression, tension, bending, etc). Ultrasound offers alternative methods of measurement with some advantages over mechanical techniques. Smaller specimens of simpler shapes can be used and the non-destructive nature permits several measurements to be undertaken on a single specimen. Two parameters are measured when using ultrasound to infer the material properties namely velocity and attenuation.

Velocity measurement could be achieved using either pulse-echo or transmission technique. Pulse-echo technique utilises a single transducer both to transmit and receive the signal. The generated ultrasonic pulse travels through the sample and is reflected at an interface, back into the same transducer where it is detected. This method implies that the pulse interrogate the specimen twice. In a transmission method, one transducer acts as transmitter and a second acts as receiver. In the application to cancellous bone the transmission technique is preferred because of its highly attenuating nature. In applying this method to the clinical environment where the bone is surrounded by soft tissue, correction may be allowed for the soft tissue thickness.

Ashman et al. [1984], Ashman et al.[1987], Ashman and Rho [1988] used continuous waves to excite the transmitting piezoelectric transducers. The propagation time was measured from the phase shift between transmitted and received ultrasonic signals. Lang [1970] among other researchers have used pulse or wave trains for excitation. The wave generated is received on the opposite side of the specimen with another transducer. The time ($\delta t$) associated with the propagation of the wave through the specimen was measured from the start of the transmitted wave to the start of the received wave. Ashman et al. [1984] believed that measurement of the propagation time is inherently more accurate with the continuous wave method than pulse method. Assuming or measuring the thickness (x) of the specimens and the measured propagation time, ultrasonic velocities can be calculated as,

$$V = x/\delta t \tag{3.9}$$

Antich et al.[1991] have proposed an alternative method for measuring velocity by using ultrasound reflection. In this approach the critical angles for which total internal reflection occurs at an interface between soft tissue and bone are measured. The phase velocities are calculated in correspondence to these angles

$$V = c/\sin\phi_c \tag{3.10}$$

where c is the velocity of sound in soft tissue. Antich et al.[1991] were able to demonstrate that velocity obtained by transmission and by reflection were in excellent agreement ($r^2 = .9993$).

This velocity of propagation is strongly dependent upon the elastic properties of the material (see Section 3.1.4). Several modes of wave propagation are possible depending on the overall specimen geometry, the internal structure of the specimen and the type of acoustic excitation (longitudinal or distortional wave propagation), but the bar wave relationship (Eqn 3.6) is normally used. The condition for the application of this Equation(3.6) is that the wavelength of the ultrasonic wave be greater than the cross-sectional dimension of the specimen. The wavelength must also be greater than the characteristic dimension of the structure if the structure is to be considered as a continuum. This is important since it is the structure which is being measured not the material. Unfortunately a defined rule for how much larger the wavelength must be inorder to satisfy these requirements does not exist. However, the specimen must be large enough that a representative section of pores and struts can be analyzed, yet small enough to resolve the inhomogeneity. Ashman et al.[1987] were able to fulfil this requirement by using low frequencies (50-75 KHz) whose wavelength are approximately 1-2cm.

Ashman et al. [1984] have given detail of a method of obtaining the elastic properties using the velocities of propagation. Ashman et al. [1987] tried to validate ultrasonically measured moduli with mechanically measured moduli using bovine specimens. Ultrasonic specimens were cut from the centre of mechanically tested specimen after mechanical testing was completed . They found a good correlation between the two techniques, giving

$$E_{mech} = E_{ult} + 23.3MPa, \qquad R^2 = 93.5\%. \quad (3.11)$$

The elastic modulus measured ultrasonically and mechanically ranged from 304- 3648 MPa and 337-3534 MPa respectively. The shear modulus measured ultrasonically and mechanically ranged from 164-484 MPa and 137-660 MPa respectively. The good correlation between the ultrasonic and mechanical technique opens way for more experimentation using ultrasound. Ultrasound would be a better way to characterise

the anisotropy of bone structure. This is because ultrasound test result are not time dependent.

The porous nature of cancellous bone lends itself to both structural and material properties description. The preceeding sections measures the structural properties. A similar technique to the one used in measuring the structural properties of cancellous bone [Ashman et al.,1986] can be used for material properties measuements. The major condition for material properties measurement is that the wavelength of the ultrasonic wave must be shorter than the characteristic dimension of the structure in order to interact with the trabeculae rather than the structure. Ashman and Rho [1988] used pulse transmission technique with transducer tuned to resonate at 2.5 MHz. the wavelength of the waves were of the order 1 mm which is greater than the cross sectional dimension of the trabeculae (0.1-0.5 mm). Ashman and Rho [1988] obtained trabecula modulus of 13.0 ± 1.47 GPa for human distal femur averaged from 53 specimen. They noticed that the values for bovine specimen 10.9±1.57 GPa were much less than human. The advantages of using ultrasound include the ease of specimen preparation and small specimen size. There also exist limitations which are inherent to the method, the major one being the possibility that 1 mm wavelength may not be small enough to allow for only material properties to be measured.

## 3.2.2 Attenuation Measurement

The attenuation of ultrasound through bone is determined by measuring the reduction in ultrasound signal amplitude resulting from the propagation through bone. The method of ultrasound attenuation applied in this investigation uses Broadband Ultrasound Attenuation (BUA). A single short pulse of ultrasound is produced by a 1 MHz transducer and, after passing through the sample, is received by another transducer positioned on the other side. The frequency content of the received signal is found either using a spectrum analyser or Fourier transform and is then stored. At each frequency the received signal amplitude is compared with that received in the absence of sample (usually degassed water). Using a reference material compensate for the variation in ultrasound signal amplitude with frequency for a particular pair of

ultrasound transducers. The difference between these two is attributed entirely to bone attenuation and a graph of attenuation against frequency can be plotted. Langton et al.[1984] demonstrated a linear relationship between attenuation and frequency for cancellous bone between 0.2 MHz and 0.6 MHz, to which a linear regression may be applied, yielding the BUA index.

## *3.3 Review of Previous Studies*

### 3.3.1 Introduction

A number of techniques which uses ultrasound in the diagnosis of bone disease have been reported in the literature over the years. The techniques uses one or both of the ultrasonic parameters namely:- ultrasound velocity and attenuation. This section reviews these techniques and explains why the present work was necessary.

### 3.3.2 Velocity Measurements

Studies of ultrasonic velocities for clinical purposes in bone have been reported for at least 30 years. Most of the early reported data for bone velocity were for cortical bone, measured at various anatomical positions and studied both *in vivo* and *in vitro* ( see Table 3.2). A variety of technique can be employed to acquire these measurements but, time of flight (TOF) measurements and pulse echo are the most commonly used methods in clinical applications.

Fry and Barger [1978], Ashman et al. [1987] and Turner and Eich [1992] have reported values for the velocity in cancellous bones measured *in vitro*. A number of authors have evaluated the correlation between Velocity and another parameters which have a relationship to fracture risk (see Table 3.3). Avioli et al., [1988] compared velocity measurements in patella with SPA of the radius shaft and concluded that they had an equal sensitivity. DPA was used by Heaney et al. [1989] who found that velocity measurements were equally sensitive indicators of bone fragility in post menopausal and osteoporotic women as BMC of the spine and also that the velocity generally decreased with increasing age after menopause. Evans and Tavakoli [1990] demonstrated a highly significant correlation between velocity and physical density of

bovine femur. Other interesting relationships which have been discussed include the work of Rubin et al. [1987] who demonstrated changes in velocity to immobilsation and sporting activity.

*Table 3.2: Published values of velocity of ultrasound in cortical human bone*

| Reference | Location | Method | Velocity |
|---|---|---|---|
| Siegel et al., 1958 | Tibia | *in vivo* ,TOF | 3481 |
| Rich et al., 1966 | | *in vitro, -* | 2880 |
| Abendschein & Hyatt, 1970 | Tibia | *in vitro, -* | 3526 |
| Martin et al., 1971 | Skull | *In vitro, -* | 3050 |
| Cravern et al., 1973 | Radius | *in vivo*, Pulse echo | 3406 |
| Whiting, 1977 | Tibia | *in vivo*, Pulse echo | 3550 |
| Yoon and Katz, 1979 | Femur | *in vitro*, TOF | 3550 |
| Andre et al., 1980 | Femur | *in vivo*, Pulse echo | $3250 \pm 190$ |
| Behari and Singh, 1981 | | *in vivo*, TOF | 3457 |
| Greenfield et al., 1981 | Radius | *in vivo*, Pulse echo | Male 3311±205 |
| | | | Female 3359±195 |
| Rubin et al., 1987 | Tibia | *in vivo*, TOF | Male 2383± 133 |
| | | | Female 2192±120 |

The precision of velocity measurement is usually assessed by repeated measurements on one or several subjects. The precision is usually quoted as the coefficient of variation given as a percentage of standard deviation divided by the mean value of successive readings. Different precision values in clinical applications have been reported by different authors. Rossman et al.[1989] reported a precision of 1%, but, Heaney et al.[1989] reported a lower precision of 2.2%.

In clinical environment three types of velocities can be identified namely: heel velocity, bone velocity and time of flight velocity

*Heel Velocity* = (Distance between transducer)/Transit time

$Bone\ Velocity$ = (Distance between transducer - soft tissue thickness)/(Transit time- Transit time through soft tissue)

*Time of flight* velocity is defined as:
$$V_{TOF} = \frac{V_w}{1-(\frac{t}{x}V_w)}$$

where $V_w$ is the velocity in water, $x$ is bone thickness and $t$ is the difference between transit in water with no bone and transit time in water with bone.

These three types of velocities have been investigated by Miller et al.[1993] and demonstrated that the velocities correlated closely with each other. $V_{tof}$ had the optimum precision but the smallest range (CV = 0.70% but $V_{bone}$ (CV = 2.71%) had the largest range, a factor that enhances its sensitivity for distinguishing normal from abnormal results.

*Table 3.3: Published Correlation Between Velocity and Physical Parameter.*

| Reference | Physical Parameter | r-values | Comment |
|---|---|---|---|
| Rich et al., 1966 | Calcium content | 0.99 | Cortical bone , Poor for cancellous bone |
| Abendschein & Hyatt, 1970 | Physical density | 0.866 | Tibia |
| Evans and Tavakoli, 1990 | Physical density | 0.85 | Bovine Femur |
| Rossman et al., 1989 | SPA (Radius) DPA (Spine) DPA (Femur) | 0.66 0.63 0.52 | Calcaneus 1535±20 Normal 1505±20 Abnormal |
| Zagzebsky et al., 1991 | SPA (Radius) DPA (Spine) DPA (Femur) DPA (Calcaneus) | <0.4 <0.4 <0.4 0.72 | Calcaneus 1571±36 |
| Waud et al., 1992 | DXA(Calcaneus) | 0.66 | Calcaneus(all): 1721± 110 Premenopause: 1744± 75 Postmenopause 1689± 92 |

### 3.3.3 Attenuation Measurement

Until 1984 the literature on the diagnostic potential of ultrasonic attenuation has been sparse. Garcia et al. [1978] used an immersion transmission method, excited by both continuous wave and broadband pulse technique. They demonstrated decrease in attenuation of bovine cortical bone with decrease in mineral content. Cancellous bone attenuation was investigated by Fry and Barger [1978] and Smith et al. [1979]. Their work however was confined to the skull for the purpose of finding the optimum parameters for trans-skull diagnostic imaging.

Significant interest developed in the application of ultrasound to bone pathology after the work of Langton et al. [1984]. They demonstrated that the attenuation of ultrasound over a frequency of 0.2 - 0.6 MHz (Broadband Ultrasound Attenuation,-BUA) was linear and the slope of this graph could differentiate between normal and osteoporotic bone. As is the fate of any new technique coming into a well established field, the questions asked are:

- How does BUA compare with ionising radiation methods ?

- What is the role of ultrasound in the assessment of bone pathology ?

- What is ultrasound measuring ?

The ability of ultrasound to discriminate between normal and osteoporotic subjects are cited in the literature (see Table 3.4). The differences reported between the normal and osteoporotic volunteers are statistically significant. Resch et al.[1990] found a significant difference in BUA between 37 caucasians women (mean age, 65±1 years) with one or more atraumatic vertebral fractures and 23 healthy women (mean age. 63± 2 years). Variants in age do not account for this significance, although a negative correlation between BUA and age has been reported [Herd et al., 1992; Waud, 1992]. Damilakis et al.[1992] demonstrated using multiple regression analysis that the difference between normal and osteoporotic patients was more disease related (p<0.001) than age related (p<0.05).

*Table 3.4:* *Published BUA demonstrating discrimination between normal and osteoporotic subjects*

| Author | No of subjects | Selection criteria | BUA(dBMHz$^{-1}$) range | Mean BUA |
|---|---|---|---|---|
| Langton et al. 1984 | N40 O20 | FFN | 55 - 90 20 - 50 | |
| Baran et al. 1988 | N29 O22 O10 | Osteopenia at 2SD or VCF FFN | | 54.5(2.2) 40(2.5) 32(3.4) |
| McCloskey et al. 1990a | N24 N10 O21 | Premenopausal Perimenopausal VCF | 65 - 90 70 - 85 20 - 80 | 79.6(1.1) 79.6(1.1) 55(4) |
| Resch et al. 1990 | N23 O37 | VCF | 40 - 90 20 - 80 | 62.6(2.9) 54(2.2) |
| Agren et al. 1991 | N17 O21 O20 | without fracture VCF or FFN | | 70(3) 56(3) 51(2.7) |
| Herd et al. 1992 | N200 O33 | VCF | 40 -120 33- 92 | 55 |
| Damilakis et al. 1992 | N74 O19 | Radiograph | | 66.5(12) 48.8(6) |

Where N is normal, O is osteoporotic, VCF is vertebral crush fracture, FFN is fracture of femoral neck and SD is standard deviation

A series of *in vivo* comparative studies between BUA and bone mineral density (BMD) have been reported in the literature. Table 3.5 represents some of the published correlation coefficient between BUA and various densitometric techniques which vary from r = 0.41 to r =0.92. The interpretation of the data is complicated by many factors including:

- measurement site assessed by BUA and bone densitometry techniques,

- effects of different ultrasound system used,

- the mode of interaction of ultrasound and photon based techniques are different,

- age range of the samples

From a clinical view point, correlation studies could be criticize on the ground that it fails to provide information about the predictive value of one test against another. The diagnostic value of a clinical test can be calculated using either Z-score or receiver operating characteristic (ROC) analysis [Eastell, 1992]. The ROC curves are generated from sensitivity and specificity of the method. The sensitivity/specificity of BUA have been reported at 70 $dBMHz^{-1}$ by Baran et al. [1988] to be 80%/80%; at 50 $dBMHz^{-1}$ by McCloskey et al. [1990a] to be 81%/93% and at 63 $dBMHz^{-1}$ by Agren et al. [1991] to be 76%/76%. From these works it appears that BUA measurements can have a similar diagnostic accuracy to lumbar spine BMD.

The relationship between BUA and physical density has also been investigated *in vitro*. McCloskey et al. [1990b] reported measurements of BUA and physical density on samples of calcaneus obtained from cadavers and concluded that there was a good correlation of r = 0.85. McKelvie et al.[1989] obtained similar correlation (r = 0.83) between BUA and physical density of the calcaneus. Evans and Tavakoli [1990] found a poor correlation (r = 0.33) between BUA and physical density of bovine femur. Tavakoli and Evans [1991] investigated the dependence of velocity and BUA on bone mineral content. The bone mineral content (BMC) of bovine femur specimens were demineralized by nitric acid. They showed a good correlation between BUA and BMC, but velocity measurements showed a better correlation greater than 0.97.

*Table 3.5: Published Correlation Coefficient Between BUA and BMD in vivo and Precision of BUA Measurement.*

| Reference | BMD Site | BMD method | Correlation Coefficient | Precision (%) | n |
|---|---|---|---|---|---|
| Gluer et al. 1992 | Calcaneus | SXA | 0.72 | 2.76 | 33 |
| Waud et al. 1992 | Calcaneus | DXA | 0.73 | 2.8 | 64 |
| Zagzebski et al.,1991 | Calcaneus | DPA | 0.56 | 10 | 42 |
| McCloskey et al. 1990b | Calcaneus | QCT | 0.80 | | 25 |
| McKelvie et al. 1989 | Calcaneus | QCT | 0.83 | | 33 |
| McCloskey et al. 1990a | Distal radius | SPA | 0.77 | 3.1 | 61 |
| Evans et al. 1988 | Distal radius | SPA | 0.45 | 2.1 | - |
| Petley et al. 1987 | Distal radius | SPA | 0.80 | 3.9 | 44 |
| Poll et al. 1986 | Distal radius | SPA | 0.80 | 3.9 | 44 |
| Rossman et al. 1989 | Radius shaft | SPA | 0.64 | 10 | 76 |
| Hosie 1987 | Radius shaft | QCT | 0.85 | - | 44 |
| Hosie 1987 | Ultradistal radius | QCT | 0.66 | - | 24 |
| Massie et al. 1993 | Spine | DXA | 0.42 | 2.6 | 328 |
| Agren et al. 1991 | Spine | DXA | 0.61 | 2.3 | 58 |
| Baran et al. 1991 | Spine | DXA | 0.83 | 2.9 | 22 |
| McCloskey et al. 1990a | Spine | DPA | 0.72 | 3.1 | 61 |
| Rossman et al. 1989 | Spine | DPA | 0.66 | 10 | 76 |
| Evans et al. 1988 | Spine | QCT | 0.64 | 2.1 | - |
| Baran et al. 1988 | Spine | DPA | 0.61 | 2.6 | 61 |
| Massie et al. 1993 | Femoral neck | DXA | 0.32 | 2.6 | 328 |
| Agren et al. 1991 | Femoral neck | DXA | 0.68 | 2.3 | 58 |
| Baran et al. 1991 | Femoral neck | DXA | 0.87 | 2.9 | 22 |
| Rossman et al. 1989 | Femoral neck | DPA | 0.41 | 10 | 76 |
| Baran et al. 1988 | Femoral neck | DPA | 0.59 | 2.60 | 61 |

where BMD is the bone mineral density and n is the sample size

Due the different modes of interaction of ultrasound with bone compared to photon based techniques, the question has been raised on several occasions [Gluer et al.,1992; Waud et al., 1992; Baran et al., 1988]

◆ Is ultrasound measuring another quantity in addition to density ?

◆ Is this quantity structure ?.

Langton et al. [1990a] confirmed the structural dependence of BUA. However, a more rigorous three dimensional analysis of cancellous bone structure and the ultrasound attenuating mechanisms is warranted and form the basis of this investigation.

### 3.3.4    Clinical Ultrasonic Bone Measurement Systems

Since the arrival of the Walker Sonix UBA575 (Worcester, USA), other clinically available systems have appeared on the market. These include McCue CUBAClinical (Winchester, UK), Lunar Achilles (Madison, USA) and Osteo Signature (Framingham, USA). The various parameters measured and the locations are given in Table 3.6. Contact Ultrasonic Bone Analyser (CUBA) was used in this investigation and a brief description will be presented in Chapter 4.

*Table 3.6 :  Clinical Ultrasonic Bone Measurement Systems*

| System | Parameters Measured | Measurement site | Comment |
|---|---|---|---|
| Walker Sonic | BUA | Calcaneus | Fixed distance Rectilinear scanning |
| Osteo Signature | V(heel) | Patella | Contact |
| Lunar Archiles | V(tof), BUA | Calcaneus | Fixed distance |
| CUBA Clinical | V(heel and bone), BUA | Calcaneus | Contact Soft tissue corrections |

# Chapter

# 4.   EXPERIMENTAL METHODS

## 4.1 Introduction

Previous chapters have introduced the concepts  relevant to this investigation. The various methods of measurement both for mechanical properties and ultrasonic parameters have been of a broad nature. This chapter will describe in greater detail the specific methods applied.  The following parameters were investigated;

- Mechanical parameters: Young's modulus (E), strength($\sigma$) and apprent density ($\rho$)
- Ultrasonic properties: velocity (V) and broadband ultrasonic attenuation (BUA)
- Structural properties: permeability ($\kappa$)

The experimental set-up to acquire these parameters will  be described with special emphasis on the precautions  taken to achieve accurate and reproducible readings.

The *in vitro* measurements were performed in the following order:

1.   Samples  prepared.
2.   Samples  degassed.
3.   Ultrasonic measurements (BUA and Velocity).
4.   Samples defatted and degassed.
5.   Ultrasonic measurements .
6.   Permeability  measured.
7.   Mechanical properties (Young's modulus and strength)  measured
8.   Apparent density  measured

## 4.2 Specimen

For the *in vitro* studies, proximal and distal bovine femi, human calcaneus and human vertebrae were investigated.

## 4.2.1 Preparation

The bovine samples were obtained fresh from a local butcher. No information on the sex, age and weight of the bovine samples were provided. The femi were cleaned and soft tissue removed. Large blocks of cancellous bone were then cut out using a band saw. These blocks were then cut down into 20 mm cubes under constant irrigation using a 220 grit diamond wafering blade, with fine smoothing on fine carborundum grit if necessary. These specimen were cut out at different locations from both the proximal and distal ends of the femi. The edges of the cubes were approximately in line with the longitudinal ( proximal-distal PD), anteroposterior (AP) and mediolateral(ML) axes of the bones from which they were obtained. The orientation with respect to the bone axis was noted and the sample's physical dimension measured.

The vertebrae specimens were obtained dried. No information of age, sex nor pathology were available. Cubes of variable sizes were cut out as described in the preceding paragraph. They were hydrated before any measurements were carried out.

The calcaneus samples were obtained post mortem from 20 different cadavers(ten males and ten females) with age range of 59 to 90 years. No pathological information on the specimens was available.

- After removal of soft tissue, a coring drill with an internal diameter of 21 mm was used to remove samples in the mediolateral direction. This is approximately the area where clinical(*in vivo*) measurements are carried out.

- The cortical end surfaces were removed to leave a cylinder of trabecular bone using 220 grit diamond wafering blade under constant irrigation.

- The fat was then removed from the samples. This involves subjecting the specimen to high speed jet of water, and then compressed air. This process is repeated until no fat is visible. The specimen is then tumbled overnight in excess of 2:1 chloroform-methanol mixture.

For all samples, care was taken to produce smooth parallel surfaces. This is crucial for accurate determination of Young's modulus [Currey, 1970]. The specimens were kept

frozen ( -20$^{\circ}$C) until required for testing, then they were thawed and allowed to attain room temperature before measurement.

During preparation, all specimen were kept wet and cool. All measurements were carried out at room temperature.

### 4.2.2 Specimen Degassing

Any slight introduction of air bubbles would increase the attenuation substantially since an air interface effectively acts as a total reflector. In the clinical situation ( *in vivo),* no air bubbles would be present. So, to ensure that no air bubbles are left inside the samples, they were thoroughly degassed  under water using a water powered vacuum pump connected to a dessicator. The samples were left degassing overnight at a pressure of 30 inches of mercury (1 bar) on bowden gauge. The specimens were transferred to the water bath without exposure to air. A wetting agent (tepol) was applied to the water during degassing to enhance gas removal.

## *4.3 Ultrasonic Methods*

Conventional ultrasonic technique are based on the pulse-echo technique which utilises a single transducer both to transmit and to receive the ultrasonic signals. An ultrasonic pulse  generated by  the transducer travels through the sample and is reflected from the far side interface, back into the transducer where it is detected. The pulse therefore travels twice through the measured sample. Due to the highly attenuating nature of cancellous bone,  the reflected signal is very weak and thus difficult to detect. Therefore the pulse-echo technique is not applicable to cancellous bone and a transmission technique must be adopted. The transmission technique uses two transducers placed at opposite ends of the samples, one as the transmitter and the other as the receiver.

This technique has been incorporated into the  Contact Ultrasonic Bone Analyser (CUBA) system [Langton et al., 1990b] which was used throughout this investigation. CUBA consisted of a portable PC interfaced to a spike generator (transmitter ) and digital receiver (Thurlby DSA 524) with dedicated menu driven software (Figure 4.1).

Two 1 MHz (nominal frequency), broadband ultrasonic transducers were mounted on a hand-held sliding calliper. One transducer acts as the transmitter and the other as the receiver. Two pairs of broadband ultrasonic transducers were used during the investigation; a 19 mm and 13 mm diameters. The former were used for phantom studies while the later for *in vitro* studies. The calliper was attached to a digital vernier gauge to measure specimen thickness. The transmitting transducer was excited by a fast rising 600V pulse (width 1 μs), producing a short RF pulse of broadband ultrasound (Figure E.6). This signal after propagating through the sample (submerged in water) is received by the other transducer positioned on the other side of the specimen.

Coupling is an important consideration when performing ultrasound measurement since an air interface effectively acts as a total reflector. Water provided the coupling in this case. The samples were submerged in a water tank and all the measurement carried out under water. Immersion contact technique was used in the *in vitro* studies reported in this thesis. Tap water was used with tepol detergent to improve sample wetting and to increase the cavitational threshold [Njeh , 1990]

At the start of the measurements, the system is switched on after setting up and initially allowed 30 minutes before commencing measurements. This allows the water to settle, air bubbles to disperse and the electronics to warm up. Samples were also allowed a setting time of 5 minutes in the water. This stabilising period is to allow air bubbles introduced by placing the sample to escape.
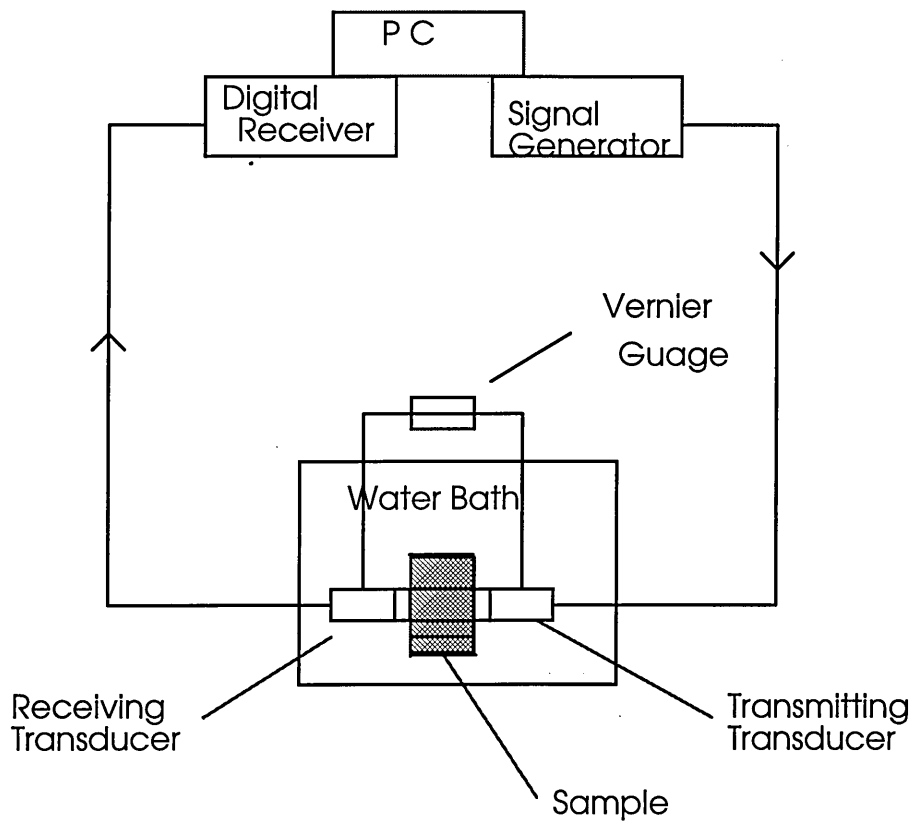
*Figure 4-1: Schematic Diagram of CUBA*

As discussed in Chapter 3, ultrasound may be used to characterise the physical properties of a material such as cancellous bone. The two characterisation parameters are velocity and Broadband Ultrasound Attenuation(reduction in ultrasound signal amplitude -dB/MHz). The next section discusses how they are measured using the CUBA system.

## 4.3.1 Ultrasonic Velocity

Ultrasonic Velocity (V) can be defined as

$$V = \frac{\text{Measured Sample Thickness}}{\text{Measured Transit time}}.$$

If the thickness of the sample and the transit time for the ultrasonic pulse through it are measured the ultrasound velocity can thus be calculated. The CUBA system collects data in the time domain thus allowing for the transit time to be measured. During

operation, the initial screen displays a transmission ultrasonic pulse. The amplitude and time sensitivity are controlled via the keyboard. The transit time is obtained through a digital timebase expansion method controlled manually by the operator but the clinical version of the CUBA has been updated to do it automatically. Also the clinical version has the facility to measure the overlying soft tissue using ultrasonic pulse-echo technique [Langton et al., 1990b]. The 4096 collected data points are initially represented using only 256 horizontal screen pixels. By expanding a small region (window) of the screen, 256 data points may be displayed on the 256 pixels. Transit time is measured from the begining of the first window (trigger pulse) to the arrival of the transmitted ultrasonic pulse. The precision of velocity measurement is typically 0.2% (based on 4 cm bone sample at 2500 m s$^{-1}$ measured at 5 $\mu$s per division), since the resolution of time measurement is 1% of time base sensitivity and the resolution of transducer separation is 0.01 mm.

## 4.3.2 Broadband Ultrasonic Attenuation (BUA)

To determine BUA, the frequency amplitude spectrum for a selected portion of the received time domain signal was calculated using a Fast Fourier Transform(FFT) algorithm. The frequency amplitude spectrum of the signal through a reference material, (chosen to be degassed water without the specimen ) was first recorded and stored as the reference trace. The reference trace is usually recorded at transducer separation of 90 mm. The frequency spectrum of the signal after passing through the specimen was subtracted from that of the reference to yield directly the attenuation as a function of frequency (Figure 4.2). This subtraction method corrects for the frequency dependence of the transducer efficiency and beam profile for a particular pair of ultrasound transducers [Langton et al., 1984]
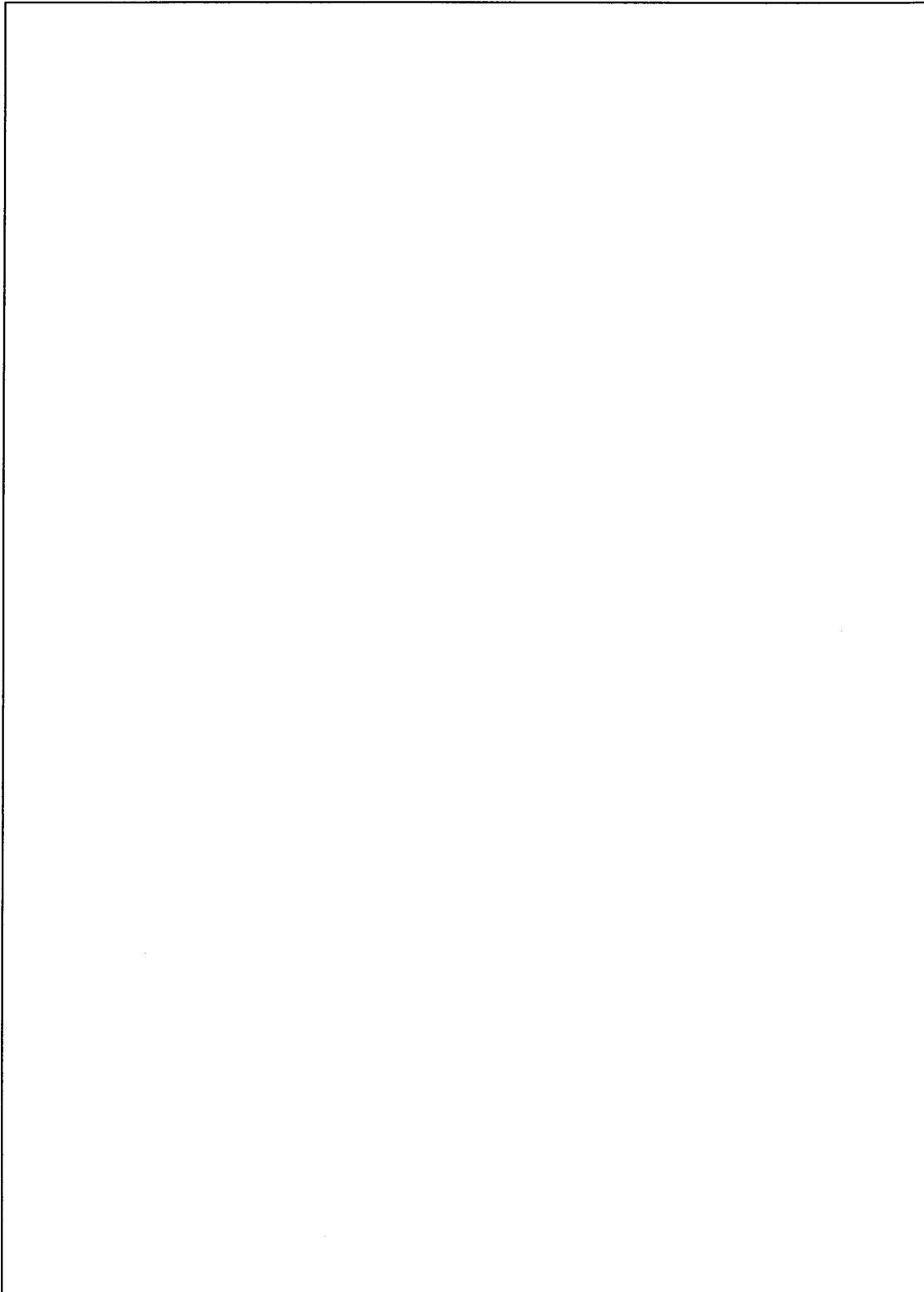
*Figure 4-2:* Description of BUA(a) The amplitude spectra for a sample and reference are compared. (b) Typical attenuation trace. (c) Regression analysis is performed over a selected frequency range

There is a linear relationship between attenuation and frequency for cancellous bone between 0.2 MHz and 0.6 MHz [Langton et al., 1984] (Figure 4.4b). Therefore, a linear regression was fitted for the plot of attenuation against frequency between 0.2 MHz and 0.6 MHz and the slope computed, to give BUA index of units dB MHz$^{-1}$ (Figure 4.2c). The BUA is nomalised for the fact that the reference trace and sample trace are collected at different transducer separations denoted nBUA(dB MHz$^{-1}$). To obtain a true volumetric parameter, the nBUA is further divided by the specimen thickness to give nnBUA(dB MHz$^{-1}$cm$^{-1}$). All these calculations have been incorporated in the CUBA software. The software also stores both the time domain (received signal) and frequency domain (amplitude spectrum) for the test sample on disc thus enabling additional data analysis if required.

## 4.3.3 Evaluation of CUBA

The evaluation of clinical equipment involves investigating its reproducibility (precision), accuracy, sensitivity and specificity.

**Reproducibility** is the ability of a technique to produce identical result for the same sample on separate occasions, and is often referred to as the precision. The numerical representation of reproducibility can be made in several ways. If many samples are measured twice, the mean difference between the pairs of readings can be used. Equally, the standard deviation from this mean (sd), or the standard error of measurement (SE$_m$), may be quoted. This is given by

$$SE_m = Z(\frac{sd}{\sqrt{n}}) \qquad (4.1)$$

where n is the number of observations in the sample, and Z is the value from the standard normal distribution corresponding to K percent confidence. The confidence levels most commonly used in practice are 95%, 99% and 90%. If the confidence level is not specified 95% is used with z value of 1.96 [Bowman and Robinson, 1990]. This often produces the largest error, so very often the coefficient of variation (CV) defined as a percentage of the mean reading is used.

It is generally accepted medically that precision (reproducibility) in a research environment is better than that of the daily hospital situation [Cummings and Black, 1986]. However, measurements to check things such as the long term drift of equipment are often taken using ideal phantoms. This is one of the reasons for a bone phantom which will be treated in the next chapter. Reproducibility tests for the present work were carried out using low density polyethylene. This is one of the reference materials that was used to validate the CUBA system [Langton et al., 1990b].

**Accuracy** is the term given to the ability of a technique to measure a known quantity correctly, but can also be used to describe the correlation of one measuring system with an independent measurement. The other parameters for the evaluation of a system are sensitivity and specificity of the technique. For a clinical system this covers the ability of a technique to diagnose a problem correctly or not (**Sensitivity** = abnormals detected/total abnormals, **Specificity** = normals detected/ total normal). These last two parameters are of vital importance in the hospital environment but are not relevant to the present studies, so will not be considered further .

### 4.3.3.1 Short Term Reproducibility

Three 90 mm (A, B, C) long and 50 mm diameter polyethylene blocks were used at the beginning to investigate both the short term and long term reproducibility. Six successive independent measurements were recorded for each of the three blocks. The results are given in Tables 4.1 and 4.2. BUA has a CV range of 1.75% - 3.5% with a mean value of 2.75%. The implication of this is that a less than 2.75 % change in BUA can no be attributed to change in the measured parameter. Positioning could not have been a source of error in the precision measurement for these blocks. This is because at the macroscopic level they are homogeneous and the diameter were 140% larger than the transducer's diameter. The probable source of error could have been phase cancellation artefacts[Personnal communication-C Langton]. Velocity has a better precision (0.6%) than BUA, this could be attributed to the ability to measure the transit time accurately.

*Table 4.1:* BUA Short Term Reproducibility

| Measurement | BUA | | | |
|---|---|---|---|---|
| No | Block A | Block B | Block C | ALL |
| 1 | 36.45 | 36.75 | 38.23 | |
| 2 | 37.62 | 39.28 | 39.98 | |
| 3 | 36.25 | 38.70 | 38.31 | |
| 4 | 38.33 | 38.28 | 39.78 | |
| 5 | 40.16 | 38.94 | 38.79 | |
| 6 | 38.50 | 38.80 | 38.66 | |
| Mean | 37.89 | 38.46 | 38.96 | 38.35 |
| Stdev | 1.33 | 0.82 | 0.68 | 1.055 |
| CV(%) | 3.5 | 2.13 | 1.75 | 2.75 |

*Table 4.2:* Short Term Reproducibility of Velocity

| Measurement | Velocity | | | |
|---|---|---|---|---|
| No | Block A | Block B | Block C | ALL |
| 1 | 2083 | 2049 | 2046 | |
| 2 | 2073 | 2049 | 2047 | |
| 3 | 2074 | 2050 | 2052 | |
| 4 | 2043 | 2050 | 2043 | |
| 5 | 2041 | 2051 | 2040 | |
| 6 | 2074 | 2053 | 2044 | |
| Mean | 2065 | 2050 | 2045 | 2053 |
| Stdev | 16.4 | 1.37 | 3.73 | 12.72 |
| CV(%) | 0.8 | 0.07 | 0.18 | 0.62 |

### 4.3.3.2 Long Term Reproducibility

The same blocks as in short term reproducibility were measured over a period of one month and the results are given in Table 4.3 and 4.4

*Table 4.3: Long Term Reproducibility of BUA*

| Days | BUA | | | CV(%) | | | All |
|---|---|---|---|---|---|---|---|
| | Block A | Block B | Block C | Block A | Block B | Block C | |
| 1 | 37.89 | 38.44 | 38.96 | 3.50 | 2.13 | 1.75 | |
| 2 | 41.05 | 38.58 | 39.97 | 3.1 | 5.13 | 0.85 | |
| 5 | 40.21 | 39.32 | 40.02 | 2.07 | 1.74 | ·1.7 | |
| 10 | 37.71 | 36.5 | 37.42 | 1.09 | 2.93 | 1.84 | |
| 17 | 37.6 | 37.52 | 38.23 | 1.86 | 1.25 | 1.12 | |
| 20 | 37.18 | 36.14 | 36.79 | 2.7 | 3.24 | 3.7 | |
| 25 | 37.88 | 37.27 | 38.1 | 4.44 | 2.57 | 2.32 | |
| Mean | 38.50 | 37.68 | 38.50 | 2.68 | 2.71 | 1.90 | 38.23 |
| Stdev | 1.38 | 1.071 | 1.13 | 1.04 | 1.17 | 0.86 | 1.26 |
| CV | 3.58 | 2.84 | 2.94 | 38.7 | 43 | 45 | 3.31 |

*Table 4.4: Long Term Reproducibility of Velocity*

| Days | Velocity $(m\ s^{-1})$ | | | CV(%) | | | All |
|---|---|---|---|---|---|---|---|
| | Block A | Block B | Block C | Block A | Block B | Block C | |
| 1 | 2065 | 2050 | 2045 | 0.75 | 0.07 | 0.18 | |
| 2 | 2057 | 2045 | 2048 | 0.5 | 0.38 | 0.19 | |
| 5 | 2093 | 2084 | 2079 | ·0.37 | 0.31 | 0.21 | |
| 10 | 2054 | 2048 | 2038 | 0.21 | 0.21 | 0.001 | |
| 17 | 2079 | 2076 | 2074 | 0.21 | 0.01 | 0.16 | |
| 20 | 2096· | 2091 | 2079 | 0.17 | 0.18 | 0.45 | |
| 25 | 2079 | 2090 | 2090· | 0.34 | 0.23 | 0.23 | |
| Mean | 2075 | 2069 | 2065 | 0.36 | 0.20 | 0.20 | 2070 |
| Stdev | 15.41 | 19.19 | 18.96 | 0.19 | 0.12 | 0.12 | 18.39 |
| CV | 0.74 | 0.93 | 0.92 | 52 | 59.9 | 60 | 0.89 |

The blocks correlated well with each other. For example a regression analysis between block B and C gave an R-squared value of 95% with a coefficient of 0.978 (p= 0.00) and a non significant intercept (p =0.846). There was no significant drift in the long term mean values for both BUA and velocity. The short term mean BUA was 38.35 ±2.75% while the long term mean BUA was 38.23±3.31. There was a non significant daily fluctuation in the mean values measured. The cause of such fluctuation could arise from the water trace being recorded under different conditions or variation in room temperature. So, the non-significant variation could be attributed to the measuring conditions rather than the equipment.

# 4.4 Permeability Measurement

Permeability is an expression relating to the flow rate of a fluid through a porous material, the hydraulic pressure which causes the flow, the material thickness and the cross-sectional area. This relationship is known as the Darcy's Law (section 2.4).

## 4.4.1 Apparatus

There are many ways of measuring the permeability of media. Depending on the method the variables to be measured are volume of discharge, and time at constant pressure head or velocity and time at falling pressure head. For this experiment the falling pressure head was used. The schematic representation of the set-up is shown in Figures 4.3, 4.4. The two metre transparent perspex tube provides the pressure head. The lower end is attached to the specimen holder. The pipe was of internal diameter of 34 mm. It was graduated from 2m to 0m at 0.2 m intervals
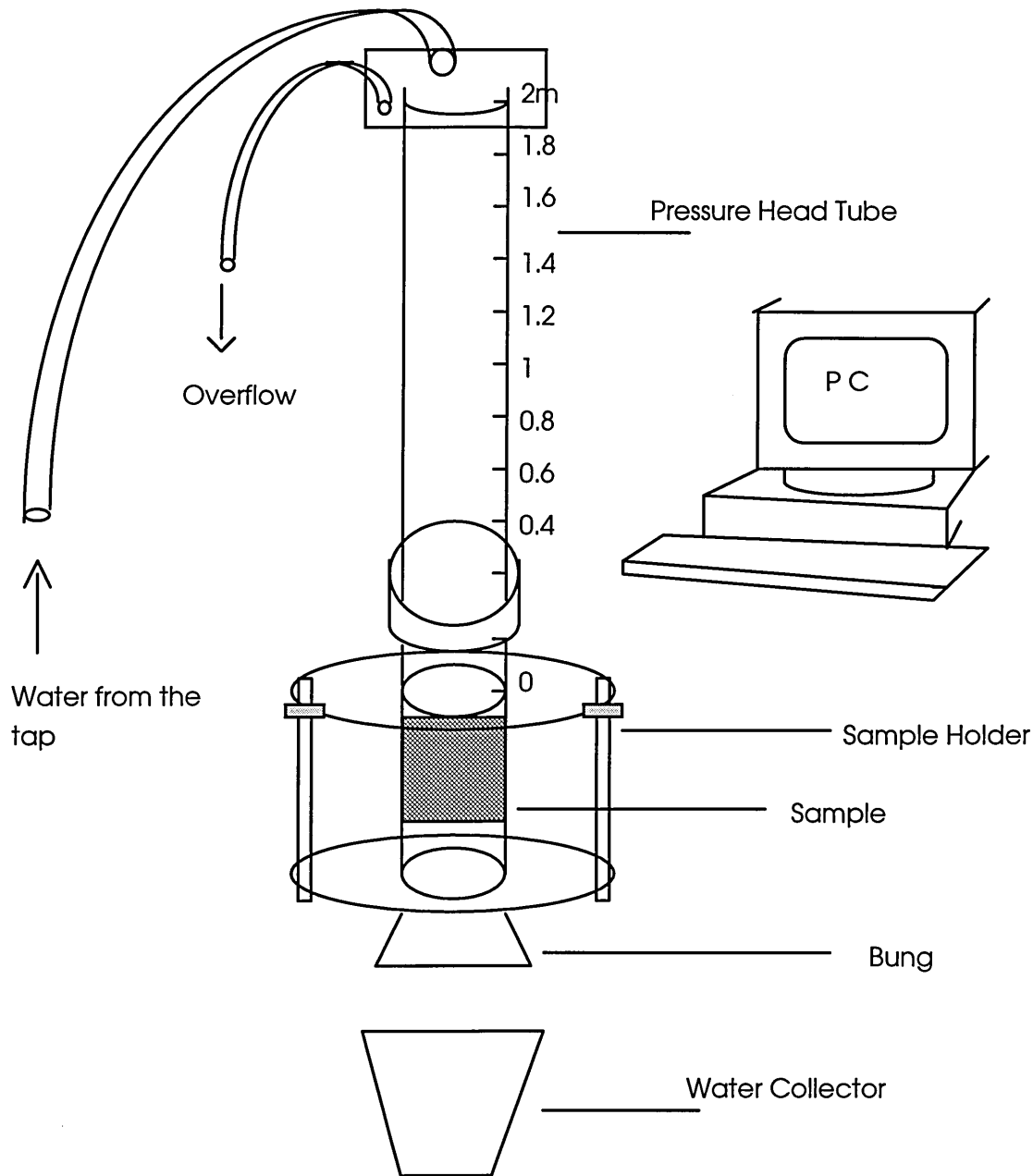
*Figure 4-3: Schematic Representation of Permeability Measurement*

The specimen holder consists of 51 mm long cylindrical perspex casing of 34 mm inside diameter. The perspex casing is held between two brass plates, the top brass plate has an inner threaded surface which is used to screw it onto the long perspex tube. Two securing nuts fasten the plastic casing onto the brass casing . Two O-rings are fitted at the top and at the bottom of the specimen to keep the specimen in position as well as acting as a sealant in preventing the water from flowing through the sides rather than through the specimen. The O-rings had an outside diameter of 41.5 mm and inside diameter of 34 mm.

For cubic specimens, a cylindrical perspex casing to fit into the original perspex casing with an internal cubic dimension was made. The cubes were made to fit well with no leakage by winding PTFE tape around them. For cylindrical specimens of diameter less than 34 mm, an adaptable casing was made. Water flow was prevented until the start of the experiment by applying a stopper bung at the bottom of the specimen holder. A computer program was used to carry out the measurements and calculate the permeability values.
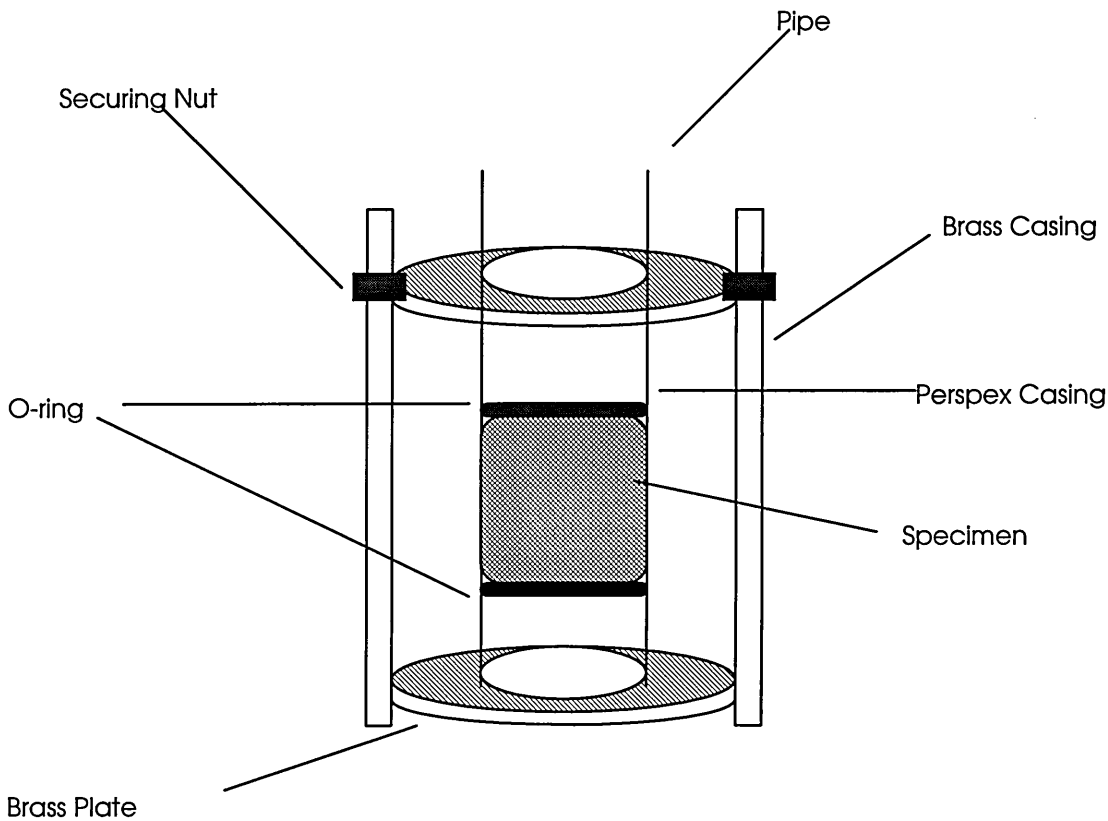


*Figure 4-4: Specimen Holder*

## 4.4.2 Method and Procedure

If the liquid level changes from height $H_0$ to $H_1$ in time $t_{01}$ then from Equation 2.13, the flow velocity may be written as

$$v = \frac{\kappa A \, \rho g \Delta H}{\eta d \, A_p} \qquad (4.2).$$

On the other hand , at a specific height H, then Equation 4.2 becomes

$$\frac{dH}{dt} = \frac{\kappa A \rho g H}{\eta d \, A_p} \tag{4.3}$$

$$\Rightarrow \quad \int_{H_0}^{H_1} \frac{dH}{H} = \frac{\kappa A \rho g}{\eta d \, A_p} \int_{t_0}^{t_1} dt \tag{4.4}$$

giving

$$ln(H_1/H_0) = \frac{\kappa \, A \rho \, g \, t_{01}}{\eta \, d A_p} \tag{4.5}$$

where $v$ is velocity (m s$^{-1}$) of fluid flow, $\eta$ is the viscosity (kg m$^{-1}$s$^{-1}$) of the fluid, A is the area (m$^2$) of the specimen , $\rho$ is the density (kg m$^{-3}$) of the fluid , $A_p$ (m$^2$) is the area of the pipe and $\kappa$ is the permeability with units m$^2$. In petroleum engineering, permeability is expressed in Darcy (10$^{-8}$ cm$^2$).

A two metre column of water was used to produce the initial hydraulic pressure through the specimen. The system was checked for leaks and when the water level in the pipe was static the bung was removed to initiate the flow and begin the measurements. The time $T_{01}$ to drop through each graduation was recorded by the operator pressing the space bar of the computer, the time calculated from the internal clock.

The permeability coefficients ($\kappa$) could be calculated using either Equation 4.2 (method 1) or 4.5 (method 2).

**Method 1:** The variables are velocity and height. The level velocity changes from zero at maximum height to a maximum at zero height. There are various ways by which this velocity could be measured including:

a.  Measuring instantaneous velocity at various points and taking an appropriate weighted mean.

b.  Measuring the velocity at a point 3/4 of the way from the pipe centre to the wall, since it is well known that in a fully developed profile the velocity at that point is approximately equal to the mean velocity.

c. Measuring the time for the meniscus to travel a specific distance from a known pressure height.

The third method was used with 0.2 m being the specific distance. Equation 4.2 implies that a linear plot of velocity versus height could be obtained provided all the other parameters remain constant. A linear regression was fitted for the plot of velocity versus height and the slope computed. The permeability coefficient was extracted from this gradient.

**Method 2:** This method uses Equation 4.5 and by-passes the necessity of calculating the velocity. The time taken for the meniscus to fall from 2 m ( zero time) to the defined graduations was recorded. A linear regression was fitted to the plot of time versus natural log of height, and the gradient computed. The permeability coefficient could be calculated from this gradient.

## 4.4.3 Validation of the Technique

Sintered high density polyethylene (HDPE) gaseous filters were chosen for the porous media in the validation study due to the availability of manufacturers permeability values (Accumatic Filtration Limited) listed in Table 4.5. It is noted that the highest mean pore size of 125 μm is below those found in cancellous bone.

*Table 4.5 : Properties of the Filters Used in Validation*

| Sample | Pore | size | distribution | Gas Permeability |
|---|---|---|---|---|
| or Grade | min. | mean | max. (μm) | $10^{-8} \, m^2$ |
| P 05 | 4 | 15 | 35 | 30 |
| P 10 | 7 | 30 | 75 | 40 |
| P 20 | 10 | 60 | 100 | 70 |
| P 30 | 15 | 75 | 175 | 70 |
| P 40 | 20 | 90 | 275 | 280 |
| P 50 | 30 | 125 | 350 | 440 |

Filters of 6 mm thickness and 35 mm diameter of each grade were used for this investigation. The following investigations were carried out :

♦ The permeability values were measured for one filter, then the number of filters ( thickness) was progressively increased to 5 filters (30 mm) of the same grade.

♦ One P50 filter was studied with the diameter being progressively decreased by 4 mm to investigate the effect of specimen dimension.

### *4.4.3.1 Results*

The results are given in Figure 4.5 and 4.6
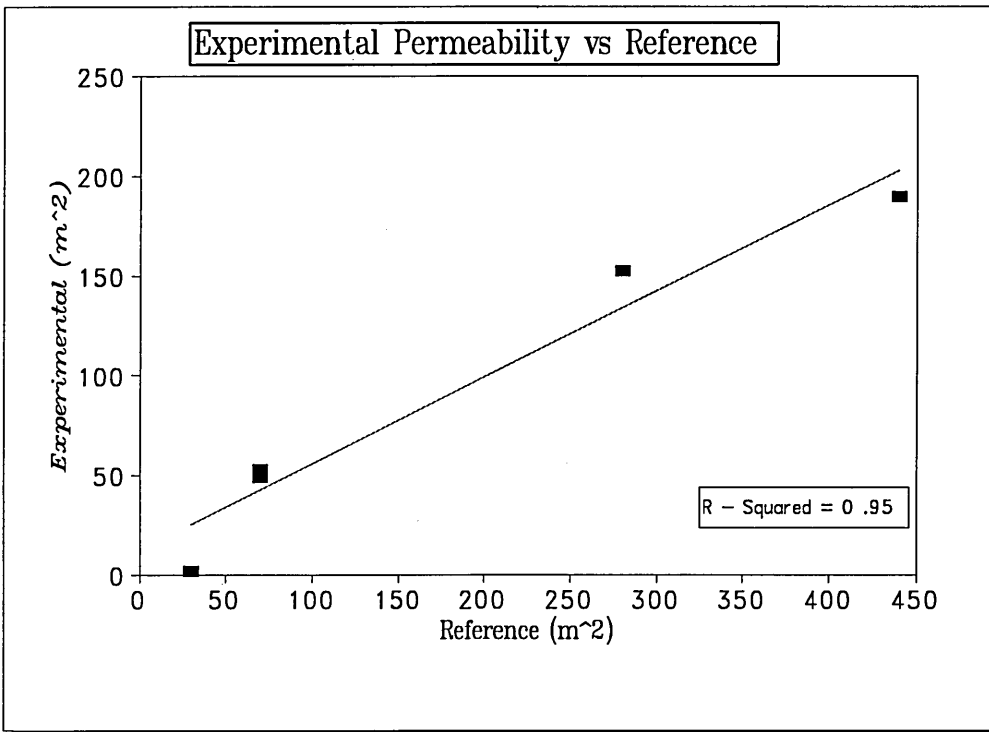


*Figure 4-5 : Comparison Between Experimental Permeability Values and References Values*

It can be seen from Figure 4.5 that the values correlate very well with an R-square value of 95%. The linear regression fit gives the x-coefficient of 0.433. This implies that the experimental values are approximately a factor of 0.5 less that the references values, due to the reference values quoted for gaseous permeability rather than liquid

permeability. The permeability results obtained using the two different methods as outlined in the preceding section were compared in Figure 4.6.
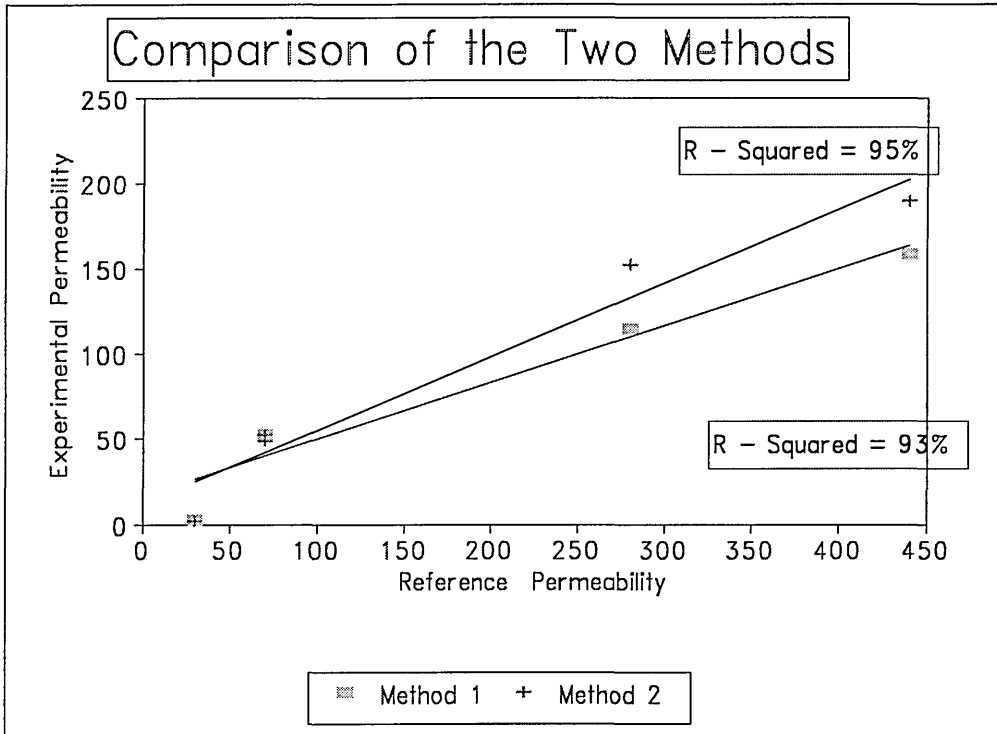


*Figure 4-6: Comparison of the Two Experimental Methods*

Method 2 has a higher R- squared value (95%) indicating a better accuracy. On the other hand the difference in R-squared values between the two methods is not statistically significant. Method 2 was found to have a short term reproducibility of 2-2.5% (cv) while method 1 was 7-8% (cv). The poor results of method 1 could have arisen from the method of velocity calculation. The change in velocity from the top of the pipe to the specimen is a continuous function and to calculate the discrete values requires a very sensitive device (which we did not have). Method 2 by-passes this problem by measuring the time. Further results of permeability in this report will refer to those obtained by method 2 except otherwise stated.

The effect of varying the specimen diameter is given in Figure 4.7.
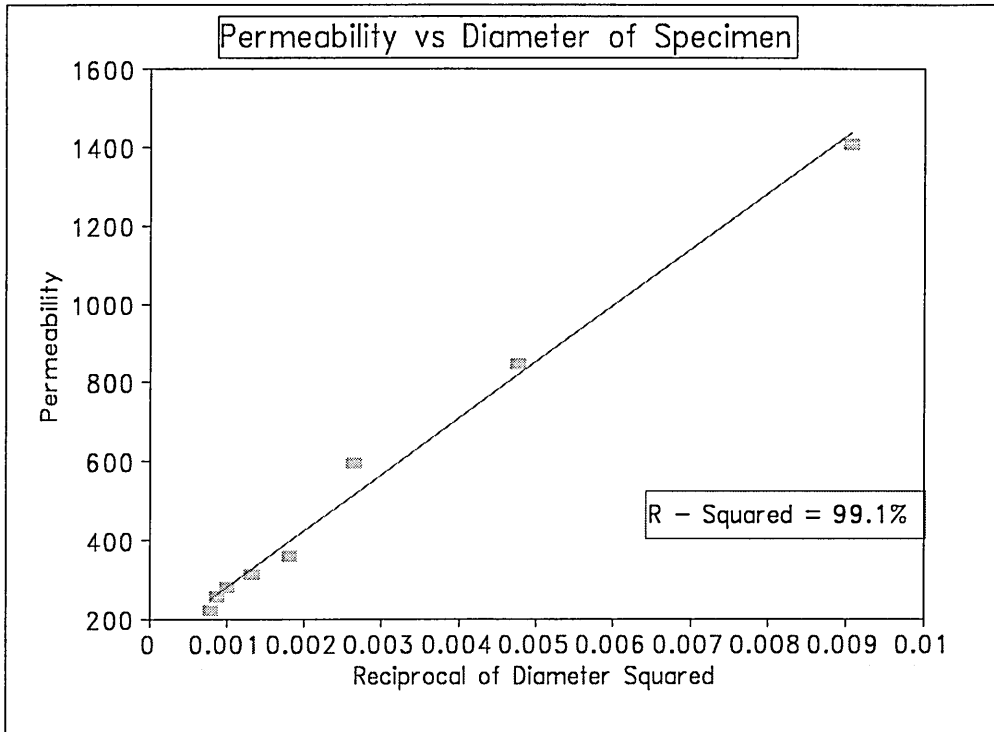
*Figure 4-7: Permeability versus the Reciprocal of Specimen Diameter Squared*

Figure 4.7 indicates that the areas A and $A_p$ in Equation 4.2-4.5 represent the area surface of the specimen and the area through which the fluid is collected respectively, which are equal.

## 4.5 Mechanical Properties

### 4.5.1 Apparatus

To obtain the mechanical properties ( Young's modulus and compressive strength) an 1122 Instron Universal Table Testing machine was used (See Figure 4.8), consisting basically of a cross head, loading column, water bath (to regulate the temperature), 3 kN loading cell and chart recorder. The loading column is fabricated from stainless steel with flat, smooth but unpolished end. The base of the water bath is a 5 mm thick stainless steel plate. The full scale load had a range of 100N to 5000N.

Cross Head

Loading Column

Water Bath

Load Cell

Chart
Recorder

Control
Panel

Specimen
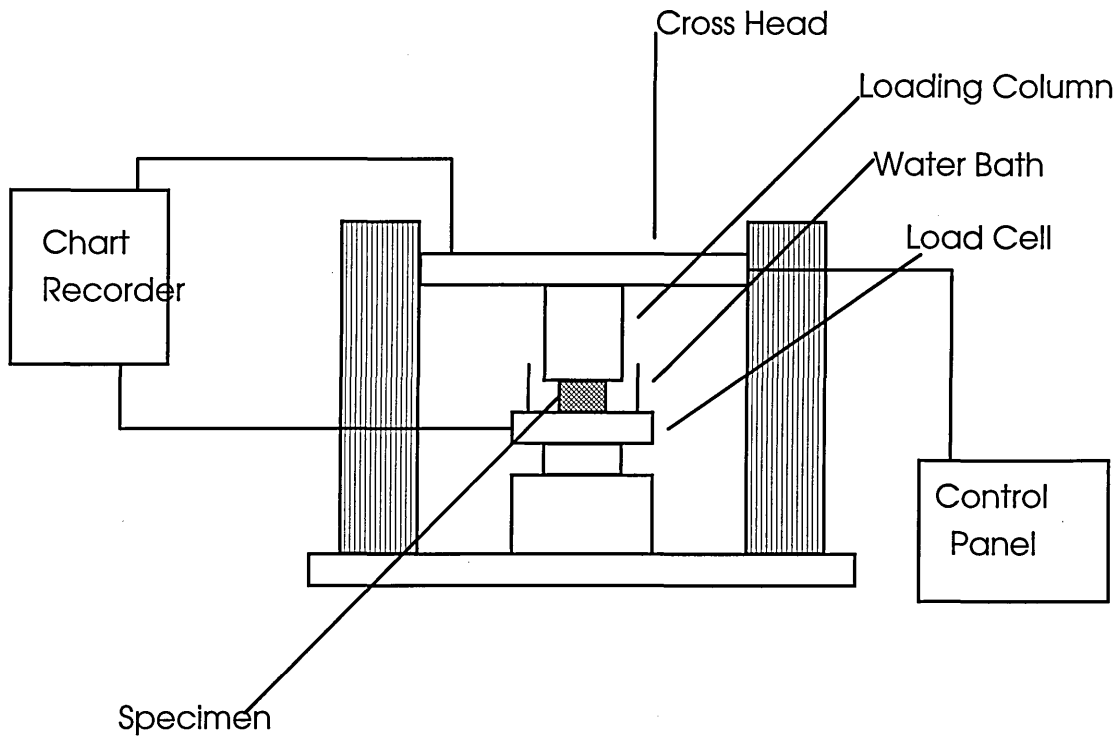
*Figure 4-8: Schematic Representation of the Instron Table Testing Machine*

## 4.5.2 Procedure

The measurements were carried out in compression. The cubes and cylinders of cancellous bone were compressed directly between the flat end of the loading column and the base of the water bath, which itself sat directly on a 5 kN load cell. Load and deformation were recorded on the machine's pen recorder, at a cross head speed of 1 mm minute$^{-1}$ and chart speed of 500 mm minute$^{-1}$. This gave a magnification of 500 and strain rate of 0.0017 s$^{-1}$.

The maximum load to which the bone is loaded is important. For example if too low a load is used the load-deformation trace would not reach the linear portion. On the other hand if too high a load is used, the trace begin to bend over, that is the onset of yielding. If that happens, it introduces an error in the measured values of Young's modulus in other directions for cubic specimens. This is because of the onset of irreversible micro damage. Very different maximum loads were found appropriate for different specimens, mainly according to their apparent density. To minimise the possibility of loading the specimen into its yield region, ( since the elasticity was being

measured in the 3 orthogonal direction for the cubic specimens), the compression load was gradually increased over several cycles until the load deformation curve was linear. Due to the viscoelastic nature of cancellous bone, this repetition was carried with the minimum time possible.

After measuring in the 3 directions for cubic specimen , one direction (proximal - distal ) was compressed into its plastic region, in order to record the ultimate strength. Ultimate strength is the maximum load sustainable by the sample, was defined as the point where a deflection was not observed with increased in load (Figure 4.9).
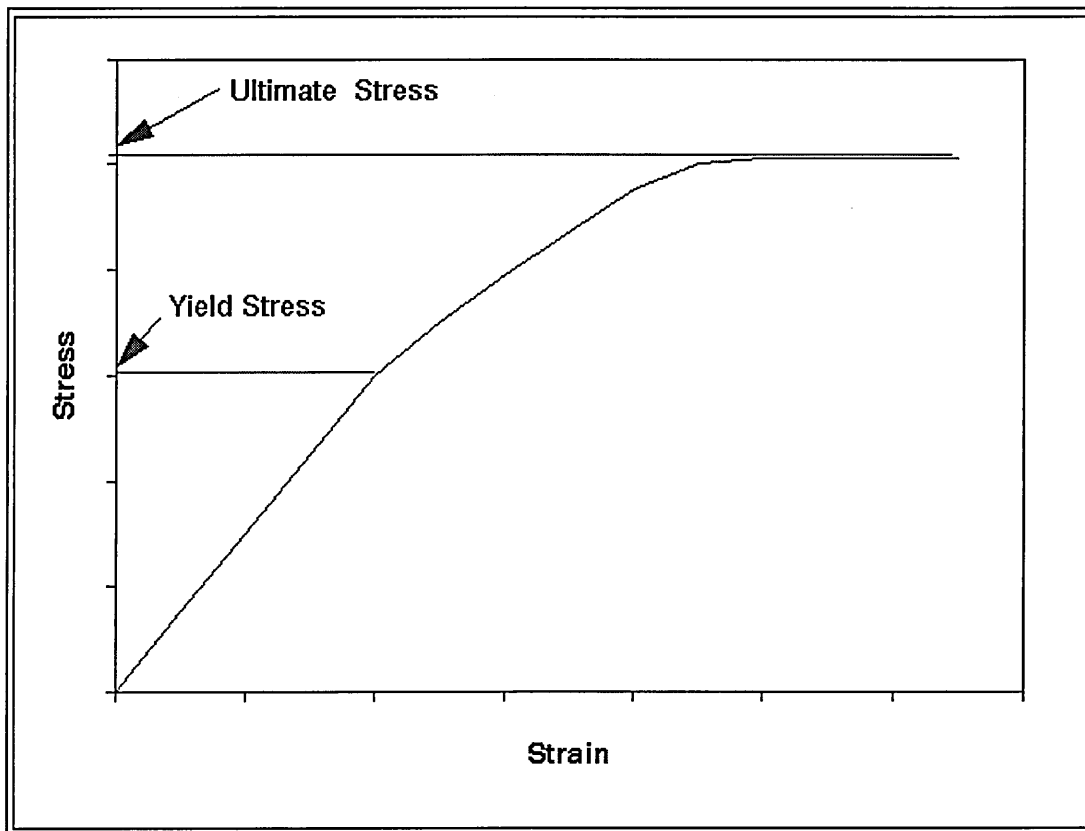


*Figure 4-9: A Typical Stress - Strain Used to Define Ultimate Stress*

The compliance of the loading system was determined at appropriate loads, by loading it against itself (that is no specimen present). The full scale load was increased from 100N to 5000N and the deflection measured. This loading system compliance was corrected for in subsequent elasticity calculations. Although temperature has a slight effect on the mechanical properties [Brear et al., 1988] and on the velocity [Evans and

Tavakoli, 1992] room temperature was used rather than physiological temperature to ease comparison with reported data.

The set up of the sample in measuring the mechanical properties introduces variation. This has been investigated by Linde and Hvid [1987] who demonstrated that different constraints on the loaded specimen, that is whether placed directly on wet platens, as here, or cemented to the platens, or constrained in a jacket, can produce differences in the strain at any particular load. This study was particularly constrained by the fact that loading was needed in three orthogonal directions, so cementing was not possible. This system was regarded as suitable for the purpose of this particular investigation, which was to demonstrate orientational dependence.

Mechanical measurements were done on defatted samples. This is because permeability measurements were required prior to compressing them. Fortunately the works of Pugh et al.[1973] and Carter and Hayes [1977] showed that the fluid in the inter-trabecular spaces has no effect on the mechanical behaviour of trabecular bone at the strain rate used in our investigation.

## 4.5.3 Calculations

Young's modulus was defined as the maximum slope of stress - strain curve in the most linear portion of the preyield region. With the modulus defined in this manner, the small initially non-linear behaviour due to surface irregularities of the specimen is disregarded.

$$\text{Young's modulus} = \frac{\text{Stress}}{\text{Strain}}$$

$$= (\text{Load/ cross-sectional area})/$$

$$(\text{deflection/height})$$

To correct for the instrument's compliance the real deflection is calculated by dividing deflection by the magnification factor and then subtracting the correction factor. The correction factor is calculated using the regression Equation obtained from the linear fit

of the load deflection graph of the instrument. A simple computer program was written by Dr. R. Hodgskinson to do the Young's modulus calculation in which the following inputs were required; height of the specimen(mm), cross-sectional area of the specimen(mm$^2$), deflection(mm), full scale load(N), and the magnification.

Ultimate strength was obtained by dividing the maximum load by the cross sectional area. For the cubic specimens this measurement could only be carried out in one of the orthogonal directions. This was chosen to be the proximal distal direction.

## *4.6 Apparent Density*

The apparent density is defined as the ratio of dehydrated tissue mass to total specimen volume. The density measurements were carried out after the mechanical and ultrasonic testing. To obtain the dehydrated tissue mass, the soft tissue and fat were removed from the specimen as described by Brear et al.[1988]. This involves subjecting the specimen to high speed jet of water, and then compressed air. This process is repeated until no fat is visible. The specimen is then tumbled overnight in excess of 2:1 chloroform-methanol mixture. The defatted cubes were then dried at 60 - 70 $^\circ$C to constant weight. The pre-testing specimen external dimension were measured using a micrometer and the volume calculated. The dried weight is divided by the volume to give the apparent density.

# Chapter

# 5. DEVELOPMENT OF BONE PHANTOMS

## 5.1 Introduction

This chapter demonstrates the attempt to develop a physical model for cancellous bone. The model will then be used to study the various parameters which affect the transmission of ultrasonic wave through a porous material. The structure of bone, especially cancellous, is both heterogeneous and anisotropic. This makes it difficult to model cancellous bone. Examining the structure of bone from the work of Whitehouse et al. [1971], Gibson [1985] proposed four structure for cancellous bone (see Chapter 1). The models are idealised ones, in real bones, a combinations of the models are observed and they are continuous, that is, one model fuses into another without a distinct separation. The following sections will describe an attempt to mimic various bone components.

### 5.1.1 Materials

There are many attributes required in a bone phantoms which is to be tested ultrasonically and these include the following :

♦ Physical (density) and acoustical (velocity and attenuation) parameters must approach those for bone (See Table 5.1).

♦ The elimination of air bubbles. This is because air bubbles are highly attenuating and thus their presence will falsify the results.

♦ It must also be variable, that is the physical and acoustical properties may be changed.

♦ It must be easily available and inexpensive.

♦ It must be manageable, that is it could easily be prepared under normal laboratory conditions.

♦ Durability and stability, this means the phantom could last for a long period of time without degradation.

In the search for bone phantom the following have been studied: Plaster of Paris, perspex, agar gel, lard, castor oil, aluminium mesh in agar gel and filters. The following sections will describe them in great detail.

*Table 5.1:* *Velocities and Attenuation of Common Medical and Industrial Materials, Wells, 1977*

| Material | Velocity $m \, s^{-1}$ | Attenuation $dB \, MHz^{-1} cm^{-1}$ | Density $kgm^{-3}$ |
|---|---|---|---|
| Subcutaneous Fat | 1450 | 0.5 | 952 |
| Muscle | 1580 | 1.5 | 1075 |
| Water | 1480 | - | 1000 |
| Cortical Bone | 3000-4000 | 3.5 | 1800-2000 |
| Cancellous Bone | 1600-2500 | 5- 20 | 100-1000 |
| Perspex | 2680 | 2 | 1180 |
| Aluminium | 6400 | 0.02 | 2700 |

## 5.2 Cortical Bone Phantom

- Plaster of Paris (POP)

- PMMA (Perspex)

### 5.2.1 Plaster of Paris (POP)

Laboratory grade Plaster of Paris (calcium sulphate, BDH production no 27622) was studied. Specimens were prepared by mixing water with powder POP. The mixture was then left to set in an open ended cube whose internal dimensions were approximately 40 mm cubed. The cube so produced was then soaked in water for a number of days. This was necessary so as to eliminate the air pockets formed in the specimen during preparation. The optimum soaking time was not determined.

*5.2.1.1 Results*

The weight ratio, 3:2 of POP to water yielded density and velocity values close to those of cortical bone (see Table 5.2) The exact value of density and velocity depended on the length of soaking. This was a critical drawback of the specimens, because virtually none of the specimens had identical values (see Table 5.2). From the results given in Tables 5.2, 5.3 and 5.4, POP was considered not to be practical as a cortical bone phantom:

♦ It was rather difficult to manufacture two specimens of identical BUA.

♦ The velocities came short of those quoted for cortical bone and nnBUA was more than two order of magnitude greater.

♦ It is impracticable as a phantom to study the effect of variation in structure.

The possible good feature of POP was the ability to vary the nnBUA by the introduction of holes into the block (see Table 5.3,5.4). The wide variation in nnBUA ($6.47$ - $20.97$ dB MHz$^{-1}$cm$^{-1}$ ) makes POP a good candidate for inter-equipment comparison.

*Table 5.2: The Attenuation and Velocity in POP Specimens (numbers in bracket are CV)*

| Specimen | nBUA dB MHz$^{-1}$ | nnBUA dB MHz$^{-1}$cm$^{-1}$ | Velocity m s$^{-1}$ | Density Kg m$^{-3}$ |
|---|---|---|---|---|
| 1 | 58.91(6) | 12.56(10) | 1750(0.4) | 1654 |
| 2 | 64.53(2) | 13.59(2) | 2057(0.5) | - |
| 3 | 83.97(3) | 18.34(3) | 1877(1) | - |
| 4 | 26.59(10) | 6.47(10) | 2240(0.5) | 1722 |
| 5 | 28.88(8) | 7.04(8) | 2227(0.7) | 1784 |
| 6 | 27.27(3) | 6.65(3) | 2194(0.5) | 1784 |
| Mean | 48.36 | 10.78 | 2056 | 1736 |
| Stdev | 22.13 | 4.43 | 186 | 53.7 |
| CV | 45.8% | 41.1% | 9% | 3.1% |

Table 5.2 illustrates that there is a 46% variation in nBUA with a 3.1% change in density. The coefficient of variation in velocity is much lower than that for nBUA, probably because velocity is less sensitive to gas pockets in the sample. It can be noted that the last three specimens with higher density have a lower nBUA but higher velocities. This is an indication that these two ultrasonic quantities have different behaviour with changing physical parameters.

***Table 5.3:*** *The BUA and Velocity Values in a POP Specimen with 9, 3 mm Diameter Holes Measured over Period of Time and Density 1631 Kg $m^{-3}$.*

| Days | nBUA | nnBUA | Velocity |
|---|---|---|---|
| 0 | 83.43(4.1) | 20.35(4.1) | 1997 |
| 2 | 68.1(2) | 16.61(2) | 1997 |
| 4 | 85.98(2) | 20.97(2) | 1974 |
| 180 | 47.05(7) | 11.4(7) | 2188 |

***Table 5.4:*** *The BUA and Velocity values in a POP Specimen with 16, 4.1 mm diameter holes measured over period of time and density 1325 Kg $m^{-3}$*

| Days | nBUA | nnBUA | Velocity |
|---|---|---|---|
| 0 | 90.86(10) | 22.61(10) | 1952 |
| 10 | 80.94(4) | 19.74(4) | 1943 |
| 180 | 106.22(2.3) | 25.98(2.3) | 1966 |

It can be noted in Tables 5.3 and 5.4 the effects of introducing holes in POP and also changes in attenuation with time. Velocity for the two cases studied above is invariant with number of holes nor with duration after manufacture.

## 5.2.2 Polymethylmethacrylate(PMMA) - Perspex Block

A brief description of polymers will be given so as to introduce the importance of some of the measurements made on polymers. High density polymers are long chain molecules with relative molecular masses from thousand to many millions. The polymer molecule may consist of a single chain-linear polymer, it may have secondary

chains branching from the main. A branched polymer or the polymer chain may be bonded together at various points by covalent bonds (cross-linked polymer).

Polymers, depending on the rate of cooling from liquid(molten) state, can give rise to an amorphous or crystalline structure. In the amorphous state the polymers are randomly oriented. In the crystalline state the polymers chains are aligned. Polymers are further classified as thermoplastics, elastomers and thermosetting depending on their response to load and temperature. The mechanical properties as well as ultrasonic characteristic will depend on the type of polymer. For detail mechanical properties the reader is referred to standard texts of polymers [Gibson and Ashby, 1984, Sprackling, 1985].

*Table 5.5: Examples of a Few Thermoplastic Polymers*

| Material | Condition at room temp. | Density $Kg\, m^{-3}$ | Velocity $m\, s^{-1}$ | E(GPa) |
|---|---|---|---|---|
| Polyethylene(LD) | P C | 910-940 | 1950 | 0.15-0.24 |
| Polyethylene(HD) | P C | 950-970 | 1950 | 0.55-1.0 |
| PMMA | Amorphous | 1180 | 2670 | 3.3 |
| Nylon | P C | 1150 | 2620 | 2-3.5 |
| (PVC) | Amorphous | 1400 | | 2.4-3 |

Where PVC is Polyvinyl chloride and P C represents partially crystalline polymers

It has been shown that polymers and fibre composite solid are example of materials with high attenuation coefficients[Hartmann and Jarzynski, 1972]. Although the densities and velocities of the polymers come short of those for cortical bone (See Tables 5.1, 5.5), the structure of these solids has been intensively studied and is considerably simpler than that of bone tissue [Hartmann and Jarzynski, 1972]. It was anticipated that an insight into the mechanism of ultrasound transmission through bone may be achieved by first studying these simple polymers.

### 5.2.2.1 Results

The velocity and BUA values of perspex, polyethylene, polystyrene, and nylon were measured and the results are presented in Table 5.6. As a cortical bone mimics, none of the polymers met all of the requirements of a good cortical bone phantom. For

example polyethylene has a very low density and the attenuation is quite high. Nylon on the other hand has too low an attenuation (52%) Perspex was the polymer with the closest properties to cortical bone.

♦      It has an nnBUA value of $3.97 \pm 7$ dB MHz$^{-1}$cm$^{-1}$ which is a few percentage above quoted values for cortical bone.

♦      The velocity and density (see Table 5.5, 5.6) were not significantly less than those of cortical bone.

♦      Perspex is a popular polymer with most of its physical and acoustical properties well defined.

*Table 5.6: BUA and Velocity Values of the Polymers*

| Material | Density Kgm$^{-3}$ | nBUA dB MHz$^{-1}$ | nnBUA dB MHz$^{-1}$cm$^{-1}$ | Velocity m s$^{-1}$ | Velocity* m s$^{-1}$ |
|---|---|---|---|---|---|
| Polyethylene | 940 | 26.37 | 4.19 ± 6% | 2052.80 | 1950 |
| Polystyrene | 1060 | 42.58 | 4.73 ±11% | 2078.81 | 2350 |
| Nylon | 1150 | 16.76 | 1.67 ±9% | 2222.23 | 2620 |
| PMMA | 1180 | 27.90 | 3.97 ±7% | 2624 | 2670 |

where velocity* is reference data velocity.
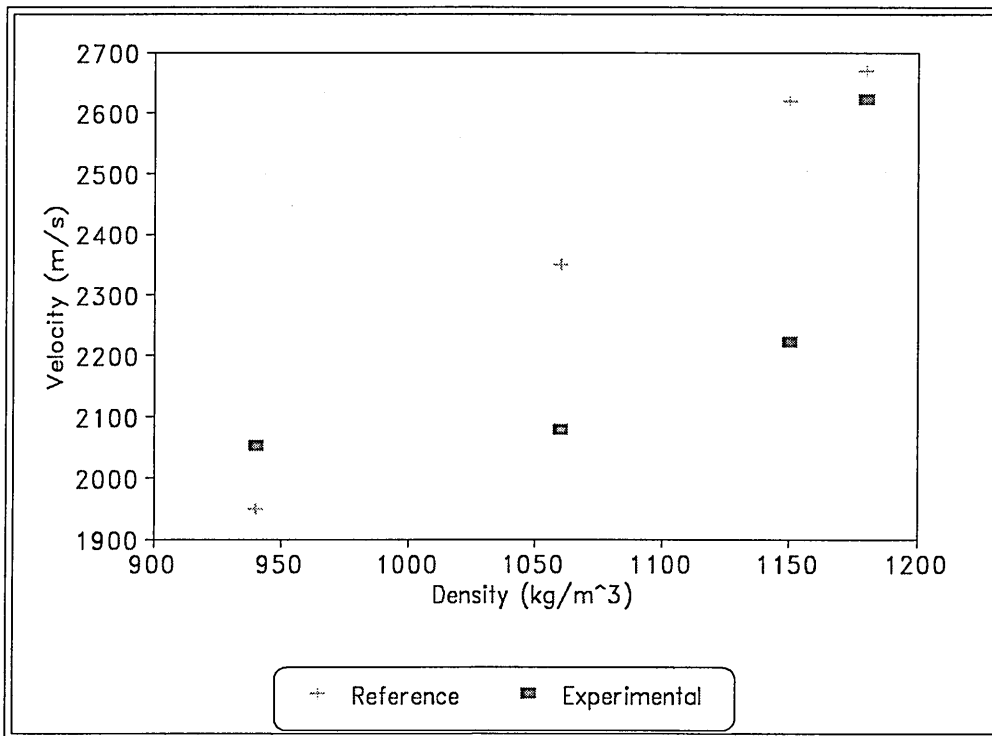


*Figure 5-1: Experimental and Reference Velocity of the Polymers versus Density*

From Table 5.6 no specific relationship seems to emerge. For example the BUA does not increase with density. But Garcia et al. [1978] suggested that there exists an inverse relationship between increased attenuation and increased density for polymers. A regression analysis gave an $R^2$ value of 60.83% for the graph of density versus velocity and an $R^2$ value 21.7% for the graph of density versus nnBUA. There are possible explanations to the absence of a relationship or poor correlation. The trivial one being the low number of data points. Other explanations may be the fact that

density is a scalar quantity while velocity and BUA are apparently vector quantities. So their values are dependent on the density and structural properties of the material in question.

As seen from Table 5.5, although the four materials are all polymers they have structural differences. Nylon and polyethylene are partially crystalline, while PMMA and polystyrene are amorphous. The mode of interactions of ultrasound waves with these two types of polymers are fundamentally different. These concept is in line with the hypothesis of Hartmann and Jarzynski [1972] that a hysteresis mechanism is operative in the low megahertz frequency range. According to this concept attenuation in polymers depends on the structural geometry of the constituent long chain polymer molecules, and their inter-association. Thus, a given degree of crystallinity determines a set of possible structural states, an associated set of critical activation energies. Hysteresis absorption is then related to these energies. These differences could also be observed from the frequency spectrum output. While crystalline materials show approximately uniform attenuation with frequency, amorphous exhibits ringing.

The velocity showed an increase with density. Fundamentally the ultrasound velocity is a function of density of the medium. The poor correlation of the velocity of polystyrene and nylon and with reference data velocity can be attributed to the specimen size. The blocks had the following length: polyethylene- 63 mm, polystyrene- 90 mm, nylon - 100 mm and perspex -70 mm. For long specimen the material attenuates most of the signal and thus increasing the error associated with transit time measurement. Finally, a more rigorous theoretical insight into the mechanism of ultrasound interaction will elucidate these results.

## 5.3 Fat Phantom

- Agar Gel
- Lard
- Castor Oil

The physical characteristic of fat which are of importance in ultrasonic interaction are density and viscosity. The viscosity of the fluid affects the level of viscous loss in ultrasonic interaction in composite porous materials. It has been shown [Evans, 1986]

that in a fluid of changing viscosity, the attenuation increases with viscosity. The state of the fat (that is solid or liquid) is also important in ultrasonic interaction. Bone marrow is solid at room temperature but liquid at body temperature. The liquid state and the temperature affect the ultrasonic velocity and attenuation (Figure 5.2 and 5.3). Many materials have been suggested to mimic bone marrow among which are agar gel, lard and castor oil.

## 5.3.1 Agar Gel

The sample consisted of a powdered graphite suspension (averaged particle diameter, 7 μm), in a solid matrix of agar, distilled water and n-propanol. The graphite powder concentration (99.5g/litre of material) determines the attenuation. The n-propanol concentration (8.6% in the matrix material) determines the speed of sound [Burlew et al., 1980]. The agar gel phantom had a velocity of 1472 m $s^{-1}$ and density of 1100 kg $m^{-3}$ which are quite comparable to real fat of 1450 m $s^{-1}$ and density 952 kg $m^{-3}$. The phantom has the advantage of very low air spaces inside and good coupling. The most likely problem is the semi-solid state of the phantom, because bone marrow is supposed to be viscous. The viscous state affects the ultrasonic measurements. Agar gel could be prescribed as a good soft tissue mimic than bone marrow mimic.

## 5.3.2 Lard

The velocity of the original household lard was measured to be 1574.5 m $s^{-1}$ and attenuation of -1.0 dB $MHz^{-1}cm^{-1}$. When the lard was melted and allowed to solidify into a 40 mm cube, the acoustic properties measured thereafter were different . This is indicative of the fact that ultrasound measurement are dependent on both structure and density. When the lard is melted some of the covalent bonds are broken and when allowed to solidify the conditions such as temperature affects the bonding. For example the values of velocity measured for lard which solidified under room temperature were different from those for lard which solidified at -20$^o$C.

On the other hand, lard was melted and the temperature raised to 70$^o$C and then allowed to cool, while BUA and velocity were measured. The results are presented in Figures 5.2 and 5.3 From this, it appears no trend exist between BUA and

temperature, but a line plot presented in Appendix E (E.1) reveals three phases. The first phase is the steady decrease in BUA with decrease in temperature up to 35 $^{\circ}$C, then there is a jump in BUA (phase II ) and a gradual increase in BUA with decrease in temperature up to 18$^{\circ}$C, where there a fall in BUA (Phase III) and then a gradual increase in BUA thereafter with decrease in temperature. These phases coincide approximately with the three state of lard: phase I - liquid, phase II- molten, and phase III - solid. This therefore supports the argument that BUA is dependent on the structure in addition to density.

There was a predictable trend between velocity and change in temperature with two different rate of change in velocity with temperature. From 70 $^{\circ}$C to 27$^{\circ}$C there is a 2.91 m s$^{-1}$ per $^{\circ}$C fall in temperature, from 27$^{\circ}$C to 0$^{\circ}$C there is a rapid fall in velocity at 9.29 m s$^{-1}$ per $^{\circ}$C. These are presented in Equations 5.1 -5.3 and Figure E.2.

[70 $^{\circ}$C - 27$^{\circ}$C]    $V = 1514 - 2.91*(Temp)$    $R^2 = 99\%$    (5.1)

[27$^{\circ}$C - 0$^{\circ}$C]    $V = 1704 - 9.29*(Temp)$    $R^2 = 90\%$    (5.2)

[70 $^{\circ}$C - 0$^{\circ}$C]    $V = 1642 - 5.61*(Temp)$    $R^2 = 89\%$    (5.3)

Ultrasonic wave propagation is supported by the elasticity of the media and therefore explains why there is a decrease in velocity with increase in temperature. The difference in Figure 5.2 and 5.3 points to the fact that BUA and velocity are determined by different parameters of the medium.

Lard will be a good marrow phantom if it is maintained in a liquid state.
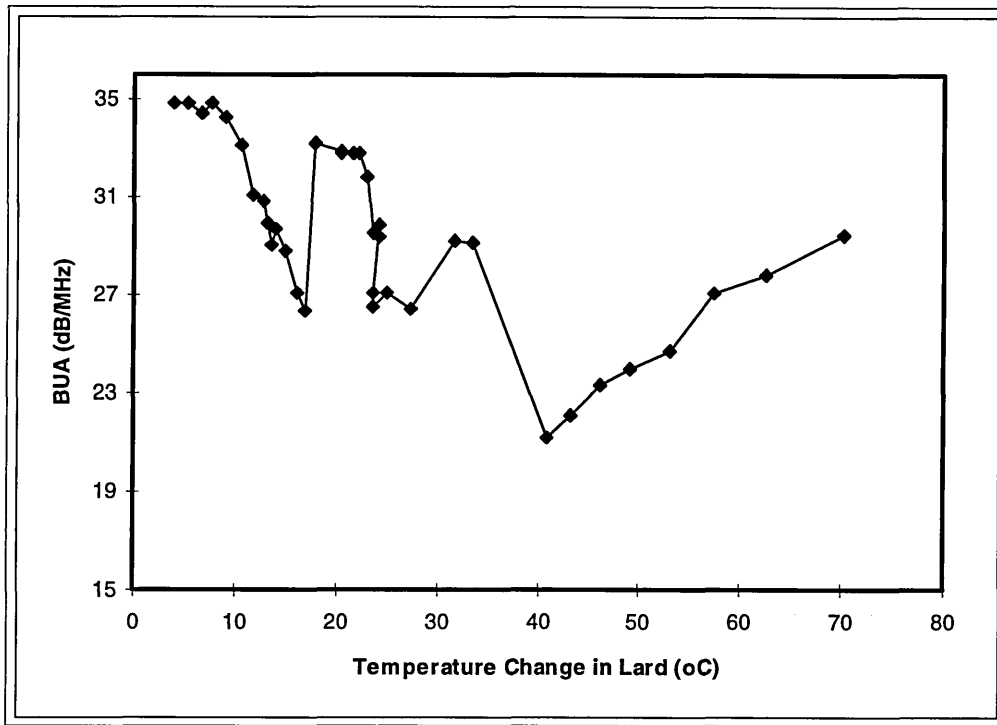
*Figure 5-2: The BUA in Lard with Changes in Temperature ($^{O}$C)*
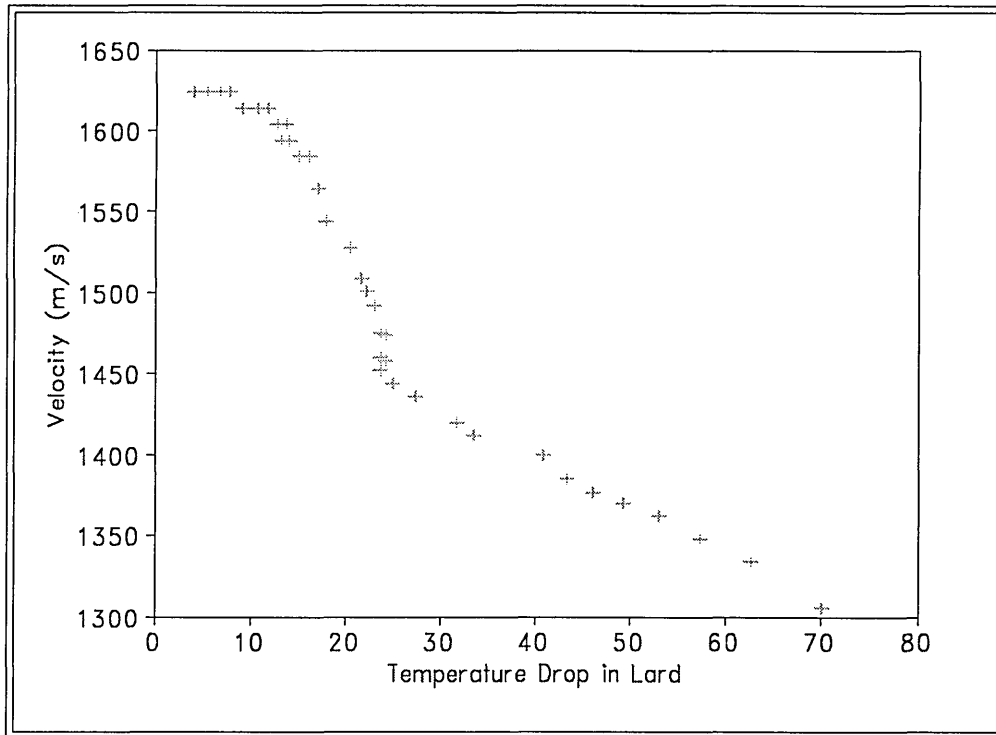


*Figure 5-3: The velocity of ultrasound in lard with fall in temperature*

101

### 5.3.3 Castor oil

It is a liquid at room temperature. This property makes it a very plausible mimic, although the viscosity may be different from that of bone marrow. Castor oil has a density of 969 kg m$^{-3}$ and velocity at room temperature of 1472 m s$^{-1}$.

## 5.4 Cancellous Bone Phantom

The following structure have been investigated as possible cancellous bone mimics:

- Aluminium mesh in agar gel,

- Filters,

- Porous perspex.

### 5.4.1 Aluminium Mesh in Agar Gel

The phantom was made up of aluminium mesh (supplied by David and Sons Ltd) placed in setting gel (agar). The mesh was approximately 1 mm in hole size. Aluminium has the following properties- Density 2700 kg m$^{-3}$, longitudinal velocity of 6420 m s$^{-1}$ and transverse velocity of 3040 m s$^{-1}$. Human trabeculae has the following properties: density 1820 kg m$^{-3}$, longitudinal velocity 3300 m s$^{-1}$, transverse velocity of 1800 m s$^{-1}$. Therefore the probable disadvantage of aluminium is its high density and velocity of transmission compared to trabeculae which may magnify the effect of reflection at interfaces.

In the investigation three samples were prepared with the following specifications

1. The holes of the mesh placed parallel to each other,

2. The mesh placed criss-crossed,

3. Parallel mesh allowed to float in setting gel.

The ultrasonic velocity and attenuation were measured using water as coupling medium. Measurements of the attenuation and velocity were obtained as follows

a) The direction of propagation was perpendicular to the plane of the mesh at 90 mm transducer separation,

b) The direction of propagation was parallel to the plane of the mesh at 90 mm separation,

c) The transducer were touching the sample (42 mm thick) and perpendicular to the plane of the mesh,

d) The transducer were in contact with the sample and parallel to mesh plane.

The results are presented in Table 5.7

*Table 5.7 : The Results of the Al Mesh in Agar Gel Phantom*

| Measurement Method | Specimen Specification | BUA dB MHz$^{-1}$ | nnBUA dBMHz$^{-1}$cm$^{-1}$ | Velocity m s$^{-1}$ |
|---|---|---|---|---|
| a | 1 | 20 (4) | 2.26 | 1529(0.3) |
| | 2 | 81(5) | 9 | 1517(0.2) |
| | 3 | 33(1) | 4 | 1525(0.2) |
| b | 1 | 67(3) | 7.41 | 1555(1.2) |
| | 2 | 58(4) | 6.44 | 1557(0.7) |
| | 3 | 72(1) | 8 | 1545(0.5) |
| c | 1 | 30.2(1) | 7.28 | 1534 (0.4) |
| | 2 | 48(6) | 14.71 | 1519 (0.5) |
| | 3 | 37(7) | 9 | 1514(0.4) |
| d | 1 | 72(2) | 13.37 | 1567(0.6) |
| | 2 | 57(10) | 10 | 1567(0.2) |
| | 3 | 73(1) | 13 | 1589(0.6) |

The following observations can be made from Table 5.7;

• The velocity recorded was on the lower band of cancellous bone velocity range. There is no significant change in velocity in the three different samples for the four measurement procedures. It could be noted that the velocity value is closer to soft tissue velocity than cancellous bone.

- The attenuation in the phantom was in the range quoted for cancellous bone but the variation was not significant between specimens. The criss-cross arrangement produced a higher nnBUA than the parallel arrangement in the perpendicular direction.

## 5.4.2 Filters

Sintered high density polyethylene (HDPE) filters manufactured by Accumatic Filtration Limited were also considered as possible cancellous bone phantom (see Section 4.5.3). These filters are produced from powdered polyethylene, with controlled particle size distribution. The result of the acoustic properties are given in Table 5.8.

*Table 5.8: Acoustic Properties of HDPE Filters*

| Grade | Mean Pore size ($\mu$m) | BUA dB MHz$^{-1}$ | nnBUA dB MHz$^{-1}$cm$^{-1}$ | Velocity m s$^{-1}$ | Density kgm$^{-3}$ |
|---|---|---|---|---|---|
| P05 | 15 | 10.1(4.5) | -0.23 | 1709 | 454.3 |
| P20 | 60 | 21.14(1.6) | 3.45 | 1732 | 500.7 |
| P30 | 75 | 33.18(0.27) | 7.46 | 1800 | 542.0 |
| P40 | 90 | 36.30(0.5) | 8.5 | 1776 | 553 |
| P50 | 125 | 102.5(1) | 30.43 | 1745 | 571.8 |
| Mean | 73 | 40.64 | 10.01 | 1752 | 524.36 |
| Stdev | 40.4 | 36.10 | 10.62 | 35.98 | 42.07 |
| CV | 55 | 88.83 | 100 | 2.1 | 8 |

The following observations can be made from Table 5.8;

* The density values for the filters fall within the range of cancellous bone densities (100 - 1000 kg m$^{-3}$) but the range of densities was small with a CV of only 8%.

* Velocity values are also within the range quoted for cancellous bone (1600 - 2500 m s$^{-1}$). It should be noted that although the densities were similar to those found in dense cancellous bone, the corresponding

velocities were lower than expected. There was no significant change in measured velocity across the different filters, with a CV of 2%.

* The nnBUA values are within the range quoted for cancellous bone (5-20 dB MHz$^{-1}$cm$^{-1}$) The variation from filter to filter was significant especially in grade P50 (1%).

* The mean pore size were lower than observed in both human calcaneus (471 - 1469 $\mu$m, Hans, 1993) and human vertebrae (670 - 1390 $\mu$m, Bergot et al., 1988).

The drawbacks of HDPE filters as a phantom for the study of ultrasound propagation are the limited range of the pore size and density. It could be concluded that the filters are good phantoms for calibration because of the 100% CV range.

## 5.4.3 Porous Perspex

Perspex has previously been shown to be a favourable cortical bone phantom. Based upon the argument that the trabeculae of cancellous bone are of similar mechanical and ultrasonic properties to cortical bone, perspex was used to develop a simulation of cancellous bone. The perspex was first made heterogeneous by introducing an array of holes to mimic the marrow pores drilled using a computerised system. The object of the experiment was to investigate how the number and distribution of holes affected the BUA and velocity. The experiment was implemented as below:

36 (6x6) symmetrical and vertical holes were drilled on a perspex cube of 41x41x41 mm dimension. The number of holes was kept constant but the hole diameter was increased from 1 mm to 5.5 mm in 0.5 mm step. One block was used continuously, that is, the hole size increase was done on the same specimen. The 36 holes covered an area of 34x34 mm$^2$ (Figure 5.4).
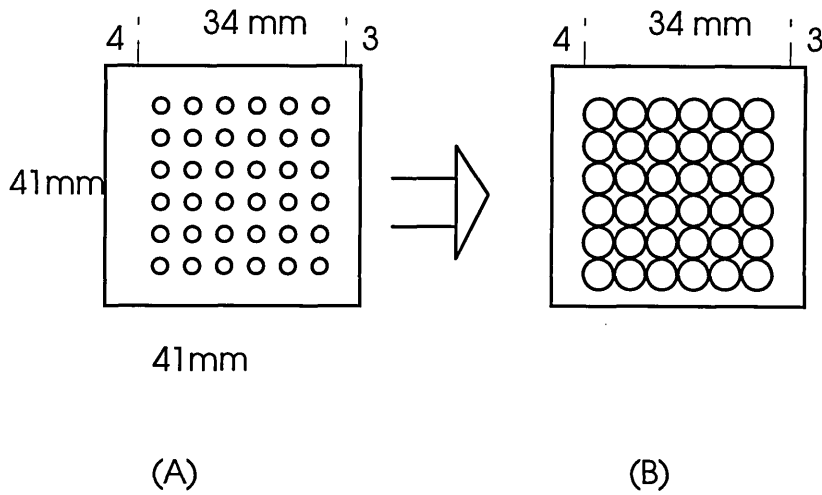
*Figure 5-4: Schematic Representation of Holes in Perspex Cube, (A) hole diameter of 2 mm, (B) maximum hole diameter 5.5 mm*

### 5.4.3.1 Results of Perspex Studies

Porosity is a characteristic of a porous medium and is defined here as the fraction of the holes to the total volume covered by the holes.

$$\text{Porosity} = (\text{Volume of Pore/Vol. of Solid}) \times 100. \tag{5.1}$$

$$\text{Porosity} = N\pi\phi^2/4A \ , \tag{5.2}$$

where N is the total number of holes, $\phi$ is the diameter of the holes and A is the area covered by the holes.

The results are given in Table 5.9, where d represents inter-hole spacing, $\phi$ hole diameter and the numbers in bracket are the coefficients of variation. Substituting the values (N = 36, A = 1156 and $\pi$) in Equation 5.2 gives $2.45\phi^2$. nnBUA was obtained by dividing nBUA with the specimen thickness.

*Table 5.9: The effect of increase in hole diameter on BUA and velocity for 36 holes on an area of 34x34 mm$^2$*

| $\phi$ (mm) | d (mm) | Porosity $(2.45\phi^2)$ | nBUA (dB MHz$^{-1}$) | nnBUA (dB MHz$^{-1}$cm$^{-1}$) | Velocity (m s$^{-1}$) |
|---|---|---|---|---|---|
| 0 | 5.7 | 0 | 21.9(7) | 5.34(7) | 2657 (0.5) |
| 1 | 4.7 | 2.5 | 23.06(9) | 5.63(9) | 2657 (0.5) |
| 1.5 | 4.2 | 5.5 | 31.83(4) | 7.62(4) | 2646 (0.6) |
| 2 | 3.7 | 9.8 | 39.70(1.4) | 9.68(1.4) | 2636 (0.6) |
| 2.5 | 3.2 | 15.3 | 46.88(2.2) | 11.44(2.2) | 2637 (0.7) |
| 3.0 | 2.7 | 22 | 54.60(5) | 13.32(5) | 2634 (0.6) |
| 3.5 | 2.2 | 30 | 56.02(2.3) | 13.61(2.3) | 2570 (0.8) |
| 4.0 | 1.7 | 39.1 | 43.11(3.5) | 10.51(3.5) | 2457 (0.6) |
| 4.5 | 1.2 | 49.5 | 27.94(6) | 6.81(6) | 2457 (0.6) |
| 5.0 | 0.7 | 61.1 | 15.98(10) | 3.90(10) | 1969 (0.5) |
| 5.5 | 0.2 | 74 | 8.68(12) | 2.12(12) | 1805 (0.4) |

* The values in bracket are the coefficient of variation for the measurement

The discussion of the mechanism of ultrasound attenuation in the porous perspex will be presented in Chapter 6. It will suffice in this Section to analyse Table 5.9 in terms of its ability to mimic cancellous bone. The following can be observed from Table 5.9:

* The apparent density range (1180 - 295 Kg m$^{-3}$) produced by drilling holes into the perspex block are within range of quoted values for cancellous bone.

* A large nnBUA range ( 2.12 - 11.44 dB MHz$^{-1}$cm$^{-1}$ ) with a mean of 8.18 $\pm$ 45% dB MHz$^{-1}$cm$^{-1}$ also apparent.

* Velocity values are on the upper quartile of those quoted for cancellous bone and the only change in velocity value was observed for very large porosity samples.

* The behaviour of BUA was non-linear with changes in hole size.

It can be concluded that porous perspex is a good cancellous bone phantom. It will be further used to study the effect of different number, size and distribution on BUA.

## 5.5 Conclusions

Pop was found not to be a good cortical bone phantom because it was not possible to manufacture identical phantoms and the attenuation was largely dependent on the length of soaking. Perspex was a better cortical bone phantom in terms of durability, stability, and manageability. Perspex also had the highest velocity and density of all the polymers studied and thus was the most appropriate of all the polymers as a substitute for cortical bone.

Agar gel was more of a soft tissue phantom than fat because of its high viscosity. Lard and castor oil were found to have properties close to fat. It was also demonstrated that both velocity and attenuation in the lard were dependent on temperature.

The ultimate objection was to be able to model cancellous bone. as 3-dimensional network of struts with the spaces filled by bone marrow. Aluminium mesh in agar gel did not satisfy the requirement of a cancellous bone phantom. It has been established that perspex with holes drilled in them provided a convenient phantom to study the propagation of ultrasound through porous material. On the other hand HDPE filters was found to be a good phantom for reproducibility study.

# Chapter

# 6. EVALUATION OF CANCELLOUS BONE PHANTOMS

## 6.1 Ultrasonic Studies of Porous Perspex

The cancellous bone phantoms developed in Chapter 5 were then used to study the ultrasonic and material properties. Perspex was shown previously as a favourable cortical bone phantom. Based on the argument that the trabeculae of cancellous bone is similar to cortical bone, perspex was used to simulate cancellous bone. This was achieved by drilling cylindrical holes into the cube. The objective of the experiment was to investigate the effect of hole size, number and distribution on the BUA and possibly velocity. The experimental details are given below in Section 6.1.1.

### 6.1.1 Experimental Procedure

Initially, the perspex was made heterogeneous by introducing scatterers as holes. The holes were an exaggerated representation of the pores found in cancellous bone. The holes were drilled using a computerised system. The following set up of holes were investigated .

♦ Constant number of holes but variable hole diameter .

36 (6x6) symmetrical and vertical holes were drilled into a 41 mm perspex cube. The number of holes was kept constant but the hole diameter was increased from 1 mm to 5.5 mm in 0.5 mm steps. One block was used continuously, that is, the hole size increase was done on the same specimen. The 36 holes covered an area of 34x34 mm$^2$ (Figure 6.1). The procedure was repeated for 25 (5x5) and 16 (4x4) hole array

covering an area of 30x30 mm$^2$ and 25x25 mm$^2$ respectively. In addition, 16 (4x4) symmetrical holes on an area of 34x34 mm$^2$ was investigated.

◆ **Constant hole diameter but variable number of holes.**

The second group of investigations commenced with 4 holes (of 3 mm diameter) and progressed with an increase in the number of holes. The hole diameter was constant throughout. The various configurations studied are illustrated in Figures 6.2 and 6.3. The small arrows indicate the direction of propagation of the ultrasound wave and the large arrows indicate the direction of increase in number of holes. For example after measuring directions A1 and A2, the number of holes were increased and direction B1 and B2 were measured.

◆ **Non symmetrical arrays of holes.**

The third arrangement consisted of a non symmetrical arrays of holes as illustrated in Figures 6.2C, 6.2D, 6.3F, and 6.3G. To further investigate the non-symmetrical arrays effect, two random hole patterns were generated with the following specifications (see Figure E.5):

1.    25 holes , 10 of which were of diameter 1.5 mm and 15 of diameter 2 mm

2.    30 holes , 10 holes were of diameter 1 mm, another 10 of diameter 22 mm and the remaining 10 holes of diameter 2.5 mm.

The cubes were measured in four directions, that is on each cubic corners.

◆ **Coupling and degassing effect.**

The effects of changing the fluid in the holes, changing the couplant and degassing were investigated. Castor oil was used to replace water in some of the arrangements and investigations were carried out on the water and gel couplant.
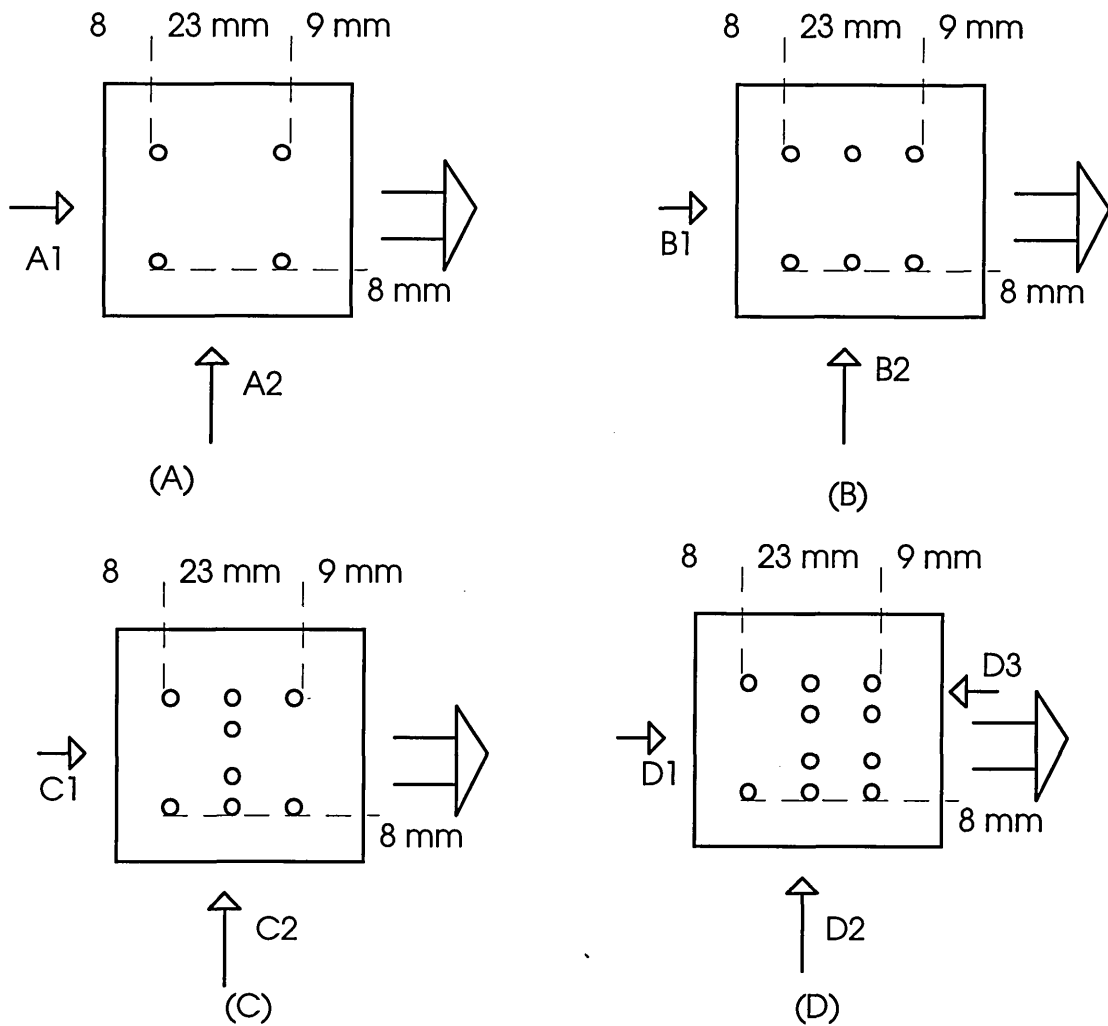
**Figure 6-1:** *Schematic Representation of Variation in Hole Numbers at Constant hole Diameter: A(4 holes), B(6 holes), C(8 holes) and D(10 holes)*
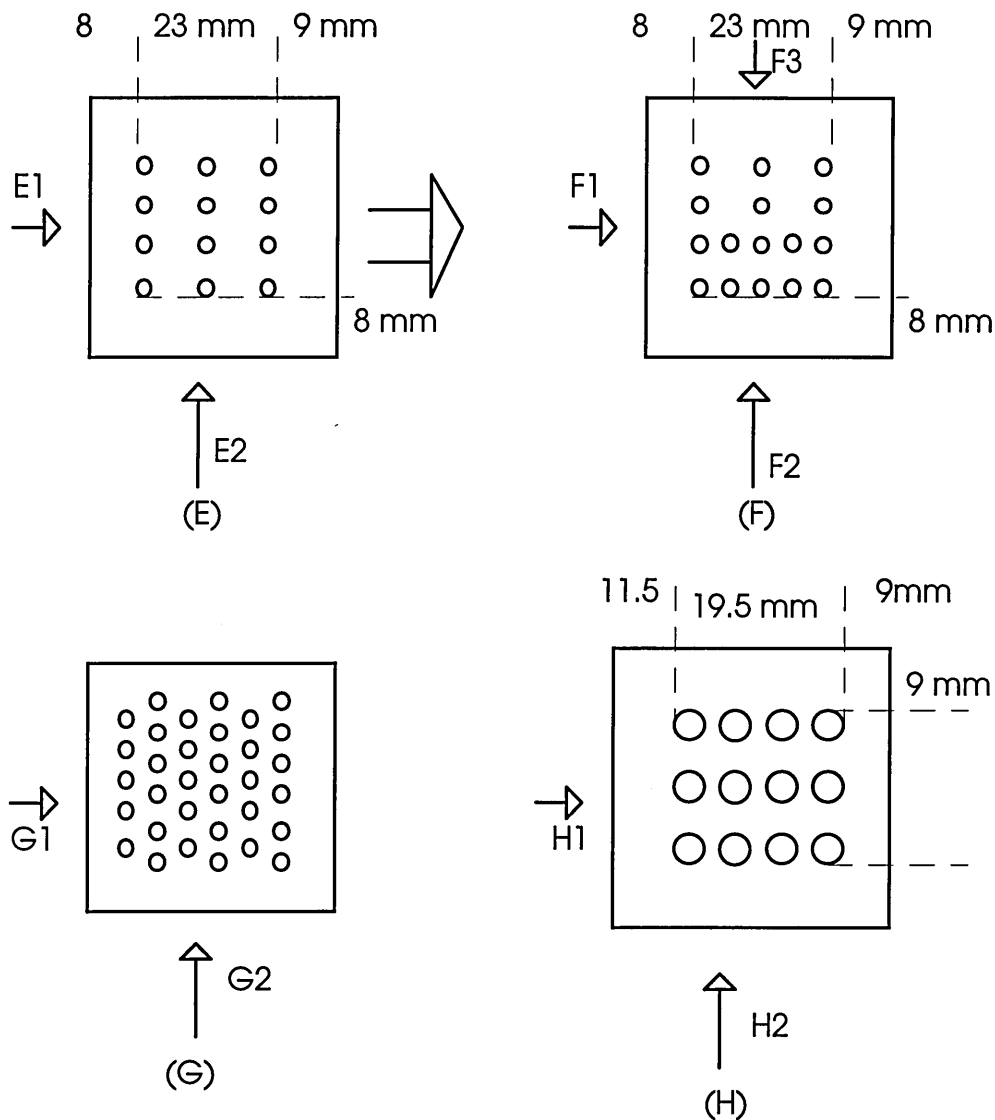
*Figure 6-2: Schematic Representation of Variation in Hole Numbers: E(12 holes), F(16 holes), G(33 holes) and H( 12 holes at 4 mm diameter)*

In all the experimentation CUBA system was used and the velocity and BUA obtained are as described in Chapter 4. The measurements were carried out in wetted water (wetting increases the threshold of cavitation [Njeh 1990]). Water has a different acoustic impedance and absorption coefficient to perspex. Thus the interface between water and perspex acts as scatterers to incoming waves.

## 6.1.2 Results of Perspex Studies

The results are given in Appendix A, Tables A.1, A.2, A.3, A.4, A.5, A.6 and A.7, where d represents inter-hole spacing, $\phi$ hole diameter and the numbers in bracket are the coefficients of variation (stdev/mean*100). Table A.1 represents nBUA, velocity

and porosity for 25 holes (5x5) on an area of 900 mm$^2$. Porosity is a characteristic of a porous medium and is defined in Section 5.4.3.1 as $(N\pi\phi^2)/4A$, where N is the total number of holes, $\phi$ is the diameter of the holes and A is the area covered by the holes. Substituting the values (N = 25, A = 900 and $\pi$) in Equation 5.2 gives $2.18\phi^2$. Since the specimen thickness was constant it was thought unnecessary to include nnBUA for the tables. Table A.2 represents the results for 16 holes (4x4) on an area of 1156 mm2. Table A.4 represents the results for constant hole diameter with variable number of holes. The notation of the directions are as presented in Figures 6.1 and 6.2. Table A.5 is a subset of Table A.4 including only those specimens with same hole size (3mm) and same number of rows(3). Table A.6 represents results for asymmetric setup.

## 6.1.3  Discussion for Porous Perspex Cancellous Bone Phantom

### 6.1.3.1  Broadband Ultrasonic Attenuation(BUA)

As mentioned earlier in Chapter 4 a contact method for ultrasonic measurement was used. The transducers were placed in contact with the perspex, submerged in degassed water with one transmitting and one receiving.

The plots of attenuation as a function of hole diameter and porosity are given in Figures 6.3 and 6.4. It can be observed that the attenuation (nBUA) increases with increase in hole diameter up to 3.5 mm and decreases rapidly thereafter. As would be expected the behaviour is similar for both hole diameter and porosity, the difference being a shift in the symmetry of the parabolic curve.
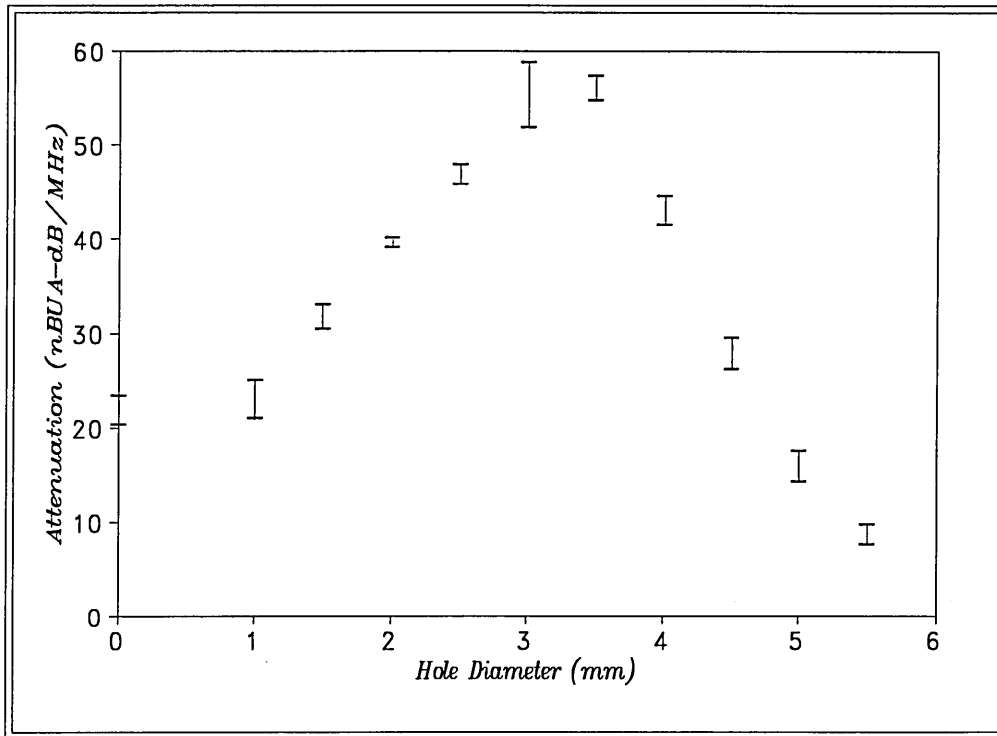
**Figure 6-3:**The Relationship Between BUA and Hole Diameter
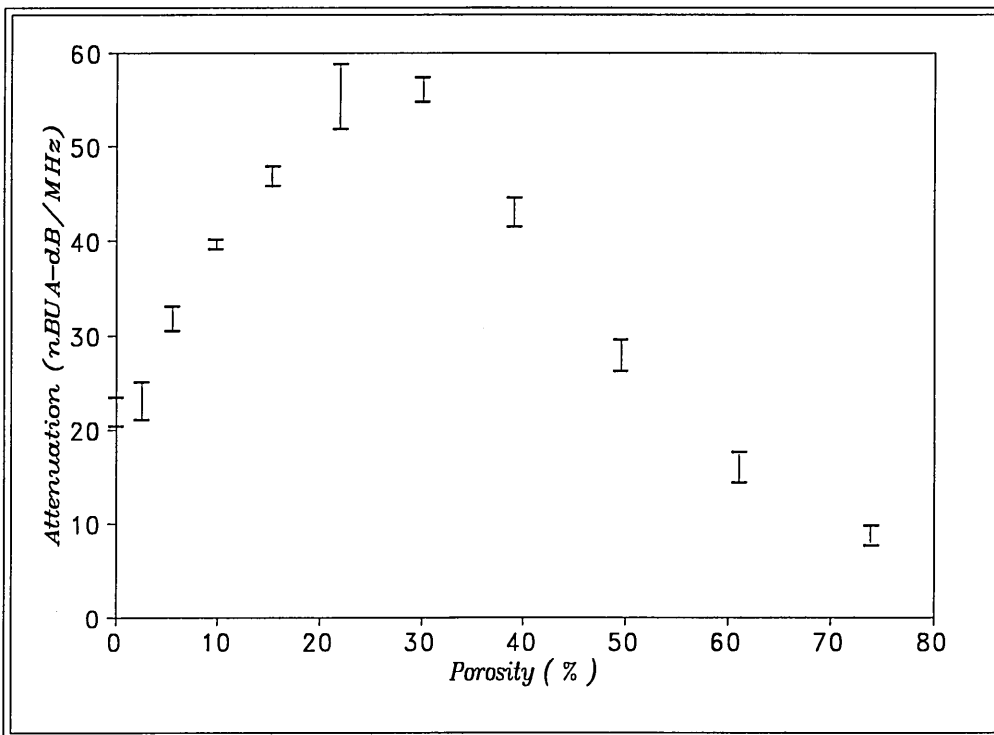


**Figure 6-4**: The Relationship Between BUA and Porosity

114

The above results (Figures 6.3 and 6.4) could be explained in terms of the modes of interaction of ultrasound with perspex. The attenuation of the received signal could arise from geometric divergence (diffraction), absorption, scattering or a combination of the processes (see Chapter 3). The geometric divergence arises when the sound beam diverges from the centre of the beam in the far field. As shown in Table 6.1 and Equation 3.2 the onset of divergence depends on the frequency of the propagating wave and the diameter of the transducer (in this case 19 mm). The perspex blocks were 41 mm cube and the end of the near field occurred within the specimen, therefore divergence loss was a contributory factor to the attenuation. This contribution is constant and therefore will not account for the behaviour of attenuation with changing hole diameter (Figures 6.3 and 6.4).

*Table 6-1: The Wavelength and Near Field Range with Perspex*

| Frequency (MHz) | Velocity (m s$^{-1}$) | Wavelength (mm) | $z_{max}$ (mm) |
|---|---|---|---|
| 0.2 | 2657 | 13.29 | 6.79 |
| 0.6 | 2657 | 4.43 | 20.37 |
| 1 | 2657 | 2.66 | 33.93 |

In the perspex block without holes, the main attenuation mechanism is absorption (absorption in perpex ($\sigma_a$p)) and reflection at the perspex - water interface ($\sigma_s$pw). This is because perspex is amorphous and has no appreciable voids. The type of absorption mechanism has been described by Hartmann and Jarzynski [1972] as hysteresis. They further postulated that absorption mechanism occurs at the molecular level as the trapping of the polymer in one of its many local potential energy minima.

The introduction of voids in the form of cylindrical holes increases the attenuation processes (Figure 6.6). the additional attenuation processes being:

♦ Absorption in water ($\sigma_a$w),

♦ Scattering at perspex - hole interface ($\sigma_s$ph) and hole - perspex interface ($\sigma_s$hp).

Total attenuation coefficient ($\sigma_T$) can be expressed as follows

$$\sigma_T = \sum (\sigma_a p + \sigma_a w + \sigma_s tp + \sigma_s pt + \sigma_s ph + \sigma_s hp). \qquad (6.1)$$

The author does not use this model to predict the experimental results but to qualitatively explain the observations. The effect of reflection coefficients at the transducer-perspex interface and perspex-transducer with changing hole diameter are constant and thus could be eliminated from the equation. The contribution to attenuation with changing hole diameter are therefore absorption and scattering at the pore interface. The total absorption component of the attenuation is given by

$$\mu_{aT} = w_p \sigma_a p + w_w \sigma_a w, \qquad (6.2)$$

where $w_p$ and $w_w$ are the fractional width of perspex and water respectively. Since the attenuation in water is used as the reference, its attenuation is therefore taken to be zero. Therefore Equation 6.2 becomes

$$\mu_{aT} = w_p \sigma_a p. \qquad (6.3)$$

The fractional width of perspex is given by (Area of perspex($A_p$)/Total area of cube($A_t$))

$$\mu_{aT} = \frac{A_p}{A_t} \sigma_a p. \qquad (6.4)$$

but $A_p = A_t - A_w$ (where $A_w$ is the area of water), substituting in Equation 6.4,

$$\mu_{aT} = \frac{(A_t - A_w)}{A_t} \sigma_a p. \qquad (6.5)$$

The area of the cube is $4.1^2$ cm$^2$, $A_w = 36\pi\phi^2/4$, and the measured attenuation in the perspex without holes ( Table 6.1) was 5.34 dB MHz$^{-1}$cm$^{-1}$. Substituting all these into Equation 6.5 gives

$$\mu_{aT} = 5.34(1 - \frac{36\pi\phi/4^2}{4.1^2}). \qquad (6.6)$$

116

The results of Equation 6.6 are given in Figure 6.6. It shows that total absorption decreases with increase in hole diameter. Therefore the observed increase in attenuation with increase in hole diameter is due to the scattering effect.



Transducer                           Attenuation

1 Transmitting             3 Absorption in perspex           5 Scattering ph

2 Receiving                4 Absorption in water           6 Scattering hp

(A)  2 mm holes                           (B)  5.5 mm holes
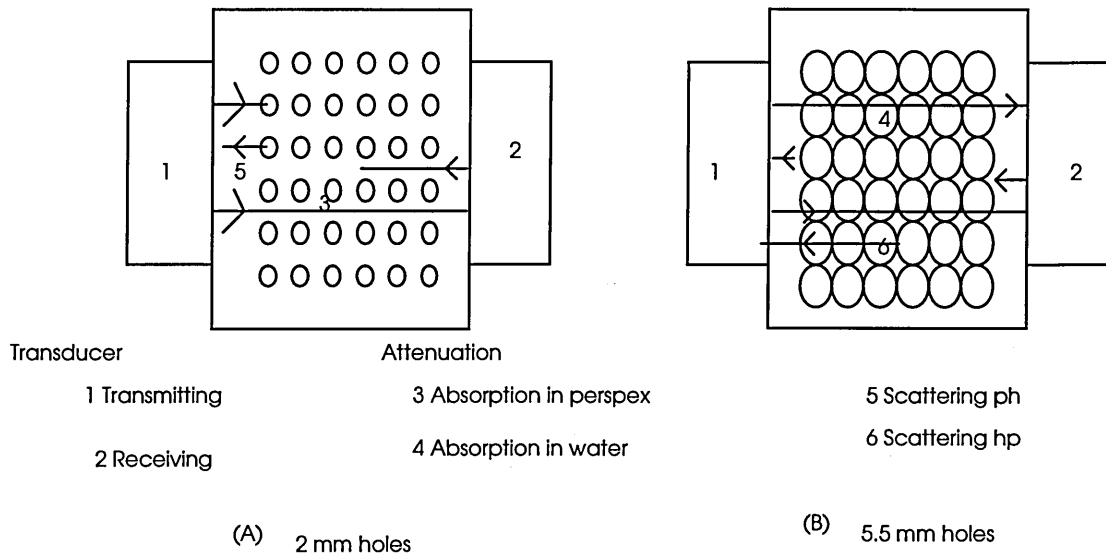
*Figure 6-5: The Attenuation Processes in the Perspex Cube*
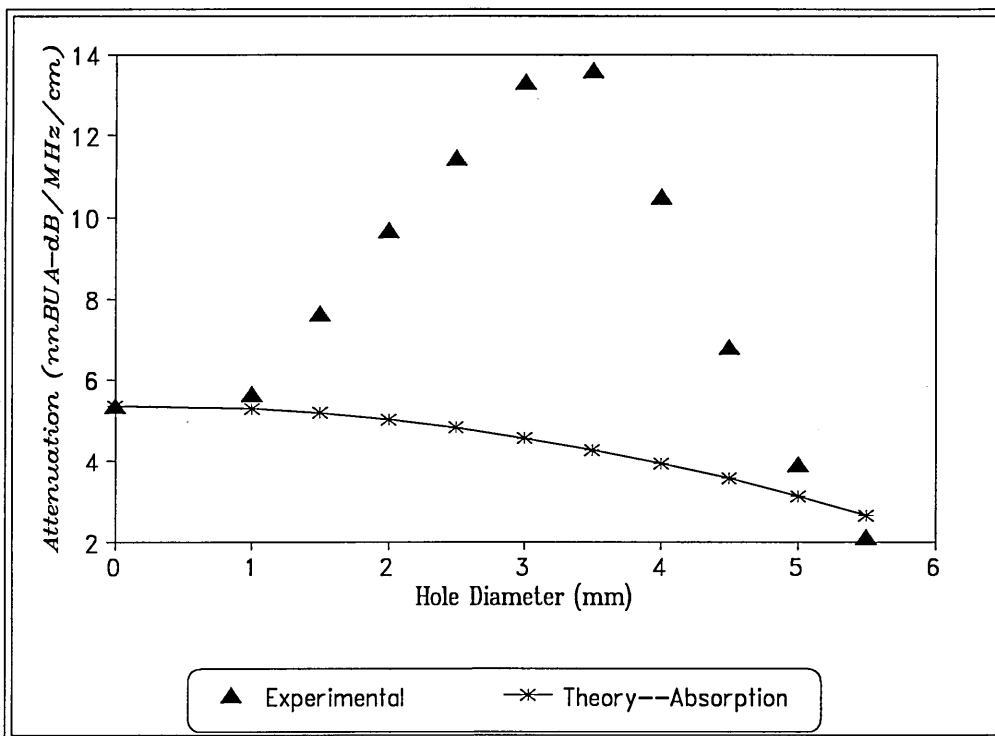


*Figure 6-6: The Relationship Between Attenuation and Absorption with Hole Diameter*

The relationship between scattering contribution to attenuation and pore diameter($\phi$) depends on the wavelength of the propagating signal. For $\lambda \gg \phi$, it has been proposed that $\sigma_s(f) = constant*\phi^3 f^4$ [Sanie et al. , 1987]. The cubic dependence of this relationship comes from the volume of the sphericals inclusions, therefore in this case of cylindrical holes quadratic dependence may be more appropriate. A linear regression of  log to base ten of nBUA versus log of hole diameter  for hole diameter of 1 to 3.5 mm resulted in Equation 6.7,

$$log(nBUA) = 1.371 + 0.735log(\phi) \qquad\qquad R^2 = 99.2\% \qquad (6.7).$$

Equation 6.7 shows that attenuation (nBUA) in this particular investigation was approximately  related to hole diameter raised to 0.74 power. This is to be expected because as $\lambda \to \phi$, the scattering coefficient becomes far less sensitive to pore size and $\sigma_s(f) \to constant*\phi$. Qualitatively looking at Figure 6.6, it can be seen that  as the hole diameter increases from 0 mm to 3.5 mm, the scattering cross section increases. This is because below 3.5 mm some of the waves go through the cube without passing through the holes. After about 3.5 mm the scattering cross section becomes constant and the dominant attenuation process becomes the absorption. Also, in terms of frequency,  high frequency components are scattered with large intensity compared to low frequency component. The same experiment was carried out but reducing  the total number of holes and the results are presented in Figures 6.7 and 6.8.
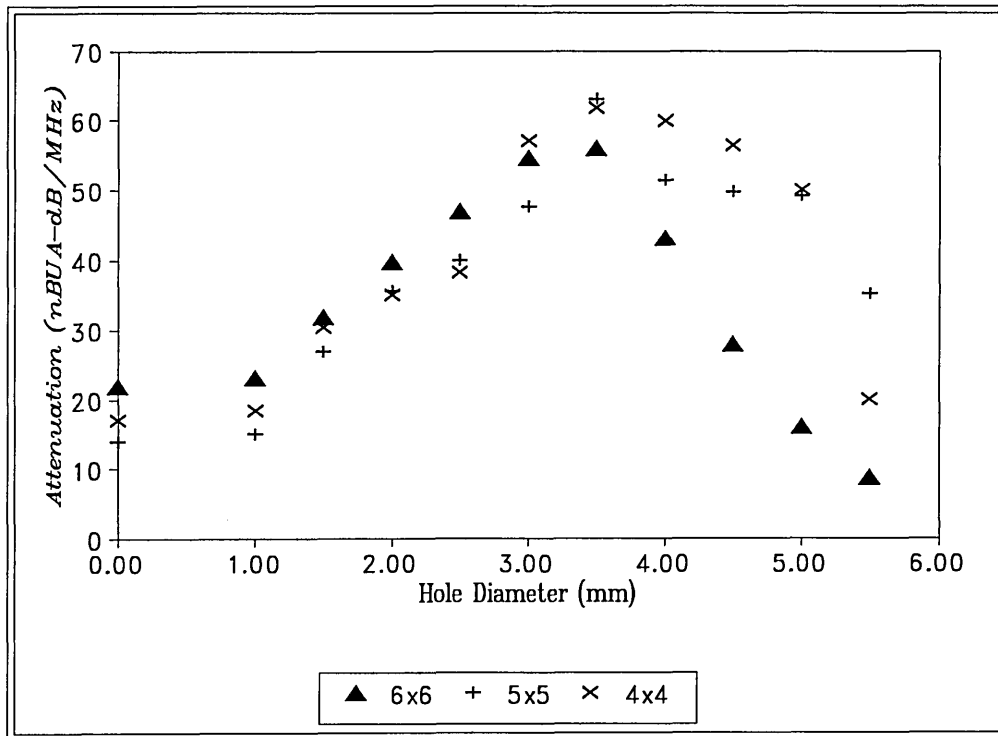
***Figure 6-7:*** *The Effect of Number of Holes on BUA as a Function of Hole Diameter*
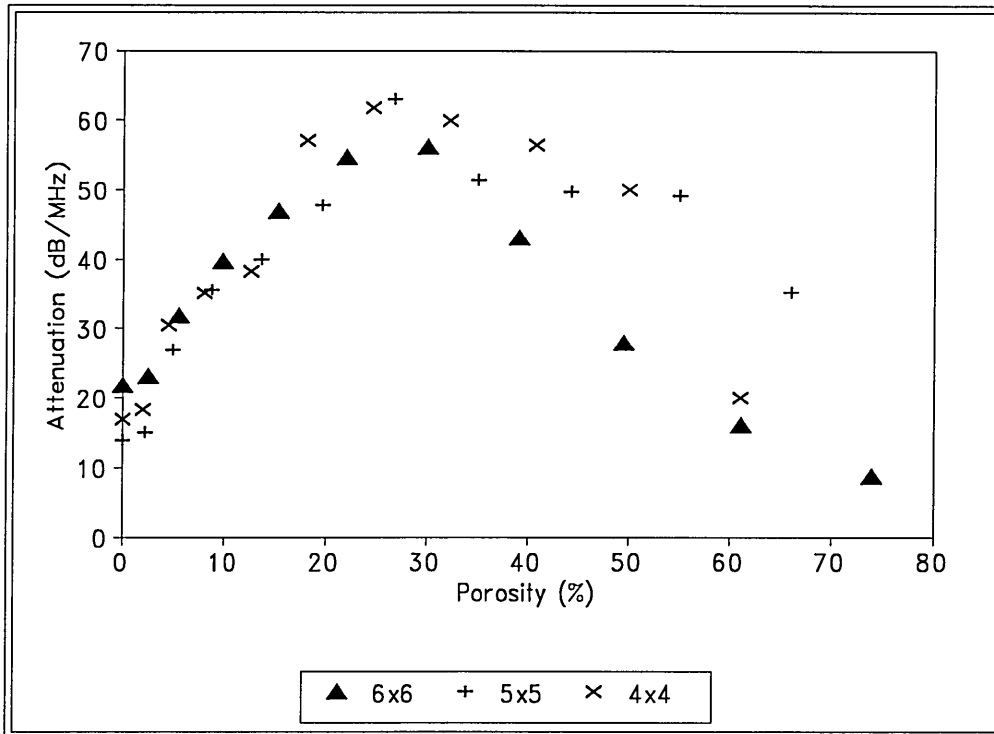
*Figure 6-8: The Relationship Between BUA and Porosity for Different Numbers of Holes*

Figures 6.7 and 6.8 illustrate the following :

♦   The three configurations all peaked at a hole diameter of 3.5 mm and inter hole spacing (d ) of $2 < d < 3$ mm.

♦   The peak porosities were 30 %, 26.7 % and 24.6 % for 36 holes, 25 holes and 16 holes, respectively.

♦   36 hole configuration has higher nBUA at hole diameters of less than 3.5 mm.

♦   A linear regression of log nBUA against log of hole diameter from 1 mm to 3.5 mm (number of samples 6) gives the following gradients $0.735\pm$ 0.034. $1.057\pm0.078$ and $0.933\pm0.096$, and $R^2$ = 99.2%, 97.9% and 95.9%, for 36 holes, 25 holes and 16 holes,  respectively, where $\pm$ is the standard deviation.

120

♦ The fall in attenuation with hole diameter after 3.5 mm is not very smooth for 25 holes and 16 holes.

The above observations could be explained thus: The 3.5 mm hole diameter correspond to an inter-hole spacing of less than 2.75, hence less than the wavelength (nominal) of the transducer. Therefore after 3.5 mm absorption dominates and hence the decrease in nBUA. If the contribution to attenuation from the holes is additive then one would expect the attenuation at any particular hole diameter to decrease with decrease in number of holes. But the results show no significant change. This anomaly may be explained by one or both of the following:-

I. Although the number of holes changed the area was not fixed, hence the wave interacted with the same total number of scatterers in all the three cases.

II. Also, changing hole number and maintaining the symmetry, maintains the structure but changes the density.

An attempt to verify the first statement was performed by repeating the experiment with 16 holes but on 34x34 mm$^2$ area. The results are presented in Table A.3. BUA peaked at 3 mm hole diameter, 5.5 inter hole spacing and 9.8 % porosity. Therefore the explanation of the results presented is highly possible.

The dome shape behaviour of nBUA with porosity poses a problem in predicting the porosity of a sample when the nBUA is measured. A look at Figure 6.9 shows some of the complications in using BUA as a predictor. BUA of specimen 1 is equal to BUA of specimen 3 but at any frequency $f_0$, specimen 1 is more attenuating than specimen 3. On the other hand specimen 2 is more attenuating than specimen 3 but has a lower BUA. In the application of BUA to bone, the impact of the second problem is small because A1 differs from A3 in the absorption and this value will be the same.

The author proposes that a combination of attenuation at a particular frequency (0.4MHz) with nBUA could linearize the response of nBUA with porosity. The attenuation values are given in Tables A.1, A.2 and A.4. The attenuation at 0.4MHz was not recorded for 36 holes because the software used in that case did not allow access to attenuation at particular frequencies.

**121**
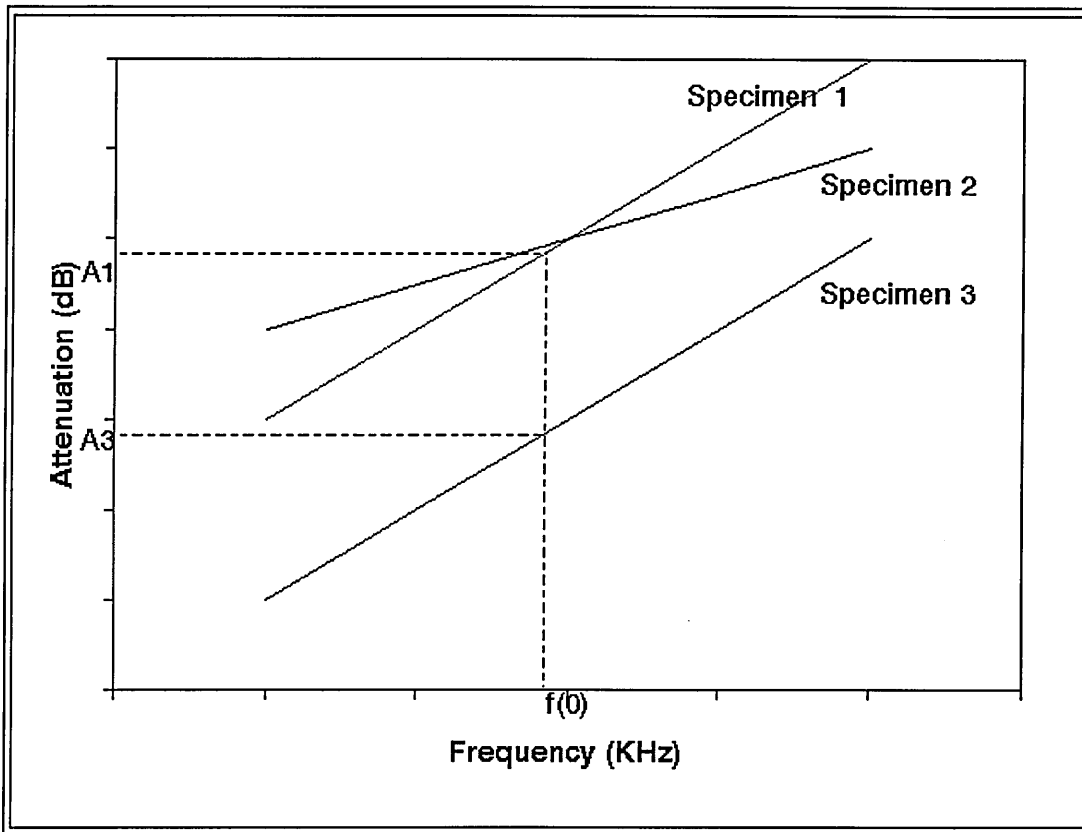
*Figure 6-9:* *Schematic Representation  of  the Problem with BUA in Prediction*
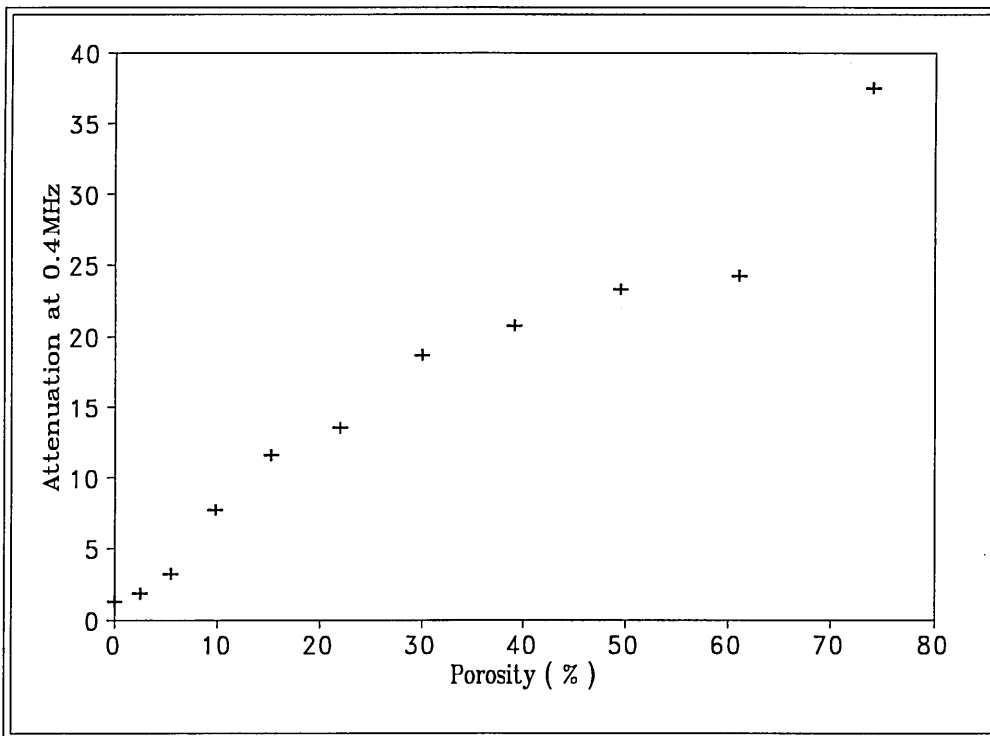


*Figure 6-10:* *Attenuation at 0.4MHz for 25 Holes versus Porosity*

The attenuation for 25 holes shows an increase with increase in porosity (Figure 6.10 ), while the response for 16 holes has a peak at 3 mm hole diameter. The attenuation at 0.4MHz was then multiplied with nBUA and the result is given in Figure 6.11. The effect of linearize the behaviour of nBUA with porosity was not achieved. The nBUA was then divided by the attenuation at 0.4MHz and an exponentially decaying response was obtained (Figure 6.12). Dividing nBUA by attenuation results in a quantity with physical meaning of $MHz^{-1}$. A plot of log of nBUA/attenuation as function of porosity produce a linear response (Figure 6.12). The result of a linear regression fit applied to this graph is given in Equation 6.8,

$$Log(nBUA/att) = 1.102 - 0.025(Porosity) \qquad R^2 = 96.7\% \qquad (6.8).$$
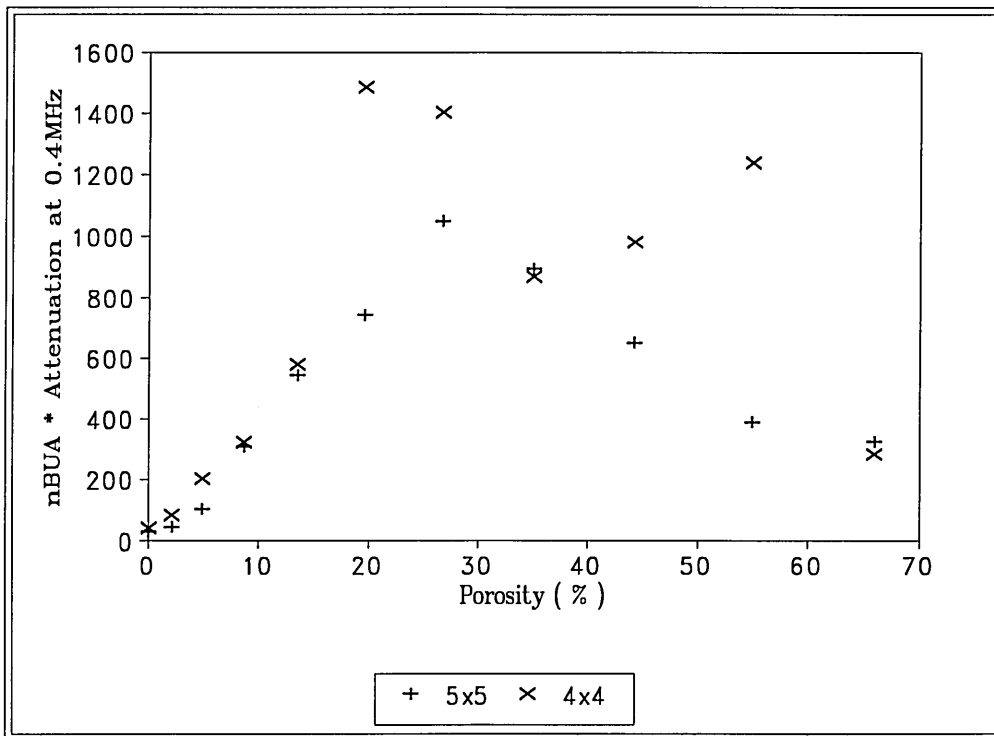


*Figure 6-11: nBUA Multiplied by Attenuation and Plotted against Porosity for 25 and 16 Holes*
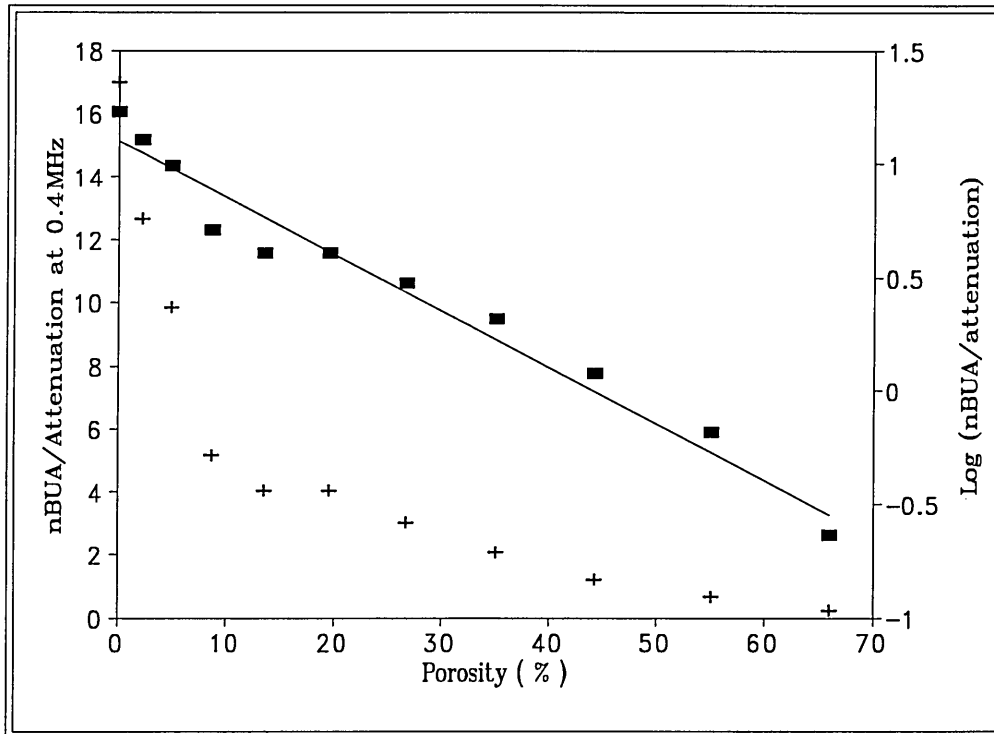
***Figure 6-12:** nBUA divided by Attenuation Plotted against Porosity*

The second and third group of experiments were aimed at identifying the structural effect on BUA and velocity values. The results are given in Table A.4 and A.5 (Appendix A). The inter-hole spacing, d was given because it is also a structural index. This spacing is analogous to trabeculae width in cancellous bone. It can be observed from the Tables that
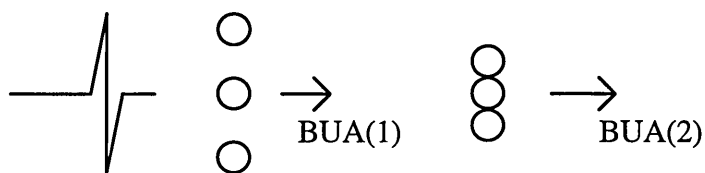


BUA(1)  ≠    BUA(2) and d(1)  ≠    d(2)

The nBUA depends on the number of rows, number of holes, inter-hole spacing (d), hole diameter and spatial distribution (direction) of holes. The various factors affecting the nBUA is indicative of the complexity of the system. In order to demonstrate an

accurate correlation between BUA and one other influencing factors everything else must remain constant. This is rather difficult, for example when the number of rows is increased, the number of holes also increases. This makes it difficult to extract the independent effect of a single factor. So it is rather difficult to predict the effect of each factor on nBUA from Table A.4. Prediction of the influence of a particular configuration on the total attenuation would require analysis of a complex situation.

There is no prominent trend in the measured BUA in Table A.4, but when the set up with the same hole diameters and same number of rows are separated into Table A.5, a gradual increase in BUA with number of holes was observed.

The observations recorded in Table A.4 and A.5 may be qualitatively explained as follows:-

♦ Increase in hole number at constant hole diameter results in an increase in scattering cross section as long as the diameter is less than 3.5 mm. Therefore an increase in nBUA with increase in hole number would be expected (Table A.5).

♦ Attenuation is linearly related to distance of the specimen propagated, therefore the amplitude of the scattered wave will depend on the position or spatial arrangement of the scatterers in the sample. Hence the observed effect of number of holes and direction on nBUA.

♦ The effect of inter-hole spacing relates to the wavelength of the wave in determining the magnitude of absorption and scattering cross sections

The results of the random hole pattern is presented in Table A.6. It could be seen that the difference between X and Y directions are significant, but no significant difference was observed between XX and X, nor between YY and Y.

The last set of experiment was designed to demonstate the effect of coupling fluid, type of liquid in the holes and the effect of gas bubbles. The results are given in Table A.7. The results confirmed the fact that if the fluid of different density and viscosity is used the resultant BUA values are going to differ. The density affects the coefficient of reflection at the interface while viscosity affects the viscous loss. The effect of the couplant is not significant because it affects only the transducer perspex interface.

### 6.1.3.2 Velocity

The velocity was measured as described in Chapter 4. Velocity values were measured for all the perspex investigations discussed above. A plot of velocity as function of hole diameter for 36 (6x6) holes configuration is given in Figure 6.13 and 6.14. There is no significant change in velocity before 3.5 mm (porosity 30%) at which point it starts to decrease with hole diameter. This same effect was also observed in the other symmetric hole configurations.

Below 3.5 mm the material could be considered homogeneous for velocity calculation purposes. Hence the velocity recorded is that through the frame (perspex). After 3.5 mm the material becomes inhomogeneous and the velocity becomes the velocity of the system which in this case is perspex and water. A linear regression fit to the linear portion produces equation 6.9. From this equation the velocity at 100% porosity (that is water velocity ) could be predicted to 1414 ± 120 (± standard error of estimate). This value is within experimental error close to the quoted value for water.

$$V = 3080.983 - 16.66(porosity) \qquad R^2 = 90.1 \qquad (6.9)$$
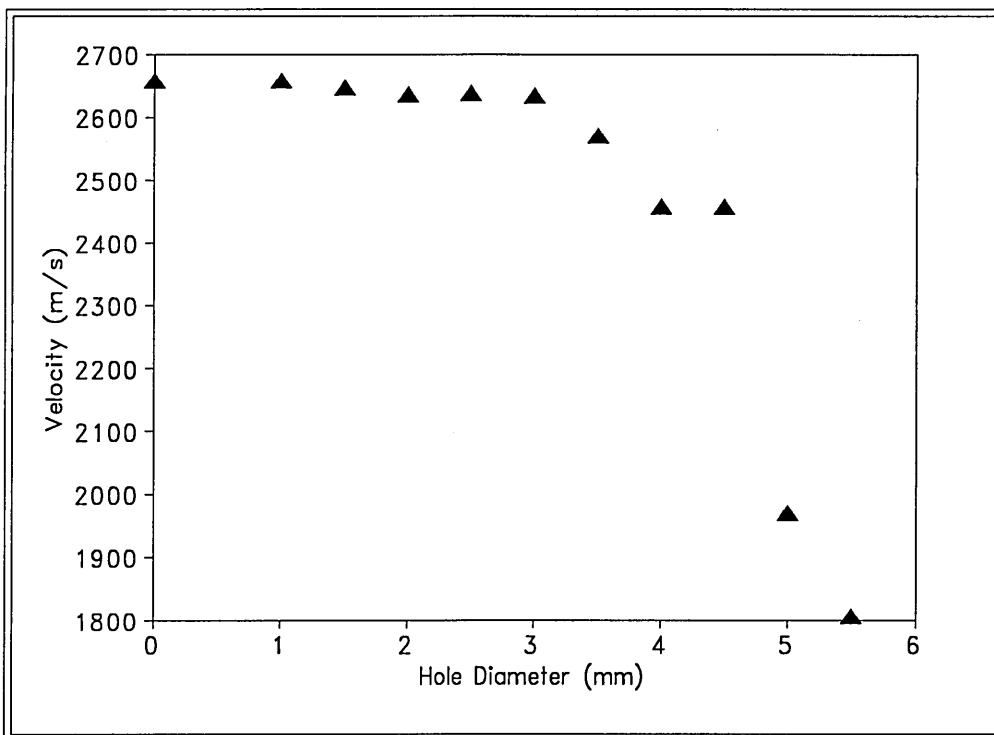
**Figure 6-13:** *The Effect of Change in Hole Diameter on Velocity*
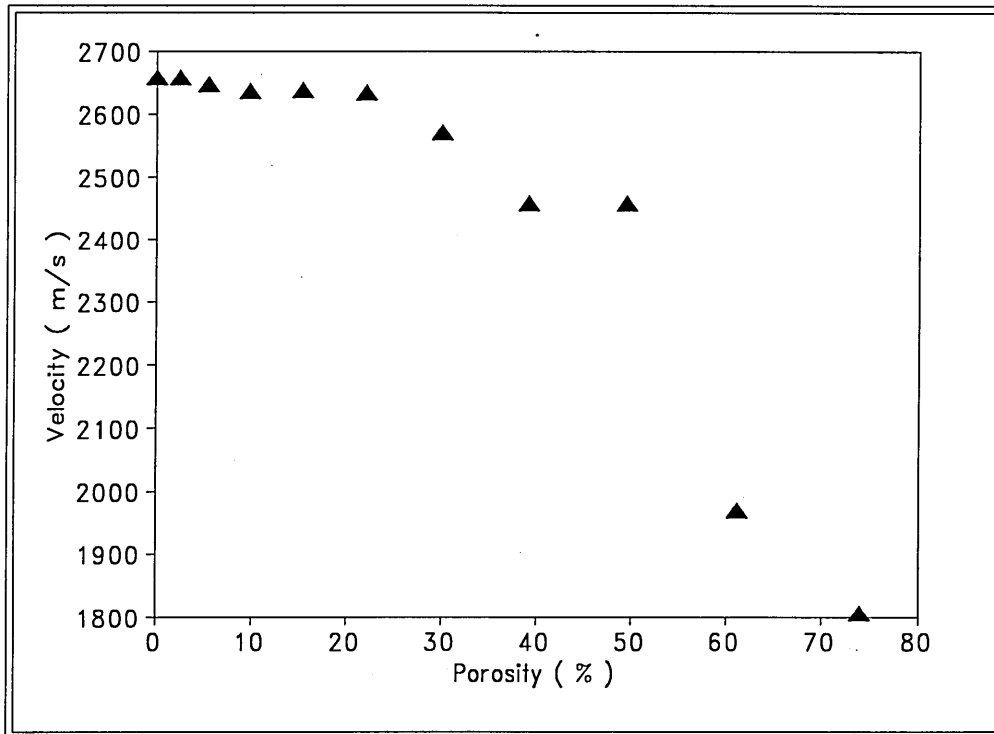
*Figure 6-14: The Relationship Between Velocity and Porosity*

The behaviour of velocity with hole diameter observed for the 6x6 hole configuration was poorer for the other hole configurations (5x5, 4x4) because the area covered by the holes was smaller hence exposing the set-up to repositioning problems.

There was no significant variation in the velocity measured for the second group of experiment (keeping the hole diameter constant, but varying the number). This is in line with the explanation given for the behaviour with varying hole diameter, because at 3 mm hole diameter the specimen is still homogeneous and hence no variation in velocity

There is little in the form of theory that can be used to explain or predict these observations. Multiple scattering theory of Waterman and Truell[1961] have been adapted to porous solids but these theories are only applicable at low porosities ($<10\,\mu$ m) and very high frequencies ($>2$ MHz $<40$ MHz). It has therefore been suggested [Mckelvie and Palmer, 1991] that Biot theory could be adapted to explain attenuation in our frequency band and high porosity.

Over a relaxation region of the acoustic frequency spectrum the velocity of sound is also observed to vary with frequency. In practice, however, the total variation is

127

usually less than 1% of the actual speed and requires accurate measurements if quantitative deductions are to be made. Kramer and Kronig[Hughes et al., 1987] have developed a relationship between frequency dependent attenuation and phase velocity. The usefulness of these exact equations is limited by the fact that data are required over a frequency range extending from 0 to ∞ [Hughes et al., 1987].

### *6.1.3.3 Sources of Error*

The size of the specimen was 41x41x41 and the diameter of transducer was 19 mm. Measurements were performed with the transducers in contact with the specimen, so the Fresnel region of the wave propagation is also used. The intensity of the wave is not uniform across the beam.

The scatterers introduced in the form of holes were not within the 19 mm diameter. Hence it was not possible to account for the effect of holes outside the field of the waves.

Further errors in attenuation and velocity measurement may arise from a number of sources including sample thickness measurement, digitisation, electronic noise and presence of gas bubbles in the water.

The temperture of the water bath was assumed to be room temperature. No control apparatus was set up to maintain it at a constant value so any fluctuation in the room temperature may have introduced some of the experimental errors.

## 6.2 Structural Studies

### 6.2.1 Perspex Modelling of Permeability

The permeability technique for quantitative assessment of cancellous bone was further validated by development of theoretical models. Since the actual geometry of the cancellous bone is often much too complicated for any mathematical analysis, the media was represented by theoretical models which can be treated mathematically. The level of complexity can then be increased to simulate the real porous media. The

simplest models are those consisting of capillaries [Scheidegger, 1974]. There is also the "ball and Stick" proposed by Koplik [Koplik et al., 1984]. The straight capillaries model was investigated and is reported in this report. This model represent a porous medium by a bundle of straight parallel capillaries of uniform diameter $\phi$ ( Figure 6.1). The flow Q through a capillary is then given by the well known Hagen-Poiseuille Law

$$Q = \frac{\pi \phi^4}{128\eta} \frac{\partial p}{\partial x},$$
(6.1)

where $\eta$ is the viscosity and $\frac{\partial p}{\partial x}$ is the pressure gradient. If there are n such capillaries per unit area of cross-section of the model, then the flow per unit area q will be

$$q = n\frac{\pi \phi^4}{128\eta} \frac{\partial p}{\partial x}.$$
(6.2)

Substituting Equation 2.12 to 6.2 yields the value of permeability to be

$$\kappa = \frac{n\pi \phi^4}{128}$$
(6.3)

A comparison between the theoretical prediction and the experimental results are presented in Table A.8 and Figure 6.15 and shows a high correlation.
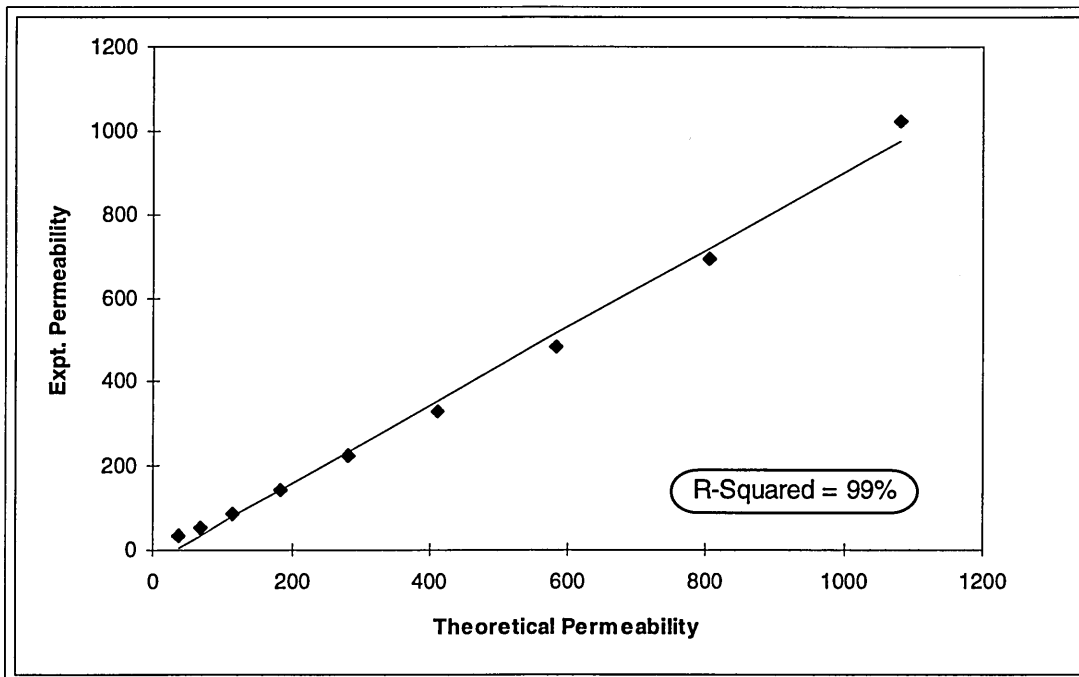


*Figure 6-15: Comparison Between Experimental and Theoretical Permeability*

## 6.2.2 Filter Studies

Porous sintered polyethene filters as explained in Chapter 4 were used to validate the experimental method of permeability measurement and were used in this section to investigate the relationship between permeability and BUA.

The permeability values were measured for one filter (6 mm thick and 40 mm diameter). The number of filters (thickness) was progressively increased to 5 filters (6 mm - 30 mm) for a particular grade. The same procedure was repeated for all the grades. BUA values were also measured using the same sequence as described for permeability.

## 6.2.3 Results and Discussion of Filter Studies:

A plot of permeability against thickness for grade 400 (P40) is presented in Figure 6.16. From the graph it could be observed that the permeability value increases with increase in thickness, from 5 mm to 15 mm and level off thereafter. From the equation for permeability (4.2) it would be expected that the permeability to be independent of thickness. The only possible explanation is that for the small thickness the rate of flow is not laminar and the application of Darcy law is not totally valid. This is confirmed by the fact that for lower permeability filters, the increase is less significant.

A plot of permeability versus grade is given in Figure 6.17. Grade values represent an indication of pore size distribution. The higher the grade the higher the porosity and the lower the density. The measured apparent density values showed a small range $0.4543$ g cm$^{-3}$ - $0.5718$ g cm$^{-3}$. Figure 6.17 shows that permeability is linearly related to porosity. This is expected and was demonstrated in the modelling.
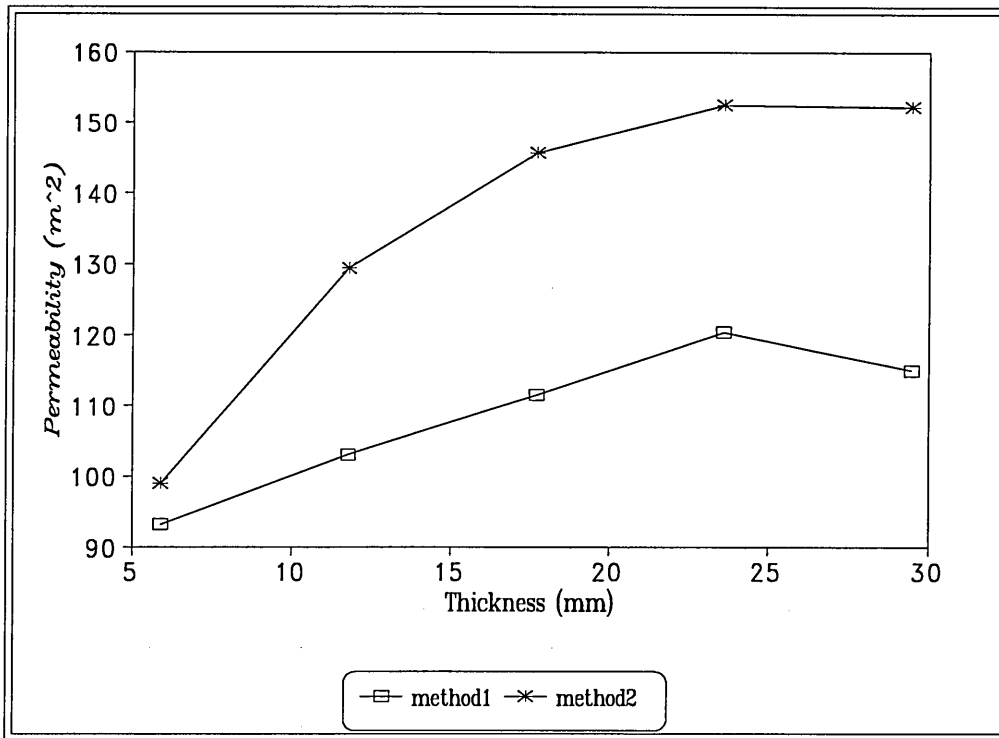
*Figure 6-16: A Plot of Permeability against Thickness for Grade 400 Filters*
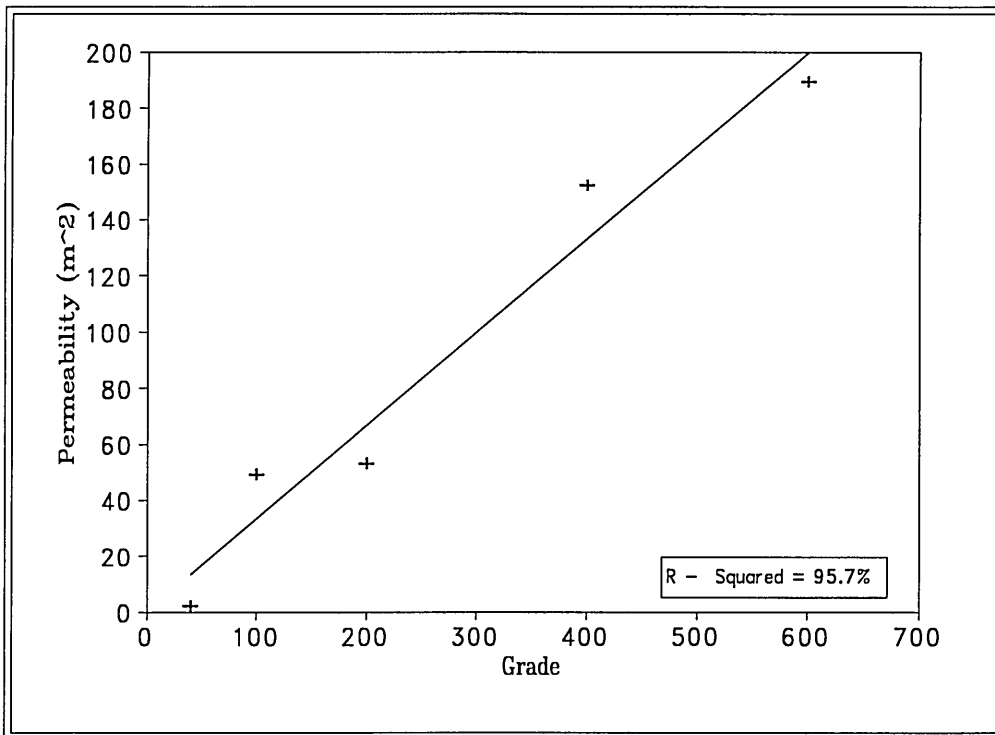


*Figure 6-17: A Plot of Permeability versus Grade for Five Filters per Grade*

To further verify the relationship between BUA in the filters and theoretical expectations, the attenuation values were recorded as a function of filter thickness. That is, the filters were progressively increased from 6 mm to 30 mm. The results are given in Figure 6.18. The R- squared value of 99.7% confirms the linear dependence of attenuation with thickness. This also justifies the use of this filter to study the relationship between BUA and permeability.

A plot of BUA versus grade is presented in Figure 6.19. BUA is highly correlated with grade, with an R-squared value of 85%. BUA in a porous material as explained in the preceeding section on perspex, is a function of pore size. The filters had a pore size distribution of 4 $\mu$m - 350 $\mu$m (Table 4.3). The pore size ($\phi$) satisfied the condition of $\lambda \gg \phi$. So, a plot of natural log of BUA versus pore size is given in Figure 6.20 and the linear regression fit given in Equation 6.9,

$$ln\ (BUA) = -2.65 +\ 1.37ln(pore\ size) \qquad R^2 = 96\% \qquad (6.9)$$

The high correlation coefficient ($R^2 = 96\%$) shows that BUA could be related mainly to the $\phi^{1.37}$ in the filter. It is worth noting that the structure in the filter was constant since they were produced by the same procedure with only increase in the diameter of the pores. A look back at the perspex results confirms the theory that as $\lambda \rightarrow \phi$, then the dependence of BUA on pore diameter approaches one and then becomes inversely proportional.
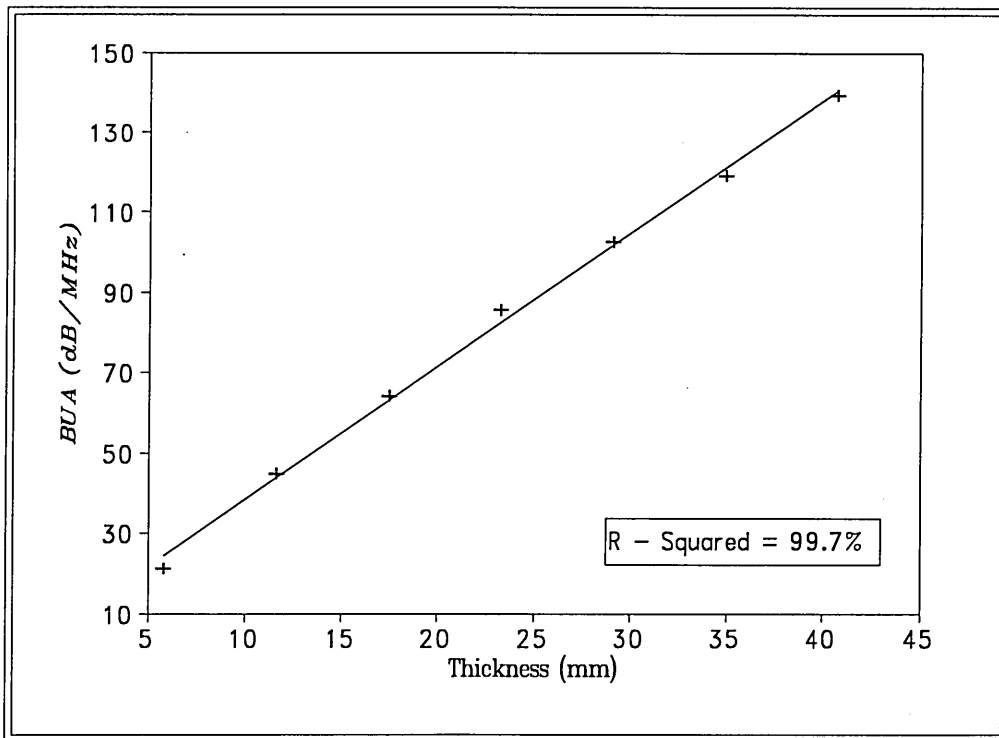
*Figure 6-18: A Plot of BUA versus Thickness for Grade 600 Filters*
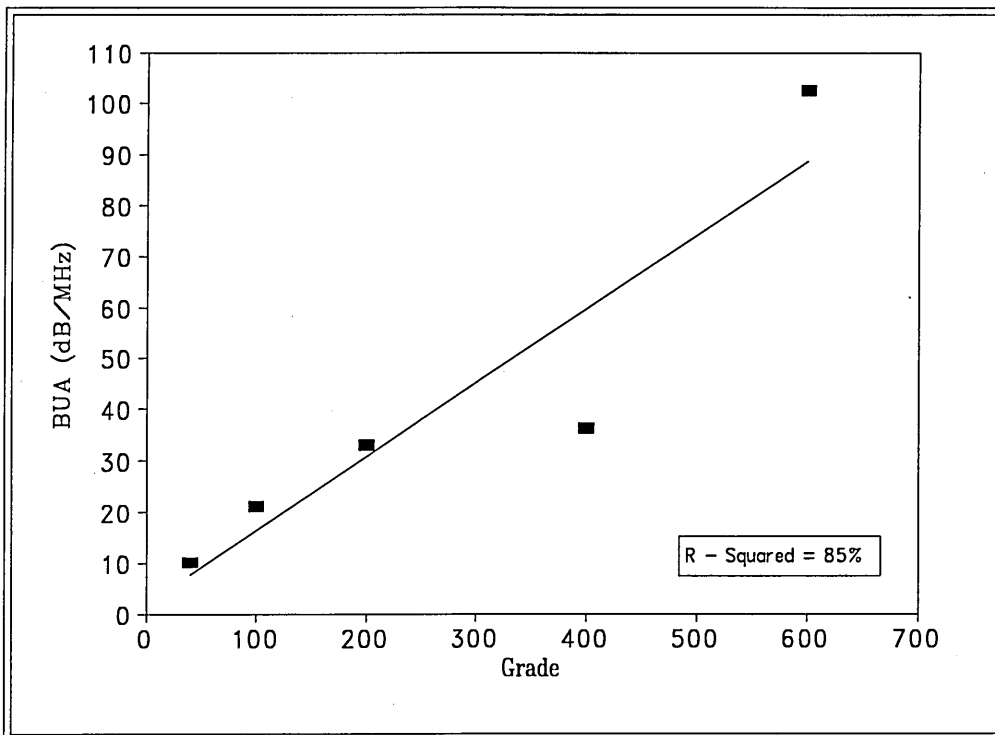


*Figure 6-19: A Plot of BUA versus Grade for 5 Filters of Each Grade*
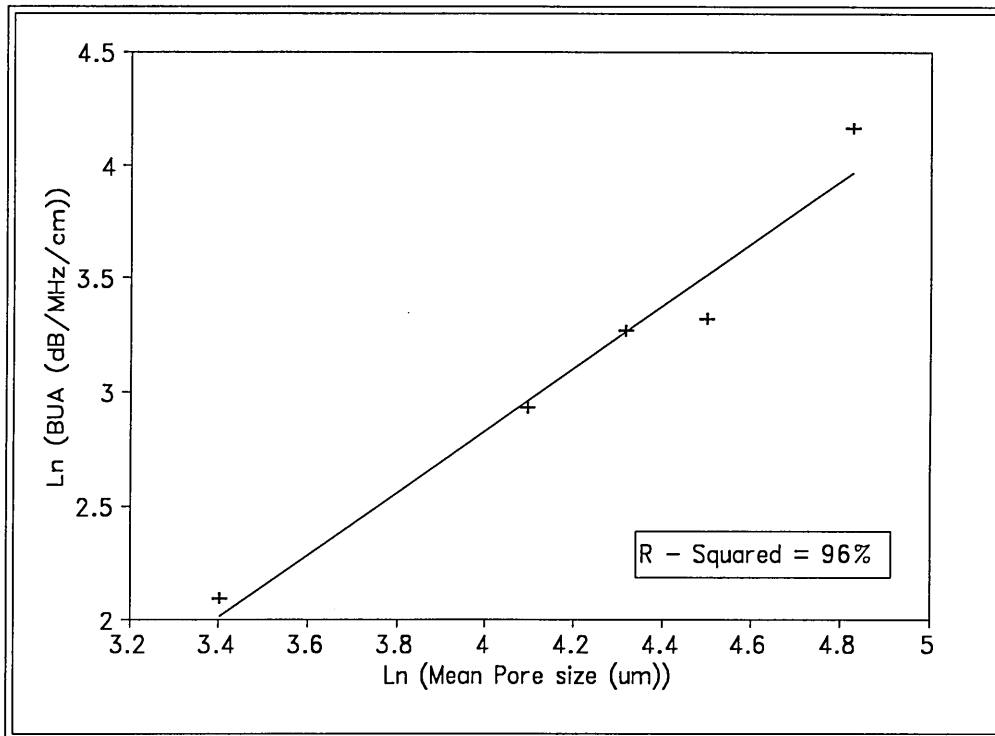
*Figure 6-20: The Relationship Between BUA and Mean Pore Size*

The BUA was plotted against the reference permeability and experimental permeability (Figures 6.21 and 6.22 respectively). Attenuation(BUA) as would be expected increases with increase in permeability. The filters were of low porosity and will correspond to the rising part of the relationship between BUA and porosity in Figures 6.4 and 6.8. So as porosity increases permeability increases and so does BUA. The low number of samples makes a formulation of an empirical equation to predict BUA from permeability studies poor.
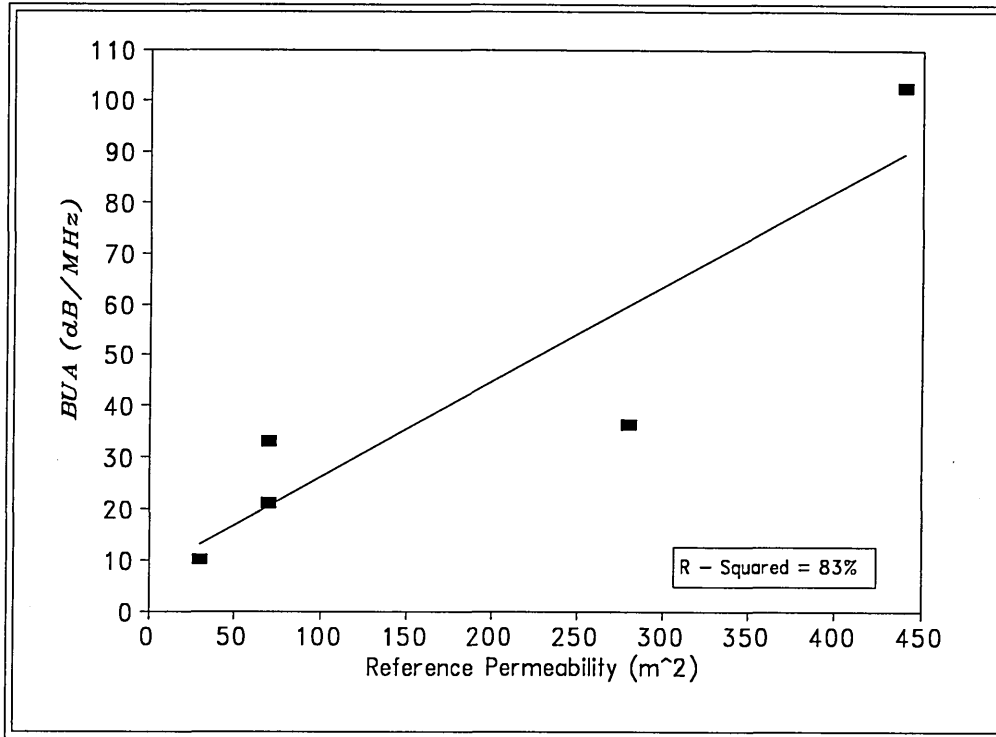
*Figure 6-21: A Plot of BUA against Manufacturer(Reference) Quoted Permeability*
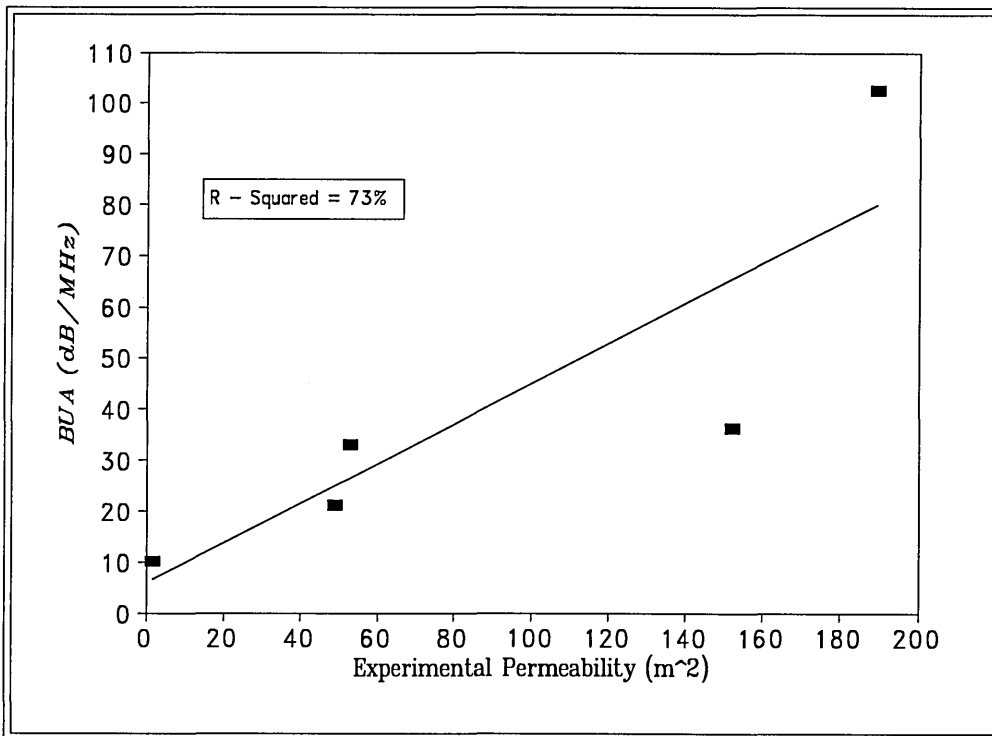


*Figure 6-22: A Plot of BUA versus Experimental Permeability*

135

## *6.3 Conclusions*

BUA in perspex with holes varies as a function of hole diameter with the peak occurring at around 3.5 mm. The scattering and absorption processes were used successfully in qualitative explanation of the results. A combination of attenuation at mid frequency (0.4MHz) could not linearize the behaviour of attenuation with hole size. Velocity on the other hand remained constant until a hole diameter of 4 mm where it started to decrease.

BUA was also found to vary according to spatial distribution of holes, hole number, inter-hole spacing and number of holes. These factors are an indication of the structure of porous perspex block. Therefore, the structural dependence of BUA has been proven by deduction. More rigorous experiment will be required to quantitative the structural dependence of BUA. A separation of the effect of absorption and scattering mechanism in attenuation will facilitate the above goal.

The permeability method was validated by comparing experimental methods with results from modelling using perspex models and by comparing the experimental results with manufacturer quoted values using filters.

The dependence of attenuation (BUA) on pore size was further demonstrated on filters. BUA was highly correlated with permeability. Permeability is proposed to give an indication of volumetric structure and therefore a correlation between permeability and BUA further substantiates the structural dependence of BUA.

# Chapter

# 7. THE RELATIONSHIPS BETWEEN ULTRASONIC, MATERIAL AND STRUCTURAL PROPERTIES OF BOVINE CANCELLOUS BONE.

## 7.1 Introduction

Proximal and distal bovine femi were chosen for this investigation because they are readily available and there are reported mechanical data for comparison. The experimental methods used are described in Chapter 4. Specimens were obtained from various locations on the proximal and distal femi (Figure 7.1) of three different bones. Specimen numbers 1- 4 were obtained from the tronchanter of the proximal femur, and specimens 5 and 6 obtained from head of the distal femur of the same bone. Specimens 7 - 10 were obtained from the distal femur and specimens 11 and 12 from the proximal femi, and specimens 13 and 14 from the distal femi of the same bone. The remaining four specimens were obtained from the third bone.

A resume of the measuring procedure is as follows:

1. The samples were prepared and machined into cubes (see Figure E3, E4)
2. They were then defatted and the acoustic properties and their permeability values measured.
3. The mechanical properties were then investigated.
4. The samples were then dried to obtain the dehydrated mass.

The specimens were maintained moist during all the mechanical and ultrasonic measurements.

In the following section the author will summarise the results obtained. This will then be followed by a discussion of the results with respect to the material, ultrasonic and structural properties.

**Head**                    **Tronchanter**

Proximal Femur

Distal Femu
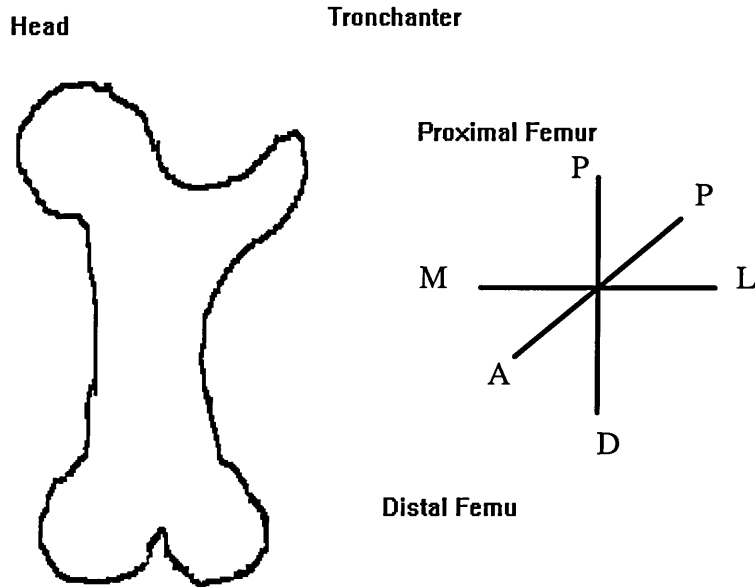
*Figure 7-1:*   *Schematic representation of a bovine femur*

## 7.2 Experimental Results

Measurements were carried out in  three directions namely; proximal-distal (PD), anterior-posterior (AP), and mediol-lateral (ML) (see Figure 7.1). For ultrasound measurements six conservative measurements were recorded for each direction per specimen. The mean of the six measurements are presented in Appendix B. The mean coefficient of variation(CV) was 3.53% and 2.1% for BUA and velocity respectively. The error associated with Young's modulus calculation is a combination of the errors associated with the following: area (A-0.17%), length(l-0.12%) and strain($\Delta$x-1.7%). Therefore the error of Young's modulus calculation could be estimated from

$$\partial\, E = \sqrt{\left(\frac{\partial\, A}{A}\right)^2 + \left(\frac{\partial\, l}{l}\right)^2 + \left(\frac{\partial\, \Delta\, x}{\Delta\, x}\right)^2}$$

as 1.68%. The error associated with permeability is 1.84%.

The results are given in Appendix B and the mean values, standard deviations and ranges summarised in Table 7.1.  To examine the difference between the different

directions, a two tail student paired t-test was carried out and the value P< 0.05 (95% confidence) was chosen as the significance level. The t-test results are presented in Table 7.2 and includes the operation (difference), the mean of the differences and the p-values. For a sample size of 18 and within 95% confidence limit, the significant t-value is $\geq 2.12$ ($t_{16, p = 0.975} = 2.12$).

The relationships between the variables were determined by conventional least square linear regression analysis. Some of the relationships were believed to be power functions hence logarithmic transformation (to base ten) was used to linearize them as shown below:

$$\text{If} \quad y = Ax^B \tag{7.1}$$

$$\text{Then} \quad \log(y) = \log(A) + B\log(x) \tag{7.2}$$

Confidence intervals (Bowman and Robinson, 1990) were used to verify the significance of the intercepts and gradients of the transformations in relation to the different directions. This theory states that to estimate some quantity $\Phi$ using an estimate $\hat{\Phi}$ which is constructed in a linear fashion from the element of an independent normal random sample, the form of a confidence interval is $\hat{\Phi} \pm t_{n-2, p} \, s.e(\hat{\Phi})$, where SE is the standard error of estimate.

***Table 7.1:*** *Mean values, standard deviation (SD), population coefficient of variation (CV) and ranges of the properties of the bovine cubes*

| Quantity | Direction | Mean | SD | CV(%) | Range |
|---|---|---|---|---|---|
| Young's Modulus (MPa) | PD | 1195 | 617 | 52 | 429 - 2380 |
| | AP | 770 | 453 | 59 | 187 - 1573 |
| | ML | 931 | 496 | 53 | 285 - 1908 |
| Strength(MPa) | PD | 8.05 | 4.15 | 52 | 2.9 - 15.20 |
| Velocity $(m\ s^{-1})$ | PD | 2252 | 170 | 7.5 | 2041 - 2543 |
| | AP | 2094 | 155 | 7.4 | 1814 - 2354 |
| | ML | 2171 | 148 | 6.8 | 1948 - 2400 |
| nnBUA $(dB\ MHz^{-1}cm^{-1})$ | PD | 42.15 | 14.83 | 35 | 24.73 - 70.54 |
| | AP | 34.02 | 7.05 | 21 | 23.76 - 50.03 |
| | ML | 41.69 | 12.46 | 30 | 27.73 - 64.29 |
| Permeability $(*10^{-13}m^{2})$ | PD | 1809 | 1712 | 95 | 52 - 5000 |
| | AP | 2533 | 1986 | 78 | 203 - 6440 |
| | ML | 2256 | 1909 | 85 | 200- 6411 |
| Density $(kg\ m^{-3})$ | - | 495 | 122 | 25 | 309 - 697 |

*Table 7.2:* The t-test results for Young's modulus, Velocity, BUA and Permeability in the different directions (n = 18).

| | Operation[1] | Mean[2] | T Value | P Value |
|---|---|---|---|---|
| Young's modulus (MPa) | PD-AP | 424 | 5.63 | 0.000 |
| | PD-ML | 263 | 5.10 | 0.0001 |
| | ML-AP | 161 | 3.47 | 0.0029 |
| Velocity $(m\ s^{-1})$ | PD-AP | 158 | 4.09 | 0.0008 |
| | PD-ML | 81 | 2.79 | 0.013 |
| | ML-AP | -77.3 | -2.34 | 0.032 |
| nnBUA $dB\ MHz^{-1}cm^{-1}$ | PD - AP | 8.14 | 2.94 | 0.0091 |
| | PD - ML | 0.46 | 0.16 | 0.87 |
| | ML - AP | 7.67 | 2.65 | 0.017 |
| Permeability $m^2$ | PD-AP | -724 | -5.98 | 0.000 |
| | PD-ML | -447 | -4.20 | 0.006 |
| | ML-AP | -277 | -3.62 | 0.0021 |

# 7.3 Discussion of the Mechanical Properties of Bovine Cancellous Bone.

## 7.3.1 Comparison with Reported Data

There is an extensive amounts of information on the mechanical properties of bovine cancellous bone measured *in vitro*. The data is marked by large variations in Young's modulus (stiffness) and strength reported. These variations have been shown to be a function of anatomical position, loading direction and testing conditions (see Chapter 2). Some of the reported work performed in compression with the exception of Ashman et al. [1987] performed in tension, are stated in Table 7.3. From the Table it

---

[1]Difference of two directions

[2]Mean of the differences

can be seen that the data currently reported lies within the range of previous work, especially those of Hodgkinson and Currey [1990]. The relatively high values of the work of Ashman et al. [1987] could be due to the fact that they were confined.

*Table 7.3:* *Some of the reported mechanical data of bovine cancellous (femi ) bone.*

| Source | Young's Modulus (MPa) | Strength (MPa) | Density (kg m$^{-3}$) |
|---|---|---|---|
| Cassidy and Davy (1985) | 168.6 ± 39 | 7.94 ± 1.57 | 478 ± 23 |
| Ashman et al. (1987) | 337 - 3534 | - | 323 - 652 |
| Hodgskinson & Currey (1990) | 35 - 1732 | - | 174 - 705 |
| Turner & Eich (1991) | 20.7 - 954 | 0.54 - 9.52 | 207 - 1125 |
| Present Studies | 187 - 2380 | 2.9 - 15.20 | 330 - 697 |

## 7.3.2 Orientational Dependence of Young's Modulus

Tables 7.1 and 7.2 illustrates the directional dependence of Young's modulus. The lowest significance was between mediol-lateral and anterior-posterior ( $p < 0.0029$, t =3.47). The anisotropy is not surprising since cancellous bone remodels to external stress hence the arrangement of the trabecular struts will depend on location and direction. This is in line with the functional adaptation postulated by Wolf [ 1889]. As expected the proximal-distal direction gave the highest Young's modulus (Table 7.1) which is the load bearing direction. The directional dependence of the mechanical properties of cancellous bone has been investigated by other researchers. These include the work of William and Lewis[1982], Bensusan et al. [1983], Ciarelli et al. [1986] and Cassidy and Davy [1986]. William and Lewis [1982] were able to demonstrate anisotropy in elasticity of cancellous samples from human proximal tibia. They found out that the ratio of vertical (PD) to lateral (ML, AP) stiffness ranged up to a factor of 10, with an average value of 3 to 4.

Results from the present studies (bovine proximal femi) showed average ratio of a factor of 1.5. A possible source of low ratio in the directions as compared to William and Lewis [1982] who used a 6 mm cubic specimens could have arisen from the size of the test specimen. In this study the 20 mm cubic specimens encompassed different

structures. As seen from Figure 1 different locations were used and Young's modulus has been shown to vary with the anatomical position, since different positions have different functional needs and hence different stiffness. William and Lewis's findings led them to suggest that Young's modulus anisotropy was caused by the difference in deformation mode with direction. Our Young's modulus values agree well with the work of Bensusan et al. [1983] who also carried out their investigation on femi samples and reported the transverse direction to be significantly less than the longitudinal direction. Their reported Young's modulus was in the range of 150 - 2500 MPa.

### 7.3.3 Power Law Relationship

The general consensus in the literature is that there is a power relationship between Young's modulus and apparent (structural) density. This is because of the similarity to rigid foams [Gibson, 1985] and also because the power law equation provides an improvement in extrapolation to zero density [Currey, 1986]. Using this knowledge, raw data of the present work was thus transformed into log to base ten scale. A linear regressional analysis was then applied to the log of Young's modulus (E) versus log of density ($\rho$). The results are given in the Equations 7.3 - 7.5

$$\log E_{PD} = -2.30 + 1.98 \log\rho \qquad R^2 = 81\% \qquad (7.3)$$

$$\log E_{AP} = -3.70 + 2.42 \log\rho \qquad R^2 = 83\% \qquad (7.4)$$

$$\log E_{ML} = -2.53 + 2.03 \log\rho \qquad R^2 = 87\% \qquad (7.5)$$

The ultimate compressive strength ($\sigma$) (previously explained in Chapter 4) was measured for one direction (PD) only. A linear regression analysis of log of strength versus log of density resulted in Equation 7.6.

$$\log\sigma = -5.05 + 2.21 \log\rho \qquad R^2 = 91\% \qquad (7.6)$$

$$\log E_{PD} = 2.26 + 0.83 \log\sigma \qquad R^2 = 71\% \qquad (7.7)$$

The close correlation between Young's modulus and density, (Equations 7.3 - 7.5) indicate that density is an important predictor of Young's modulus (stiffness). The 20%

variation may be due to structural differences between specimens and/or also from experimental errors in both density and Young's modulus measurement.
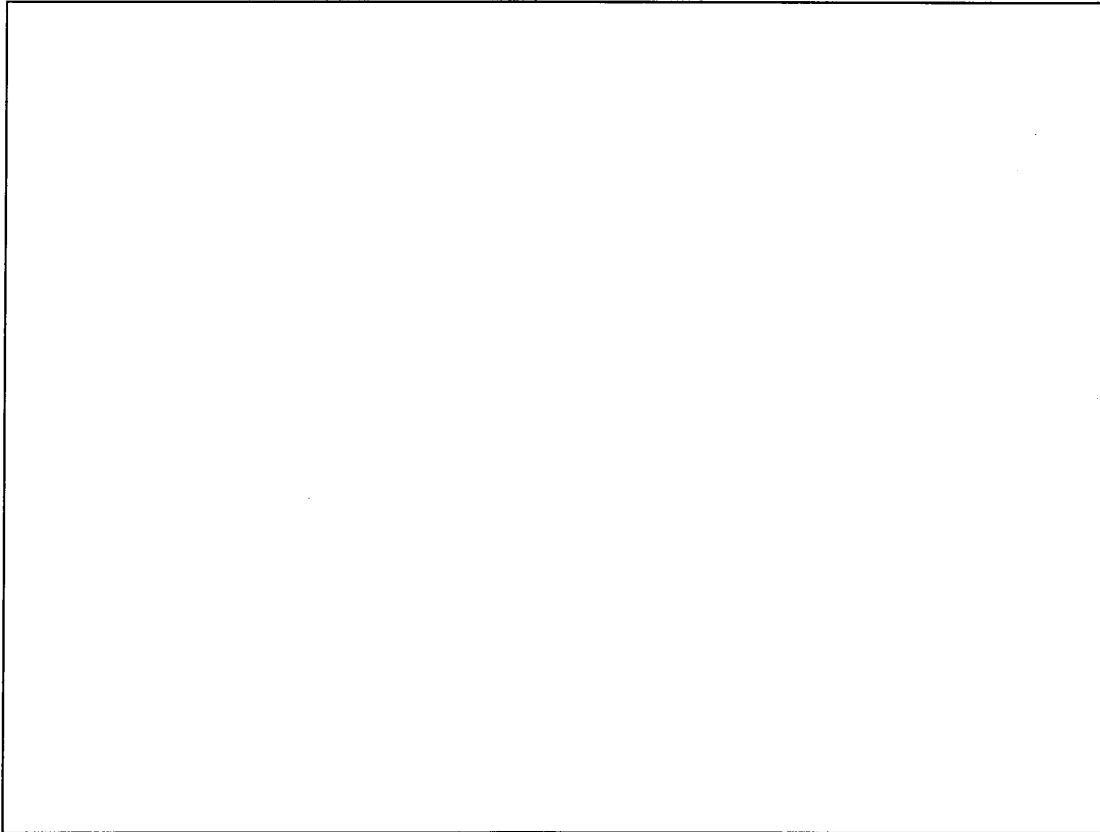


*Figure 7-2: The Relationship Between Young's Modulus and Density for the Three Orthogonal Directions*

There is no general consensus in the literature concerning the power of density in relationship to Young's modulus. Rice et al. [1988] comprehensively analysed a pool of data on the subject and came to the conclusion that Young's modulus varies as the square of the apparent density. Carter and Hayes who pioneered these studies, suggested a cubic relationship [Carter and Hayes, 1976, 1977]. Gibson [1985] and Gibson and Ashby [1988] used beam theories to propound cubic, quadratic and linear relationships depending on the cell structure and direction in which measurements were carried out.

From Equations 7.1 and 7.2, the gradients of Equations 7.3 - 7.5 are the power coefficients of density. An 80% confidence (since the $R^2$ values are in that range) was used to examine the significance of the gradients. Power coefficients of 1.98 ± 0.21, 2.03 ± 0.17, 2.42 ± 0.24 for PD, ML and AP, respectively (where ± is the

144

confidence interval calculated at a 80% confidence, and n = 18) were obtained. This demonstrates that Young's modulus (in the PD and ML) is proportional to the square of density, whereas in the AP it is well above the power of 2. This further supports the directional dependence of Young's modulus. Theoretically, the cell structure determines the mode of deformation, consequently directional variation in structure will affect the Young's modulus dependence on density. The curious finding was that the direction with the highest Young's modulus values had the smallest power coefficient. This is in contrast to the hypothesis of Gibson [1985] which states that more dense material have a close cell structure and have a higher power. The same trend is observed for the intercept values. These results demonstrate that stiffness is dependent on the direction of measurement as well as density. Caution must therefore be exercised when an accurate prediction of Young's modulus is performed from measured density.

The results presented in Equations 7.3-7.5 agree with the works of Bensusan et al. [1983] and Hodgskinson and Currey [1990] who carried out their investigation on bovine femi. They found out that Young's modulus more closely followed a density squared relationship over the density range investigated. It is important to note that although Hodgskinson and Currey[1990] carried out their investigation in three perpendicular directions, the correlation analysis was only done for the mean of the three directions. It is difficult to compare these results with theoretical predictions because these studies employed different regions of the femur which encompasses different structures. The theoretical predictions are for homogeneous structures only. The variety of structure in the femur is evident from the work of Whitehouse and Dyson [1974] on human femur who demonstrated that rod-like structures develop in regions of low stress and plate-like structures occur in regions of higher stress.

There is also controversy concerning the relationship between strength and density. Gibson's [1985] theoretical predictions depend on the cell structure and the mechanism of deformation. For an asymmetric cell (open and closed) structure which fails by elastic buckling or plastic yielding, the model predicts a quadratic dependence. For a columnar cell structure being compressed in the longitudinal direction, which fails by uniaxial plastic yielding, the model predicts a linear dependence. If the columnar structure is compressed in the transverse direction and it fails by elastic

buckling then the model predicts $\rho^{3/2}$, or $\rho^2$ or if it fails by plastic yield then it predicts $\rho^3$. The scope of this investigation did not warrant us to study the mode of failure of the specimen. Assuming that all the specimens investigated had asymmetric cell structure, then a quadratic density dependence should be expected. Therefore the linear regression analysis of the results given in Equation 7.6 and Figure 7.4 are in close agreement with the theoretical predictions. This agreement is also supported by the statistical analysis of Rice et al. [1988] and the pioneering work of Carter and Hayes [1976, 1977] who came to the conclusion that compressive strength was proportional to the square of the apparent density.

It follows from Equations 7.3 and 7.6 that Young's modulus and strength of bovine cancellous bone are linearly proportional to each other (Equation 7.7 and Figure 7.4). This basic proportionality has been substantiated by works such as those of Brown and Ferguson [1980], Goldstein et al. [1983] and Bensusan et al. [1983]. It was deduced that the circled data points on Figure 7.4 were the greatest contributors to the variation and hence the poor correlation ($R^2 = 71\%$) of this study. Large experimental errors could have incurred in measuring these two points.
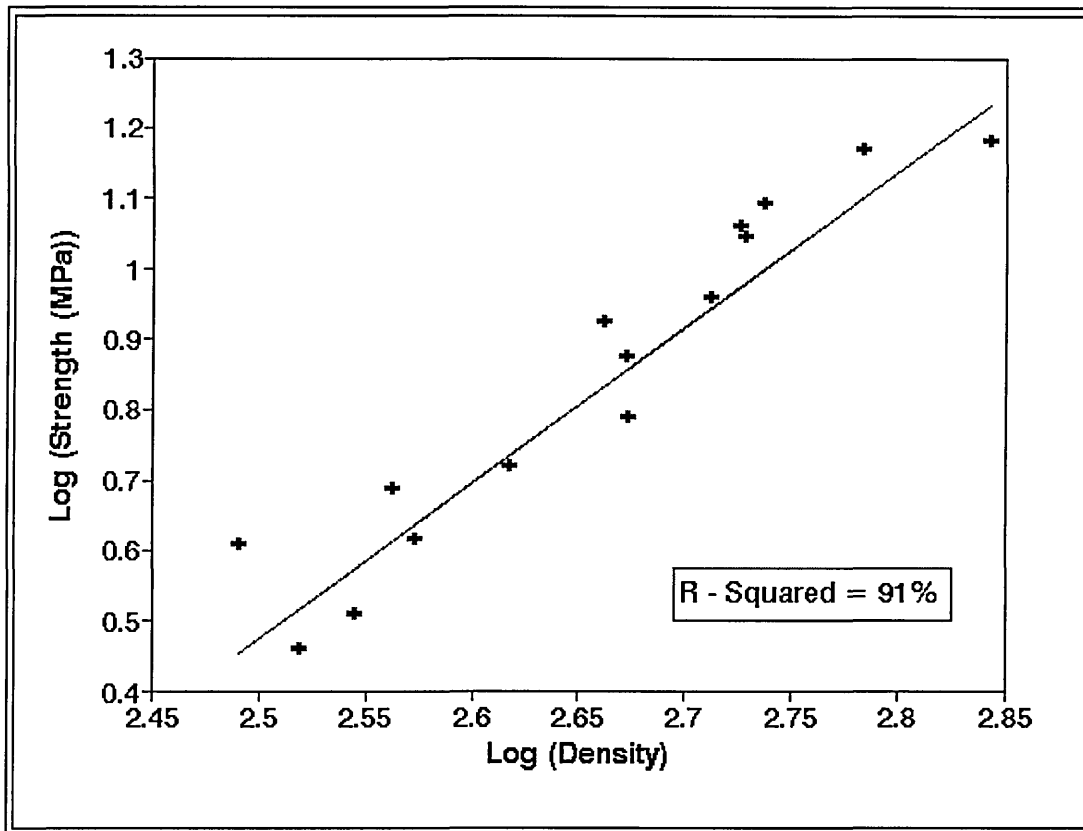
*Figure 7-3: The Relationship Between Ultimate Strength (in the PD direction) and Density*
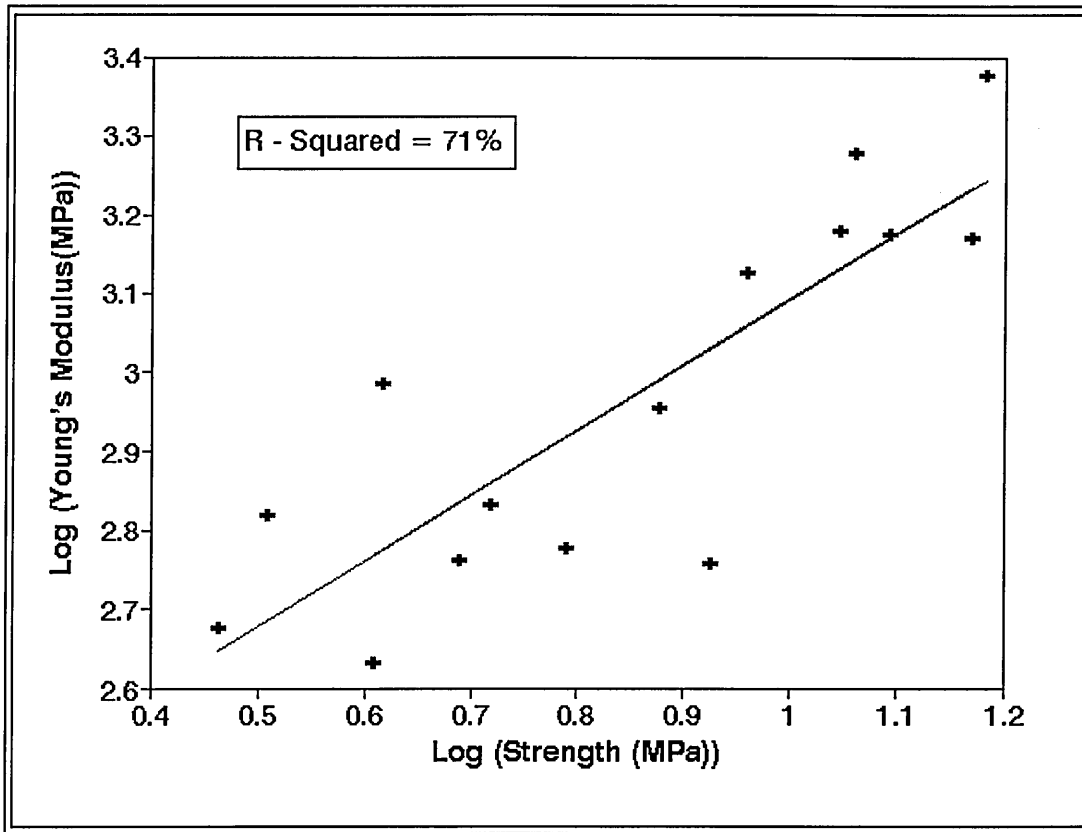
*Figure 7-4: Young's Modulus in the PD Direction Plotted Against Ultimate Strength*

## 7.4 Ultrasonic Properties of Bovine Cancellous Bone

### 7.4.1 Ultrasonic Velocity

Table 7.1 shows that velocity varies with direction and the significance of this variation is highlighted by the t-test (Table 7.2), and found to be significant (as expected). Velocity and Young's modulus are vector quantities which will vary with direction in any anisotropic medium. It therefore implies that a correlation between these two quantities will show no directional dependence. Within 80% confidence level (as used earlier) both the gradient and intercepts of Equations 7.8 -7.10 showed no difference.
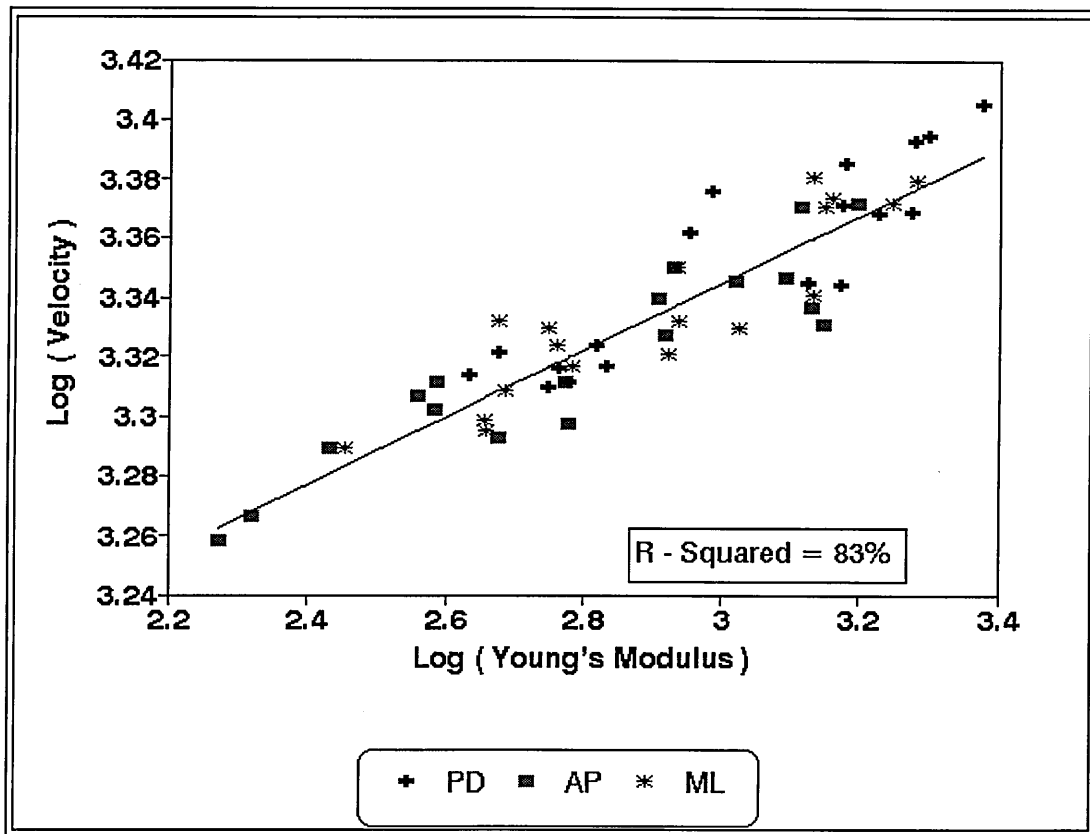
***Figure 7-5:*** *Velocity Plotted against Young's Modulus for three orthogonal directions (R - Squared is for all specimens)*

$$\log V_{PD} = 3.02 + 0.112\log E_{PD} \qquad R^2 = 77\% \qquad (7.8)$$

$$\log V_{AP} = 3.04 + 0.101\log E_{AP} \qquad R^2 = 83\% \qquad (7.9)$$

$$\log V_{ML} = 3.04 + 0.103\log E_{ML} \qquad R^2 = 78\% \qquad (7.10)$$

$$\log V_{All} = 3.0 + 0.113\log E_{All} \qquad R^2 = 83\% \qquad (7.11)$$

Velocity was also correlated to apparent density and the linear regression analysis are presented in Equations 7.11 - 7.13 and in Figure B.2 (Appendix B).

$$\log V_{PD} = 2.80 + 0.206\log\rho \qquad R^2 = 49\% \qquad (7.12)$$

$$\log V_{AP} = 2.67 + 0.243\log\rho \qquad R^2 = 69\% \qquad (7.13)$$

$$\log V_{ML} = 2.77 + 0.212\log\rho \qquad R^2 = 70\% \qquad (7.14)$$

The correlation coefficient of velocity with density is lower than for Young's modulus. The relationship between velocity and density is still not well understood because the mode of propagation is influenced by many factors such as wavelength and the structure of the propagating media.

In isotropic and homogeneous solids, both transverse and longitudinal waves can be propagated (see Section 3.4). In a straight uniform bar with small radius compared with the wavelength of the propagating waves, a bar wave represented by

$$V_{bar} = \sqrt{E/\rho} \qquad (7.15),$$

is propagated. In cancellous bone, Young's modulus has been reported to be linearly related to strength ($\sigma$) [Carter and Hayes, 1976, 1977, Rice et al. ,1988]. This has been supported by present findings (Equation 7.7, 8.3). Therefore Young's modulus could be represented as

$$E = C\sigma_u \qquad (7.16),$$

substituting Equation 7.16 into 7.15 gives

$$V_{bar} = C_1\sqrt{\sigma_u/\rho} \qquad (7.17).$$

However, the velocity measured in this investigation is the longitudinal velocity as defined by the following Equation

$$V_{long} = \sqrt{\frac{K+(4/3G)}{\rho}} = \sqrt{\frac{E(1-v)}{\rho(1-2v)(1+v)}} \qquad (7.18)$$

where K is bulk modulus, G is rigidity modulus, $v$ is the Poisson ratio and E is the Young's modulus. The bar wave relationship (Equation 7.15) was used instead of Equation 7.18 because Poisson ratio was not measured and it is impossible to measure *in-vivo,* hence

$$V_{Long} \approx \sqrt{E/\rho} \qquad (7.19)$$

Data from Kay and Laby [1989] were used to verify the feasibility of this relationship (see Appendix C). An R-Squared value of 98% was obtained for $V_{long}$ versus

$\sqrt{\dfrac{K + 4/3G}{\rho}}$ (Equation B4) but the R-Squared dropped to only 94% when the

longitudinal wave velocity were correlated with $\sqrt{E/\rho}$ (Equation B2). Therefore no

significant error was introduced in correlating $V_{long}$ with $\sqrt{E/\rho}$ . Applying this

Equation (7.19) to the data of this study gives:

$$V_{PD} = 1317 + 627\sqrt{E_{PD}/\rho} \qquad\qquad R^2 = 88\% \qquad\qquad (7.20)$$

$$V_{AP} = 1455 + 543\sqrt{E_{AP}/\rho} \qquad\qquad R^2 = 80\% \qquad\qquad (7.21)$$

$$V_{ml} = 1349 + 625\sqrt{E_{ml}/\rho} \qquad\qquad R^2 = 82\% \qquad\qquad (7.22)$$

$$V_{All} = 1441 + 574\sqrt{E_{All}/\rho} \qquad\qquad R^2 = 85\% \qquad\qquad (7.23)$$

$$V = 1149 + 7815\sqrt{\sigma/\rho} \qquad\qquad R^2 = 75\% \qquad\qquad (7.24)$$

These relationships are illustrated in Figures 7.6 and B.3. At 80% confidence limits, the application of Equation 7.19 to the data (Equations 7.20 - 7.22) showed no directional dependence. This is expected since density act as a normalising factor. Combining all the directions gave Equation 7.23 which is not significantly different from the others. The $R^2$ values of 85% is significant and similar to that reported by Ashman et al. [1987]. It is worth noting that $V_{long}$ was measured in this investigation while Ashman et al. claimed to have measured the bar wave velocity, however $V_{long}$ is thought to be more appropriate to *in vivo* investigation.
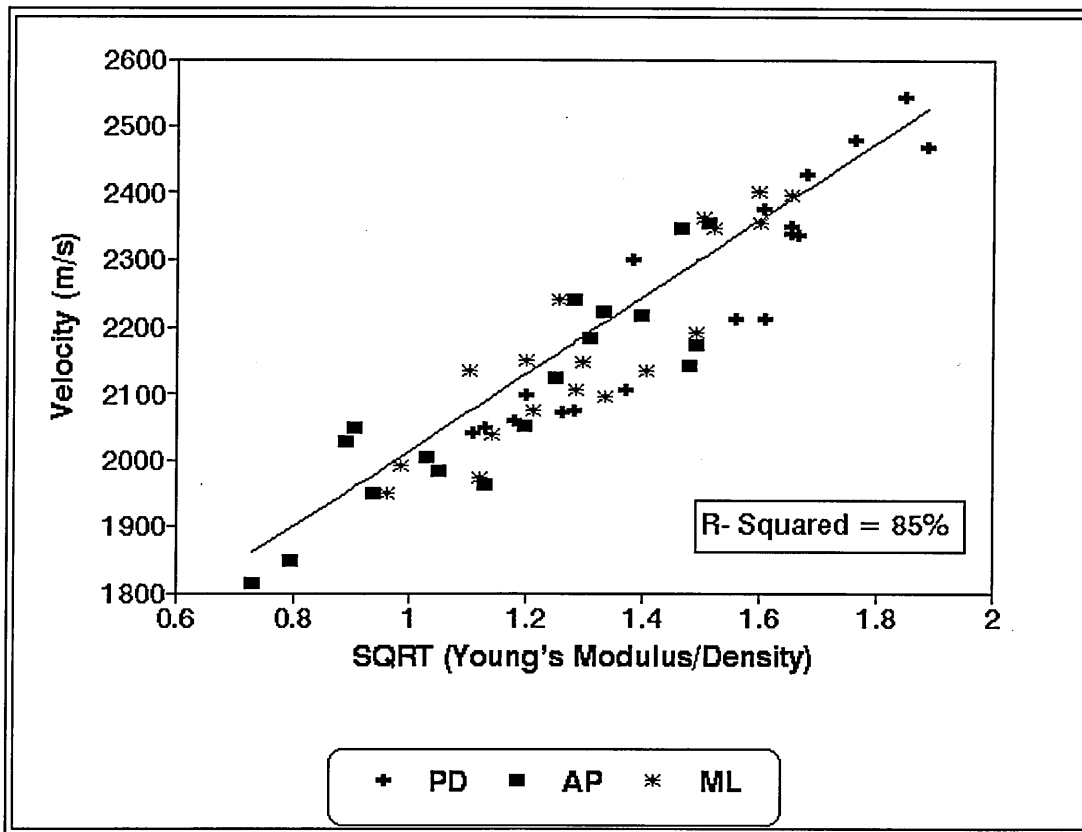
*Figure 7-6: The Relationship Between Velocity, Young's Modulus and Density*

On the other hand, when the predictive power, for Young's modulus and compressive strength were examined, they showed a high goodness of fit (Figures 7.7 and B.4).

$$E = -460 + 5.9*10^{-7}V^2\rho \qquad\qquad R^2 = 91\% \qquad (7.25)$$

$$\sigma = -280 + 4.92*10^{-7}V^2\rho \qquad\qquad R^2 = 92\% \qquad (7.26)$$

The increase in correlation coefficient, could be due to the fact that the experimental errors were lower in measuring velocity and density than in measuring Young's modulus and strength. On the other hand the reason could be more to do with the fact that by squaring you remove the need to define whether it is bar or longitudinal wave is being measured. These results are interesting because velocity and density (using QCT) are the only measured parameters *in vivo*. These findings (Equations 7.25, 7.26) have far reaching implications with respect to the management of skeletal illnesses. For instance, it could be proposed that ultrasound and QCT be complimentarily used in the determination of bone stiffness and strength, whereby the velocity from ultrasound and density from QCT are used in Equation 7.25 and 7.26.

152
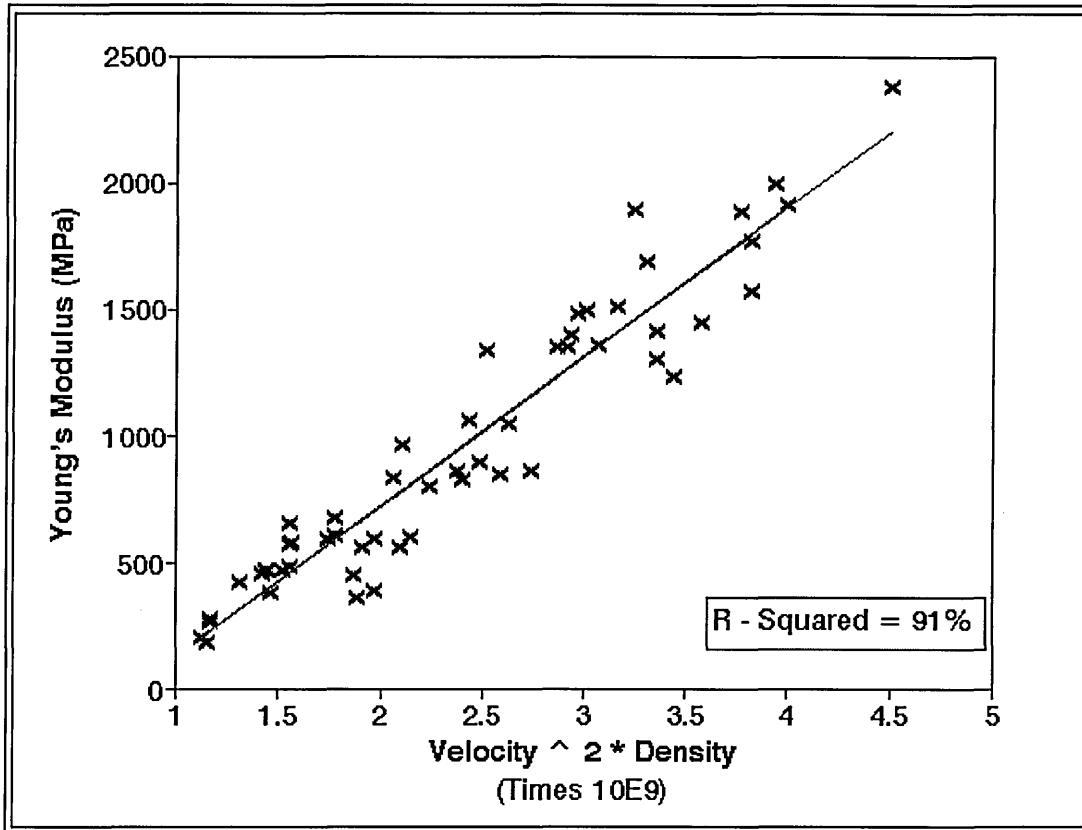
*Figure 7-7: Young's Modulus Plotted as a Function of Density and Velocity*

## 7.4.2  Broadband Ultrasonic Attenuation

The attractiveness of BUA  in cancellous bone characterisation has been its assumed ability to  provide structural information. There are few *in vitro* studies  investigating the relationship between BUA with physical and structural properties. Studies by Langton et al. [1990b], Tavakoli and Evans [1992] and Gluer et al., [1993] have thrown some light to the matter. This investigation was aimed at advancing the knowledge of the relationship between these factors. Table 7.1 and 7.2 show that BUA (like the other vectorial properties) is dependent on direction. This is in agreement with the pilot *in vitro* study of Langton et al. [1990b] who failed to show a significant relationship between BUA and density in equine third metacarpal cancellous bone, and supports the structural dependence of the BUA hypothesis.

### *7.4.2.1  The Density Dependence of BUA*

This study further investigated the relationship between BUA and density. The nnBUA values were plotted against density as shown in Figure 7.8 and it was observed that nnBUA decreases as the density increases. At lower density (higher porosity) the spread in nnBUA  was significantly greater than at higher density (lower porosity) where the bone structure approaches cortical bone and hence the structural effect diminishes. At lower density the effect of structure is greater, hence a higher spread in nnBUA values.
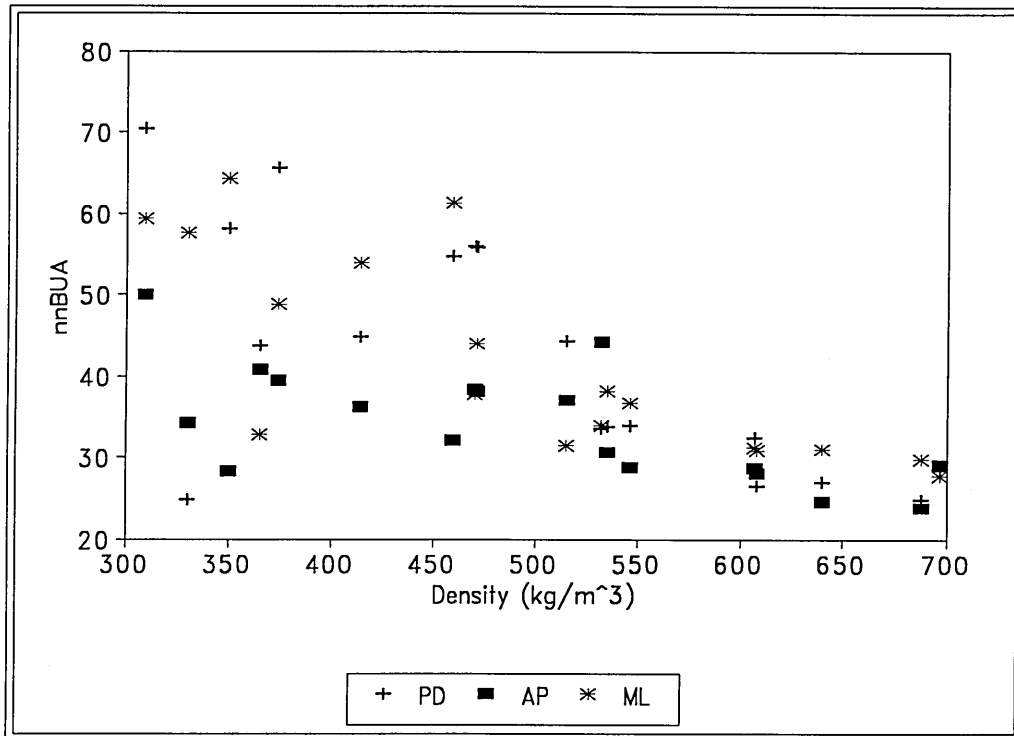
*Figure 7-8: Scatter Plot of nnBUA Against Density for the Three Orthogonal Directions*

The nnBUA values were then separated into the three different directions and plotted independently as a function of density. Logged values were used in the correlation since the dependence of BUA on density is not known.

## A :   PD  Direction



*Figure 7-9: Plot of log nnBUA Against log Density in the PD Direction*

In Figure 7.9 a linear relationship was observed for the log of nnBUA and log of density. The correlation coefficient was improved when the point circled in the Figure was not included in the analysis. This point corresponded to specimen number 2.

$$\log(\text{nnBUA}_{PD}) = 4.94 - 1.24\log\rho \qquad R^2 = 79\% \qquad (7.27)$$

The R-squared value of 79% (Equation 7.27) implies that in this particular direction density accounts for 79% of the variance in BUA. Reducing the correlation to one direction will result in a reduction in the structural variation thereby improving the relationship between BUA and density. The value of specimen 2 is out of range by approximately a factor of 2. This large deviation cannot be totally explained by experimental error, however, it is suspected that due to the low density there is a large structural deviation from the other specimens in this direction.

## B: AP Direction
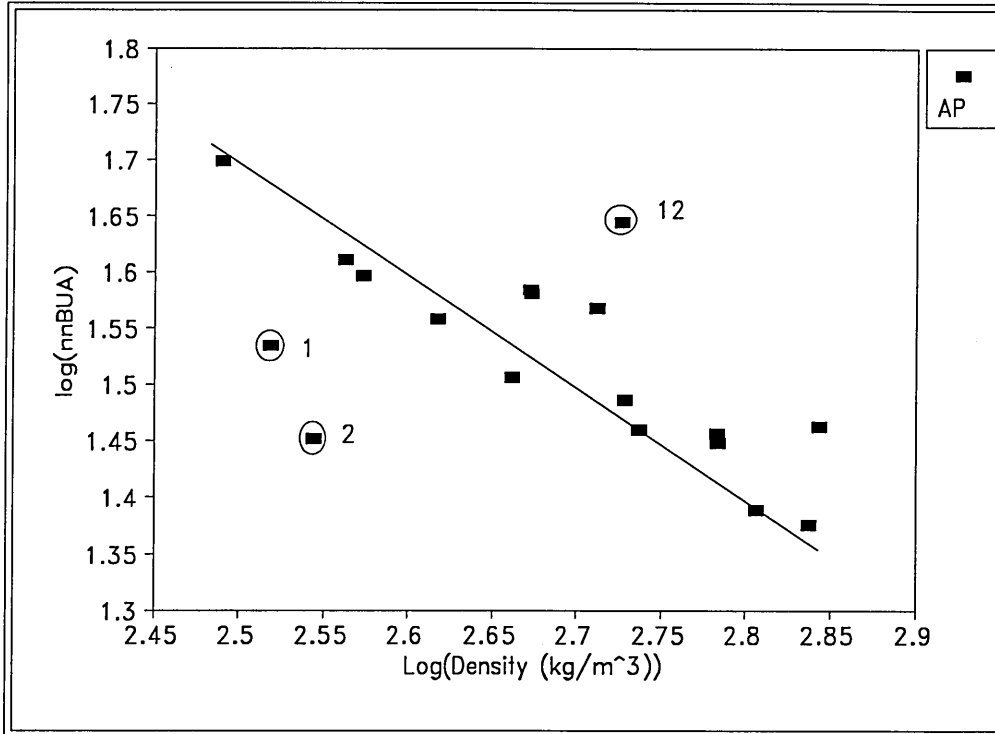


*Figure 7-10:* Plot of log of nnBUA Against log of Density in the AP Direction( the line is hand drawn).

Figure 7.10 exhibits a similar trend to that observed in Figure 7.9, however, the scatter along the linear regression line was higher. In this case three specimens 1, 2 and 12 were the highest contributor to the poor correlation. These specimen are circled on the graph(Figure 7.9)

$$\log(\text{nnBUA}_{AP}) = 2.94 - 0.527\log\rho \qquad R^2 = 43\% \qquad (7.28)$$

The same explanation as given for Figure 7.9 will hold true for Figure 7.10. As explained in Section 7.3.1, a map of the structure of the femur will reveal that open cell, rod-like structures develop in regions of low stress, while higher density, closed cell, plate-like structures occur in regions of higher stress. Unfortunately, this claim cannot be substantiated because micrograph of the specimen were not taken.

## C: ML Direction
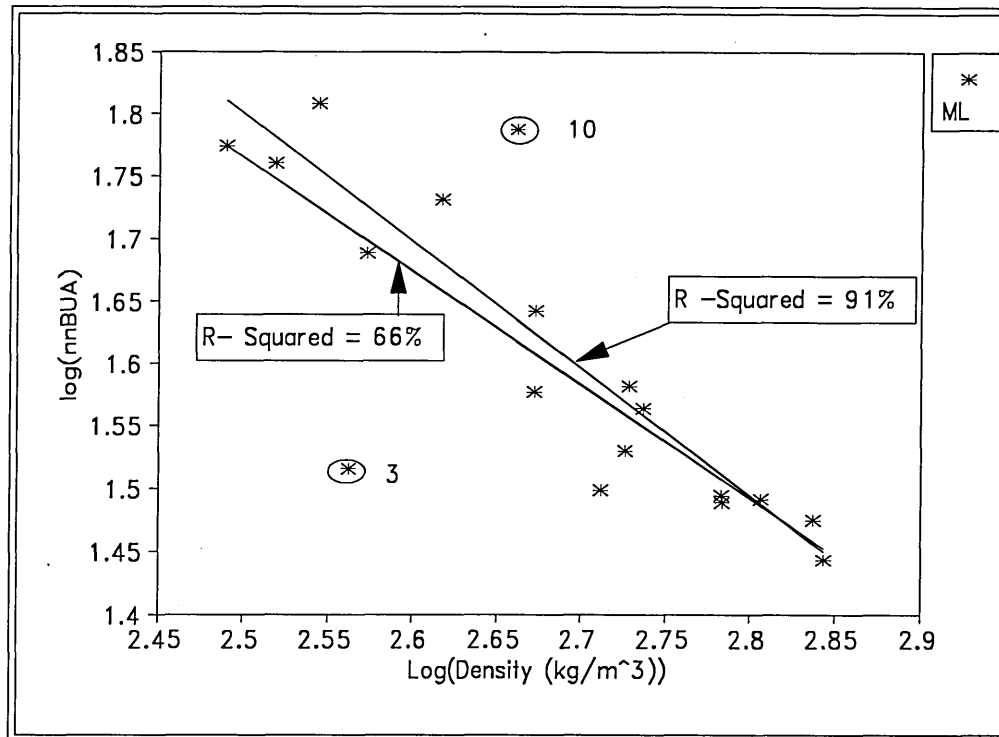


*Figure 7-11: Plot of log of nnBUA Against log of Density in the ML Direction*

The points circled in Figure 7.11 (specimen number 3 and 10) were the highest contributors to the variability. A linear regression including these points gave an R-squared value of 66% but when these points are excluded from the analysis, the R-squared value is increased to 91% and as shown in Equation 7.29.

$$\log(nnBUA_{ML}) = 4.35 - 1.02\log\rho \qquad R^2 = 91\% \qquad (7.29).$$

From the gradients of Equations 7.27, 7.28 and 7.29 one could suppose that when the structure of a set of samples is constant then BUA is linearly proportional to density.

The generally poor correlation of BUA with density was not surprising because it was shown in Chapter 6 that BUA has a parabolic relationship with porosity (density). Hence, a highly significant linear correlation could be observed if the density corresponding to the peak of the parabola could be identified and thus the graphs could be divided into two sections (ascending and descending). Among the specimens contributing to highest variability, specimen 1, 2, 3 are of lower density and thus could be at peak density values.

### 7.4.2.2  BUA as a Predictor of Mechanical Properties
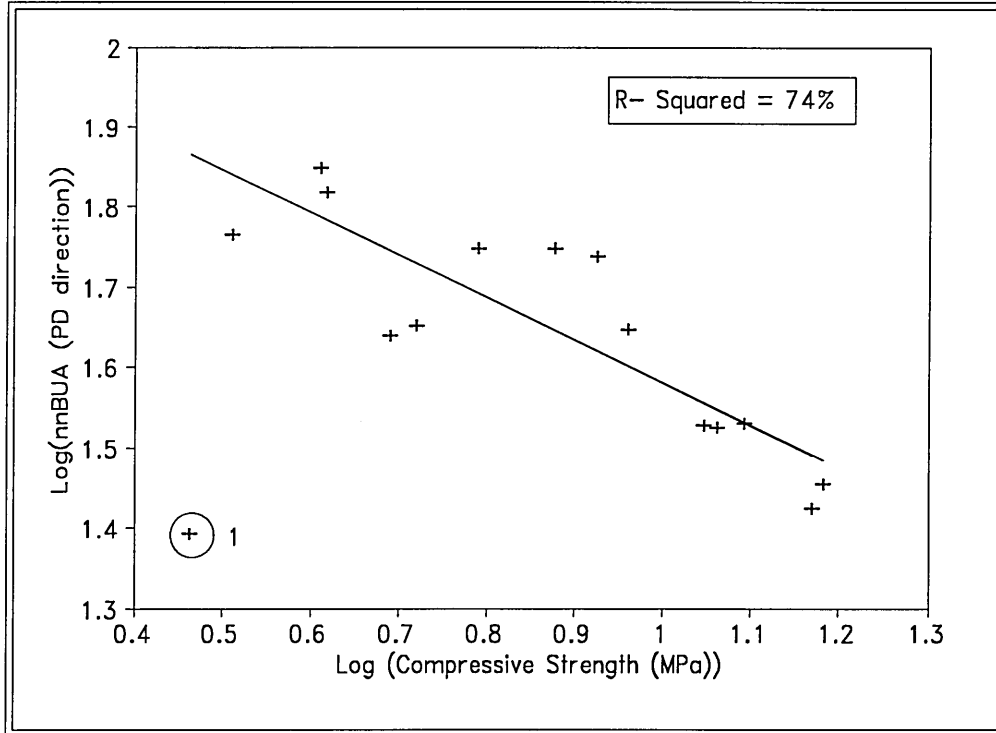


**Figure 7-12:** *Plot of log of nnBUA Against log of Strength in the PD Direction*

Specimen 1 was also the greatest contributor to the variability in the linear regression analysis of log BUA against log of strength., and excluding this point resulted in Equation 7.30; when included in the analysis an R-squared value of 24% was observed.

$$\log(\text{nnBUA}_{PD}) = 2.11 - 0.511\log\sigma \qquad R^2 = 74\% \qquad (7.30)$$

Since *in vivo* the measurements are carried in one direction, one could propose that BUA is a good predictor of strength.

The plot of nnBUA against Young's modulus(E) is presented in Figure 7.13. Two trends can be observed which are separated by a vertical line, at Young's modulus of 650 MPa. There is no defined behaviour between E and BUA below 650 MPa, even when the various directions are distinguished. Above 650 MPa, BUA decreases with increasing in E. From Figure 7.2 it can be seen that Young's modulus has a strong dependence on density, but BUA has a poor correlation with density (Figure 7.8). Hence a poor correlation between E and BUA would be expected. The relationship

159

between BUA and E (Figure 7.13) also follows the same trend as between BUA and density.

The parabolic behaviour of BUA with density observed in Figure 6.4 could be used to explain Figure 7.13. For low density and hence low E, low BUA are observed and conversely for high density and hence high E, low BUA are again observed. To be able to predict E from BUA the peak of the parabola is required.
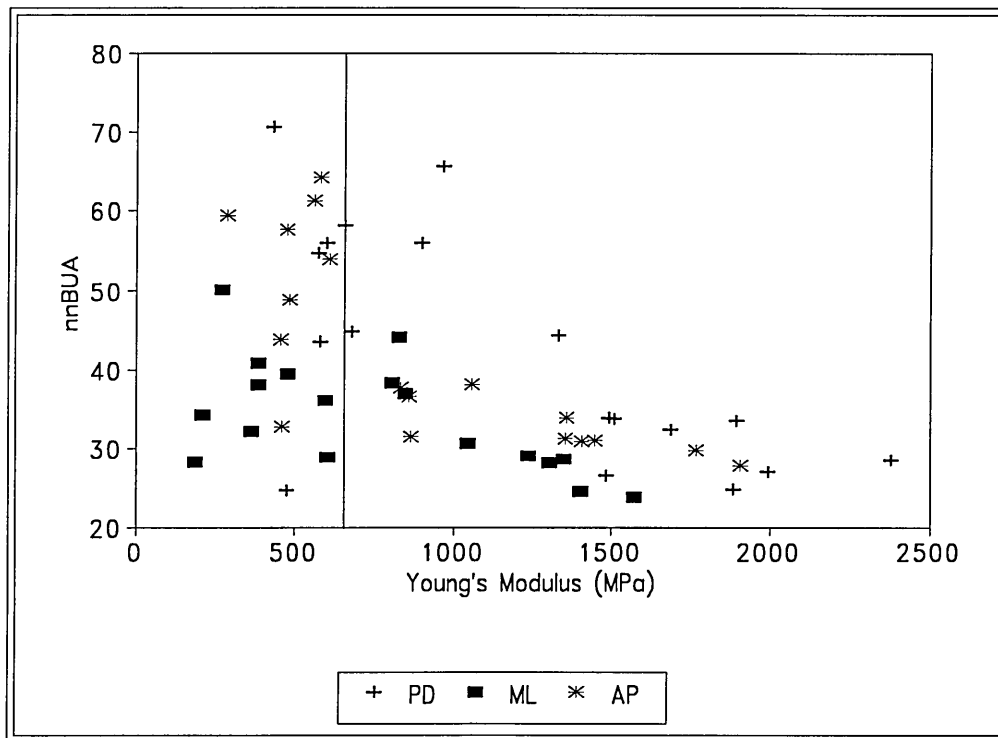


*Figure 7-13: A Plot of BUA versus Young's Modulus for the Three Orthogonal Directions*

### 7.4.2.3 BUA as a Predictor of Velocity

A plot of nnBUA versus velocity is presented in Figure 7.14. No particular relationship emerged between BUA and velocity. This could be because different parameters of varying degrees influence velocity of ultrasound propagation and the ultrasonic attenuation in cancellous bone. For instance

- Velocity of propagation will be dependent on the specimen size, density and wavelength.

- Attenuation will be dependent on wavelength, density and architecture of the specimen.

Therefore it not surprising to observe a poor correlation between velocity and BUA. A large scatter was observed in all directions at the velocity range of 1950 - 2200 (Figure 7.14). Separating the results into different directions did not improve the correlation. This is because the two parameters are vectors quantities and therefore will be direction dependent in an anisotropic material.
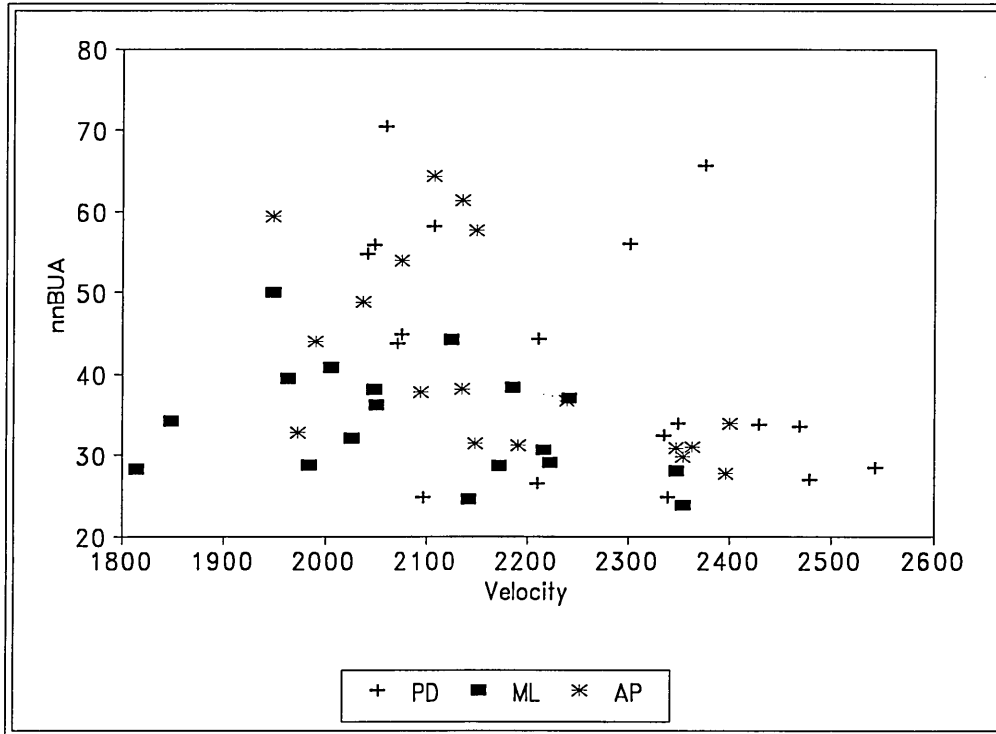


*Figure 7-14: A Plot of BUA versus Velocity for the Three Orthogonal Directions*

## 7.5 Permeability

Permeability was shown in Chapter 6 to give an indication of pore size distribution and density of the material. The permeability coefficients of the bovine specimens were measured to quantify the structure of the specimens.

The cylindrical specimen holder used for the filter experiments was fitted with a cubic adapter with bovine specimen dimensions. The cubic nature of the specimens lends itself to leakage at the edges and this was avoided by winding PFTE tape around the

cubes. The results are given in Appendix B and the means and standard deviations are presented in Tables 7.1 and 7.2. The linear regression of log of permeability versus log of density are presented in Figure 7.15 and Equations 7.31 - 7.33.

$$\log K_{PD} = 14.17 - 4.15 \log \rho \qquad R^2 = 78\% \qquad (7.31)$$

$$\log K_{AP} = 12.5 - 3.44 \log \rho \qquad R^2 = 82\% \qquad (7.32)$$

$$\log K_{ML} = 12.8 - 3.59 \log \rho \qquad R^2 = 84\% \qquad (7.33)$$

The following can be deduced from Equations 7.31 - 7.33:

* Permeability is related to the power of apparent density

* Permeability is dependent on direction with PD direction significantly different from AP and ML directions.

The strong dependence of permeability on density only leaves 16% - 22% on structure and experimental error. This statement is not totally true because the author does not know how structure is related to density in this bovine specimens, some changes in density also result in structural changes and vice versa. On the other hand the directional dependence of permeability and power coefficients confirms the dependence of permeability on structure.
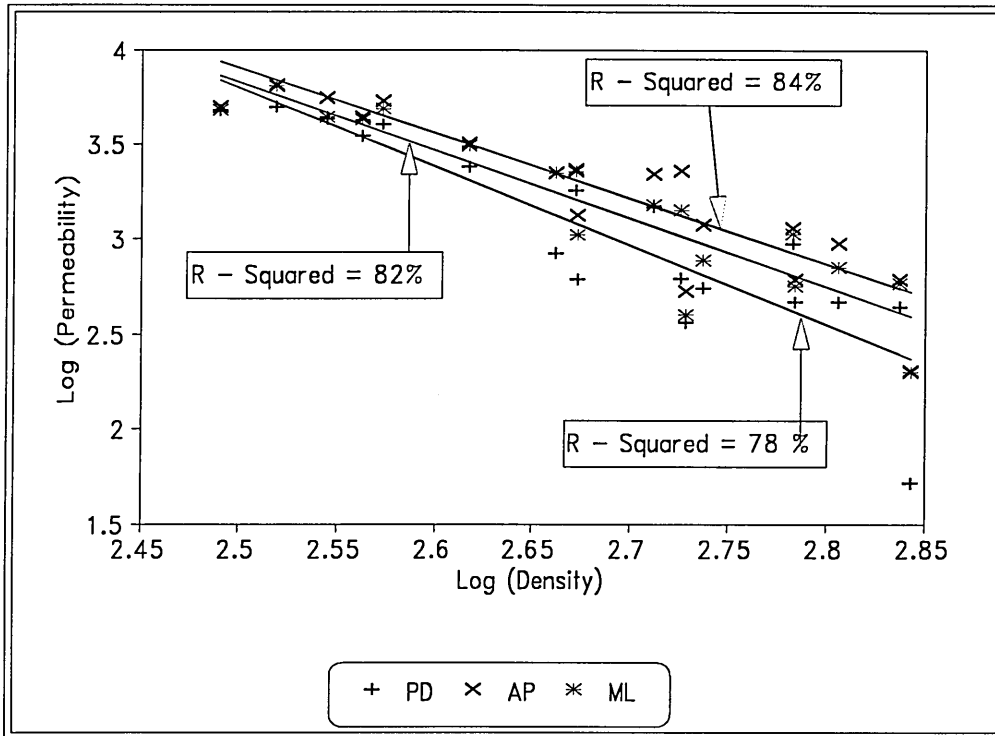
*Figure 7-15:* A plot of log of permeability versus log of apparent density for three orthogonal directions

The relationship between Young's modulus and permeability is presented in Figure 7.16. This figure demonstrates that Young modulus is inversely proportional to permeability. This is expected because permeability depends on the porosity of the sample while Young's modulus depends on the reciprocal of porosity. For example, a dense specimen will have a low porosity and low permeability but high Young's modulus.
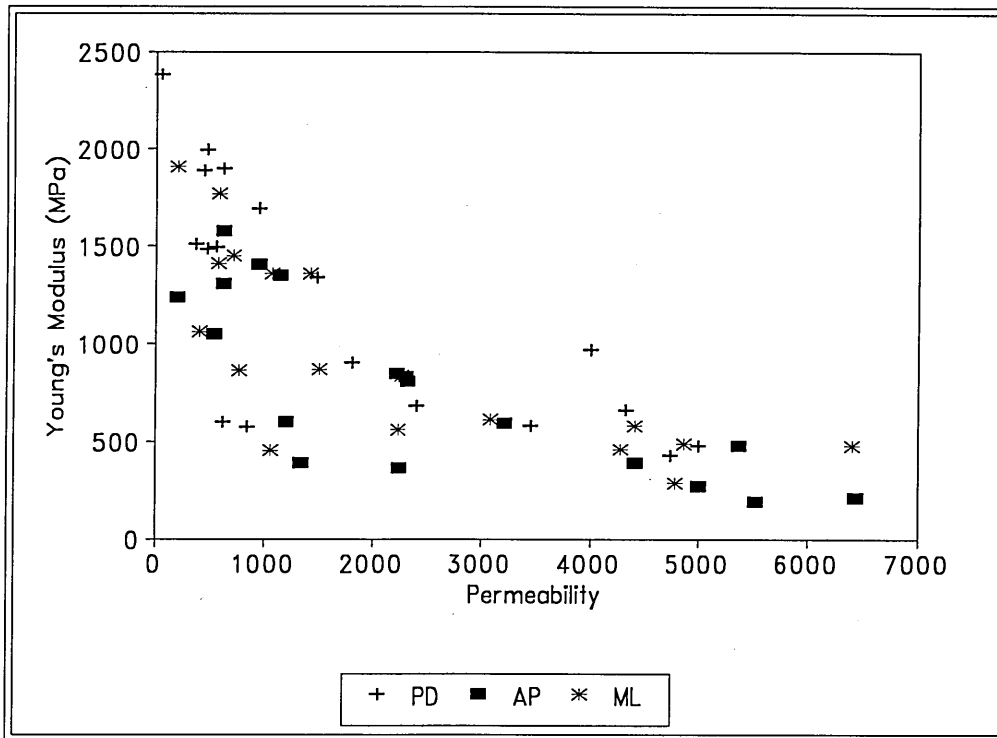
***Figure 7-16:*** *Plot of Young's Modulus versus Permeability for the Three Orthogonal*
*Directions*

A plot of strength versus permeability in the PD direction is presented in Appendix
(Figure B.1). The behaviour of strength with permeability is similar to that of Young's
modulus. A linear regression of log of strength versus log of permeability is presented
in Figure 7.17 and Equation 7.34.

$$\log\sigma = 2.013 - 0.379\log\kappa \qquad R^2 = 78\% \qquad (7.34)$$

where $\sigma$ is strength in MPa and $\kappa$ is permeability in $(10^{-13})$ $m^2$. It worth noting that
the correlation coefficient in Equation 7.34 is the same magnitude as in Equation 7.27 (
prediction of strength from BUA) and Equation 7.31 (prediction of permeability from
density). This indicates that density is a major contributor to variability in permeability
and strength.
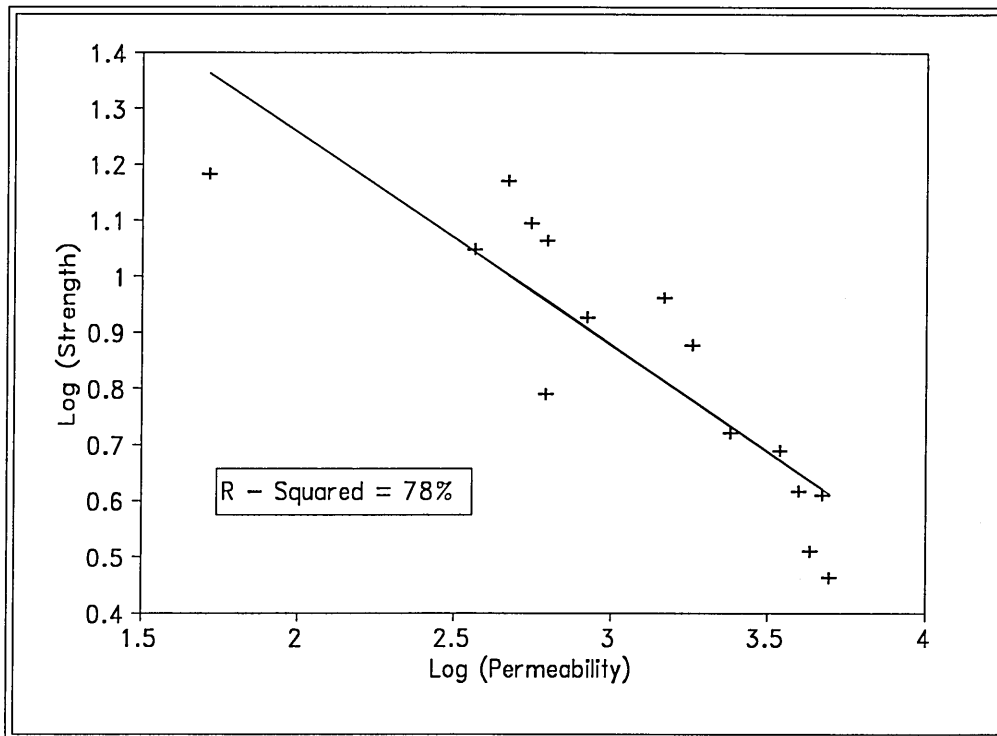
*Figure 7-17: Plot of log of Strength versus log of Permeability in PD Direction*

The relationship between velocity and permeability is presented in Figure 7.18. Velocity decreases with increase in permeability. Below a permeability value of 2000 $m^2$ there is a large scatter. At low permeability the bone structure is approaching cortical bone, but velocity is dependent on the elasticity of the sample ($\Delta E \gg \Delta \kappa$ for low $\kappa$). Hence, there is a large variation in velocity not permeability, which is a geometric parameter not material parameter.
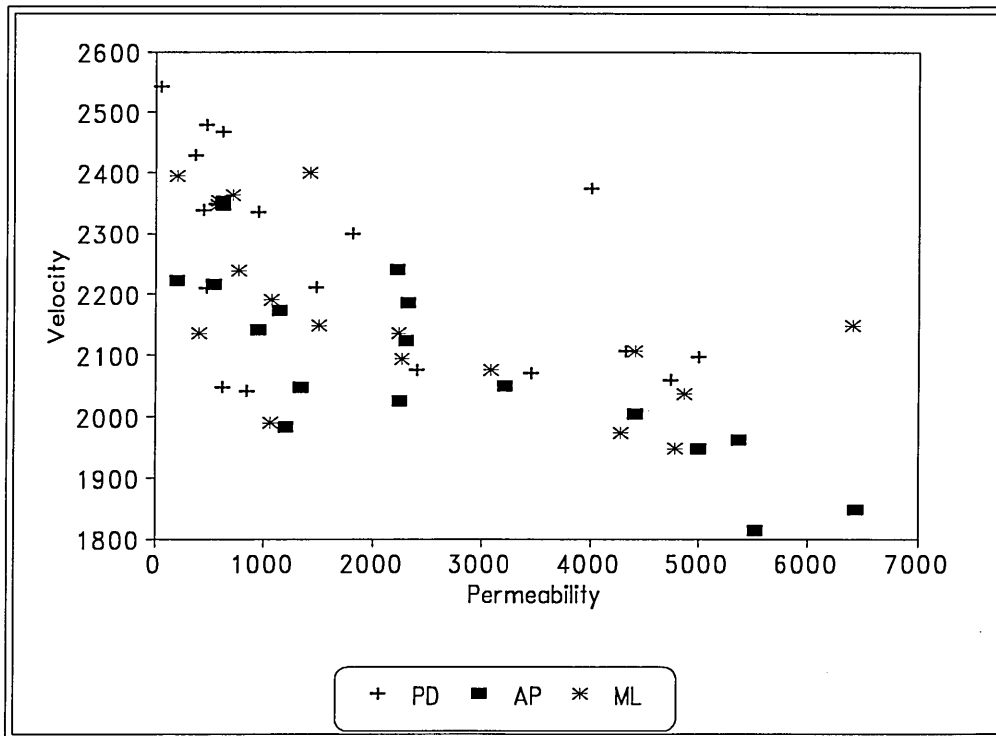
*Figure 7-18: Plot of Velocity versus Permeability for the Three Orthogonal Directions*
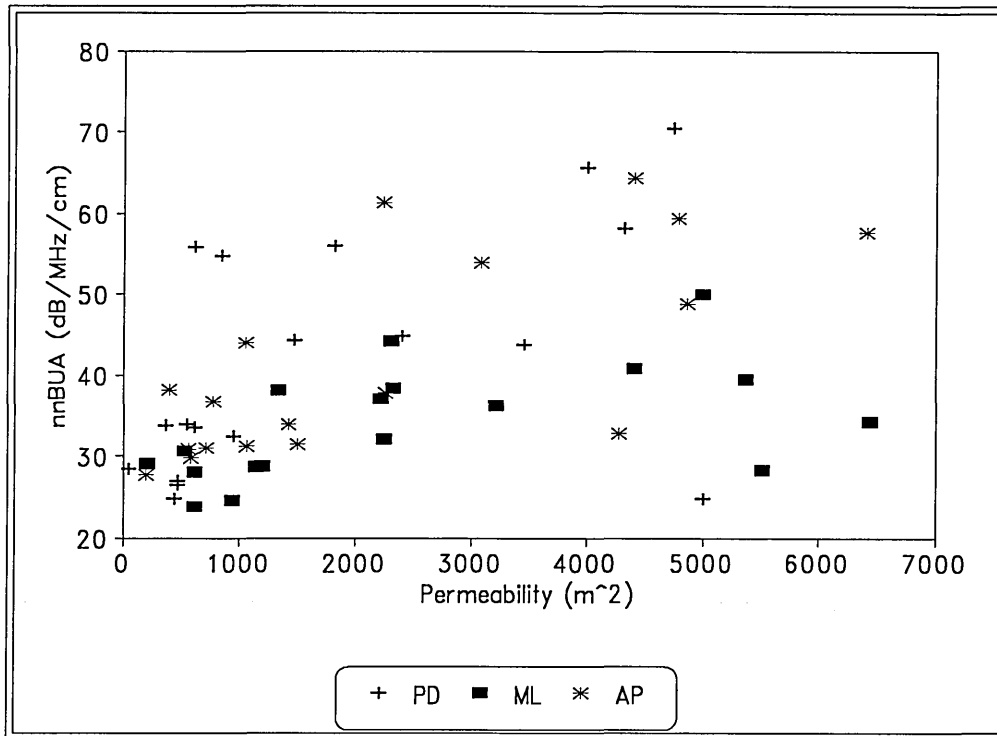
***Figure 7-19:*** *Plot of nnBUA versus Permeability*

A plot of BUA versus permeability is presented in Figure 7.19. There is an increase in BUA with increase in permeability up to a permeability value of 4500 m$^2$, and decrease in BUA thereafter. This result also confirms the parabolic behaviour of BUA with porosity. Since porosity has a large influence on permeability, the relationship between permeability and BUA would be expected to follow the same pattern as between BUA and density (Figure 7.8). There is a higher scatter observed in Figure 7.19 than in previous trends. This could be due to their differing degree of structural dependence

The major problems with permeability as a structural index is that there is a large local variation in architecture along and perpendicular to the sample length, hence permeability values may exaggerate or underestimate the structural changes occurring in the ultrasound path. Incomplete defatting present a problem with permeability measurements, resulting in low permeability values. There was no method of verifying that the defatting was completed, this problem was acute in dense samples.

# 7.6   Conclusions

The mechanical properties (Young's modulus and compressive strength) fall within reported data for bovine cancellous bone. Orientational dependence of these properties has been demonstrated. Young's modulus was related to the nth power of density, the n value being dependent on the direction of measurement( n = 1.98 for PD, 2.42 for AP and 2.03 for ML). The ultimate compressive strength in the PD direction was also found to have a quadratic relationship with density.

Ultrasonic velocity was shown to be directionally  dependent which is expected for a vector quantity measured in an anisotropic medium. Velocity correlated with Young's modulus ($R^2$ = 83%) and  there were no significant differences in the correlations when separated into the orthogonal directions. The correlation of velocity with density was lower and  dependent on direction  ( $R^2$ = 69% for AP,  70% for ML and 49% for PD). The ultrasonic velocity followed the  well established relationship between velocity,  Young's modulus and density ( $V_{bar} = \sqrt{(E/\rho)}$ and $V_{long} \Rightarrow V_{bar}$.)

BUA was also shown to be directionally dependent and the highest significance was seen between PD and AP directions. When BUA was separated into different directions and the structural variation diminished, BUA was then found to be linearly proportional to density. It worth noting that  one would not expect a correlation between BUA and density for random samples. For a specific direction (PD) BUA was found to predict strength with an $R^2$ of 74%. The behaviour of  BUA with Young's modulus also followed the  same pattern as between BUA and density. This is accounted for by the strong dependence of Young's modulus on density. There was no correlation between BUA and velocity

There was a high negative correlation between permeability and density. The gradient of the linear regression analysis varied for the different directions implying directional dependence of permeability and thus structure. A negative correlation was found between permeability with E, $\sigma$ and V. Permeability was not found  to be a good predictor of BUA for bovine cancellous bone. This is because for some of the bovine samples studied their density values are around the turning point of the BUA-density parabolic behaviour. Permeability has an inverse proportionality behaviour with density with a higher dependence than BUA.

# Chapter

# 8. THE RELATIONSHIPS BETWEEN ULTRASONIC, MATERIAL AND STRUCTURAL PROPERTIES OF HUMAN **CANCELLOUS BONE**

## *8.1 Introduction*

The samples for this *in vitro* study were obtained from the human calcaneus and the vertebrae. The calcaneus is the bone where clinical ultrasound measurements are performed, chosen for accessibility even in obese subjects, more than 90 % cancellous bone by volume, and little covering soft tissue, thus making the contribution of soft tissue and cortex negligible. In contrast to lumbar spine measurements, osteoarthritis cannot influence the results. The calcaneus is as good a site as any cancellous bone site for the prediction of hip fractures [Stewart et al., 1994]. This is because osteoporosis is a systemic disease and all bones lose mineral, albeit not all at the same rate nor in the same longitudinal profile. The calcaneus reflects this systemic nature of osteoporosis as well as any other skeletal site [Vogel et al., 1988]. The vertebrae on the other hand was chosen because of its marked anisotropy (Figure 8.26).

The methodologies employed in this study are as described in Chapter 4 . Further aspects of the sequence of calcaneus measurements were as follows:

- A coring drill was used to mark the area of interest before commencing measurement as illustrated in Figure 8.1.
- Ultrasonic measurements were carried out on the whole calcaneus samples ($nnBUA_{whole}$).

- The whole calcaneus was then cored to produce a cylindrical specimen keeping cortical end plates ($nnBUA_{core}$) intact , as shown in Figure 8.1.

- These specimens were then measured without the cortical end plates ($nnBUA_{can}$).

- The samples were then defatted and further ultrasonic measurements carried out ($nnBUA_{def}$).

- Velocities values were also measured for whole, core, cancellous and defatted samples.

- Mechanical testing was performed on the defatted cancellous cylindrical specimens. The specimens were maintained moist during all the mechanical and ultrasonic measurements.
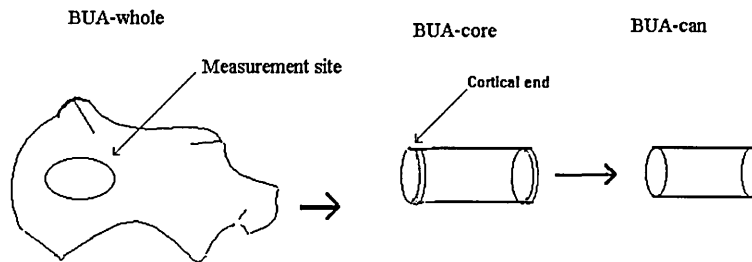


*Figure 8-1:* Calcaneus Measurement Procedure

For ultrasonic measurements six conservative measurements were recorded and the values presented in Table 8.1, D.1 and D.2 average values. The coefficient of variation are 4.4% and 1.5% for BUA and velocity respectively. The errors associated with Young's modulus density and permeability are the same as discussed in Chapter 7The next four sections will report on and discuss the results obtained for the calcaneus specimens. Section 8.6 will present and deliberate the vertebrae results and the last Section will then draw conclusions on the findings in this chapter.

## 8.2 Calcaneus Results

The results are presented in Table 8.1 and in Appendix D. The following notations and units were used in the presentation and discussion:-

- attenuation (nnBUA) - $dBMHz^{-1}cm^{-1}$;

- velocity (V) - $m\,s^{-1}$;

- compressive Young's modulus (E) - MPa;

- compressive strength ($\sigma$) - MPa;

- density ($\rho$) - $kg\,m^{-3}$ ; and

- permeability ($\kappa$) - $m^{2}$.

The correlation coefficients between $nnBUA_{whole}$, $nnBUA_{core}$, $nnBUA_{can}$, $nnBUA_{def}$, velocity, density, compressive strength and Young's modulus are provided in Table 8.2. $nnBUA_{whole}$ is the attenuation value obtained when measurements were carried out on whole bone calcaneus and represents most closely the *in vivo* situation. $nnBUA_{core}$ and $nnBUA_{can}$ are the attenuation measurements obtained on core samples with the cortical ends and on core samples without the cortical ends respectively. $nnBUA_{def}$ is the attenuation value obtained on defatted specimen.

The velocity quoted in Tables 8.1 and 8.2 represents the velocity of cancellous samples. The velocity values for whole, core and defatted samples are presented in Appendix D. The density refers to the apparent density of the cancellous samples. It was impossible to measure the apparent density of the core and whole samples as described in Chapter 4.
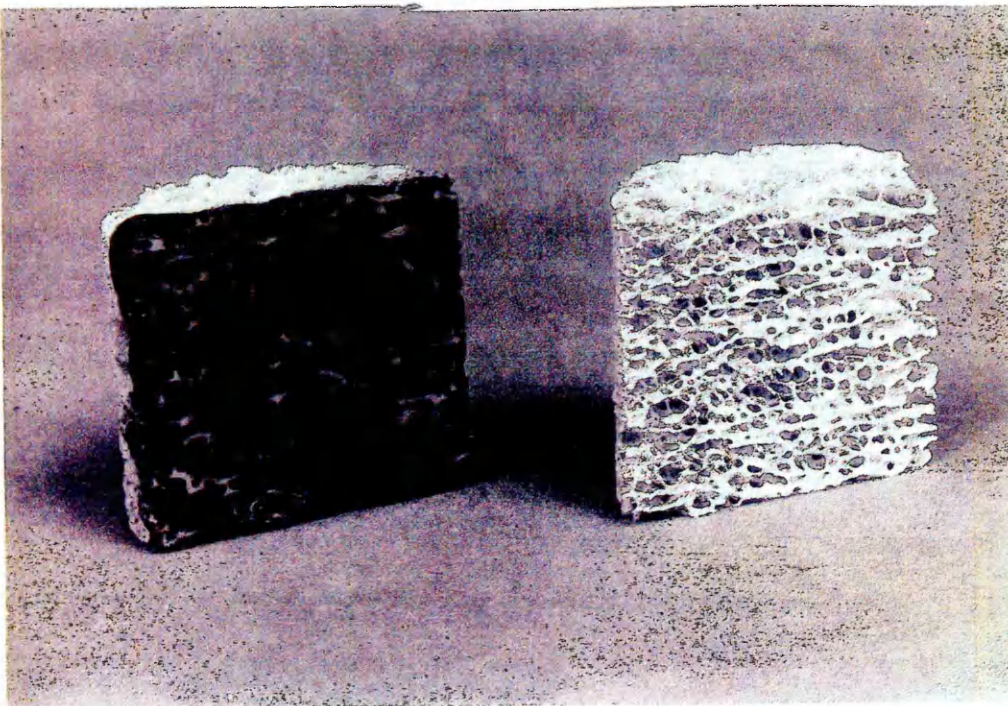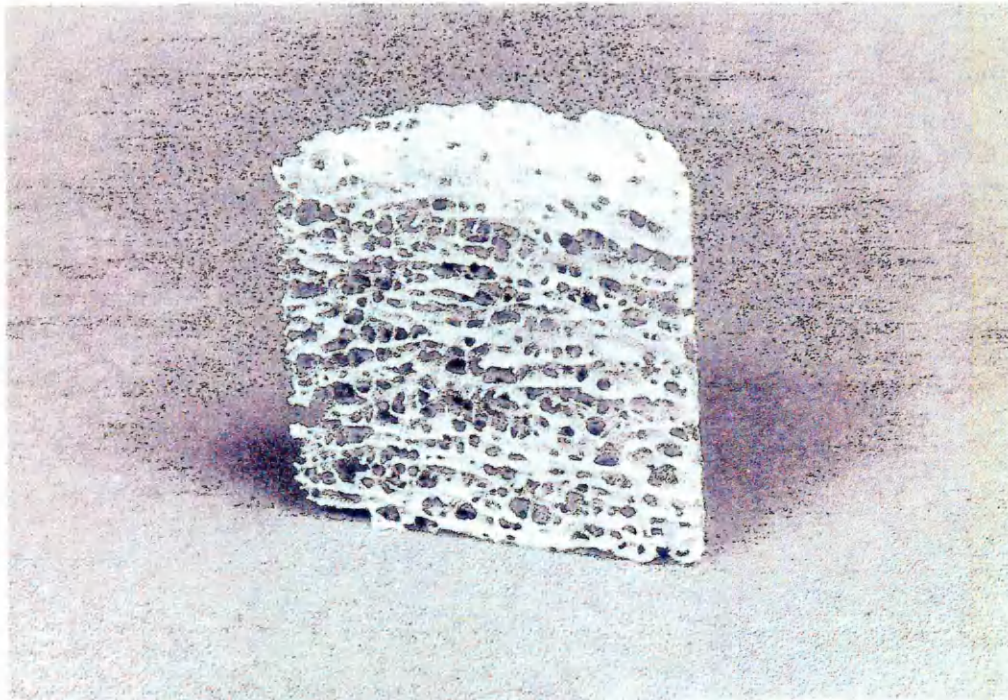
*Figure 8-2*: *Photographs of a Specimen from the Calcaneus (20 mm diameter)*

*Table 8.1:*  *Ultrasonic, Structural and Material Properties Data*

| Specimen no | Sex | Age Years | nnBUA$_{can}$ dB MHz$^{-1}$ cm$^{-1}$ | Velocity ms$^{-1}$ | Density kgm$^{-3}$ | Strength MPa | Young's modulus (MPa) | $\kappa$ m$^{-2}$ |
|---|---|---|---|---|---|---|---|---|
| 1 | F | 87 | 23.09 | 1625 | 265 | 0.623 | 41.88 | 462 |
| 2 | M | 80 | 17.87 | 1680 | 268 | 0.440 | 30.03 | 500 |
| 3 | F | 89 | 14.81 | 1490 | 236 | 0.248 | 13.45 | 527 |
| 4 | M | 84 | 31.29 | 1646 | 351 | 0.684 | 61.6 | 115 |
| 5 | F | 75 | 26.27 | 1728 | 345 | 1.028 | 70.57 | 78 |
| 6 | F | 67 | 18.10 | 1663 | 286 | 0.590 | 52.37 | 1238 |
| 7 | F | 59 | 23.84 | 1668 | 291 | 0.685 | 38.63 | 823 |
| 8 | M | 79 | 30.85 | 1776 | 354 | 1.069 | 75.0 | 114 |
| 9 | M | 71 | 25.26 | 1697 | 375 | 0.960 | 80.56 | 113 |
| 10 | F | 83 | 12.9 | 1559 | 206 | 0.129 | 7.54 | 1539 |
| 11 | F | 63 | 15.21 | 1590 | 236 | 0.483 | 29.3 | 1734 |
| 12 | M | 67 | 23.19 | 1690 | 282 | 0.679 | 48.66 | 319 |
| 13 | M | 76 | 12.82 | 1663 | 236 | 0.305 | 26.29 | 645 |
| 14 | F | 74 | 3.66 | 1500 | 143 | 0.093 | 6.03 | 2504 |
| 15 | M | 84 | 13.37 | 1610 | 245 | 0.337 | 18.84 | 1056 |
| 16 | F | 89 | 6.21 | 1517 | 182 | 0.119 | 8.20 | 1232 |
| 17 | M | 90 | 19.02 | 1637 | 265 | 0.366 | 37.56 | 875 |
| 18 | M | 59 | 16.5 | 1663 | 230 | 0.288 | 25.09 | 994 |
| 19 | F | 69 | 20.22 | 1610 | 259 | 0.265 | 33.19 | 1260 |
| 20 | M | 80 | 11.07 | 1578 | 181 | 0.105 | 7.82 | 1185 |
| Mean | | 76 | 18.28 | 1635 | 262 | 0.475 | 35.63 | 865.7 |
| Stdev | | 9.89 | 7.40 | 76.6 | 61.4 | 0.306 | 23.18 | 630 |
| CV | | 13% | 40.48% | 4.69% | 23.44% | 64.42% | 65.06% | 72.77% |

where $\kappa$ is the permeability coefficients in m$^2$ * 10$^{-13}$

*Table 8.2:* *R- Squared values ( %) for correlation between velocity, nnBUA, density, strength and Young's modulus (E) (Note that all parameters are not logged)*

| | $nnBUA_{whole}$ | $nnBUA_{core}$ | $nnBUA_{can}$ | $nnBUA_{def}$ | Density | Strength | E |
|---|---|---|---|---|---|---|---|
| Velocity | 68 | 55 | 60 | 59 | 64 | 68 | 69 |
| $nnBUA_{whole}$ | | 94 | 87 | 88 | 79 | 73 | 74 |
| $nnBUA_{core}$ | | | 89 | 85 | 76 | 69 | 71 |
| $nnBUA_{can}$ | | | | 91 | 87 | 76 | 79 |
| $nnBUA_{def}$ | | | | | 83 | 70 | 77 |
| Density | | | | | | 81 | 91 |
| Strength | | | | | | | 89 |

* Note : all the correlation coefficients in Table 8.2 are for the raw data (not logged)

## 8.3 Mechanical Properties of the Calcaneus

The discussion of the mechanical properties will be in relation to the following points:

• Firstly, how do the mechanical properties correlate with reported data.

• Secondly, The dependence of mechanical properties on density.

### 8.3.1 Comparison with Reported Data

Few studies have addressed the mechanical properties of the calcaneus. The only cited studies (to the author's knowledge) are those of Weaver and Chalmer, [1966] and Jensen et al., [1991]. Jensen et al. [1991] demonstrated a topographical variation of the mechanical and physical properties of the calcaneus. This implies that in order to obtain good comparison with previous studies and within a sample set, both sets of studies must have been carried out at the same location for all the samples. The present study was performed in the mediol-lateral direction on the flat region of the calcaneus for all the samples, that is between the medial and the lateral process of the calcaneal tuberosity. A comparison of present and previous studies is given in Table 8.3. The results reported in

174

this study (Young's modulus and strength) have a distribution lower than those reported by Jensen et al.[1991]. However the lower density reported here may explain the lower distribution. On the other hand it worth noting that our strength values are comparable to those of Weaver and Chalmer [1966] whose density values reported are ash weights

*Table 8.3: Young's Modulus, Strength and Density compared to other studies*

| Source | Young's Modulus<br>MPa | Strength<br>MPa | Density<br>$kgm^{-3}$ |
| --- | --- | --- | --- |
| Weaver and Chalmer<br>1966(Mean) | -<br>- | 0.035 - 1.06<br>(0.37) | 75 - 350<br>(186) |
| Jensen et al.<br>1991(Median) | 54 - 211<br>(83) | 1.20 - 3.20<br>( 1.70) | 270 - 450<br>(350) |
| Present Studies<br>(Mean) | 6.03 - 80.56<br>(35.63) | 0.093 - 1.06<br>(0.484) | 143 - 375<br>(261.8) |

## 8.3.2 The Power Law Relationship

The general consensus in the literature favours a power law relationship between Young's modulus and density [Carter and Hayes, 1976, 1977; Gibson, 1985; Hodgskinson and Currey, 1990], where the power lies between 2 and 3. This is due to the similarity between trabecular bone and porous engineering materials. Gibson [1985] and Gibson and Ashby [1988] have predicted the relationship between Young's modulus with density, and strength with density for the different structures found in cancellous bone using beam theories. For a structure consisting of plates connected by rods , they predicted a cubic relationship for transverse modulus, assuming the stress applied normal to the plates causes them to bend. For strength, trabecular failure can occur either by elastic buckling or by plastic yielding depending on the slenderness ratio. Gibson then predicted $\sigma \propto \rho^2$ or $\rho^{3/2}$ for elastic buckling and $\rho^3$ for plastic yield. No experimental data were used to support this model in the transverse direction.

175

Calcaneus data were logged to base ten and a linear regression analysis produced the results given in Equations 8.1, 8.2, 8.3 and Figures 8.3, 8.4, 8.5.

$$\log \sigma = -7.46 + 2.92 \log \rho \qquad R^2 = 88\% \qquad (8.1)$$

$$\log E = -6.1 + 3.1 \log \rho \qquad R^2 = 89\% \qquad (8.2)$$

$$\log \sigma = -1.73 + 0.9 \log E \qquad R^2 = 93\% \qquad (8.3)$$

The linear regression given in Equation 8.2 and Figure 8.4 demonstrated that Young's modulus was related to $3.1 \pm 0.26$ power of density. This is in agreement with the cubic prediction of Gibson [1985]. Strength was related to $2.92 \pm 0.25$ ($\pm$se) power of density, within the 95% confidence the strength is proportional to density cubed. The R-Squared values of 88% and 89% are highly significant. The power agreement with the theoretical prediction may be considered significant because the theoretical prediction is based on a regular, repeating cell, but the cell size of cancellous bone is not uniform. The cubic relationship leads to the inference from Gibson [1985] theoretical analysis that the mode of failure is plastic yielding.

Strength was related to Young's modulus by a power of $0.90 \pm 0.12$ (see Equation 8.3 and Figure 8.5). This agrees closely with the linear relationship reported in the literature [Carter and Hayes, 1977; Hodgskinson and Currey, 1990] and bovine cancellous bone findings reported in the Chapter 7. Mathematically, this is expected since both Young's modulus and strength correlates by the same power (3) with density, implying they should correlate linearly with each other.
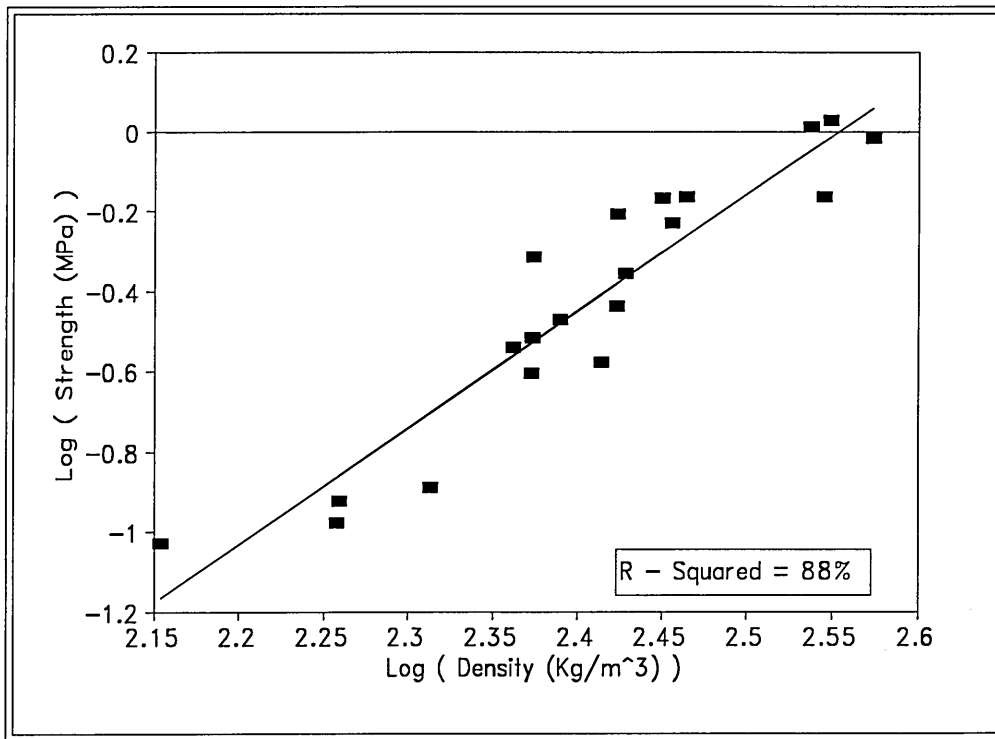
**Figure 8-3**: *The Relationship Between Compressive Strength and Density*
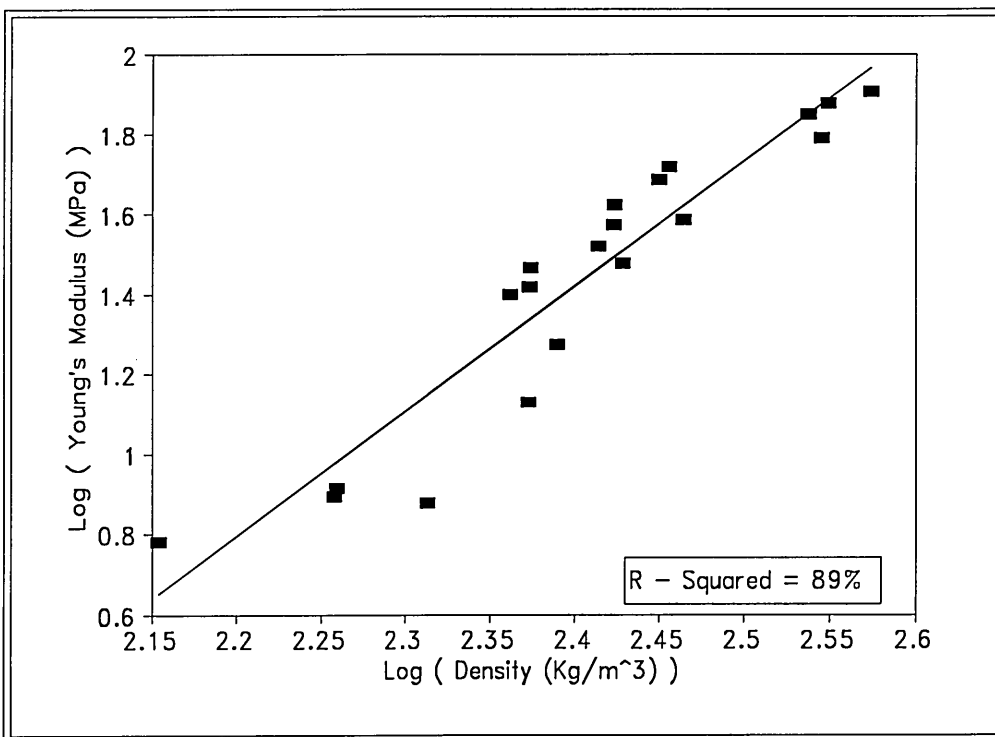


**Figure 8-4**: *The Relationship Between Young's Modulus and Density*

177
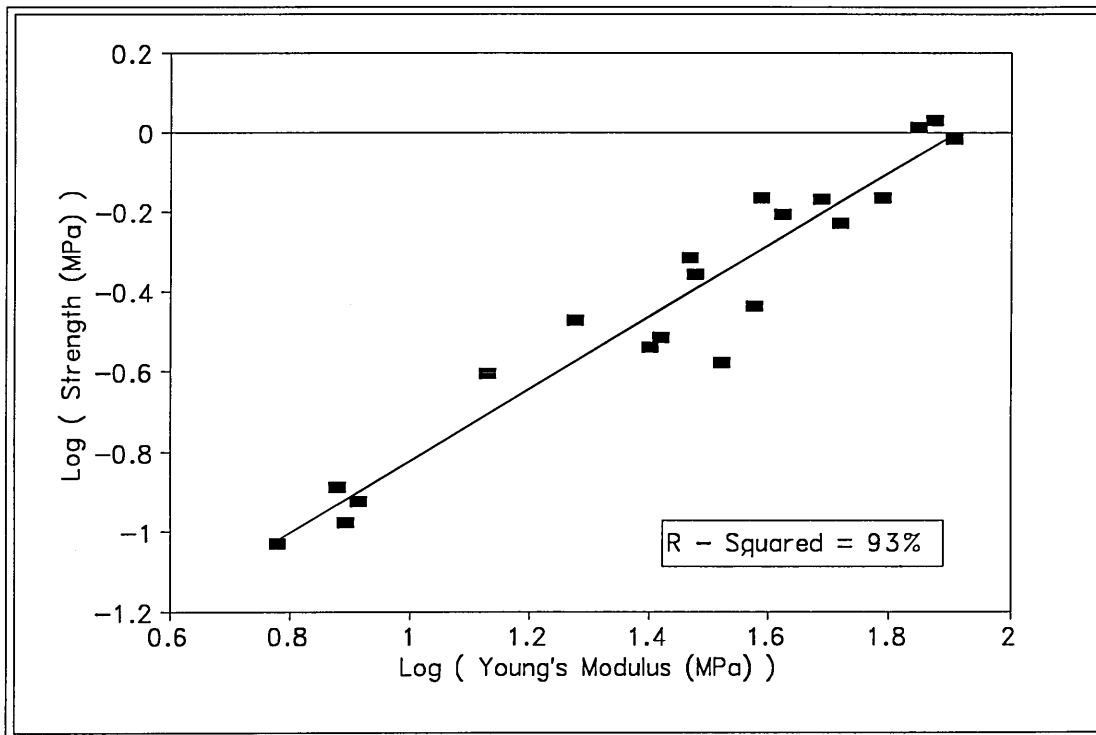
*Figure 8-5: The Relationship Between Compressive Strength and Young's Modulus*

The next step in correlating the experimental results with theoretical prediction is to determine the type of cancellous bone structure to be found in the calcaneus (Figure 8.2). The calcaneus exhibits two distinct stress patterns in the perpendicular and inferior directions [Jhamaria et al., 1983], which arises due to its functional adaptation. The perpendicular trabeculae are chiefly subjected to compressive force and inferior ones of the tuberosity are subjected to tensile forces [Gierce 1976]. The stress pattern gives rise to a structure that Singh [1977] described as plates. The plates are of irregular shape and show numerous fenestrations. They are connected by smaller plates and rods. The specimens were therefore tested along the lines of the struts and perpendicular to the plates (transverse direction), therefore the cubic relationships are in close agreement with the theoretical predictions of Gibson [1985].

# *8.4 Ultrasonic Properties of the Calcaneus*

### 8.4.1 Velocity

Velocity values were measured for whole calcaneus, core, cancellous and defatted and the results are given in Table 8.1 and Appendix D.1. The velocity values for whole and core specimen are the same within experimental error. Their mean values were 1652 and 1665 respectively. A linear regression to fit the velocity of whole specimen with that of core specimen gives the following (Figure 8.6)

$$V_{whole} = 39 + 0.969V_{core} \qquad R^2 = 91\% \qquad (8.4)$$

The coefficient of Equation 8.4 has a t-ratio of 0.32 and $p = 0.753$ . This implies that the coefficient 39 is not significant and hence $V_{whole} \approx V_{core}$ . On the other hand an analysis of the differences gives a mean value of 10.05 and a 90% confidence interval of -0.05 - 20.15. This supports the initial statement of equality of the values. The few samples whose values deviated from this general observation and hence 9% unexplained variation in Equation 8.4 could have been caused by error in thickness measurement and poor contact as illustrated in Figure 8.7.
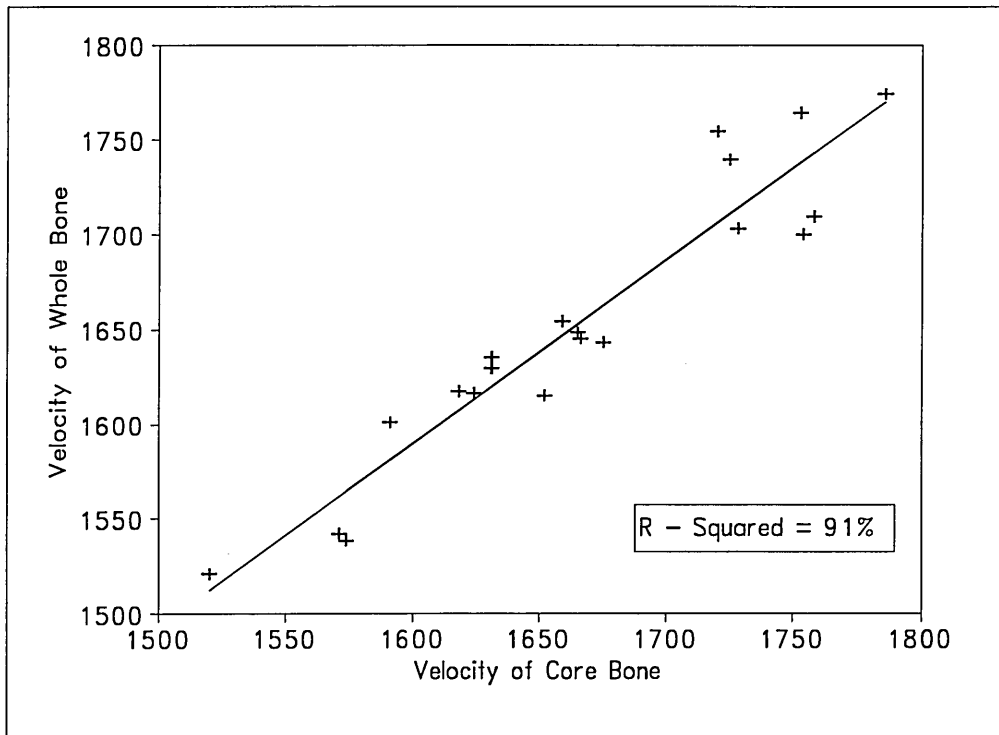
*Figure 8-6: The Correlation Between Velocity of Whole Calcaneus Bone Samples and Core Bone .*

The core and whole calcaneus bone samples are irregular and therefore posed a problem in thickness measurement and proper contact with the transducer (see Figure 8.7). The specimen diameter was 21 mm and transducer diameter was 13 mm. Therefore there was 4 mm outer radius for which the transducer position could vary. Unfortunately, these surfaces are irregular and as demonstrated in Figure 8.7 this generates contact problems and hence velocity problems, because the value obtained in Figure 8.7b will be lower than in 8.7c. This is due to the inclusion of transmission in water in Figure 8.7b. Although great effort was put into acquiring measuring condition close to the ideal situation (Figure 8.7a), it was not always possible to achieve.

Cortical End Plates

Transducer    Cancellous Bone    Transducer
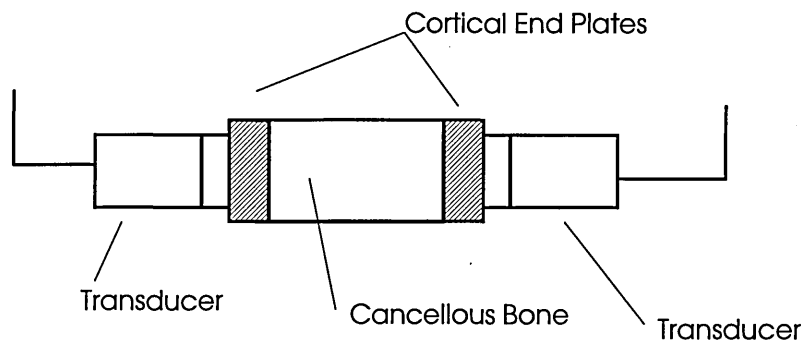
A)  Ideal Measuring Condition

Water interface
Cortical End Plates
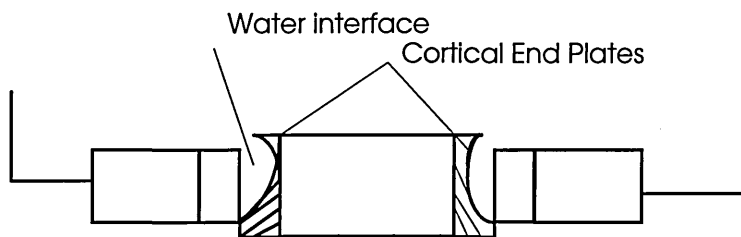
B) Measuring Condition for Core Sample
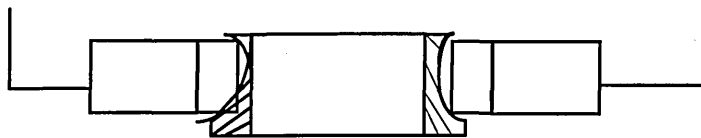
C) Another Possible Measuring Condition

*Figure 8-7:*  *Contact Problems with Whole and Core Bone Samples*

The velocity values for cancellous specimen and defatted (Appendix D.1) are also statistically the same. Their mean values were 1630 and 1626, respectively. A linear regression fit to velocity of cancellous specimen ($V_{can}$) versus velocity of defatted cancellous specimen ($V_{def}$) (Figure 8.8) gives:

$$V_{can} = -58 + 1.04 V_{def} \qquad R^2 = 93\% \qquad (8.5).$$

The coefficient of Equation 8.5 has a t-ratio of -0.54 and p = 0.599 while the gradient (constant) has t-ratio of 15.65 and p = 0.000. This implies that the coefficient value -58 is not significant and thus $V_{can} \approx V_{def}$. On the other hand an analysis of the differences gives a mean value of -3.25 and a 90% confidence interval of -10.87 - 4.37. These results are to be expected since the difference between the two cases is the fat is replaced by water, whose acoustic impedance is not significantly different from that of fat.. The 7% variation in Equation 8.5 could be attributed to experimental errors such as inadequate degassing. Also there is the problem encountered with very porous specimens where the trabeculae start to collapse when good contact is sort with the ultrasound transducers.
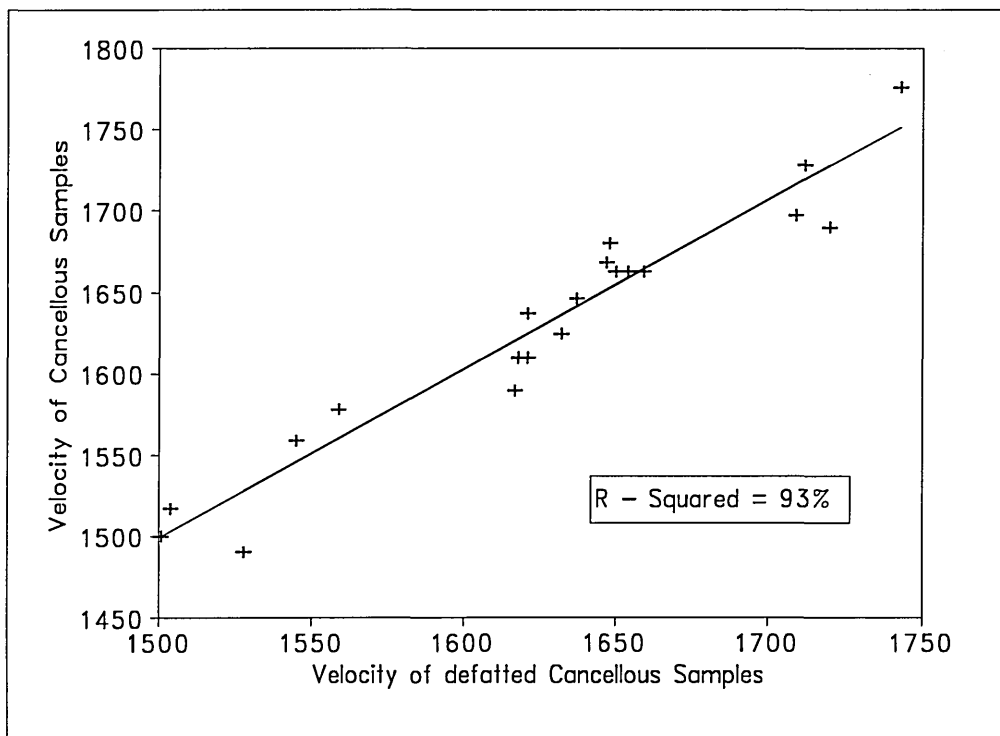


*Figure 8-8: The Correlation Between Velocity of Cancellous Bone Samples and Defatted Samples*

A correlation between velocity of whole calcaneus with cancellous specimens and whole calcaneus with defatted cancellous specimens are given below:

$$V_{whole} = 363 + 0.793V_{can} \qquad R^2 = 65\% \qquad (8.6)$$

$$V_{whole} = 225 + 0.879 V_{def} \qquad R^2 = 70\% \qquad (8.7)$$

The low correlation coefficient in Equations 8.6 and 8.7 could be related to the measuring problem described in Figure 8.7. One would expect the velocity of whole samples to be much larger than in cancellous samples due to the larger velocity value in the cortical end plates. The mean of the differences between whole velocity and cancellous velocity was 25.5 m s$^{-1}$ with a 90 % confidence interval of 7.8 - 43.2 m s$^{-1}$. There is a similar range for other combinations (whole - defatted, core - cancellous, core - defatted). The mean of the differences are statistically different but the small value could be attributed to the thin cortical endplates and reduction in velocity by the water interface in some measurements. The velocity henceforth will refer to velocity of the cancellous samples except otherwise stated.
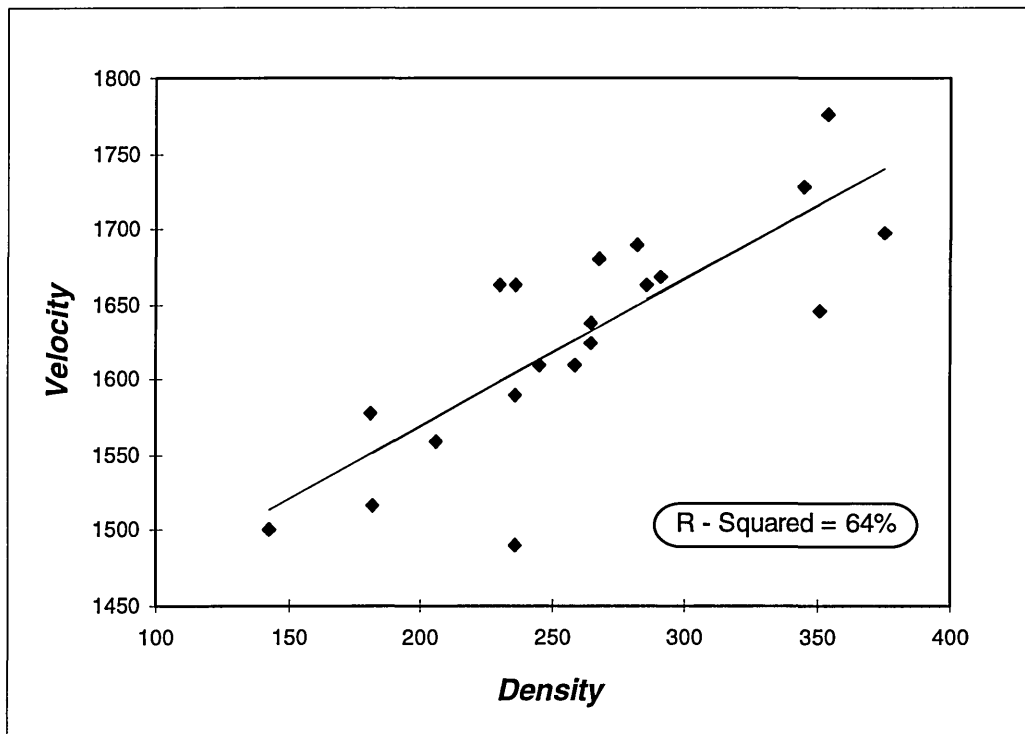


*Figure 8-9:* *Plot of Velocity Against Density*

The correlation coefficient for velocity versus density was 0.80 ($R^2 = 64\%$) (Figure 8.9). This value is lower than the 0.85 observed by Evans and Tavakoli [1990] ( $R^2 = 72\%$). Evans and Tavakoli studies were on bovine specimens, in addition Chapter 7 demonstrated a higher correlation coefficient ($R^2 = 69\%$, for logV versus log$\rho$) in the AP direction for

bovine specimen. On the other hand Waud et al. [1992] observed a lower correlation of 0.73 *in vivo* ($R^2 = 53\%$).

## 8.4.2 Velocity and Mechanical Properties

The relationship between ultrasonic velocity and mechanical properties is well established (Equations 7.15, 7.17). The problem (as discussed in Chapter 7.3) is to define the type of velocity being measured. The bar wave velocity relationship (Equation 7.18) was used and the linear regression fit given in Equations 8.8 and 8.9 and Figures 8.10 and 8.11 for Young's modulus and compressive strength respectively.

$$V = 1390 + 702\sqrt{E/\rho} \qquad R^2 = 73\% \qquad (8.8)$$

$$V = 1369 + 6460\sqrt{\sigma/\rho} \qquad R^2 = 66\% \qquad (8.9)$$
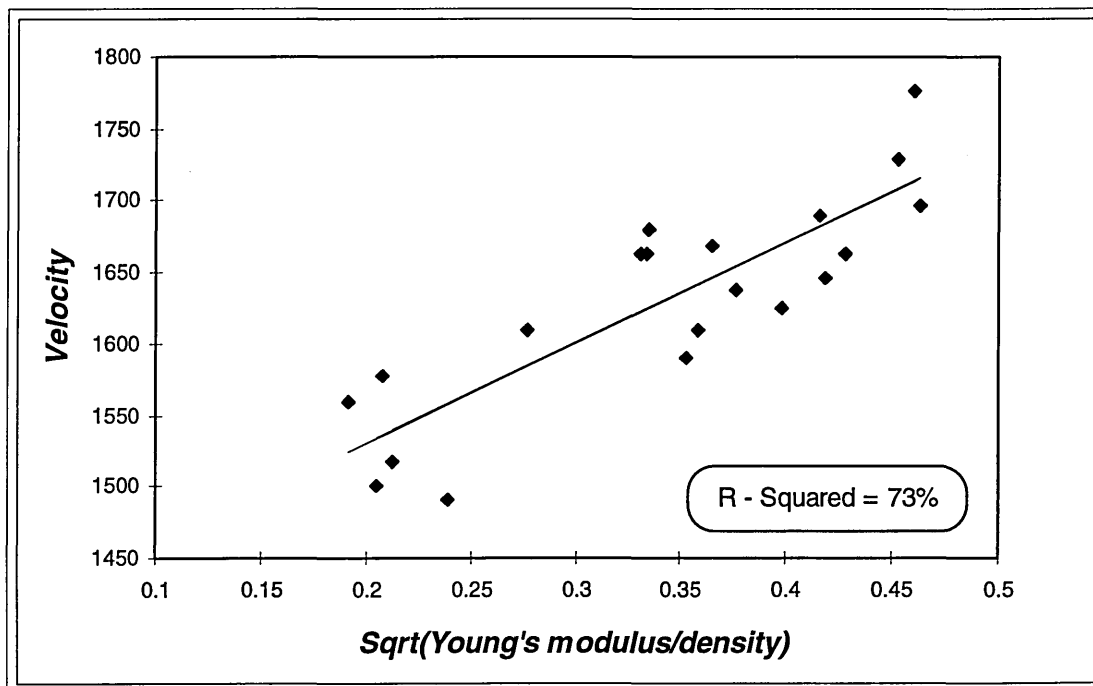


*Figure 8-10:* The Relationship Between Velocity , Young's Modulus and Density

The correlation coefficient given in Equations 8.8 and 8.9 are less significant than would be expected. One explanation could be the fact that a broadband transducer with nominal frequency of 1 MHz was used in this investigation. 1 MHz and thus a wavelength of 1.5 mm - 8.16 mm do not satisfy the condition for the application of the bar wave (Equation

7.1). On the other hand, although the 1.5 mm is greater than the cross-sectional dimension of the trabeculae, its velocity could not be considered to represent the material velocities because it has been quoted to be above 2000m/s [Ashman et al., 1987]. The correlation coefficient given in Equation 8.9 explains only 68% of the variance. Turner and Eich [1991] demonstrated a higher correlation coefficient ($R^2 = 77\%$). They carried out their experiment on bovine specimens which have a larger density range. The results reported in Chapter 7 on bovine cancellous bone over a large density range also demonstrated a higher correlation coefficient.
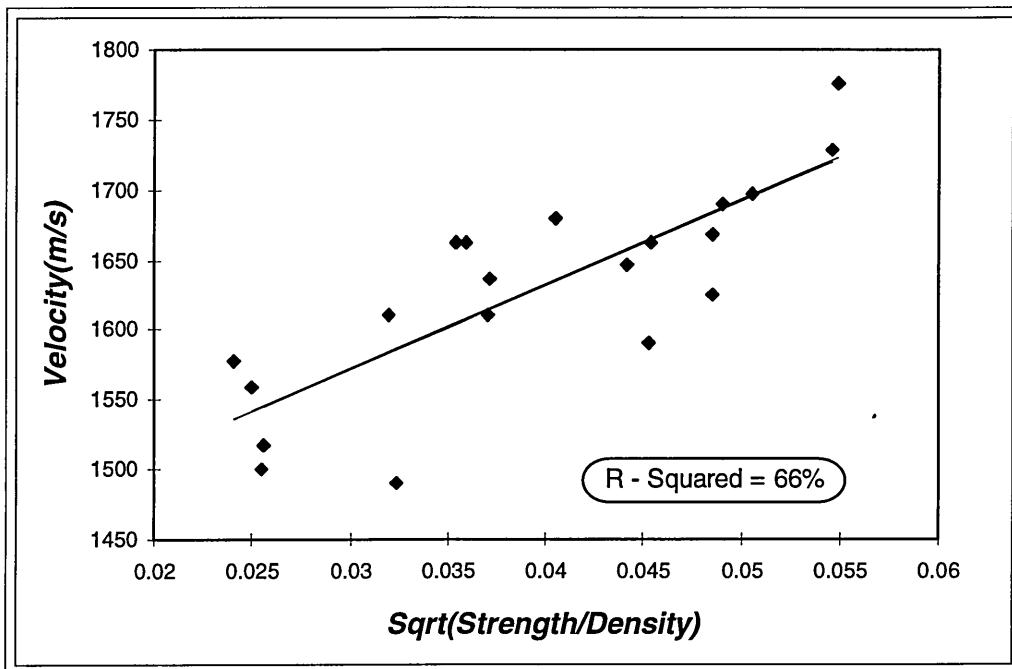


*Figure 8-11: The Relationship Between Velocity and Strength for Calcaneus*

Another possible cause of the poor correlation of velocity with young's modulus and with strength, could be that the pulse method utilised in this investigation has an inherent inaccuracy in reading the start of the received signal as illustrated in Figure 8.12. This error becomes significant if the specimen is small or if the period is of the same order of magnitude as the time delay. The reason for this is twofold:

- Firstly, there is a region called the near field of the transducer in which the waves emanating from the transducer face interfere with one another. The length of the near field of the transducer ($Z_{max}$) is given by Equation 3.2. For frequency range of 0.2 -

0.5 MHz, $Z_{max}$ is 3.14 - 12.15 mm. The specimen encountered in this investigation had thickness range of 15 - 25 mm.

- Secondly, when the specimen is short and the velocity is high enough, the interference disturbs the received signal and the time measurement is inaccurate. It was demonstrated in Chapter 4 that the system had a time delay (0.8 µs). This was thought to affect the accuracy of the measured velocity since the specimen were of different thickness. Incorporating the time delay in the velocity measurement did not improve the correlation coefficient.
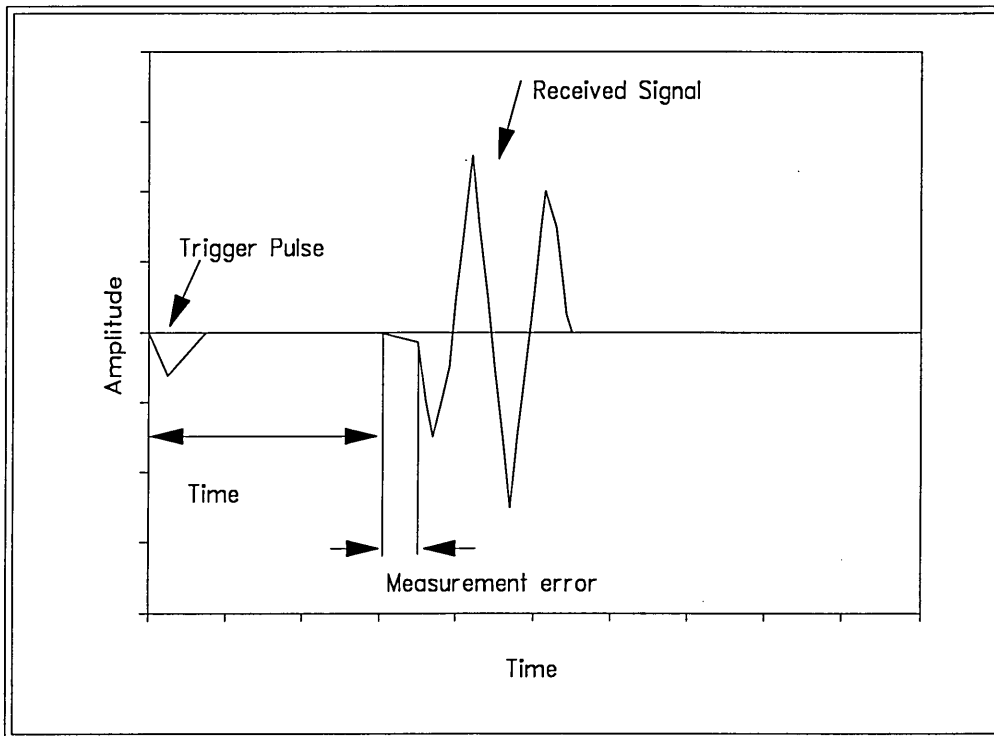


*Figure 8-12: Error Involved in Time of Flight Measurement (not to scale)*

On the other hand, the ability to use velocity to predict Young's modulus and strength given in Equations 8.10 and 8.11 and illustrated in Figures 8.13, and 8.14 respectively. The increased R-squared is due to the linearisation by squaring.

$$E = -37.6 + 10^{-7} V^2 \rho \qquad R^2 = 93.5\% \qquad (8.10)$$

$$\sigma = -0.424 + 1.3 * 10^{-9} V^2 \rho \qquad R^2 = 88\% \qquad (8.11)$$

The correlation coefficient of Equations 8.10 and 8.11 has more clinical relevance, since the main objectives is to be able to predict strength and Young's modulus from measured velocity. The standard error of estimates of Young's modulus in Equation 8.10 is 6.09 MPa and 0.106 MPa for strength in Equation 8.11. It can be seen from Table 8.2 that the correlation coefficient has increased in the above combination in comparison to the individual correlation.

The mode of ultrasound propagation through porous structure such as cancellous bone is not well understood. Further investigations is necessary to elucidate the effect of pore size and distribution on velocity, dependence of velocity on frequency or wavelength and the validity of bar wave in this application. William[1991] demonstrated that Biot theory could be used for better theoretical prediction of ultrasound transmission through cancellous bone. They further argued that at 0.5 MHz, the longitudinal wave is transmitted as a bulk wave rather than a rod wave through the material.
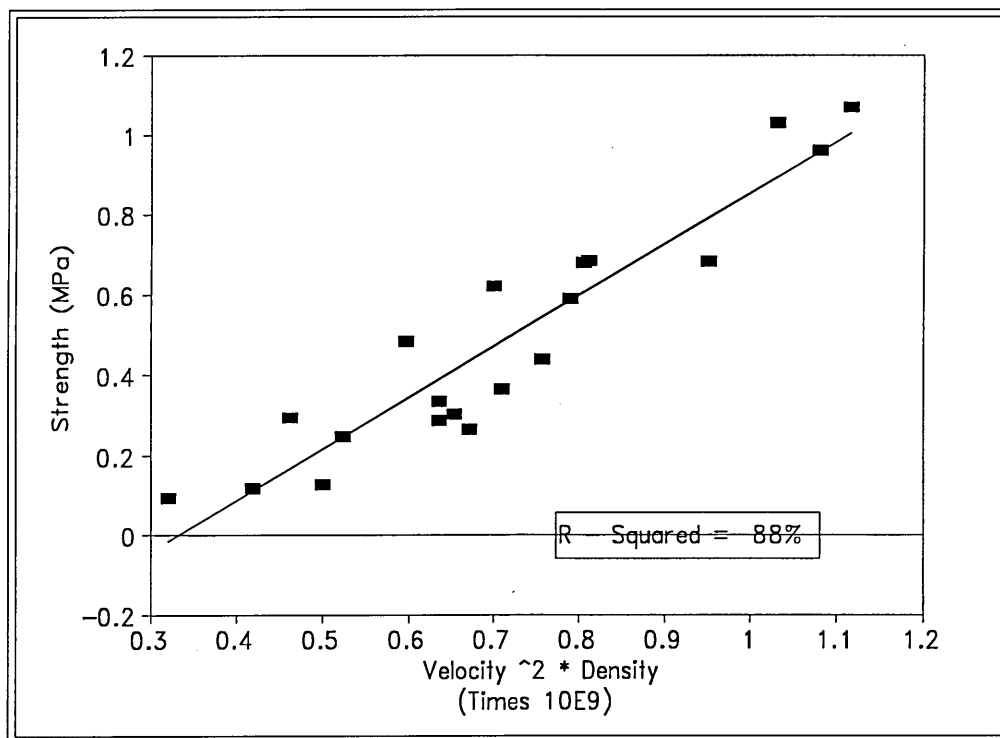


*Figure 8-13: The Relationship Between Strength, Velocity and Density*
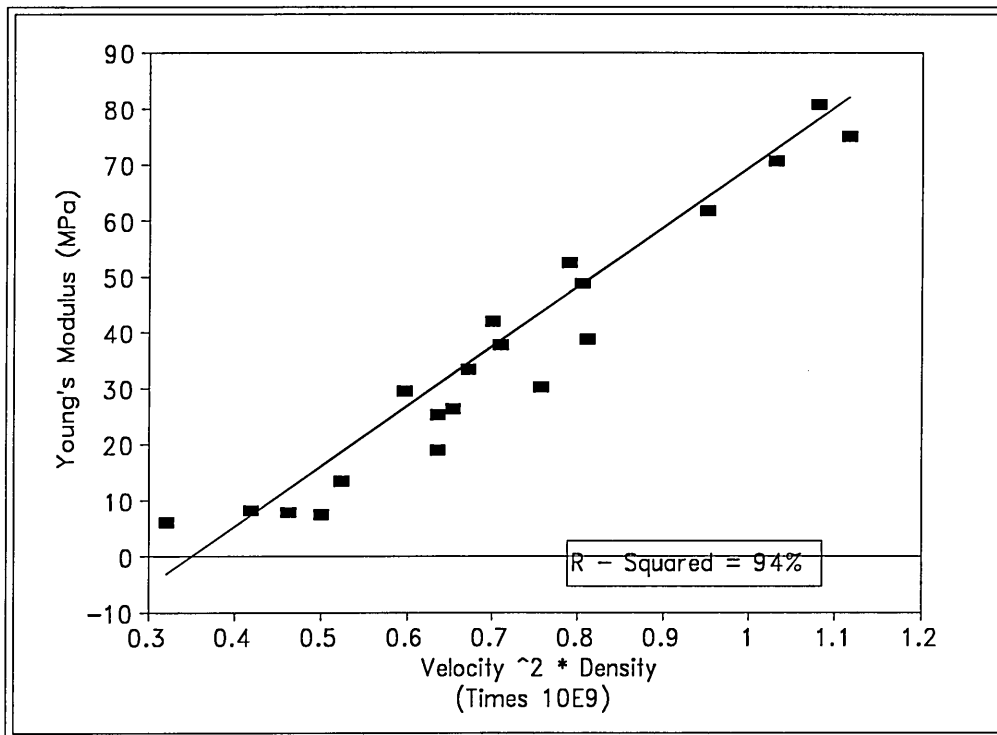
***Figure 8-14:*** *The Relationship Between Young's Modulus, Velocity and Density*

## 8.4.3 Broadband Ultrasonic Attenuation (BUA)

Since the introduction of the concept of using BUA as a discriminator of osteoporosis, little has been done to relate it to the mechanical integrity of the bone, this section examines that relationship. A commonly encountered problem with *in vitro* measurements is the extrapolation of results to *in vivo* conditions. This study has attempted to quantify this problem by first carrying out the ultrasonic measurements on whole samples before coring. The results are given in Appendix D - Tables C.1, C.2. A linear regression fit to the data are presented in Equations 8.12 - 8.14

$$nnBUA_{whole} = 0.73 + 1.08nnBUA_{core} \qquad R^2 = 94\% \qquad (8.12)$$

$$nnBUA_{whole} = 4.34 + 1.02\ nnBUA_{can} \qquad R^2 = 87\% \qquad (8.13)$$

$$nnBUA_{core} = 3.60 + 0.93nnBUA_{can} \qquad R^2 = 89\% \qquad (8.14)$$

The effect of coring the samples on the attenuation is shown in Equation 8.12 and illustrated in Figure 8.15. The standard deviation on the gradient and intercept are

188

0.06552 and 1.47, respectively. The t-ratio and p-value of the intercept are 0.51 and 0.613, respectively. Therefore as would be expected there is a slight but not significant effect of coring on the intercept. The slight effect is due to the loss of the signal that would have been scattered back from an area outside of the cylinder when the samples are cored.
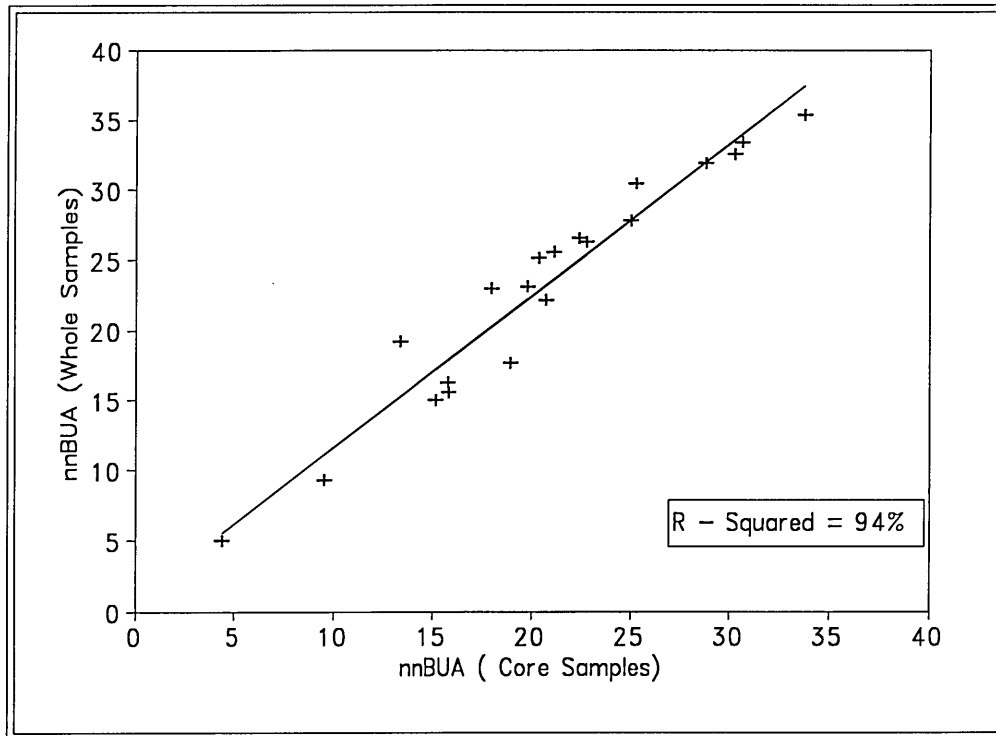


*Figure 8-15: Plot of BUA of Whole Calcaneal Against BUA of Core Samples*

The effect of the cortical end plates are shown in Equation 8.14 and Figure 8.16. The standard deviation on the gradient and intercept are 0.0757 and 1.487, respectively. The t-ratio of the gradient and intercept are 12.28 and 2.42, respectively, implying that these values are significant. Within 95% confidence limit $nnBUA_{core}$ is directly proportional to $nnBUA_{can}$. It is evident from Equation 8.14 and the statistics that the cortical end plates affect only the intercept, thus causing an offset without changing the BUA pattern. This implies that the observed attenuation *in vivo* will be determined predominantly by the cancellous component of the bone.

The combined effect of coring and cortical end plates is given in Equation 8.13 and Figure 8.16. The standard deviation on the gradient is 0.0949 and that on intercept is 2.014. The

t-ratio of the gradient is 10.79 and that of the intercept is 2.32. The offset increases from whole - core to cancellous but the $nnBUA_{whole}$ is still directly proportional to $nnBUA_{can}$ with a proportionality constant of 1 within experimental error. The correlation observed between $nnBUA_{whole}$ and $nnBUA_{can}$ ($R^2 = 87\%$) (see Table 8.2) which is presented in Equation 8.13 and illustrated in Figure 8.16 was significant. This implies that the mechanical measurements carried out on the cancellous samples could be related to the $nnBUA_{whole}$ and thus the *in vivo* condition. There is also a gradual but not significant decrease in the correlation coefficient as the specimen under went coring to defatting [see Table 8.2].
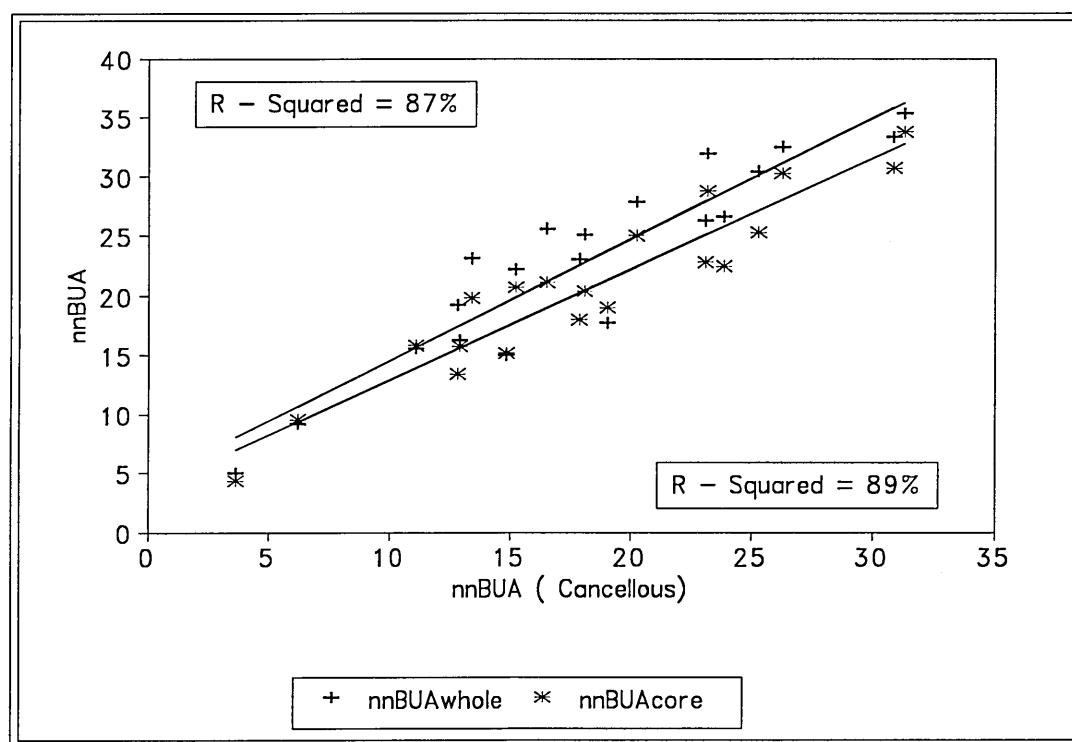


*Figure 8-16:* BUA of Whole and Core Calcaneal Samples Plotted Against BUA of Cancellous Samples

No significant difference was observed between the specimen with fat *in situ* and those without fat (pores filled with degassed water). The mean of their differences was 0.511 ±1.086 (95% confidence limit). This could be explained by the fact that the difference in acoustic impedance between fat and water is small. Although mechanical measurements

were carried out on defatted specimens the ultrasonic properties discussion will be on specimen with fat *in situ*. This is because specimens with fat *in situ* have no degassing problem for acoustic measurements, hence they were more reproducible.

$$nnBUA_{can} = 0.33 + 0.96BUA_{def} \qquad R^2 = 91\% \qquad (8.15),$$

$$nnBUA_{whole} = 3.71 + 1.03nnBUA_{def} \qquad R^2 = 87\% \qquad (8.16).$$

$$nnBUA_{core} = 3.52 + 0.91nnBUA_{def} \qquad R^2 = 85\% \qquad (8.17)$$

The standard deviations of the intercept and gradients of Equation 8.15 are 1.47 ($p = 0.824$, $t = 0.23$) and 0.073 ($p = 0.000$, $t = 13.06$). This confirms the equality of $nnBUA_{can}$ and $nnBUA_{def}$ discussed above.

There was a significant positive correlation between all the nnBUA values and density and the highest significance was between $nnBUA_{can}$ and density ($R^2 = 88\%$, see Table 8.2). To determine the relationship between $nnBUA_{can}$ and density a linear regression analysis was applied to the log transformation of the data. This is presented in Equation 8.17 and illustrated in Figure 8.17.

$$Log(nnBUA_{can}) = -3.57 + 1.99log\rho \qquad R^2 = 87\% \qquad (8.17).$$

The correlation coefficient was higher than that reported by McKelvie et al. [1989] ($R^2 = 0.69$) and McCloskey et al. [1990] ($R^2 = 71\%$). It is worth mentioning that the density reported by McKelvie et al. [1989] was actual density (total specimen mass including fat divided by the total specimen volume) not the apparent density reported here and by McCloskey. The high correlation of this study was unexpected since BUA has been reported to be dependent on both structure and density [Langton et al., 1990a; Tavakoli and Evans, 1992]. One possible explanation is that all measurements were carried out in one direction, hence the architectural variation will not be significant in comparison to the density changes. With the bovine results (see Chapter 7) significant correlation could be observed when the results were separated into the three directions. It must also be noted that some structural changes such as thinning or total loss of the trabeculae which occur in an ageing bone are not mutually exclusive of density changes (that is, a density change

implies a change in structure). From the log transformation (Equation 8.17) it could suggested that the ultrasound attenuation also follows the power relationship with density (nnBUA $\propto \rho^{1.99} \pm 0.09$ ) as compressive strength. This will further justify the architectural dependence of BUA.

There have been a host of studies correlating BUA and density measured by established densitometric techniques (Table 3.4, Gluer et al., 1992; Waud et al., 1992; Rossman et al. 1989). The reported correlation coefficients have varied from 0.41 to 0.85 ($R^2$ = 17% - 72%). Some possible reasons for the wide correlation values could be:-

1. A large age range which encompasses a large structural differences, for example Rossman et al. [1989] used 21 - 61 years females and Waud et al. [1992] used 35 - 83 years.

2. The reports correlate BUA at the calcaneus with density of a different anatomical site (Table 3.4)

3. The values of BUA are not normalised for specimen thickness

To verify the third reason, correlation coefficient between BUA $(dB/MHz)_{can}$ and density, and $BUA_{core}$ and density were calculated. The $R^2$ values fell from 88% (nnBUAcan ) to 81%($BUA_{can}$) and from 76% ($nnBUA_{core}$) to 66% ($BUA_{core}$). This decrease could have been more significant if the samples used in this study had a higher sample thickness CV (range 15 - 25 mm, mean = 19.95 mm and CV = 13.35% for cancellous samples; range 20 - 33 mm, mean = 28.28 mm and CV = 12.53% for core samples). This decrease validates the third explanation of variation in correlation values *in vivo* . It could therefore be proposed that further study *in vivo* should normalise BUA for specimen in order to give a volumetric density. Studies by Herd et al. [1994] have also come to the same conclusion.
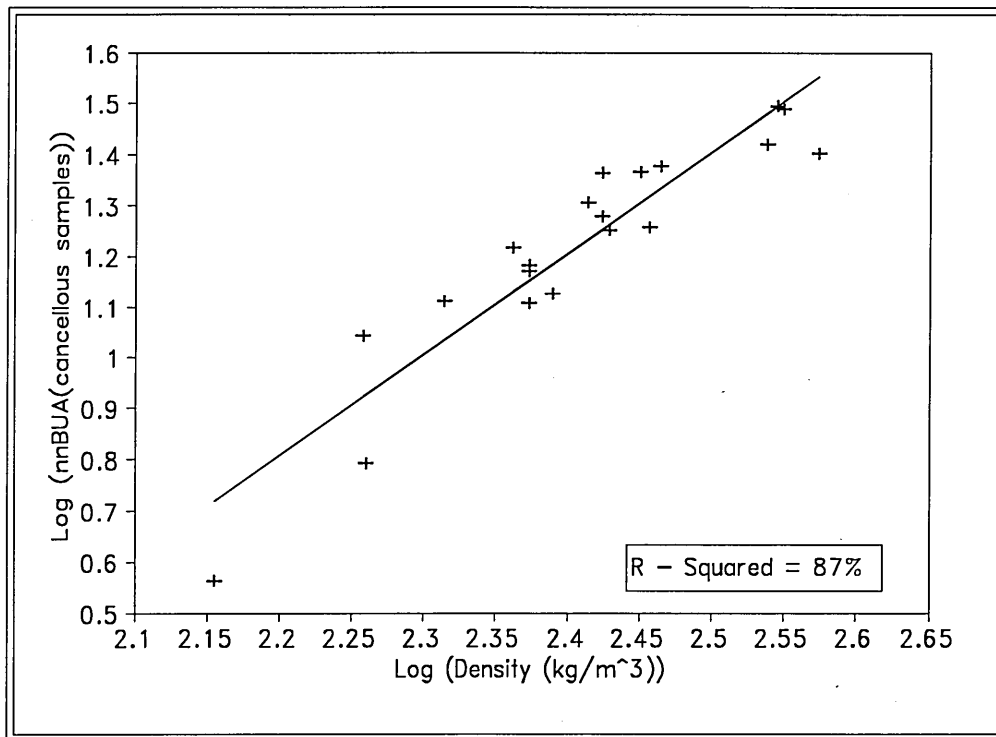
*Figure 8-17: A Plot of BUA of Cancellous Samples Versus Density*

There is a high positive correlation ($R^2$ = 75%) between $nnBUA_{can}$ and compressive strength as illustrated in Figure 8.18 ( see also Table 8.2). A linear regression analysis applied to the $\log_{10}$ transformed values is presented in Equation 8.18. A gradient of 1.18 shows that BUA is linearly proportional to strength.

$$Log\sigma = -1.84 + 1.18log(nnBUA_{can}) \qquad R^2 = 75\% \qquad (8.18)$$

$$logE = -0.220 + 1.36log(nnBUAcan) \qquad R2 = 77\%. \qquad (8.19)$$

Young's modulus was highly correlated with nnBUA, with a higher but not significant correlation than strength (see Table 8.2 and Equation 8.19). The higher values could be because E normalise the measurements for specimen thickness, while strength does not. The specimen used in this study had thickness varying from 15 mm - 25 mm. A plot of attenuation versus Young's modulus is presented in Figure D.11 (Appendix D) and the graph of the logged values presented in Figure 8.19.

Table 8.2 shows that there is no significant difference in the $R^2$ values of nnBUA$_{whole}$, nnBUA$_{core}$, nnBUA$_{can}$ and nnBUA$_{def}$ with compressive strength.
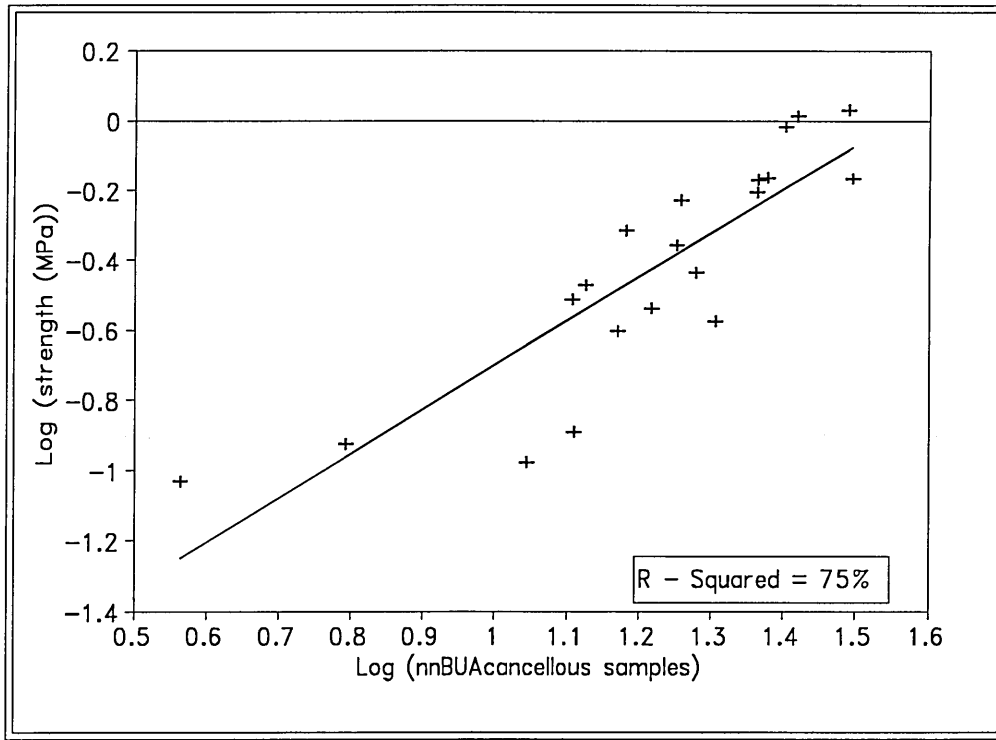


***Figure 8-18:*** *A Plot of log of Compressive Strength Against log of BUA*
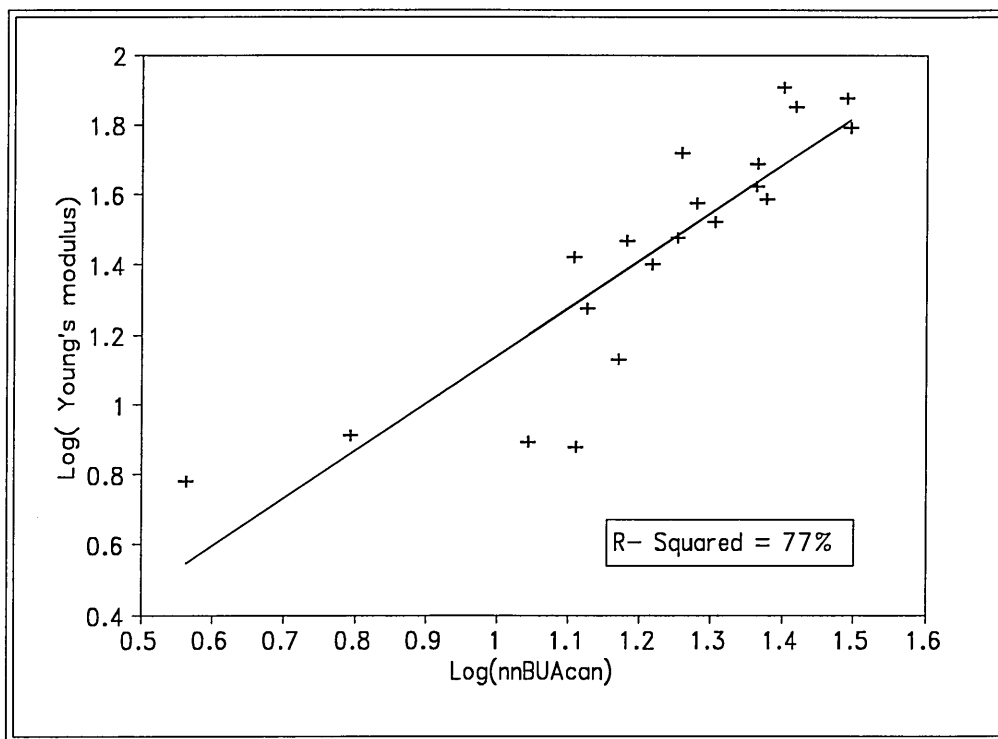
***Figure 8-19:*** *Plot of log of Young's Modulus Against log of BUA*

A plot of velocity (cancellous and defatted) against attenuation is presented in Figure 8.20. Velocity is proportional to attenuation with a correlation coefficient of 0.77 ($R^2$ = 60%). A higher correlation could have been observed if not for specimen number 3 and 4. When these two values are eliminated then correlation between velocity and attenuation becomes 0.89 ($R^2$ = 79%) as seen in Figure D.3 ( Appendix D). The 21% variance could be due to the difference in the modes of interaction of velocity and nnBUA with cancellous bone. Other researchers have found a poor *in vivo* correlation between BUA and ultrasound velocity. For example Rossman et al. [1989] observed an r = 0.53 , while Waud et al. [1992) found r = 0.74.
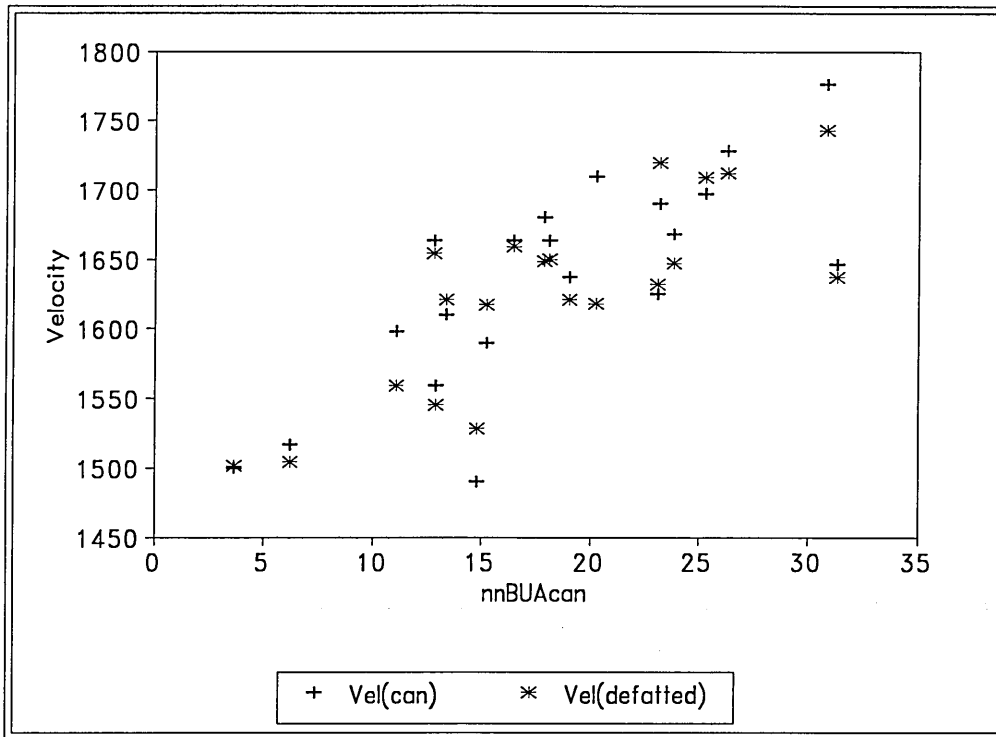
*Figure 8-20: The Relationship Between Velocity and BUA*

Preceding sections have shown that nnBUA is a good predictor of strength and Young's modulus, Nonetheless, it is a better predictor of density for the age range used, hence the author substituted density with BUA in the bar wave equation (7.18) and the following relationships were obtained (Figures 8.21 and 8.22):

$$\sigma = -0.119 + 1.18 * 10^{-8} V^2 BUA_{can} \qquad R^2 = 80\%, \qquad (8.20)$$

$$E = -10.21 + 9.11 * 10^{-7} V^2 BUA_{can} \qquad R^2 = 83\%. \qquad (8.21)$$

The standard error of strength estimate is 0.14 MPa (Eqn. 8.20) and 9.77 MPa for Young's modulus (Eqn. 8.21). This means that the strength and elasticity could be predicted with 83% accuracy using only ultrasound parameters. These two parameters could be measured *in vivo*. The correlation coefficient for strength and Young's modulus is higher from combined BUA and velocity than when used individually (Table 8.2).
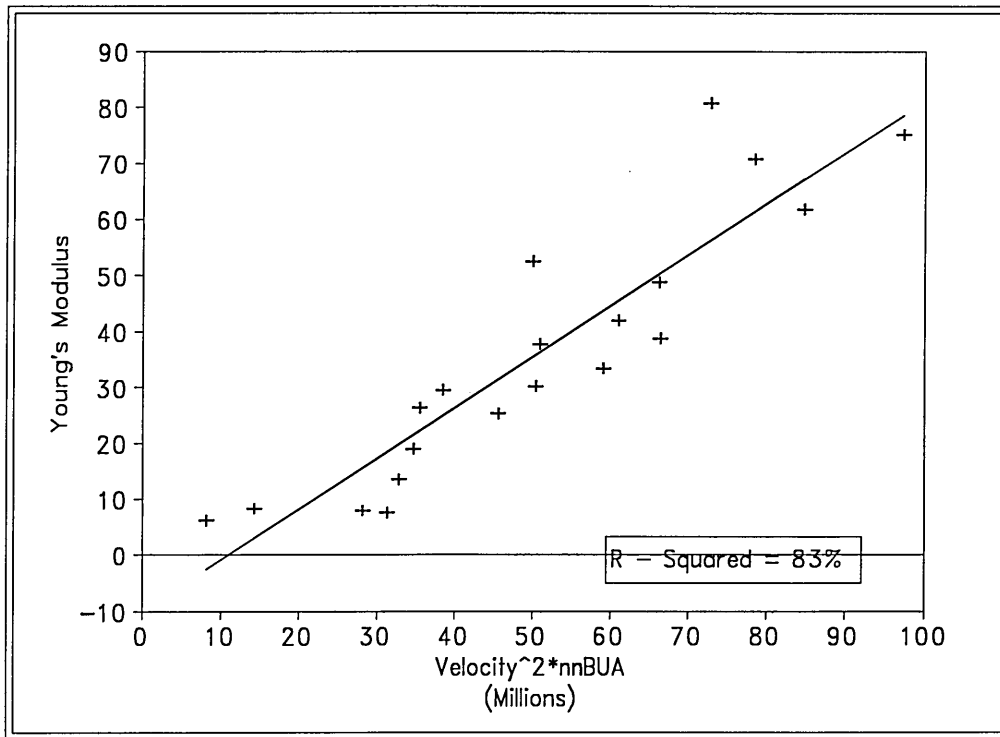
***Figure 8-21:*** *The Relationship Between Young's Modulus , Velocity  and BUA*
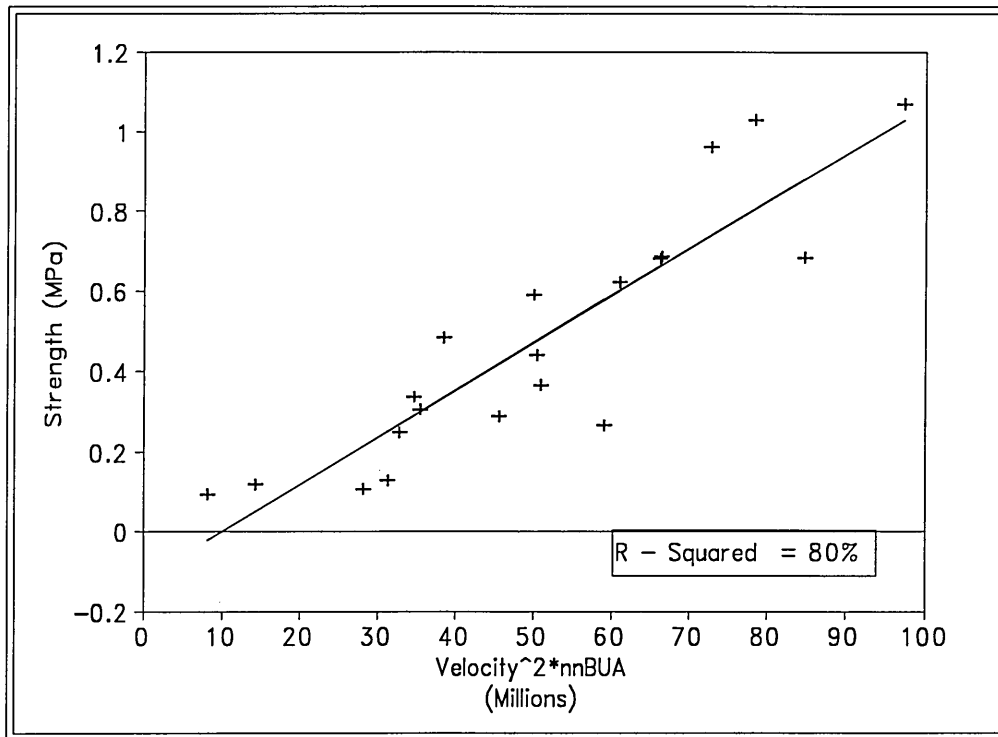
*Figure 8-22: The Relationship Between Strength , Velocity and BUA*

No significant trend between any of the measured mechanical and acoustic parameters were observed with age (Figure D.4 in Appendix D), although age has been reported as a predictor of velocity and attenuation [Heaney et al., 1989, Herd et al., 1991, Agren et al., 1991, and Waud et al., 1992]. Agren et al. [1991] observed a significant negative correlation (r = -0.448) between BUA and age, while Herd et al.,[1991] demonstrated that in addition to age, years since menopause was a significant factor in predicting BUA. In the first 5 years following the menopause BUA decreased by 2.5%/year, while in the next 5 years the decrease fell to 0.5%/year. Heaney et al.,[1989] found no relationship between age and velocity in premenopausal normal women, but in contrast, found a significant negative correlation between velocity and age between older normal subjects (r = -0.422) and osteoporotic postmenopausal subjects (r = 0.295).

The non-significant correlation between age and the measured properties (E, $\rho$, $\sigma$, velocity and BUA) in this study could be accounted for by the small age range and lack of pathological information on the specimens. This is because while a 60 years old female

198

with mobility problems could have a low bone mass, an active 80 years old female could have a higher bone mass. So the trend of acoustic and mechanical properties with age could be better studied in a normative population or in a restricted sample with the criteria governing selection including:- general health, activity, body weight, drug treatment and the time for the onset of menopause

## 8.5 Structural Properties- Permeability

Permeability as a structural index was introduced in the previous chapters. Permeability coefficients of the calcaneus were studied and the results presented in Table 8.1 and Appendix D.3. A plot of permeability versus density is presented in Figure D.5 from which an exponential decay with density could be observed. Therefore a linear regression plot of log(permeability) versus density ( presented in Figure D.6) results in an $R^2$ of 75% compared to 68% for $\log(\kappa)$ versus $\log(\rho)$ (presented in Figure 8.23). The permeability study in bovine cancellous bone showed a strong dependence on density when the results were separated into the three orthogonal directions ( $R^2 = 82\%$, AP; $R^2 = 78\%$, PD and $R^2 = 84\%$, ML). The lower dependence on density in the calcaneus samples $(R^2 = 68\%)$ could have arisen due to problems with defatting. There is no quick experimental method of determining that all the fat has been remove. Thus any sample without all the fat removed will give unnecessary low reading. This problem was more apparent with the calcaneus samples because of the method of which they were machined. The cylindrical calcaneus samples were acquired by drilling but not under constant water irrigation so the fat produced in the process were forced into the sample.
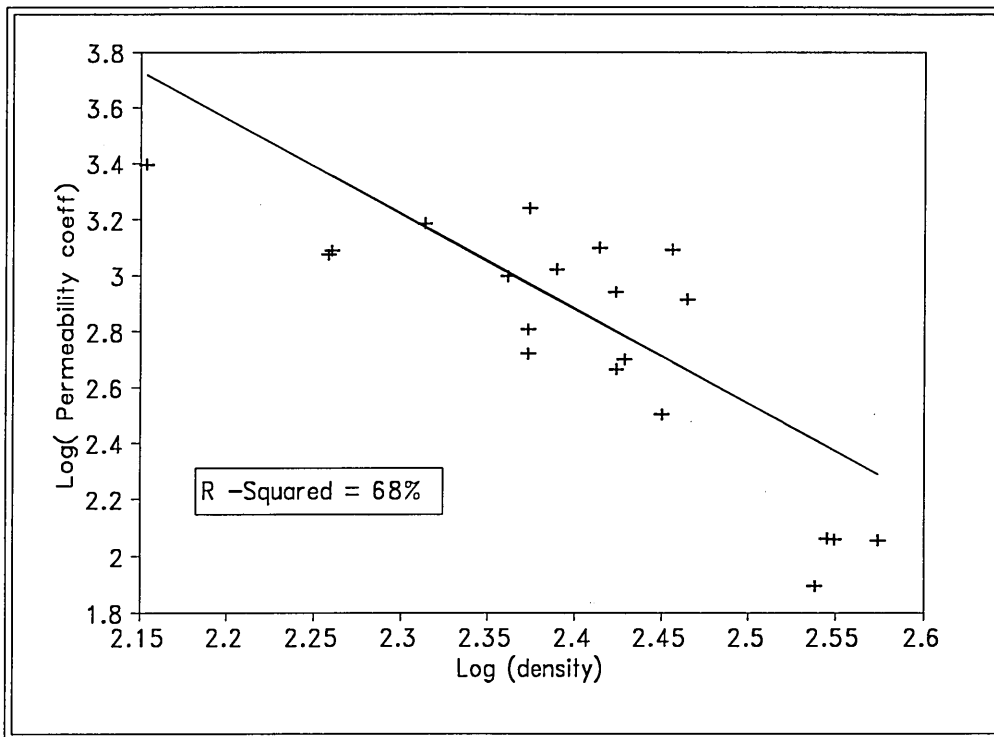
*Figure 8-23:* *A Plot of Permeability versus Density.*

Permeability is proposed here as being dependent on structure as well as density. Therefore one would expect a significant correlation between permeability and structure dependent parameters such as Young's modulus, strength and BUA. A plot of permeability versus strength presented in Figure D.7 shows an exponential decay with strength and therefore an $R^2$ of 71% was observed for a linear regression fit of $\log\kappa$ versus strength ( Figure 8.24

Permeability also decreases exponentially with BUA and a linear regression of of $\log\kappa$ versus strength gave a correlation coefficient of 67%. Permeability therefore is a poorer predictor of BUA than density in the calcaneus. Permeability experimental technique and defatting could account for some of the poor correlation.
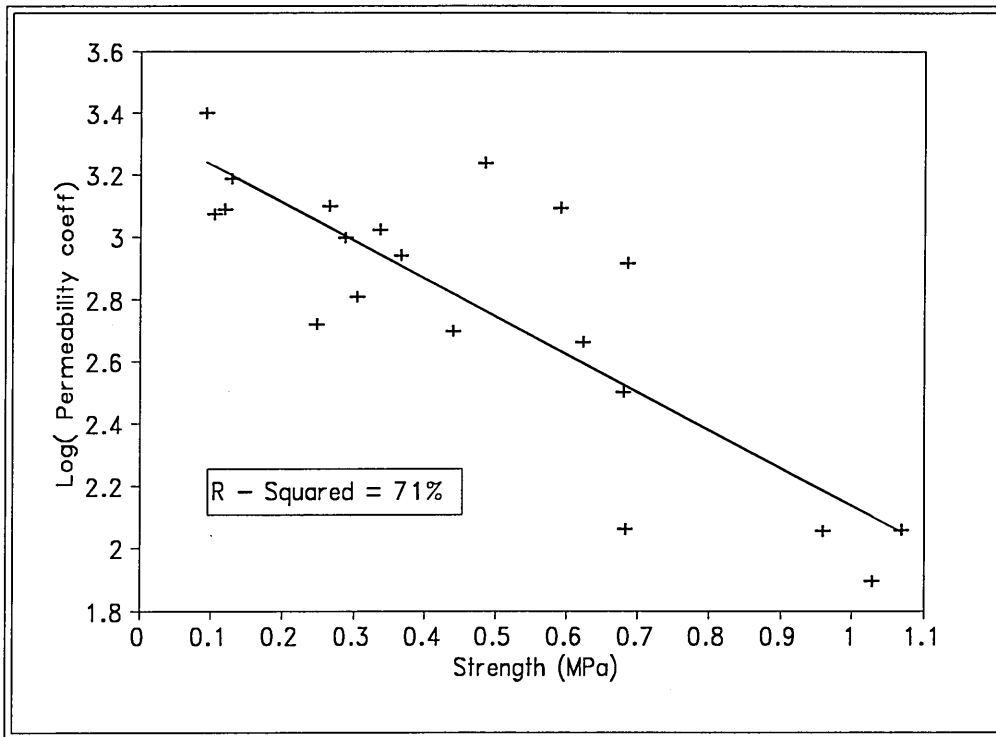
***Figure 8-24:*** *A Plot of Permeability versus Strength*
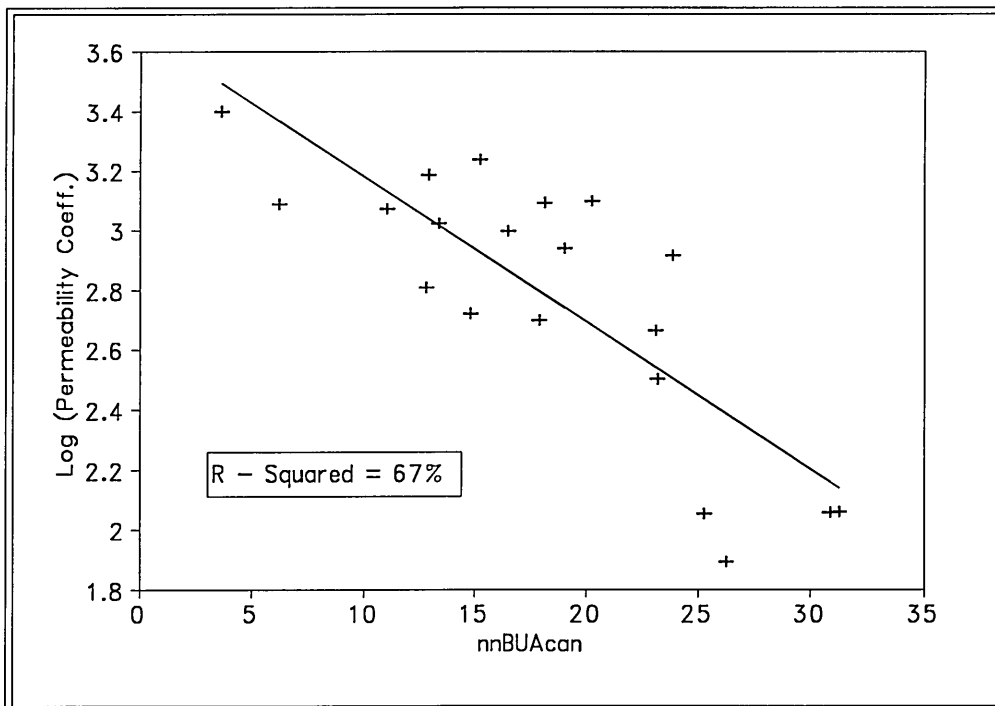


***Figure 8-25:*** *A Plot of log Permeability against BUA*

201

## 8.6 Vertebrae Results and Discussion

The other source of human specimen used for this study was thoracic vertebrae because of the distinctive anisotropy. No information on sex, age and pathology of the specimens were available. The specimens were obtained dry, and they were then soaked in water prior to any measurements. The measurement procedures are as described in Chapter 4. The vertebrae measurements were carried out in the three perpendicular directions, giving three data points per specimen. The results are given in Table 8.4, including the mean, standard deviations (Stdev) and coefficient of variation (CV = (stdev/mean)x100). Young's modulus had the highest CV (71%), while velocity had the lowest (10.43).

**Table 8.4:** *The Mechanical, Acoustic and Structural Properties of the Vertebrae*

| Specimen no | Young's Modulus(MPa) | Strength (MPa) | Density kg m$^{-3}$ | Velocity m s$^{-1}$ | nnBUA dB MHz$^{-1}$ cm$^{-1}$ | $\kappa$ m$^2$*10$^{-11}$ |
|---|---|---|---|---|---|---|
| PD1 | 55.3 | 1.3 | 205 | 1861(1.7)* | 31.62(5)* | 194.14 |
| PD2 | 113.4 | 2.05 | 254 | 1893(1.2) | 44.83(1.4) | 138.44 |
| PD3 | 151.9 | 3 | 338 | 2079(2.5) | 49.32(4.5) | 113.7 |
| PD4 | 107.6 | 1.85 | 267 | 1945(0.1) | 43.86(4.5) | 125.6 |
| AP1 | 12 | | | 1526(1.0) | 9.78(2.6) | 109.3 |
| AP2 | 30.2 | | | 1617(1.7) | 17.73(2.3) | 86.1 |
| AP3 | 47.4 | | | 1683(1.0) | 19.24(4.0) | 94.34 |
| AP4 | 48.6 | | | 1619(.01) | 18.35(4) | 91.23 |
| ML1 | 14.6 | | | 1490(1.4) | 10.87(1.0) | 111.2 |
| ML2 | 31.4 | | | 1652(1.0) | 17.86(0.6) | 94.6 |
| ML3 | 57.9 | | | 1708(1.4) | 23.22(1.6) | 90.8 |
| ML4 | 47.5 | | | 1622(1.4) | 17.93(3) | 86.1 |
| Mean | 59.82 | 2.05 | 266 | 1725(1.2) | 25.38(2.88) | 111.3 |
| stdev | 42.75 | 0.708 | 54.9 | 180 | 13.65 | 30.9 |
| CV | 71.46% | 34.53% | 20.6% | 10.43% | 53.78% | 27.76% |

* where the value in brackets is the cv for that measurement
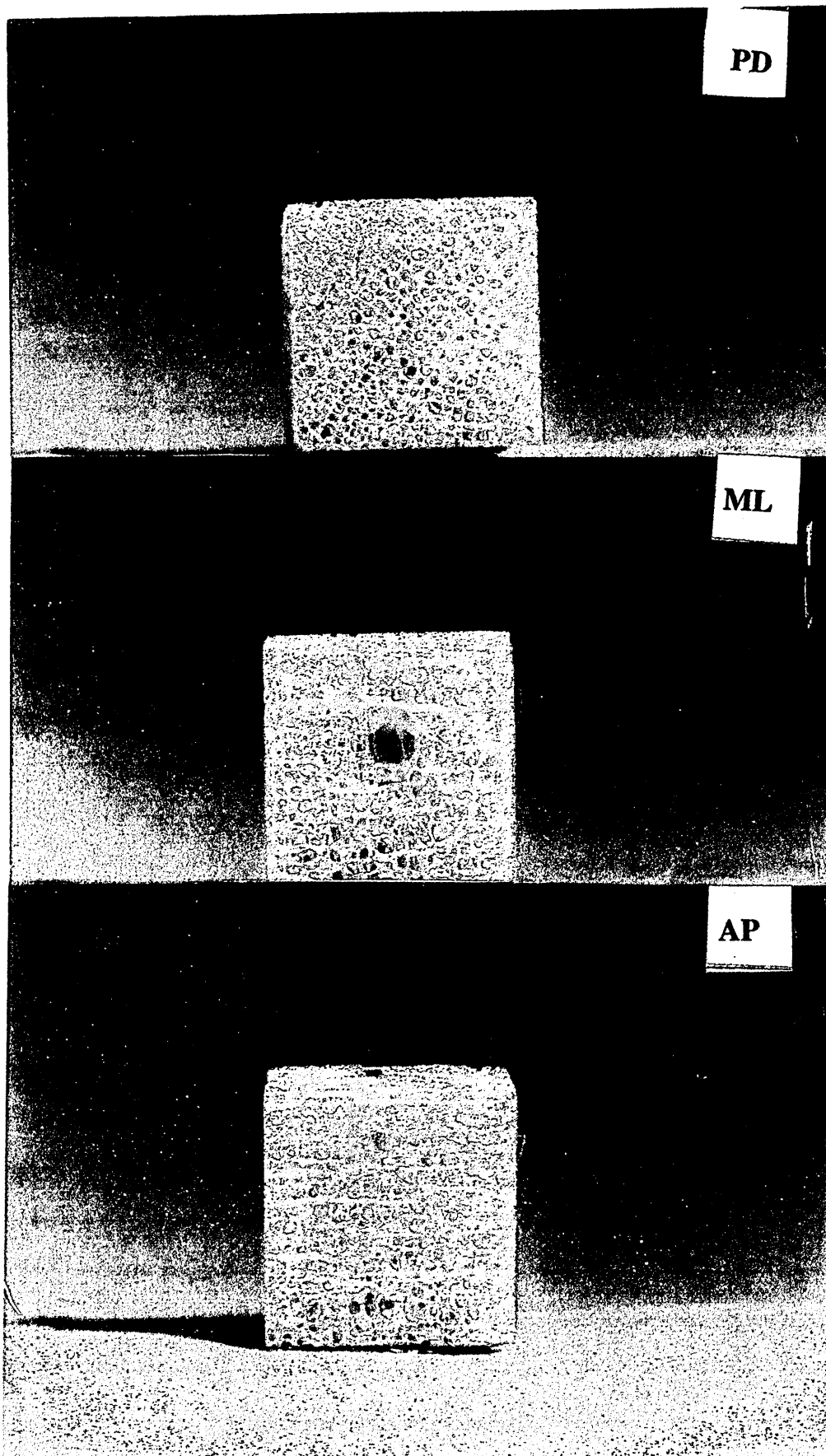
*Figure 8-26: A Photograph of a Specimen from the Thoracic Vertebrae(12\*12 mm)*

## 8.6.1 Mechanical Properties of the Vertebrae

Studies reported in the literature have looked at the mechanical properties of human vertebrae, however to the author's knowledge there is none examining both ultrasonic properties and mechanical properties apart from a recent report by Nicholoson et al. [1994]. Some of the cited work on mechanical properties are presented in Table 8.5 which illustrates that mechanical properties of this study fall within reported work.

*Table 8.5: The reported mechanical properties of human vertebrae (L = lumbar, T = thoracic)*

| Source | Strength (MPa) | Young's Modulus | Comment |
|---|---|---|---|
| Weaver & Chalmers (1966) | 4.25 <br> 2.54 | - <br> - | < 50 years L <br> > 50 years L |
| Galante et al. (1970) | 2.06 ± 0.25 | - | $L_3, L_4$ |
| Lindahl (1976) | 4.6±0.3 <br> 2.7±0.7 | 55.6±0.7 <br> 35.1±0.6 | males L2-4 <br> females L2-4 |
| Struhl et al.(1987) | 0.06-15 | 10 - 428 | Fresh |
| Present studies (1994) | 2.05±0.7 | 59.82±42 | wet defatted,T |

It can be seen in Table 8.4 that Young's modulus in the proximal - distal direction was a factor of 3 higher than the anterior-posterior and mediol-lateral directions and the values of Young's modulus in ML are approximately equal to those in AP. The higher value in PD is expected since the PD is the direction of applied load. A closer look at Figure 8.23 (photograph of the vertebrae) will reveal that the vertebrae is an example of bone where loading is largely vertically uniaxial. The trabeculae often develop a columnar structure with cylindrical symmetry. The columns of bone are oriented in the vertical direction (PD). This gives relatively high Young's modulus and strength in the direction of load with lower Young's modulus and strength in the transverse directions. This anisotropy is accentuated with age due to the loss of the thin horizontal trabecular and an increase in diameter among the remaining trabeculae (Parfitt, 1984). Bone growth is stimulated by stresses to

which it is subjected (Wolf,1889), hence when the trabecular bone mass decreases with age, the compressive force on the remaining trabecular structure will increase. To reduce this critical increase, new bone is formed on the vertical trabeculae. The horizontal trabecular which are often disconnected or have dissappered are not involved in this adaption of the trabecular bone (Parfit et al., 1983).

A plot of log to the base ten of Young's modulus versus log of density is given in Figure 8.27. The linear response of this graph indicates that Young's modulus in the vertebrae also follows the power relationship discussed for the calcaneus and bovine femi specimens. The gradient for the linear regression is 1.98±0.46, 2.78±1.12, and 2.78±0.73 for PD, AP and ML respectively. The $R^2$ values are 89.8%, 76%, and 88% for PD, AP and ML respectively. The high correlation is not surprising because the previous studies have confirmed the power relationship between Young's modulus and density. The results suggest a cubic relationship with density in the AP and ML and a quadratic relationship with density in the PD direction. It is noteworthy that the power dependence of Young's modulus on density follows the same pattern as that observed in the bovine, whereby the direction with the highest Young's modulus had the lowest exponential. A linear regression of log of strength (PD direction) versus log of density resulted in a gradient of 1.64±0.26 and an $R^2$ of 95.1%. As would then be expected strength (PD direction) correlated positively and linearly with Young's modulus (PD- direction) with an $R^2$ of 92%.
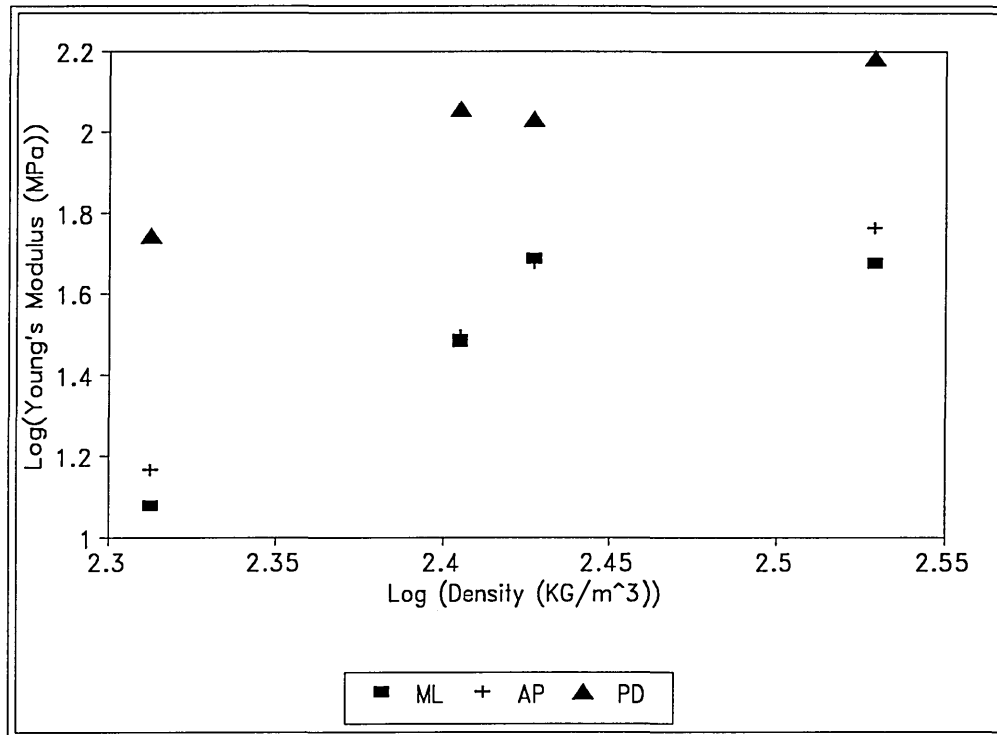
*Figure 8-27 : A Plot of log of Young's Modulus Against log of Density for three Orthogonal Directions*

## 8.6.2 Ultrasonic Properties of Vertebrae

### 8.6.2.1    *Velocity*

It can be seen from Table 8.4 that velocity had the highest values in the PD direction and it is in agreement with a recent report by Nicholson et al. [1994]. Velocity also had the lowest coefficient of variation (CV) compared to the other acoustic and mechanical properties. The lowest CV could be due to the fact that velocity is highly dependent on microstructure (collagen and hydroxapatite) and the macrostructural dependence is highly affected by the wavelength of the propagating wave. Application of the modified bar wave equation (7.18) to the vertebrae data is presented in Figure 8.28 and Equation 8.21 (sample number is 12),

$$V = 1213 + 1151\sqrt{E/\rho} \qquad\qquad R^2 = 89\% \qquad\qquad (8.21).$$

The coefficient of correlation (Eqn. 8.21, r = 0.94) is higher than that for the calcaneus (r=0.84). The reasons for lower r in the calcaneus have been discussed, however the vertebrae had smaller specimen diameter and more appropriate for the application of the bar war relationship.
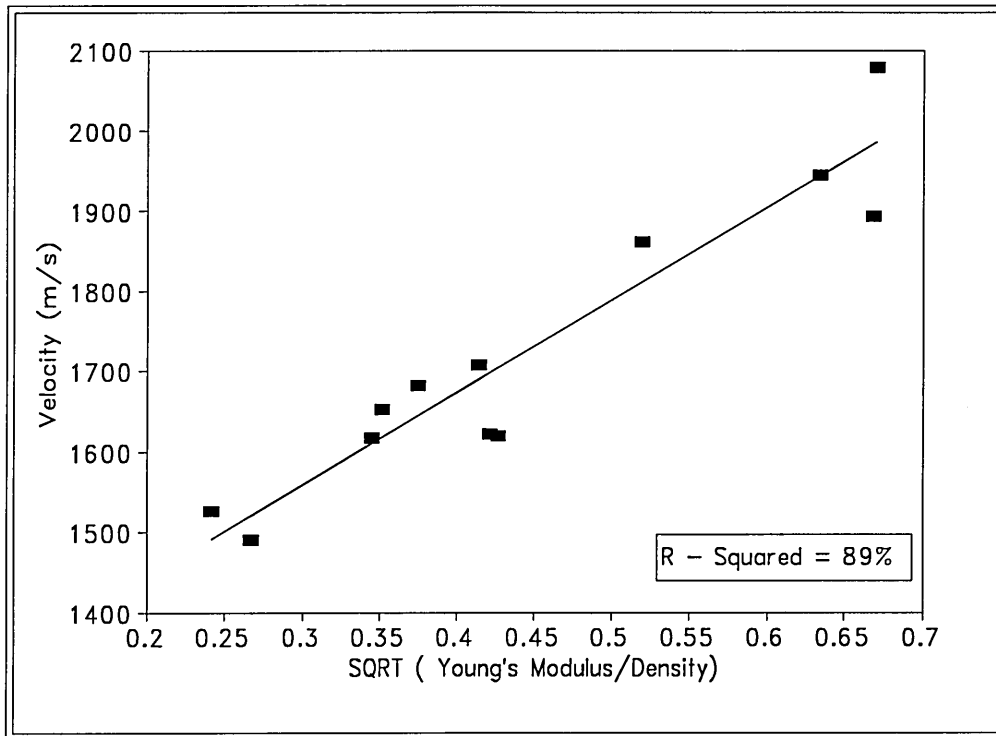


*Figure 8-28:* *The Relationship Between Velocity, Young's Modulus and Density*

### 8.6.2.2 Broadband Ultrasound Attenuation (BUA)

BUA exhibited a marked anisotropy with a factor of 2.6 higher in the PD compared to the AP and ML (see Table 8.4). The overall CV of attenuation is 54% compared with 71% for Young's modulus and 20.63% for density. This is a further indication of structural dependence of nnBUA. The coefficient of variation in the individual directions are 17.86% for PD, 26.88% for AP and 29.02% for ML. This shows that for the individual directions the coefficient of variation is comparable to density variation. This further confirms the

reasons put forward in the calcaneus studies that within a specific direction the structural changes are smaller than density changes.

The log of attenuation as a function of log density is presented in Figure 8.29. There is an increase in BUA with increase in density in the ML and AP directions but no significant trend is observed for the PD direction. The unobserved change in BUA with density in the PD direction could be due the rod like structure and would be affected by real density rather than apparent density. Similar anomaly have been observed in velocity propagation by Nicholson et al [1994]. The trend for ML and AP is similar to the calcaneus results.
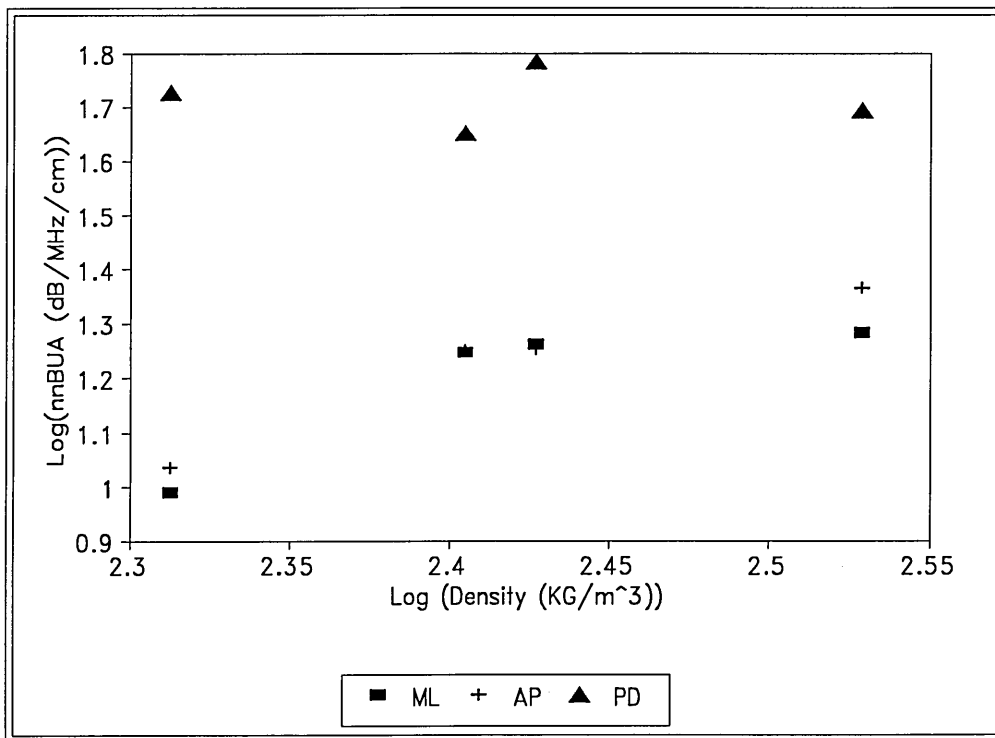


*Figure 8-29: A Plot of BUA versus Density for the Three Orthogonal Directions*

The plot of log of BUA versus log of Young's modulus is presented in Figure 8.30. The linear regression analysis resulted in Equation 8.22. The correlation coefficient $(r = 0.959)$ is highly significant and higher than observed in the calcaneus specimen ( $r = 0.877$). The high correlation between BUA and Young's modulus for these highly anisotropic samples may be attributed to them measuring similar material properties (bone mass and structure).

$$\log(E) = -0.206 + 1.39\log(\text{nnBUA}) \qquad R^2 = 92\% \qquad (8.22)$$

$$\text{nnBUA} = -102.22 + 0.074\text{V} \qquad R^2 = 95\% \qquad (8.23)$$

BUA in the vertebrae is also proportional to velocity as demonstrated in Equation 8.23 and Figure 8.31. The correlation coefficient (r = 0.975) is higher than in the calcaneus ( r = 0.889). The following factors could contribute to the higher correlation coefficient in the vertebrae:-

1.     There is a higher velocity CV  in the vertebrae than in the calcaneus.

2.     The vertebrae has a high degree of anisotropy  and thus different structures were studied, hence bringing out the dependence on structure rather than     density for both velocity and BUA.

3.     The pore size  (marrow connectivity) and trabecular  thickness which affect both attenuation and velocity are different in the calcaneus and the vertebrae.
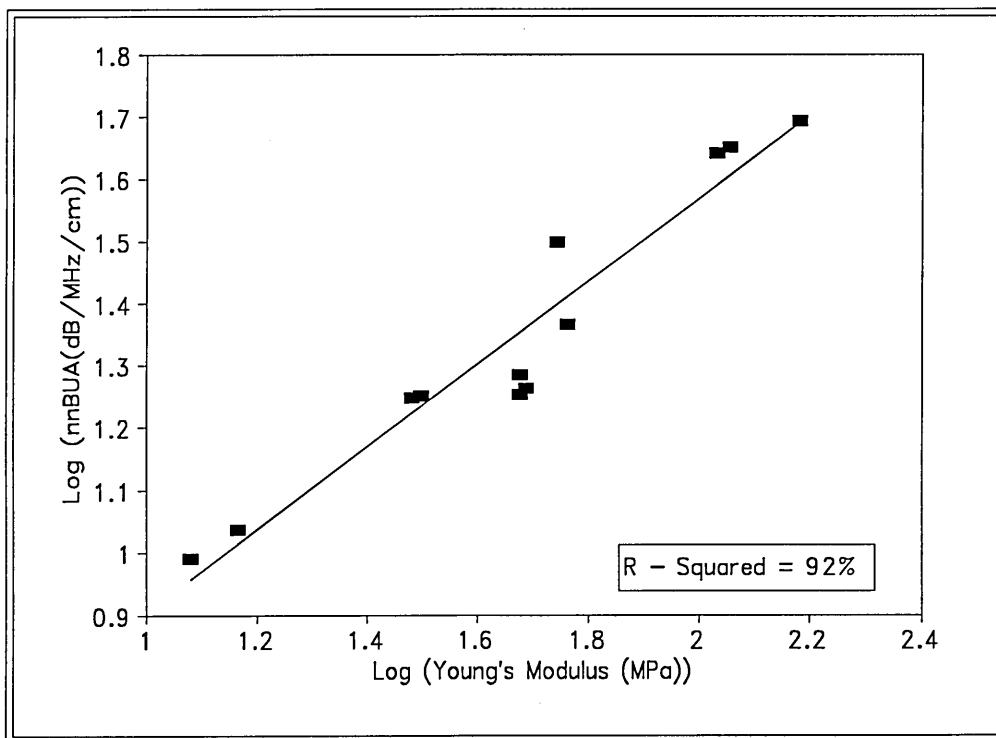


*Figure 8-30:  A Plot of log of BUA versus log of Young's Modulus*
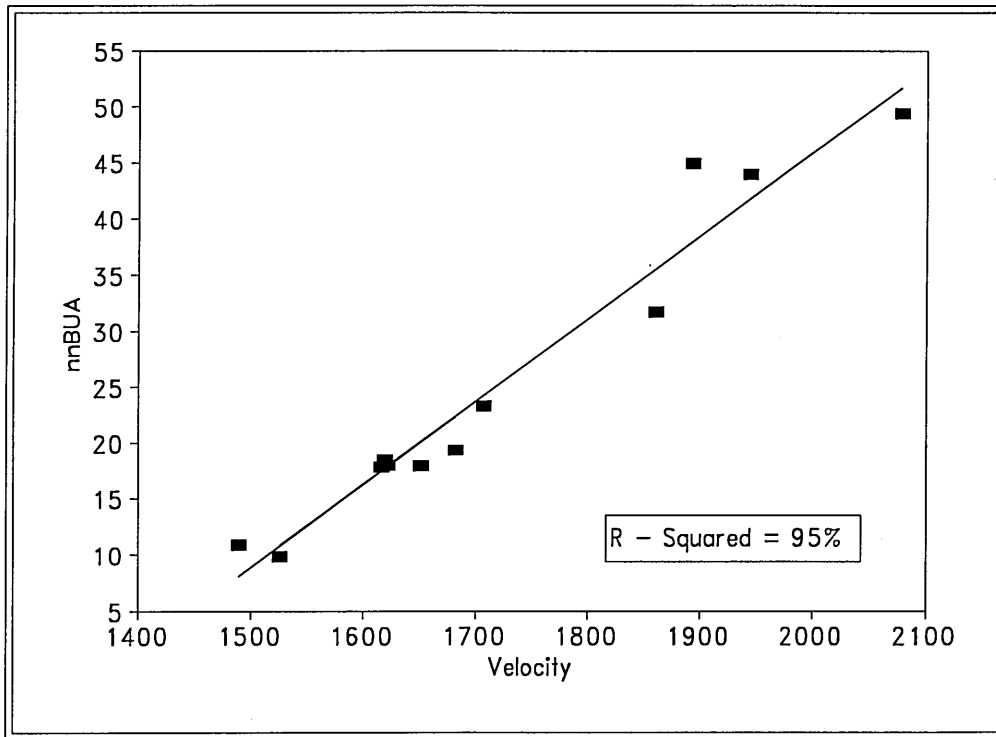
***Figure 8-31:*** *The Relationship Between Velocity and BUA in the Vertebrae*

## 8.6.3 Permeability of the Vertebrae

The permeability in the vertebrae has the highest values in the PD direction and no significant difference between AP and ML directions. This is contrary to observations in the bovine where the PD direction had the lowest permeability, this is because in the vertebrae the columns present themselves as straight capillaries and the influence of tortuous route is thus eliminated. This further supports the hypothesis that permeability can be used as a quantitative indicator of the arrangement of struts in space.

A plot of log permeability versus log density is presented in Figure 8.32. there is an inverse proportionality relationship between permeability and density as observed in the calcaneus and bovine samples. Qualitatively the PD direction showed a linear decrease in permeability with increased in density while AP and ML directions are more curved. Due to the number of sample points this observation will not be expanded upon because it could well be an experimental error.
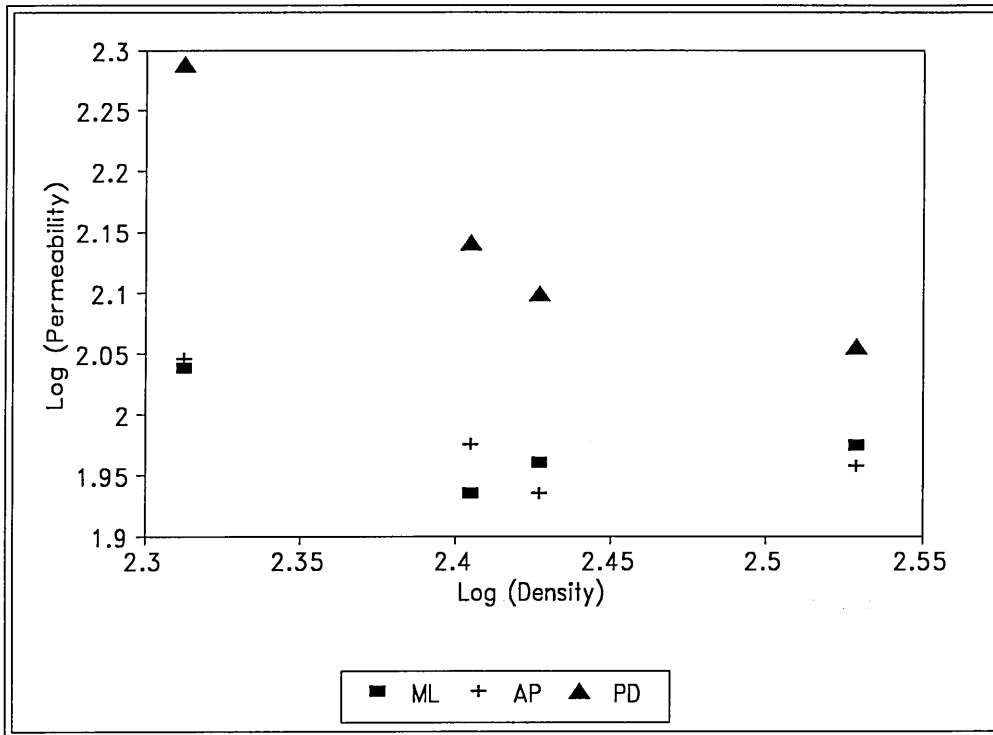
*Figure 8-32: A Plot of log of Permeability versus log of Density*

A plot of BUA with permeability showed a decrease in BUA with an increase in permeability but in two phases. The first phase involves the AP and ML directions and there is a jump to phase II involving the PD direction. The implication of this is that if the tortousity of the samples are included in the correlation then the phase transition could be eliminated. Further correlation between velocity, Young's modulus, strength and density were not carried out because they will follow the same trend as observed in Figure 8.33 since they are highly correlated with each other.
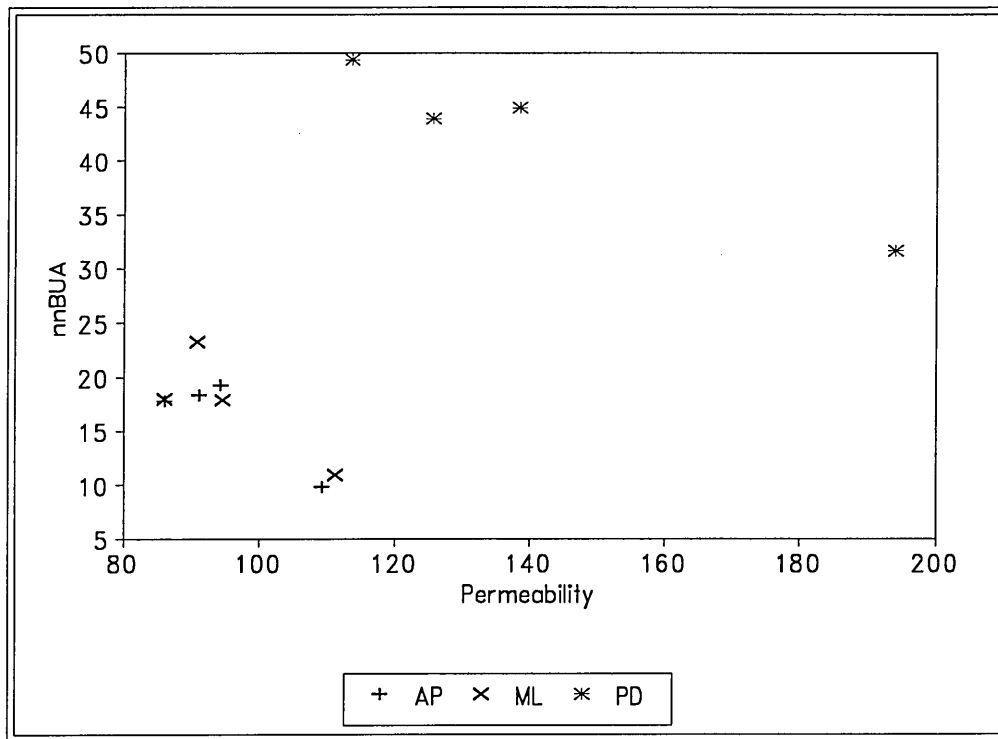
***Figure 8-33:*** *A Plot of BUA versus Permeability*

## *8.7  Conclusions*

### 8.7.1  Calcaneus

The mechanical properties are similar to those reported in the literature. Young's modulus and strength were found to be related to the cubic power of density for the mediol-lateral direction and this is in agreement with the power relationship predicted by the theoretical models of Gibson [1985].

Velocity of the core and whole samples, and cancellous and defatted samples were statistically the same. Velocity was relatively poorly correlated with density ($R^2$ = 64%). The modified wave velocity relationship was investigated and the calcaneus data explain only 73% and 68% of the variance for Young's modulus and strength respectively. On the other hand velocity was a good predictor of Young's modulus ($R^2$ = 94% ) and strength ($R^2$ = 88%).

213

The calcaneus has the measuring site advantage of accessibility and also it has more than 90 % trabecular bone by volume [ Vogel et al., 1988], hence $nnBUA_{whole} \approx nnBUA_{can}$. This was demonstrated by measuring cored samples and samples without the cortical end plates. The effect on BUA was only an offset due phase cancellation.

Broadband Ultrasonic attenuation (BUA) has been demonstrated as a good predictor of density (BUA $\alpha$ $\rho^{1.99}$ , $R^2$ = 87%) , bone strength (BUA $\approx$ $\sigma$, $R^2$ =75% ) and Young's modulus (BUA $\approx$ $E^{0.74}$, $R^2$ = 77%) of the calcaneus.

It was also demonstrated that a combination of $V^2BUA$ could predict strength and Young's modulus with 80% and 83% accuracy respectively.

There was no significant trend between ultrasonic and material properties with age . This was attributed to the limited age range .

Permeability was demonstrated to be related to density and also to predict both strength and BUA.

## 8.7.2 Vertebrae

The vertebrae was found to be distinctly anisotropic with the PD direction exhibiting the highest Young' modulus, velocity and BUA values. The mechanical properties correlated with those reported in the literature and also follow the power relationship with density found in the calcaneus and bovine samples.

The modified bar wave equation had a higher correlation than in the calcaneus. The direction dependence BUA and velocity was further demonstrated in the vertebrae. Due the distinct anisotropy in the vertebrae BUA was highly correlated with both velocity and Young's modulus more than in the calcaneus.

Further investigation is needed to understand the mode of ultrasound transmission through cancellous bone , especially the application of the Biot theory.

# 9. COMPARATIVE ANALYSIS OF BOVINE AND HUMAN CANCELLOUS BONE

## 9.1 Introduction

Three sets of cancellous specimens(18 bovine femur, 20 human calcaneus and 4 human vertebrae) were investigated and reported in Chapters 7 and 8. This chapter investigates the effect of analysing the combination of data.

## 9.2 Mechanical properties

### 9.2.1 Young's Modulus

A plot of the log (Young's modulus) versus log (density) for all samples is presented in Figure 9.1 and linear regression analysis given in Equation 9.1

$$\text{Log}E_{All} = -8.145 + 4.08\log\rho \qquad\qquad R^2 = 86\% \qquad (9.1)$$

The standard error of estimate is 0.279 and the correlation coefficient is highly significant and within the range of the individual groups ($R^2$ is 89% for the calcaneus; 82%, 83% and 87% for bovine PD, AP and ML directions respectively; and 90%, 76% and 88% for vertebrae PD, AP and ML direction respectively). At a 95% confidence limit, the intercept and slope of the whole data set are significantly different from the slope of the individual groups analysed separately, presented in Table 9.1 where SE is the standard error. The confidence interval (CI) at p confidence limit, with n-2 degrees of freedom using the student t distribution is given by $t_{n-2,p}*SE$.

**Table 9.1:** *Confidence Intervals for the Relationships Between log(Elasticity-E) and log(Strength- σ) with log(density)*

| Equation | Constant | SE | CI(±) | Gradient | SE | CI(±) | $R^2$ (%) | N |
|---|---|---|---|---|---|---|---|---|
| E(All) | -8.145 | 0.468 | 0.93 | 4.08 | 0.181 | 0.36 | 86 | 86 |
| E(All)*[1] | -8.79 | 0.590 | 1.19 | 4.31 | 0.233 | 0.47 | 89.5 | 42 |
| E(Bovine)* | -2.68 | 0.512 | 1.09 | 2.10 | 0.19 | 0.40 | 88 | 18 |
| E(Calcaneus) | -6.11 | 0.622 | 1.31 | 3.14 | 0.258 | 0.54 | 89 | 20 |
| E(Vertebrae)* | -4.4 | 1.726 | 3.26 | 2.51 | 0.713 | 1.35 | 86 | 4 |
| σ(All) | -9.48 | 0.718 | 1.44 | 3.84 | 0.286 | 0.57 | 83 | 39 |
| σ(Bovine) | -5.05 | 0.502 | 1.08 | 2.22 | 0.189 | 0.41 | 91 | 15 |
| σ(Calcaneus) | -7.48 | 0.607 | 1.27 | 2.93 | 0.252 | 0.53 | 88 | 20 |
| σ(Vertebrae) | -3.66 | 0.630 | 1.19 | 1.64 | 0.261 | 0.49 | 95 | 4 |

One weakness of this analysis is that for bovine and vertebrae samples, three values of Young's modulus were measured per specimen. Therefore one density value had three corresponding Young's moduli. Young's modulus as demonstrated in Equation 9.1 is related to the density of the whole data set by the power of four. This is higher than those reported in the literature. This could be because the literature, to the best of the author's knowledge, has no measurement of the calcaneus in the medio-lateral direction. There is no predictive significance of this correlation (Equation 9.1) because as illustrated in Figure 9.1 the overall regression line overestimates the calcaneus values, while underestimating the bovine values. Therefore, the mechanical properties of the three sample groups are distinct in relation to density and should be analysed separately. This is supported by the statistical analysis of Rice et al. [1988] who concluded that human and bovine data on elastic modulus and strength are statistically distinct and cannot be combined to form interspecies relationships between mechanical properties. This is contrary to a recent study by Hodgskinson and Currey [1992] where three evolutionary widely separated mammalian species (humans, horses and bovines)

---

[1] The linear regression was carried out using average values of Young's modulus for the bovine and vertebrae specimens

were used. They showed that the regressions for the whole data set were extremely close to the regressions for the species taken individually. One reason for the agreement observed in the work of Hodgkinson and Currey [1992] is that they used average values and included the structure index 'fabric' in their analysis. The mean Young's modulus is not a material property that is important in any give loading situation; it merely gives an indication of the overall stiffness of the specimen.
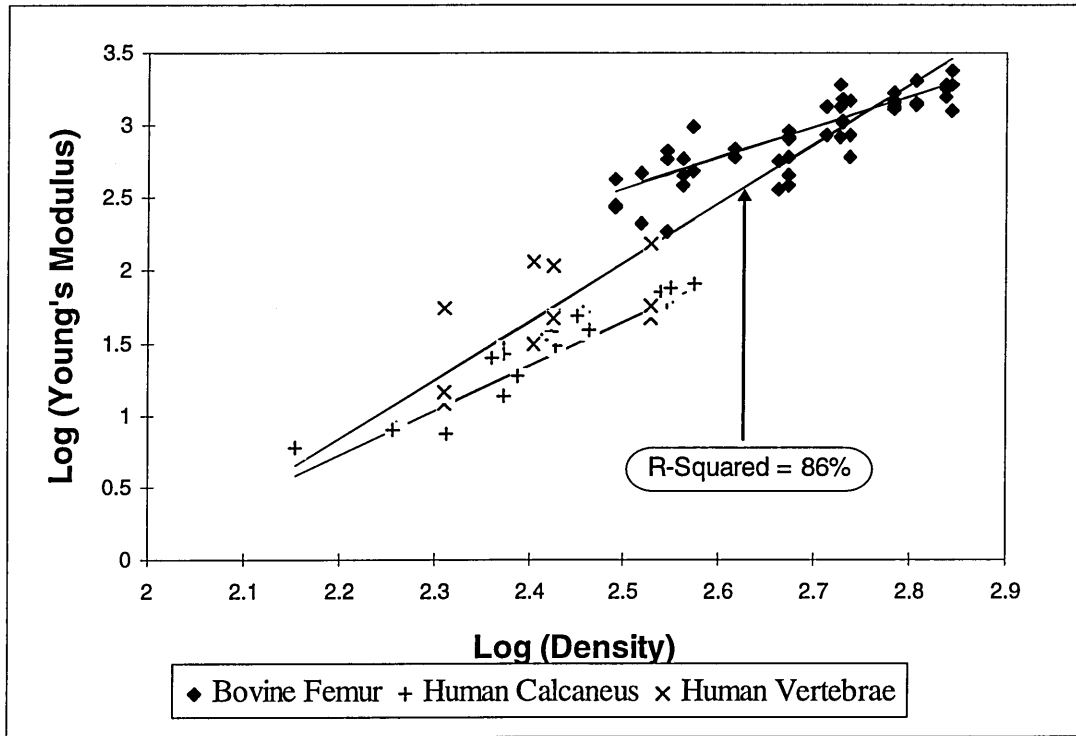


*Figure 9-1:* *The Relationship Between Young's Modulus and Density for all Cancellous Bones*

## 9.2.2 Strength

A plot of log strength versus log density of the whole data set is presented in Figure 9.2 and the linear regression analysis given in Equation 9.2

$$\text{Log}\sigma_{\text{All}} = -9.48 + 3.8\text{log}\rho \quad R2 = 83\% \quad (9.2)$$

The standard error of estimate of Equation 9.2 is 0.280. The slope and intercept are similar to those of Young's modulus (Equation 9.1), but significantly ( 95% confidence limit) different from the individual groups (see Table 9.1). Strength of the whole data set is related to density by a power of 4 which is higher than reported in the literature.

As discussed above the different groups should be analysed separately because the dependence of Young's modulus and strength on density is also affected by the orientation of the struts (open cell, closed cell, symmetric or non-symmetric) (Gibson 1984). The orientation of the struts will therefore vary from specie to specie and from location to location.
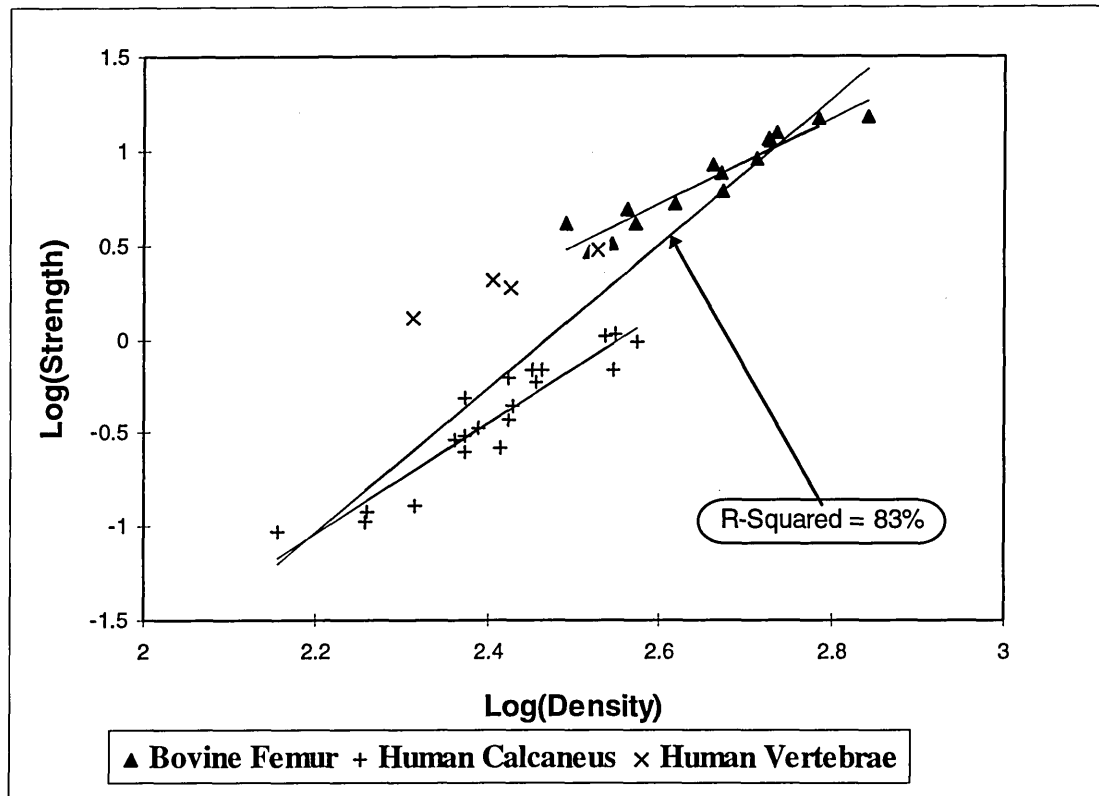


*Figure 9-2: The Relationship Between Strength and Density for Cancellous Bone*

## 9.3 Ultrasound Properties

### 9.3.1 Velocity

A plot of velocity as a function of density is presented in Figure 9.3 and the linear regression through the whole data set given by Equation 9.3

$$V_{all} = 1301 + 1.67\rho \qquad R^2 = 75\% \qquad (9.3)$$

The standard error of estimate of Equation 9.3 is 145.8 m s$^{-1}$. This value is higher than the standard error of the calcaneus implying such a relationship will be a poor predictor

of density in the calcaneus from a velocity measurement. The correlation coefficient (r = 0.87) of the whole data set is higher than observed for the calcaneus samples alone(r = 0.80) but lower than observed for the bovine samples (r = 0.92). The intercept and gradient of the whole data samples is statistically different from that of the individual groups, presented in Table 9.2. The correlation for bovine samples given in Table 9.2 was obtained from correlation of density against the average value of velocity for each specimen. The average value has no significance in characterising cancellous bone being anisotropic and thus direction dependent.

***Table 9.2:*** *Confidence Interval (CI) of Velocity versus Density and log(velocity) versus log(Young's modulus)*

| Equation | Constant | SE | CI | Gradient | SE | CI | $R^2$ | n |
|---|---|---|---|---|---|---|---|---|
| ρ(All) | 1301 | 46 | 91.5 | 1.67 | 0.11 | 0.22 | 75 | 84 |
| ρ(Bovine) | 1675 | 56.7 | 120.2 | 1.0 | 0.11 | 0.23 | 84 | 18 |
| ρ(Calcaneus) | 1374 | 46 | 96.6 | 0.97 | 0.17 | 0.36 | 64 | 20 |
| E(All) | 3.09 | 0.006 | 0.012 | 0.085 | 0.003 | 0.006 | 94 | 86 |
| E(Bovine) | 3.0 | 0.02 | 0.04 | 0.113 | 0.007 | 0.014 | 83 | 54 |
| E(Calcaneus) | 3.14 | 0.01 | 0.02 | 0.049 | 0.007 | 0.015 | 73 | 20 |
| E(Vertebrae) | 3.03 | 0.028 | 0.062 | 0.122 | 0.017 | 0.038 | 84 | 12 |

It may be concluded that when vector quantities such as Young's modulus, strength and velocity are to be predicted from scalar quantity such as density, each specie and direction must be treated individually.
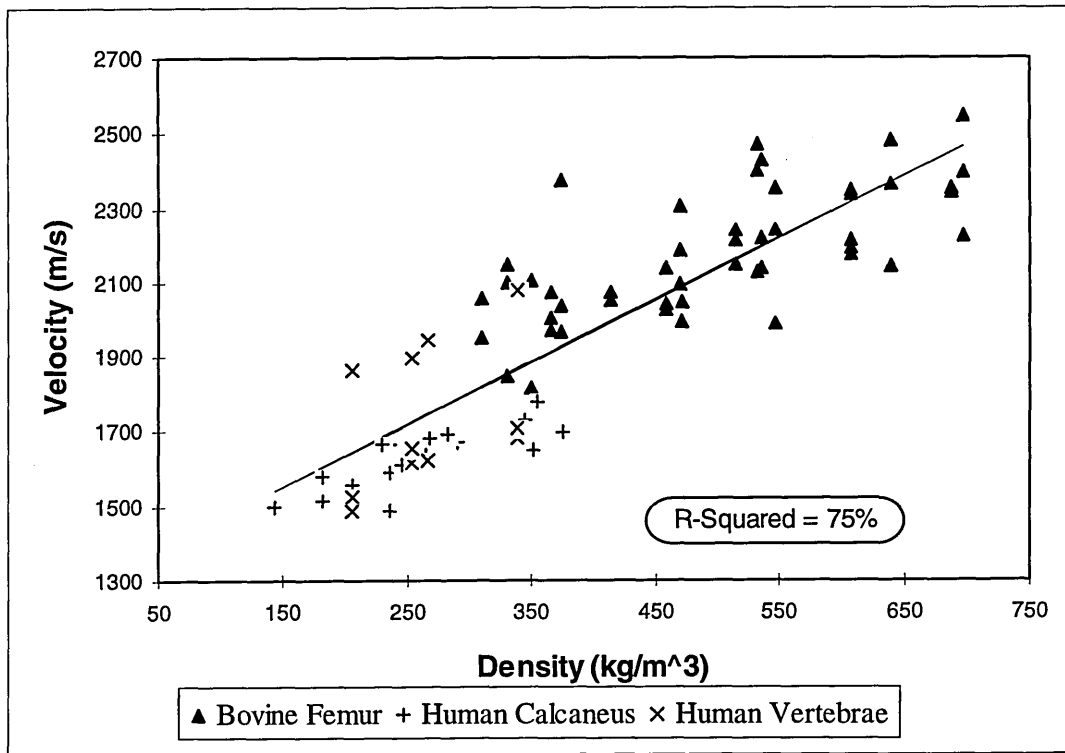
**Figure 9-3** : *A Plot of Velocity as a Function of Density:*
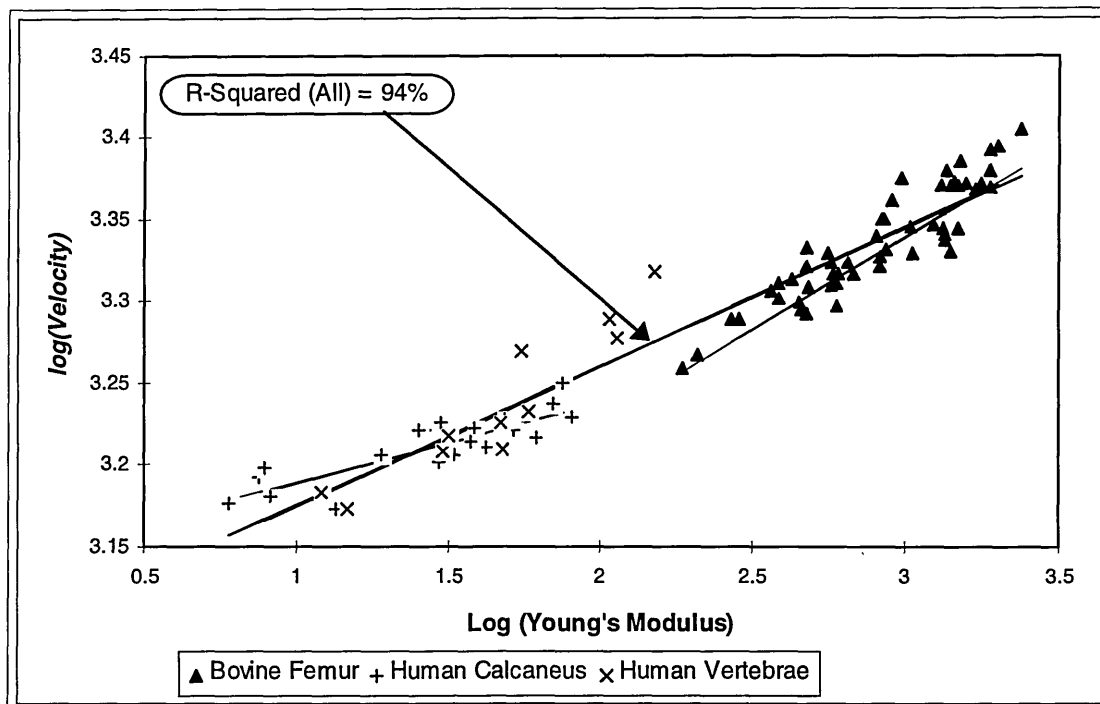


**Figure 9-4:** *A Plot of log(Velocity) as a Function of log(Young's Modulus)*

The linear regression analysis of log(Velocity) versus log(Young's modulus) and the confidence intervals of the gradient and intercept are presented in Table 9.2 and Figure

220

9.4. The line fit through the combined data has a higher correlation coefficient than the individual groups.

The plot of velocity as the combined function of Young's modulus (E) and density (ρ) is presented in Figure 9.5 and the linear analysis in Equations 9.4 and 9.5

$$V = 1446 + 551\sqrt{E/\rho} \qquad\qquad R^2 = 94\% \qquad (9.4)$$

$$E = -382 + 5.61 * 10^{-7} V^2 \rho \qquad\qquad R^2 = 94\% \qquad (9.5)$$

The plot of velocity as the combined function of strength(σ) and density (ρ) is presented in Figure 9.6 and the linear analysis in Equation 9.4.

$$V = 1382 + 6141\sqrt{\sigma/\rho} \qquad\qquad R^2 = 93\% \qquad (9.6)$$

$$\sigma = -2.84 + 4.84 * 10^{-9} V^2 \rho \qquad\qquad R^2 = 95\% \qquad (9.7)$$

**Table 9.3:** *Confidence Interval for the Equations of the Form* V = *constant* + *gradient*\* √(E/ρ) *and gradient*\* √(σ/ρ)  *Calculated at 95% Confident Limit.*

| Equation | Constant | SE | CI(±) | Gradient | SE | CI(±) | $R^2$(%) | n |
|---|---|---|---|---|---|---|---|---|
| E(All) | 1446 | 16.0 | 31.8 | 551 | 14.5 | 18.9 | 94 | 86 |
| E(Bovine) | 1410 | 45.4 | 91.2 | 574 | 33.5 | 67.3 | 85 | 54 |
| E(Calcaneus) | 1390 | 35.8 | 75.2 | 702 | 101.6 | 213.5 | 73 | 20 |
| E(Vertebrae) | 1213 | 58 | 129.3 | 1150 | 125 | 278.8 | 89 | 12 |
| σ(All) | 1388 | 25 | 50.55 | 5983 | 276 | 558 | 93 | 39 |
| σ(Bovine) | 1103 | 159 | 343.4 | 8122 | 1246 | 2691 | 77 | 15 |
| σ(Calcaneus) | 1390 | 42 | 88.24 | 6040 | 1021 | 2145 | 66 | 20 |

Table 9.3 demonstrates that both the confident ranges of bovine and human specimens lie within the same range. To further restrict the range, the confidence level was chosen to reflect the $R^2$ values, for example 80% confidence for the bovine samples. Again the confidence ranges for both species were still within the same range. This implies that the bovine femur, human calcaneus and the vertebrae behave in the same way with respect to velocity, elasticity and density. It therefore also justifies Equations 9.4

and 9.6 whereby the two species data were combined. Following from this, one could conclude that the relationship given in these equations could be applied to any anisotropic material.
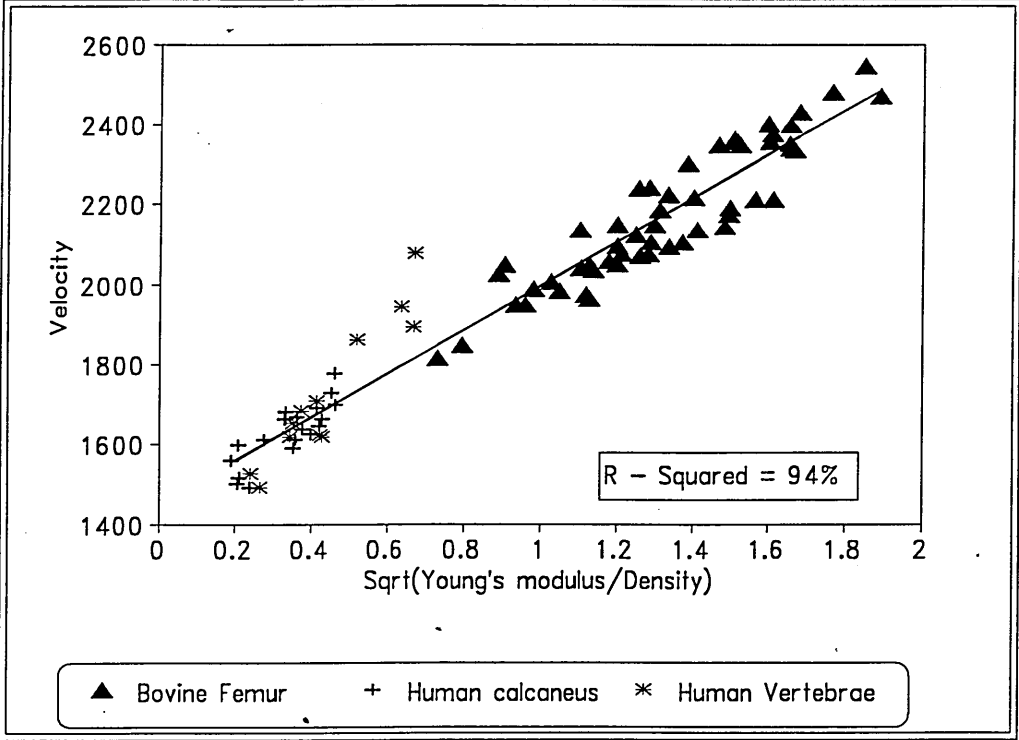


*Figure 9-5*: *The Relationship Between Velocity , Young's Modulus and Density for all Specimen*
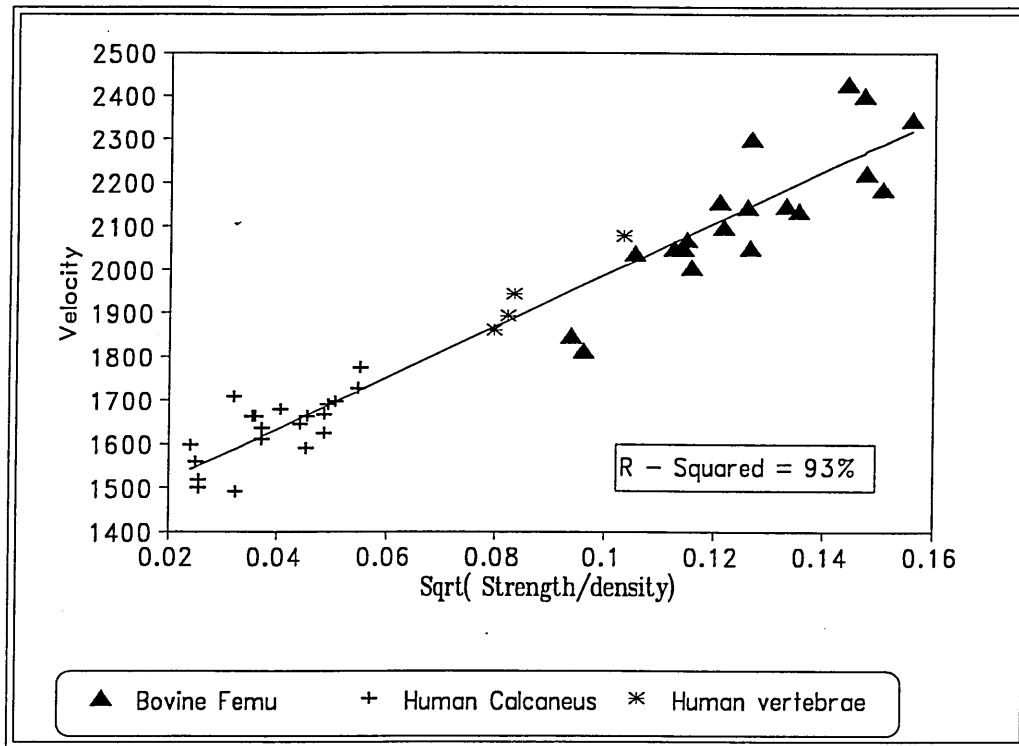
*Figure 9-6:* *The Relationship Between Velocity, Strength and Density for all Specimen*

The next question that should be addressed is to what degree can bone strength and stiffness be predicted from velocity measured using the CUBA system. The combined results have a very high correlation coefficients (Equations 9.5 and 9.7) but the individual data set have a relatively lower correlation coefficient ($R^2 = 88\%$, calcaneus; $R^2 = 92\%$, bovine). The pulse method utilised in this investigation has an inherent inaccuracy in reading the start of the received signal. This error becomes significant if the specimen is small or if the period is of the same order of magnitude as the time delay. The reason for this is twofold. There is a region called the near field of the ultrasonic beam transducer in which the waves emanating from the transducer face interfere with one another. The length of the near field region of the transducer ( $X_{max}$.) is approximately given by $X_{max} = \dfrac{(4r^2 - \lambda^2)}{4\lambda} \approx \dfrac{r^2}{\lambda}$ (when $r \gg \lambda$) where r is the radius of the transducer and $\lambda$ is the wavelength. For bovine samples of velocity 2252 ms^{-1} and frequency 0.2 - 0.6 MHz $X_{max.}$ is 1.16 - 11.66 mm and for calcaneus samples 3.14 - 15.5 mm for velocity of 1635 ms^{-1}. The human calcaneus specimens

measurements were carried out after the cortical end plates had been removed. This therefore produced specimens of varying thickness (25 mm - 15 mm) and the shorter specimens thus lend themselves to velocity measurement inaccuracy. From the previous results the effect of this inaccuracy was minimal.

The mode of ultrasound propagation through cancellous bone is not well understood. Ashman and Rho[1988] argued that for waves generated at 2.25 MHz and specimen of cross-section of 5 mm a bar wave is generated which travels along the trabecular struts. Contrary, William[1992] used Biot's theory to show that the velocities measured by Ashman and Rho are for bulk waves. Our application of the bar wave equation for simplicity yielded good correlation coefficients. Turner and Eich [1991] carried out a similar investigation on bovine cancellous femur. They measured two sets of velocity ; one with a transducer excited at 2.25 MHz and the other one at 215 kHz. The higher frequency produced higher velocity values, but the correlation with yield strength was not significantly different ( $R^2$ = 77% for 2.25 MHz and $R^2$ = 73% for 215 kHz ). Our studies on CUBA system (McCue Ultrasonic, UK) produced a higher $R^2$ value ( $R^2$ = 95% ). The numerical values between these two studies could not be compared because of difference in frequency used for velocity measurement. It was also noted that the Young's modulus reported by Turner and Eich [1991] were lower than for corresponding density in this study. The discrepancy may be due to a lack of allowance for the compliance of the Instron system in the Young's modulus calculation.

## 9.3.2 Broadband Ultrasonic Attenuation

A plot of nnBUA as a function of density is presented in Figure 9.6. It should be noted that only the PD values are included for bovine and vertebrae. It can be seen from Figure 9.6 that the behaviour of nnBUA with density was non-linear and this is similar to what was observed in the porous perspex study.

Low nnBUA values were measured for very low density calcaneus samples and very high density bovine samples. The explanation for this observation is the same as proposed for the perspex model in Chapter 6, in which the contribution of scatter determines the shape of the curve and it is structure dependent. For the calcaneus, the

224

specimens were obtained from the same position, thus limiting the structural variation, hence the linear response with density. The bovine samples were obtained from different position on the proximal and distal femur. It is generally accepted that different locations due to distinct functional requirement develop separate arrangements of struts - hence the scatter observed with the bovine samples.
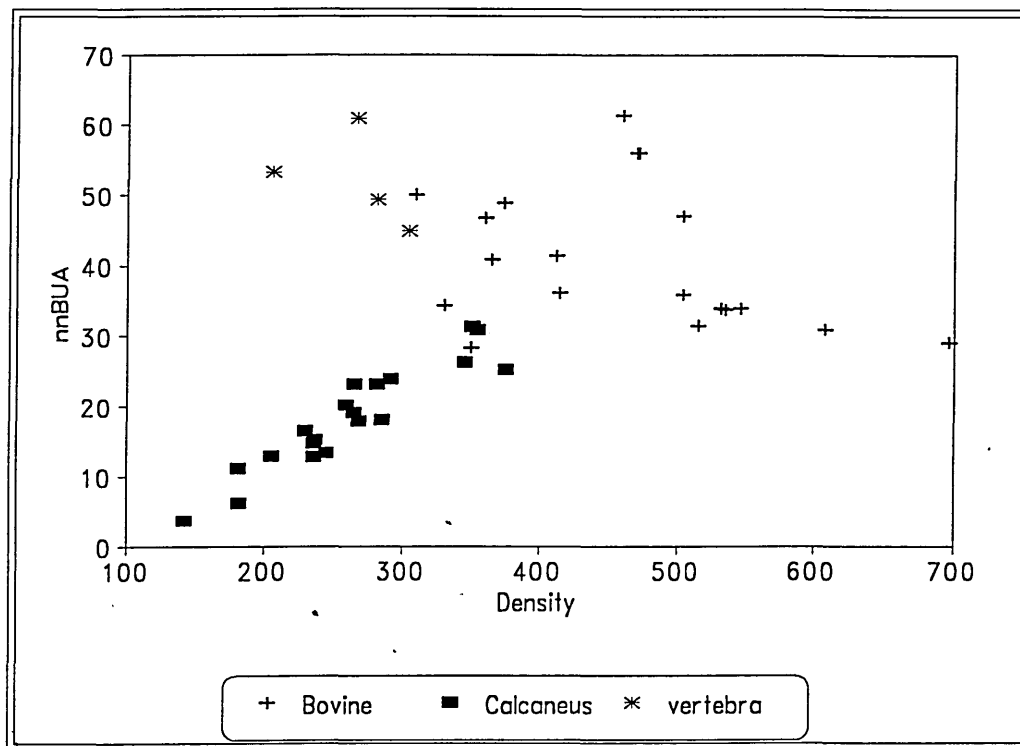


*Figure 9-7: A Plot of nnBUA versus Density for Calcaneus, Vertebrae(PD and Femur(PD)*

The plot of BUA as function of strength is presented in Figure 9.8. and the relationship is parabolic as observed with density. This is due to the strong dependence of strength on density. When the BUA values were divided by density two distinct phases were observed;-ascending for calcaneus and descending for vertebrae and bovine. Therefore BUA could be used to predict strength if the region of the curve is known.

225
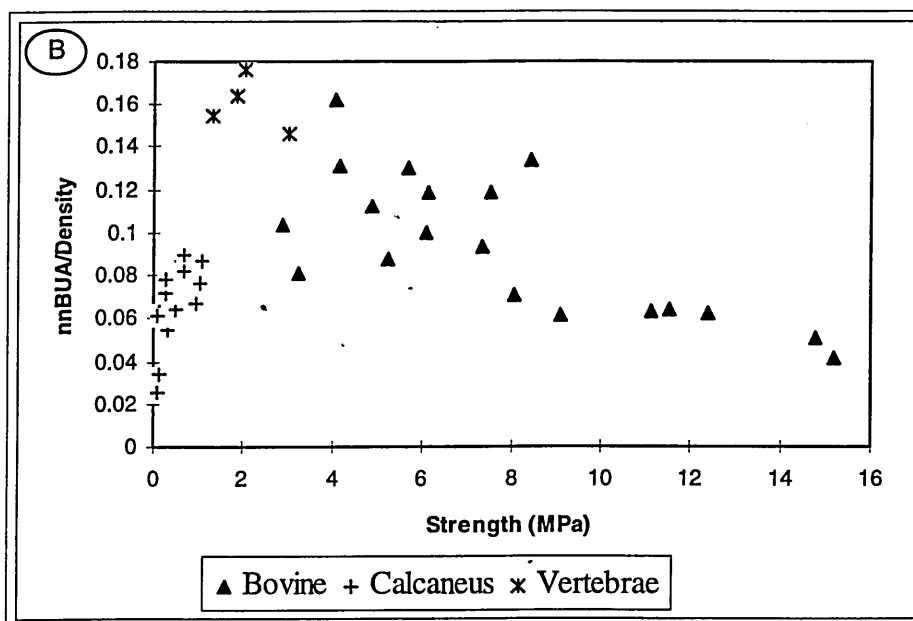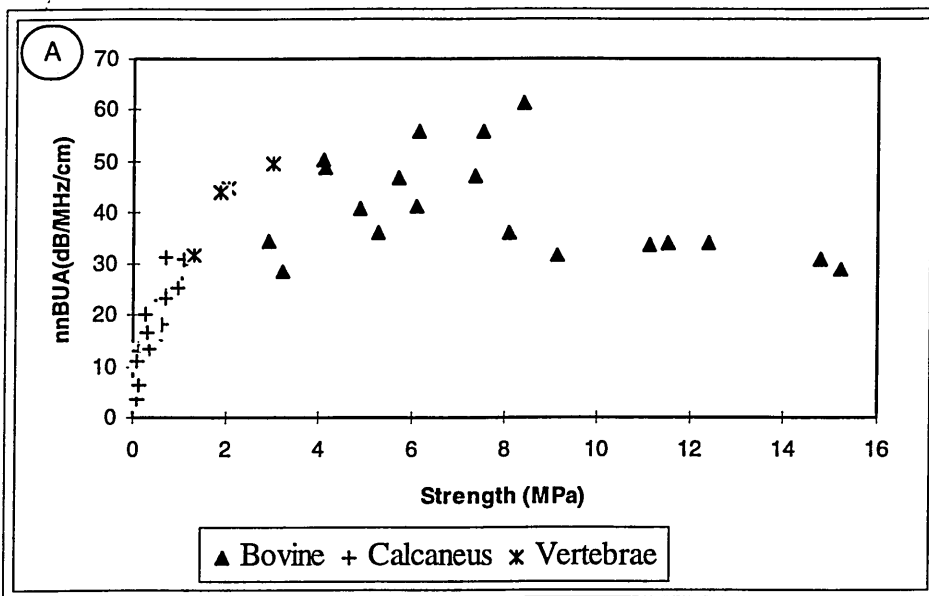
*Figure 9-8: The Relationship Between BUA and Strength (A), nnBUA divided by density (B)*

## 9.4 Conclusions

\*    Density is a high predictor of Young's modulus and strength for individual specie. The statistical analysis demonstrated that the mechanical properties are distinct and should be analysed separately for each site and each specie.

\*    Velocity had a low correlation coefficient with density and line fit through the

combined data overestimates calcaneus values, while underestimating vertebrae and bovine values. Caution should then be exercised in relating vector quantities like velocity, Young's modulus, and strength with scalar quantity like density without specifying or unifying the direction of measurement.

* Applying the modified wave equation ( $V = \sqrt{E/\rho}\ or \sqrt{\sigma/\rho}$ ) to the combined data resulted in a very high correlation coefficient ( r = 0.97 for Young's modulus and r = 0.96 for strength). Statistical analysis also confirmed that the relationship could also be applied to any bone site and specie. It was thus proposed that such a relationship could be used in-vivo with density measured from QCT to predict bone strength.

* The relationship between BUA and density for the combined data followed the same pattern as observed for the porous perspex models. The same pattern was observed for strength. A simple empirical formulation could not be derived to predict strength for the combined data.

# Chapter

# 10. DISCUSSION AND FUTURE STUDIES

## 10.1 Introduction

Osteoporosis is now recognised as a silent epidemic reiterated in the recent report by the Department of Health, [1994]. At present, clinical non-invasive assessment of osteoporosis relies mainly on bone mineral density(BMD) measurements using dual energy X-ray absorptiometry. Bone density has been shown to be a predictor of fracture, explaining about 75 - 80% of the variance. The current sentiment now believes that other properties of bone such as fatigue damage, trabecular architecture, mineralization and elasticity may be important in determining fracture.

The work of Langton [Langton et al., 1984] pushed ultrasound forward as an alternative modality to bone status assessment. Ultrasound has the advantage of being a mechanical wave and the process of fracture is mechanical. Therefore ultrasound could give information pertinent to fracture such as structure. There are few unanswered questions such as: what is ultrasound measuring?, can empirical formulae be derived to correlate the structural and density changes to ultrasound? These questions constituted my research theme and the objectives of the project were therefore:

* To develop the understanding of ultrasound transmission through cancellous bone

* To determine the relationship between ultrasonic parameters with mechanical and structural properties of cancellous bone

* To identify the structural dependence of ultrasound parameters

This chapter presents a resume of how the above objectives were achieved. The reader is referred to the preceding chapters for detail coverage.

## 10.2 Methodology

The investigation was carried out in two parts:- a phantom study and an *in vitro* cancellous bone study. For the phantom study only the factors affecting ultrasound transmission were investigated. Mechanical properties and ultrasonic properties were investigated in the *in vitro* studies.

Ultrasound properties were measured using the Contact Ultrasonic Bone Analyser(CUBA). CUBA's short term and long term precision were assessed using polymers. The short term and long term precision was 2.75% and 3.31% for BUA and 0.62% and 0.89% for velocity respectively. The lower precision in BUA was thought to be due to phase cancellation artefacts.

Permeability was introduced as a structural index because it is related to the porosity and connectivity of a sample. The method of measuring permeability was validated by comparing the experimental results with manufacture's quoted values for porous HDPE filters ($R^2$ = 95%). A straight capillary model was developed and the experimental values were highly correlated with theoretical prediction ($R^2$ = 99%).

## 10.3 Properties affecting Ultrasound Transmission in Porous Material

### 10.3.1 Development of Physical Mimics

In order to gain an understanding into ultrasound transmission through cancellous bone, mimics were developed. Various mimics for cortical bone, bone marrow and cancellous bone were investigated. Plaster of Paris (POP) was not found to be a good cortical bone phantom because it was not possible to manufacture identical phantoms and the attenuation was largely dependent on the length of soaking. Perspex was a better cortical bone phantom in terms of durability, stability, and manageability.

Perspex also had the highest velocity (V = 2670 m s$^{-1}$) and density ($\rho$ = 1180 kg m$^{-3}$) of all the polymers studied and thus was the most appropriate of all the polymers as a substitute for cortical bone whose quoted velocity and density are 3000- 4000 m s$^{-1}$ and 1800 - 2000 kg m$^{-3}$ respectively.

Agar gel was more of a soft tissue phantom than fat because of its high viscosity. Lard and castor oil were found to have properties close to fat. It was also demonstrated that both velocity and attenuation in lard are dependent on temperature.

Aluminium mesh in agar gel did not satisfy the requirement of a cancellous bone phantom. It was established that perspex with holes drilled in them provided a convenient variable phantom to study the propagation of ultrasound through porous materials. On the other hand HDPE filters were found to be a good phantom for precision studies.

## 10.3.2 Evaluation of Cancellous Bone Mimics

Perspex blocks with holes drilled in them (porous perspex) were further used to study the effect of age associated osteoporosis on ultrasound transmission. In ageing cancellous bone two types of bone loss occurs- thinning of the trabeculae or total loss of trabeculae struts. This was mimiced by increasing the hole diameter and by varying the number and distribution of the holes respectively.

Broadband ultrasound attenuation (BUA) in porous perspex varies as a function of hole diameter (porosity) with a peak occurring at around 3.5 mm. Scattering and absorption processes were used successfully in qualitative explanation of the results. The effect of scattering was dependent on the diameter of the pores compared to the wavelength of the ultrasound wave. The absorption contribution was independent of pore size. A combination of attenuation at mid frequency (0.4 MHz) could not linearize the behaviour of BUA with hole size. The dependence of BUA on pore size was further demonstrated on HDPE filters. The pore sizes found in the filters were lower than 3.5 mm (15 - 350 $\mu$m) and the parabolic relationship with pore size was

not observed. It was found that BUA could be related to $\phi^{1.4}$ in the HDPE filters ($R^2$ = 96%).

Velocity on the other hand remained constant until a hole diameter of 4 mm where it started to decrease. The form of wave propagation (bar wave or longitudinal wave) could be used to explain this observation. For a pore size less than 4 mm ( ≈ wavelength of the pulse) two wave path could be identified:- one through perspex only and one through perspex and water. Due to the signal to noise ratio only the wave solely through perspex is identified, hence resulting in the non-variant velocity with changing pore size. After 4 mm pore size, the change in velocity is inversely proportional to porosity ($R^2$ = 90%).

## 10.4 Relationship Between mechanical, ultrasonic and structural properties of cancellous bone

### 10.4.1 Bovine Cancellous Bone

The ultimate application of the ultrasound technique will be to predict the mechanical behaviour of bone from ultrasound measurements. Bovine bone samples were collected from proximal and distal femora. They were then tested both ultrasonically and mechanically.

The mechanical properties (Young's modulus- E and strength- $\sigma$) were within reported data for bovine cancellous bone. Orientational dependence of these properties was also demonstrated. Young modulus was related to the nth power of density, the n value being dependent on the direction of measurement( n = 1.98 for PD, 2.42 for AP and 2.03 for ML). The ultimate strength was also found to have a quadratic relationship with density.

Ultrasonic velocity was shown to be direction dependent which is expected for a vector quantity measured in an anisotropic medium. Velocity correlated with Young's modulus ($R^2 = 83\%$) but there was no significant difference in the correlations when separated into the various directions. The correlation of velocity with density was poor and dependent on direction ($R^2 = 69\%$ for AP, 70% for ML and 49% for PD). The ultrasonic velocity followed the well established relationship between velocity, Young's modulus and density ($V = \sqrt{(E/\rho)}$).

BUA was also shown to be direction dependent and the highest significance was seen between PD and AP directions. When BUA was separated into different directions and the structural variation diminished, BUA was found to be linearly proportional to density. It is worth noting that one would not expect a correlation between BUA and density for random samples. For a specific direction (PD) BUA was found to predict strength with an $R^2$ of 74%. The behaviour of BUA with Young's modulus also followed the same pattern as between BUA and density. This is accounted for by the strong dependence of Young's modulus on density. There was no correlation between BUA and velocity

There was a high negative correlation between permeability and density. The gradient of the linear regression analysis was different for the different directions implying directional dependence of permeability and thus structure. A negative correlation was found between permeability with E, σ and V. Permeability was not found be a good predictor of BUA for bovine cancellous bone. This is because for the bovine samples studied, their density values were around the turning point of the BUA-density parabolic behaviour, but permeability has an inverse proportionality behaviour with density. Also, the permeability dependence on density is higher than BUA dependence, thus having a lower dependence on structure than BUA.

## 10.4.2 Human Cancellous Bone

In clinical practice, ultrasound measurements are carried out at the calcaneus, patella, tibia and phalanges. However, the most popular site is the calcaneus due to its high cancellous bone content and parallel surfaces. Human samples were obtained from the calcaneus and spine. Mechanical, ultrasound and material properties were measured.

## 10.4.2.1 Calcaneus

The mechanical properties are similar to those reported in the literature. Young's modulus and strength were found to be related to the cubic power of density for the medio-lateral direction and this is in agreement with the power relationship predicted by the theoretical models of Gibson [1985].

Velocity of the whole and core samples, and cancellous and defatted samples were statistically the same. Velocity was relatively poorly correlated with density ($R^2$ = 64%). The modified wave velocity relationship was investigated and the calcaneus data explained only 73% and 68% of the variance for Young's modulus and strength respectively. Velocity was however a good predictor of Young's modulus ($R^2$ = 94%) and strength ($R^2$ = 88%).

The calcaneus has the measuring site advantage of accessibility and also it has more than 90 % trabecular bone by volume [ Vogel et al., 1988], hence $nnBUA_{whole} \approx nnBUA_{can}$. This was demonstrated by measuring cored samples and samples without the cortical end plates. The effect cortical endplates on BUA was only an offset probably due to phase cancellation.

Broadband Ultrasonic attenuation (BUA) has been demonstrated as a good predictor of density (BUA $\alpha$ $\rho^{1.99}$ , $R^2$ = 87%) , bone strength (BUA $\approx$ $\sigma$, $R^2$ =75% ) and Young's modulus (BUA $\approx$ $E^{0.74}$, $R^2$ = 77%) of the calcaneus.

It was also demonstrated that a combination of $V^2BUA$ could predict strength and Young's modulus with 80% and 83% accuracy respectively.

There was no significant trend between ultrasonic and material properties with age and this was attributed to the limited age range.

Permeability was demonstrated to be related to density and also to predict both strength and BUA.

## 10.4.2.2 Vertebrae

The vertebrae were found to be distinctly anisotropic with the PD direction exhibiting the highest Young' modulus, velocity and BUA values. The mechanical properties

correlated with those reported in the literature and also follow the power law relationship with density found in the calcaneus and bovine samples.

The modified bar wave equation had a higher correlation than in the calcaneus. The directional dependence BUA and velocity was further demonstrated in the vertebrae. Due to the distinct anisotropy in the vertebrae, BUA was highly correlated with both velocity and Young's modulus more than in the calcaneus.

## 10.4.3 Analysis of all cancellous samples

Density is a high predictor of Young's modulus and strength for individual specie. The statistical analysis demonstrated that the mechanical properties are distinct and should be analysed separately for each site and each species.

Velocity had a low correlation coefficient with density and line fit through the combined data overestimated the calcaneus values, while underestimating vertebrae and bovine values. Caution should then be exercised in relating vector quantities like velocity, Young's modulus, and strength with a scalar quantity such as density without specifying or unifying the direction of measurement.

Applying the modified wave equation ( $V = \sqrt{E/\rho} \, or \sqrt{\sigma/\rho}$ ) to the combined data resulted in a very high correlation coefficient ( $R^2 = 94\%$ for Young's modulus and $R^2 = 93\%$ for strength). Statistical analysis also confirmed that the relationship could also be applied to any bone site and species. It was thus proposed that such a relationship could be used in-vivo with density measured from QCT to predict bone strength.

The relationship between BUA and density for the combined data followed the same pattern as observed for the porous perspex models. The same pattern was observed for strength. A simple empirical formulation could not be derived to predict strength for the combined data. The existence of a peak in this relationship means that a proper interpretation of the correlation between BUA and density requires a knowledge of the density range. For example, the calcaneus has a density range far below the peak value and hence a good correlation was observed between BUA and density. The bovine femur on the other hand has a density range including the peak and hence any

linear correlation will not yield any meaningful results. This results then questions the validity of the in vivo correlation between BUA measured at the calcaneus with density measured at other sites because of the higher variation in density between sites.

When nBUA is separated into three orthogonal directions in the bovine specimens, a linear relationship was observed between nBUA and density. For the calcaneus a quadratic relationship was observed. This is analogous to the Young's modulus relationship with density in which Young's modulus relates to quadratic and cubic powers of density for bovine and calcaneus respectively.

## 10.5 Evidence of Structural Dependence of Ultrasound

BUA was also found to vary according to the spatial distribution of holes, hole number, inter-hole spacing and number of holes within the porous perspex mimic. These factors are an indication of the structure of the porous perspex mimic. Therefore, the structural dependence of BUA has been proven by deduction. More rigorous experimental analysis will be required to quantify the structural dependence of BUA. A separation of the effect of absorption and scattering attenuation mechanisms will facilitate the above goal.

The directional dependence of BUA, velocity, Young's modulus and permeability in both bovine femur and vertebrae is conclusive evidence that these parameters are influenced by the arrangement of trabeculae (structure of the cancellous samples). The higher coefficient of variation (CV) of BUA compared to density is further evidence of structural dependence. The high CV makes BUA more sensitive to osteoporotic changes in cancellous bone than density measurement.

Permeability was introduced as a structural index because it is related to the porosity and connectivity of a sample. BUA in the HDPE filters correlated well with permeability ($R^2 = 83\%$). Permeability was proposed to give an indication of structure

and therefore a correlation between permeability and BUA further substantiated the structural dependence of BUA.

## 10.6 Future Work

### 10.6.1 Methodology

Chloroform used in the defatting procedure has been reported to be carcinogenic (Private communication), therefore future studies involving defatting should use dichoromethane in conjunction with ultrasonic cleaning apparatus as described by Sharp et al. [1989].

One of the problems with permeability measurements is that poor defatting drastically affects the results and limits the ability to determine the cut off point when the Darcy equation ceases to apply. In future investigations, a method could be devised to determined whether the defatting is completed or not, and also investigate the limitation of the Darcy Law. The weakness with permeability as a structural index is its strong dependence on density. The phantom study in Chapter 5 was unable to identify the sole effect of structure on permeability. An experimental set up should be devised whereby the density is maintained constant and structure varied.

The temperature of the water bath was not controlled but was assumed to be room temperature, hence any fluctuation in temperature may affect the accuracy of the results. As demonstrated in Figure 5.2 and 5.3 and the work of Evans and Tavakoli [1992], BUA and velocity are temperature dependent. Hence it will be recommended that future studies use a temperature regulated water bath.

### 10.6.2 BUA

To investigate the sole effect of scattering to BUA, excess attenuation may be calculated. The excess attenuation may be obtained by subtracting the attenuation

coefficient of perspex without holes from the attenuation coefficient of perspex with holes

The apparent strength of cancellous bone is reduced by multiple load cycles as opposed to a single load cycle. Static methods such as the one used in this investigation do not take into account the cyclic dynamic axial loading that occurs during everyday life. An investigation could be carried out to verify whether ultrasound (Velocity and BUA) can indicate changes in bone strength with the application of multiple load cycles, ie fatigue analysis.

Another experiment could be designed in such a way that velocity and BUA were measured on a sample as the load was being progressively applied. A relationship could be derived between applied load and ultrasonic parameters (Velocity and BUA).

The pilot studies on the vertebrae confirmed the marked anisotropy, so further extensive studies could be carried out to help the understanding of ultrasound propagation through porous materials such as cancellous bone, especially the application of the Biot theory.

## 10.6.3 In-Vivo Population Studies

It has been demonstrated that both BUA and velocity are good predictors of cancellous bone strength. A large prospective population study should be carried out to find the BUA and velocity values for the highest specificity and sensitivity for fracture prediction. This may incorporate the derivation of a combined parameter. It has been demonstrated that the prediction of strength was improved by using the bar wave equation. An *in vivo* study should be carried out using both QCT and ultrasound to investigate which combination could improve prediction such as:

$$\sigma = v^2 BUA, or\_\sigma = v^2 QCT,$$

## 10.6.4 Structural Analysis and Modelling

The studies here were limited to the macroscopic changes. A microscopic study may compliment the results obtained here. Such a study would look at topological parameters such as connectivity, trabeculae spacing and trabeculae thickness.

The problem with quantification of the structure of cancellous bone is, how do you define structure. The definitions are sometimes linked with the problem to be solved. Structure does not have a universal definition. So, an alternative approach to the study of osteoporosis will be what structural changes occur in an osteoporotic bone (thinning and erosion of trabeculae) and how do these changes affect the strength of cancellous bone. Chapter 5 demonstrated that BUA and velocity change with these structural changes but a model to predict the structural changes from measured velocity and BUA is needed.

The porous perspex models demonstrated that BUA was dependent on pore size, number and distribution. A theoretical model incorporating the Biot theory is needed that could predict BUA and velocity from the material properties of the sample.

# Chapter

# 11. CONCLUSIONS

1. Perspex was demonstrated to be a good cortical bone mimic in terms of durability, stability, manageability, ultrasound velocity and attenuation.

2. It was also established that perspex blocks with holes drilled in them and HDPE filters were good cancellous bone phantoms to study the propagation of ultrasound.

3. BUA varies with porosity having a peak value at 35% porosity. Scattering phenomenon were qualitatively demonstrated to be responsible for the parabolic behaviour.

4. Velocity is inversely proportional to porosity .

5. Young's modulus is related to the nth power of density, the n value being dependent on the direction of measurement and on the site of measurement.

6. The measured ultrasonic velocity can be approximated to the well established bar wave equation which relates velocity to Young's modulus and density.

7. Velocity and BUA are good predictors of Young's modulus and strength.

8. Young's modulus, velocity, BUA and permeability are all direction dependent, validating the structure dependence of these quantities.

9. Permeability coefficient is a good structural index

10. Future work is recommended in the aspects of *in vitro* methodology and *in vivo* studies.

# 12. REFERENCES

**Aaron JE, Makins NB, Sagreiya K (1984)** The microanatomy of trabecular bone loss in normal ageing men and women. *Clin. Orthop 215*, 260

**Abenschein W and Hyatt (1970)** Ultrasonics and selected physical properties of bone. *Clin. Orthop 69: 294-301*

**Agren M, Karellas A, Leahey D, Marks S and Baran (1991)** Ultrasound attenuation of the calcaneus: A sensitive and specific discriminator of osteopenia in postmenopausal women, *Calcif. Tissue Int. 48 240 -244*

**Alhava M E (1991)** Bone density measurement, *Calcif Tissue Int (suppl)* 49 S21 -S23

**Andre M.P, Craven J.D and Greenfield M.A (1980)** Measurement of the velocity of ultrasound in the human femur in vivo. *Med. Phys. 7(4) 324 -330*

**Antich P.P, Anderson J.A, Ashman R. B, Dowdey J.E, Gonzales J. Murry R.C. Zerweky J.E and Pak C.Y (1990).** Measurement of mechanical properties of bone material in vitro by ultrasound reflection: Methodology and comparison with ultrasound transmission . *J. of bone and Mineral research, 6(4) 417- 426*

**Ashman B.R and Rho J.Y (1988).** Elastic modulus of trabecular bone material. *J. Biomechanics vol 21(3) pp177-181.*

**Ashman B.R ,Cowin S.C, Van Buskirk W.C and Rice J.C (1984).** A continuous wave technique for the measurement of the elastic properties of cortical bone. *J. Biomechanics vol 17,349-361*

**Ashman B.R, Turner C. H and Cowin S.C (1986).** Ultrasonic technique for the measurement of the structural elastic modulus of cancellous bone. *Transactions of the orthopaedic research Society P43.*

**Ashman R.B, Corin J.D and Turner C.H (1987).** Elastic properties of cancellous bone measurement by an ultrasonic technique. *J. Biomechanics vol 20(10) pp979-986.*

**Avioli LV (1991)** Significance of osteoporosis: A growing international health care problem. *Calcif. Tissue Int. (Suppl) 49: S5-S7*

**Avioli LV, Brandenburger G, Chesnut C, Gallagher JC, Heaney RP, Lappe J and Recker RR (1988)** Ultrasound transmission velocity in screening for bone fragility *J. Bone Min Res. 3, 215 -219*

**Bamber J. C and Tristam M (1988)** Diagnostic Ultrasound ; In the Physics of Medical Imaging, edited by S Webb, Adam Hilger, Bristol pp319 - 386

**Baran D T, McCarthy CK, Leahey D, and Lew R (1991)** Broadband ultrasound attenuation of the calcaneus predicts lumbar and femoral neck density in caucasian women: A preliminary study, Osteo. Int 1: 110 -113

**Baran DT, Kelly AM, Karellas A, Gionet M, Price M, Leahy D, Steutermna S, McSherry Band Roche J (1988)** Ultrasonics attenuation of the os calcis in women with osteoporosis and hip fractures, *Calcif. Tissue Int. 43 138 -142*

240

Behari J and Singh S (1981) Ultrasound propagation in in vivo bone.*Ultrasonics 81: 87- 90*

Behrens J.C, Walker P.S and Shoji H, (1974).    Variation in strength and structure of cancellous bone at the knee , *J. Biomechanics vol 7 201-207*

Bell G.H, Dunber O, Beck J.S and Gibb A (1967).    Variations in the strength of vertebrae with age and their relations to osteoporosis. *Calc. Tissue Re. 1, 75*

Bensusan J.S., Davy D.T. Heiple K.G and Verdin P.J (1983) .    Tensile, coompressive and torsional testing of cancellous bone.    *Trans 29th orthop. Res. Soc.8 132*

Bergot C, Laval-Jeantet A.M, Preteux F and Meunier F (1988) A measurement of anisotropic vertebral trabecular bone loss during aging by quanititative image analysis. *Calcif. Tissue Int. 43: 143 - 149*

Biot M.A (1962)  Generalized theory  of acoustic propagation in porous dissipative media. *J. Acoustic Soc. Am.; 34: 1254-1264*

Biot M.A (1956a) Theory of propagation of elastic waves in a fluid saturated porous solid. I. Low frequency range. *J. Acoustic Soc. Am.; 28:168- 179*

Biot M.A (1956b) Theory of propagation of elastic waves in a fluid saturated porous solid. II. Higher frequency range. *J. Acoustic Soc. Am.; 28: 179 -191*

Blair Scott G. W. (1969).    Elementary rheology    , Academic Press, London

Bowman A. W and Robinson B. R (1990) Introduction to regression and analysis of variance. (Adam Higer , London)

Brear K, Currey J.D and Raines S, (1988).    Density  and  temperature  effects  on  some mechanical properties of  cancellous bone , *Engng in  Med vol  17(4) pp163-167*

Brown T.D and Ferguson A.B, (1980).    Mechanical property  distribution in  cancellous bone of the human proximal femur , *Acta.Orthop.Scand. 51,429-437.*

Bryant J.D (1983).    The effect of impact on the marrow pressure of long bones in vitro    *J. Biomechanics, 16, 659-665*

Bryant J.D, (1988).    On the mechanical function of marrow in long bones, *Engng in Med vol 17(2) 55-58*

Buckle H, (1959). *Metall. Rev. 4, pp49.*

Burlew M.M, Madsen E.L, Zagzebski J.A, Banjavic R.A, Sum S.W (1980). A new ultrasound tissue-equivalent material. *Radiology 134, pp517-520.*

Burstein A.H and Frankel V.H (1971).  A standard test for laboratory animal bone.  *J. Biomechanics, Vol 4, 155-158.*

Burstein A .H, Reilly D.T, Martens M (1976). Aging of bone tissue: Mechanical properties. *J. BoneJt Suurg. 58A: 82-86*

Carlstrom D, (1954).    Microhardness measurement on single haversian systems in bone. *Experientia 10, 171*

Carter D.R and Hayes W.C, (1976).    Bone compressive strength: The influence of density and strain rate,    *Science Vol 194, 1174-1175.*

Carter D.R and Hayes W.C, (1977).    The compressive behaviour of bone as a two phase porous structure.    *J. of Bone and Jt Surgery, vol 59A 954- 962*

**Carter D.R and Spengler D.M, (1978).** Mechanical properties and composition of cortical bone, *Clin. Orth. and Rel. Res. No 135 192-217.*

**Carter D.R, Schwab G. H and Spengler D.M, (1980).** Tensile fracture of cancellous bone, *Acta.Orthop.Scand. 51, 733-741*

**Cassidy J.J and Davy D.T [1985]** Mechanical and architectural properties in bovine cancellous bone *Trans-Orthop. Res.Soc.* pp354

**Charnley J, (1970).** Acrylic cement in orthopaedic surgery, William and Wilkins, Baltimore, Maryland.

**Christensen R.M, (1986),** Mechanics of low density materials . *J. Mech. Phys. Solids*

**Ciarrelli M.J, Goldstein S.A, Dickie D, Ku J.L, Kapper M., Stanley J., Flynn M. J and Matthews L.S (1986).** Experimental determination of the orthogonal mechanical properties , density and distribution of human trabecular bone from the major metaphyseal regions ultilizing material testing and computed tomography. *Trans. Orthop. Res. Soc., P42.*

**Craven J.D, Costantini M.A, Greenfield M.A and Stern R (1973).** Measurement of the velocity of ultrasound in human cortical bone and its potential clinical importance. An in vivo preliminary study. *Invest.Radiol. 8: 72-77*

**Cohn S.H, Abesamis C and Yasumara S (1977)** Comparative skeletal mass and radial bone mineral content in black and white women *Metabolism 26,* 171-

**Cowin S.C (1988)** Wolff's law of trabeculae archictecture at remodeling equilibrium. *J. Biomech. Engng. 110, 213 -215*

**Cowin S.C (1985)** The relationship between the elasticity tensor and fabric tensor. *Mechanical Material 4., 137 - 147*

**Cummings S.R and Black D(1986)** Should Perimenopausal women be screened for osteoporosis ? *Ann. Inter. Med.: 104: 817 - 823*

**Cummings S.R, Black D. M, Nevitt M.C, Browner W, Cauley J, Ensrud K Genant H.K, Palermo L, Scott J and Vogt T. M (1993)** Bone density at various sites for prediction of hip fractures. *Lancet' 341: 72 -75*

**Currey J.D (1969).** The mechanical consequences of variation in the mineral content of bone. *J. Biomechanics 2, pp1-11*

**Currey J. D (1970).** The mechanical properties of bone. *Clin. Orthop. Rel. Res. Number 73, 210-231*

**Currey J.D (1984).** The mechanical adaptation of bones. *Princeton University Press, Princeton N.J.*

**Currey J.D (1986).** Power Law models for the mechanical properties of cancellous bone , *Engng in Med vol 15(3) pp153-154*

**Damikalis J.E, Drekatis E, and Courtsoyiannis N.C (1992)** Ultrasound attenuation of the calcaneus in female population: normative data. *Calcif. Tissue Int 51: 180 - 183*

**Davis E, Troxell G.E, Wiskocil C.T (1964),** Testing and inspection of engineering materials, *3rd edition, New York, McGraw- hill*

Ducheyne P, Heymans L, Martens M, Aenondt E, Meester P.D and Mulier J.C (1977) The mechanical behaviour o intracondylar cancellous bone of the femur at different loading rates. *J Biomechanics 10, 747 -762*

Dyson E,D, Jackson C.K and Whitehouse W.J, (1970).    Scanning electron microscope studies of human trabecular bone,    *Nature 225, 957-959*

*Eastel R  (1992) Expert Workshop, Cologne Germany*

Eastel R and Riggs B.L, (1987) Endocrinology and aging calcium homoestasis and osteoporosis *Endocrinol. Metab. Clin. 16, 829*

Evans F.G and King A.I, (1961).   Regional differences in some physical properties of human spongy bone.    In biochemical studies of the muscol-skeletal system. Evans F(ed). Springfield, C.C. Thomas

Evans F.G (1973)  Mechanical properties of bone . *Charles C Thomas Publisher, USA*

Evans J.A (1986) Ultrasonic wave propagation in tissue. Physics in medicine, edited by Evans JA, *IPSM Report No 47*

Evans J.A. and Tavakoli M.B (1990). Ultrasonic attenuation and velocity in bone. *Phys. Med. Biol. 35(10) 1387-1396.*

Evans J.A. and Tavakoli M.B. (1992). Temperature and direction dependence of the attenuation and velocity of ultrasound in cancellous and cortical bone. Current Research in Osteoporosis and Bone Measurement II, BAth

Evans P.G, Behiri J.C, Currey J.D and Bonfield W, (1990). Microhardness and  Young's modulus in cortical bone exhibiting a  wide range of mineral volume fractions, and in a  bone analogue, *J. Material  science: Mat. in Med.138-43.*

Evans W.D, Crawley E.O, Compston J.E, Evans C and Owen G.M (1988) Ultrasonic attenuation and bone mineral density, *Clin. Physiol. Meas 9, 163 -165*

Fry F.J and Barger J.E (1978) Acoustical properties of human skull. *J Acoust. Soc. Am. 63: 1576 - 90*

Galante J, Rostoker W and Ray R.D (1970).  Physical Properties  of trabecular bone,  *Calc. Tiss. Res. vol 5, 236-246*

Garcia B.J., Foster F.S. and McNeill R.G. (1978) Ultrasonics attenuation in bone, Ultrasonics symposium proceedings : 327- 330

Gershon -Cohen J,  Reentman A.M, Schraer H and Blumberg N (1953) Asymptomatic fractures in osteoporotic spines of the aged *JAMA 153 625-*

Gibson L.J, (1985). The  mechanical  behaviour  of  cancellous  bone,  *J. Biomechanics vol 18, 317-328.*

Gibson L.J and Ashby M.F(1988).  Cancellous Bone.   Cellular Solids, structure and properties, *Pergamon Press 316- 330    ,*

Gibson L.J and Ashby M.F (1982). The mechanics of 3-dimensional cellular materials, *Proc.R. Soc., 382, 43-59*

Gierse H, (19760.    The cancellous   structure  in the  calcaneus  and  its relation to mechanical stressing , *Anat. Embryol. 150, 63-83.*

Gillan  (1969). Material under stress, *Butterworths Press*

243

Gluer C.C, Vahlensieck M, Faulkner K.G, Engelke K, Black D, and Genant H.K (1992) Site-matched calcaneal measurement of broadband ultrasound attenuation and single X-ray absorptiometry: Do they measure different skeletal properties ? *J. Bone and Mineral Research 7(9) 1071 -1079*

Gluer C.C, Wu C.Y and Genant H.K (1993) Broadband attenuation signals depend on trabecular orientation: an in-vitro study. *Osteoporosis Int 3: 185-191*

Goldstein S. A (1987). The mechanical properties of trabecular bone : dependence on anatomical location and function , *J. Biomechanics vol 1055-1061*

Goldstein S.A, Wilson D.L, Sonstegard D.A and Matthews L.S (1983) The mechanical properties of human tibial trabecular bone as a function of metaphyseal location. *J. Biomechanics, 16: 965 - 969*

Goldstein S. A, Goulet R and McCubbrey D (1993) Measurement and significance of three-dimensional architecture to the mechanical integrity of trabecular bone. *Calcif. Tissue Int 53(suppl): S127 -S133*

Gong J.K, Arnold J.S and Cohn S.H, (1964). Composition of trabecular and cortical bone, *Ant. Rec. 149, 325.*

Gray R.J and Korbacher G.K, (1974). Compressive fatique behaviour of bovine compact bone , *J. Biomechanics vol 7, 287-292.*

Greenfield M.A, Craven JD, Huddleston A, Kehrer M.L, Wishko D and Stern R (1981) Measurement of the velocity of ultrasound in human cortical bone in vivo. *Radiology 138: 701 -710*

Hall I.H, (1968). Deformation of solids, *Thomas Nelson and Sons*

Hans D, (1993). Validation des mesures ultrasoniques sur le calcaneum; *PhD Thesis, University of Claude Bernard - Lyon, France*

Harrigan T.P , Jasty M, Mann R.W and Harris W.H, (1985).Limitation of the continuity assumption in cancellous bone mechanics , *Transaction of the 31st annual meeting of the orthopaedic research society p135, Orth. Res. Soc.*

Harrigan T. P and Mann R. W (1984) Characterization of microstructural anisotropy in orthotropic materials using a second rank tensor. *J. Materials Sc. 19, 761 -767*

Hartmann B and Jarzynski J, 1972, ULtrasonic hysteresis absorption in polymers: *J. Appl. Phy., Vol 43(11) pp 4304- 4312*

Hayes W.C and Gehart T.N (1985) Biomechanics of bone: Applications for assessment of bone strength. In peck WA (ed): Bone and Mineral Research, Annual III, Amsterdam, Elsevier pp 259 -294

Heaney R.P, Avioli L.V, Chestnut C.H, Lappe J, Rescker R.R and Brandenburger G.H (1989) Osteoporotic bone fragility, detection by ultrasound transmission velocity *J. Am. Assoc. 261, 2986 -90*

Hearmon R.F.S, (1961). An introduction to applied anisotropic elasticity , *Oxford University Press, London*

Herd R.J.M., Ramalingham T., Ryan P.J, Fogelman I. and Blake G.M. (1992) Measurements of BUA in the calcanues in premenopausaland postmenopausal women, *Osteoporosis Int. 2: 247 -251*

244

**Herd R.J.M, Blake G.M, Miller C.G, Fogelman I (1994)** Should BUA be normalised for the width of the calcaneus? (Abstract) *10th International Bone Densitometry Workshop, Italy 1994, Bone and Mineral 25(supll 2) S16*

**Hodgskinson R., Currey J.D and Evans P.G (1989).** Hardness, an indicator of the mechanical competence of cancellous bone , *J. Orthop. Res. 754-758*

**Hodgskinson R and Currey J.D, 1990.** Effect of structural variation on Young's modulus of non- human cancellous bone , *Proc Instn Mech Engrs 20 pp43-52*

**Hosie C.J, Smith D.A, Deacon AD and Langton C.M (1987)** Comparison of broadband ultrasonic attenuation of the os calcis and quantitative computed tomography of the distal radius *Calcif. Tissue Int.48, 303 -308 -*

**Hvid I and Jensen J, (1984).** Cancellous bone strength at the proximal human tibia , *Engng in Med vol 13(1), 21-25*

**Hvid I, Anderson K and Olesen S, (1984).** Cancellous bone strength measurement with osteopenetrometer, *Engng in Med vol 13(2) 73-78*

**Hvid I, Rasmussen O, Jensen and Nielsen S, (1985a).** Trabecular bone strength profiles at the ankle joint , *Clin. Orth. and Rel. Res. No 199 306-312*

**Hvid I, Jensen N.C, Bunger C, Solund K and Djurhuus (1985b).** Bone mineral assay: Its relation to mechanical strength of cancellous bone , *Engng in Med vol 14(2) pp79-83*

**Hughes M.S, Handley S.M and Miller J.G (1987)** Nearly local Kramers-Kronig relations applied to porous epoxy Ultrasonics Symposium 1987 pp 1041 - 1045

**Jernot J.P, Bhanu Prasad P and Demaleprade P (1992)** Three-dimensional simulation of flow through a porous medium. *Journal of Microscopy 167(pt1) 9 -21*

**Jensen C.N, Madsen l.P and Linde F, (1991).** Topographical distribution of trabecular bone strength in the human os calcanei , J. *Biomechanics vol 24, 49-55.*

**Jensen C.N, Hvid I and Kroner K, (1988).** Strength pattern of cancellous bone at the ankle joint, *Engng in Med vol 17(2) 71-76*

**Jhamaria N.L, Lal K.B, Udawat M, Banfri P, and Kabra S.G (1983).** The Trabecular pattern of the calcaneum as an index of osteoporosis, *J. bone and Joint Surgery 65B 195-198*

**Johnston Jr C.C, Slemenda C.W and Melton J.L (1991)** Clinical use of bone densitometry. *The New England J. of Medicine: 324(16) 1105 - 1109*

**Josefchak R.G, Finlay B.J, Bourne R.B and Rorabeck C.H, (1987).** Cancellous bone support for patellar resurfacing, *Clin. Orth.and Rel. Res. 220 192-199*

**Kaplan S.J, Hayes W.C, Stone J.L. and Beaupre G.S ( 1985).** Tensile strength of bovine trabecular bone. *J. Biomech. 18, 723-727.*

**Kaye and Laby [1986]** Tables of physical and chemical constants Longman 15th edition

**Koplik J, Lin C, and Vermette (1984)** Conductivity and permeabilityy from microgeometry. *J. Appl. Physics 56(11)*

**Ku J.L, Goldstein S.A, Choi K.W, London M and Herzig L.S(1987).** The Mechanical Properties of single trabeculae, *Orth. Res. Soc.*

**Kwiecen M.J., MacDonald I.F.,dullien F.A.L (1990)** Three-dimensional reconstruction of porous media from serial section data. *Journal of Microscopy 159(pt3) 343- 359*

**Lang P, Steiger P, Faulkner K, Gluer C and Genant H.K(1991)** Current techniques and recent developments in quantitative bone densitometry. *Radiologic Clinics of North America 29(1)49 - 76*

**Lang S.B , (1970).** Ultrasonic method for measuring elastic coefficient of bone and results on fresh and dried bovine bones. *IEEE Trans. Biomed. Engng BME 17*

**Langton C.M, Evans GP, Hodgskinson R and Riggs C.M (1990a)** Ultrasonic, elastic and structural properties of cancellous bone, *Current Research in Osteoporosis and bone mineral measurement, Bath conference 10 -11*

**Langton C.M, ALi A.V., Riggs C.M., Evans G.P and Bonfield W. ( 1990b).** A contact method for the assessment of ultrasonic velocity and broadband attenuation in cortical and cancellous bone. *Clin. Physiol. Meas., 11(3) pp243-249.*

**Langton C.M, Palmer S.B and Porter R.W(1984)** The measurement of broadband ultrasonic attenuation in cancellous bone, *Eng. Med. 13, 89 -91*

**Lanyon L.E and Smith R.N (1970).** Bone strain in the tibia during normal quadripedal locomotion. *Acta. orthop. Scan. 41, 238-248.*

**Law M.R, Wald N.J and Meade T.W (1991)** Strategies for prevention of osteoporosis and hip fracture. *BMJ 303, 453-459*

**Lindahl O,(1976).** Mechanical properties of dried defatted spongy bone. *Acta. Orthop. Scand. 47, 11-19*

**Linde F and Hvid I, (1987).** Stiffness behaviour of trabecular bone specimen , *J. Biomechanics vol 20(1) 83-89.*

**Linde F, Bentzens S, Gothgen C, Hvid I and Pongsorpetch B, (1988).** Mechanical properties of trabecular bones by a non- destructive compresion testing approach , *Engng in Med vol 17, 23-30.*

**Linde F, Hvid I and Jensen N.C, (1985).** Material properties of cancellous bone in repetitive axial loading , *Engng in Med vol 14, 173-177.*

**Lotz J.C , Gerhart T.N and Hayes W.C (1990).** Mechanical properties of trabecular bone from the proximal femur: A quantitative CT study , *Journal of computer assisted tomography 14(1) pp107-114*

**Lozupone Enrico, (1985).** The structure of the trabeculae of cancellous bone , *Anat. Anz, Jena, 159, 211-229.*

**Lozupone E and Favia A, (1990).** The structure of the trabeculae of cancellous bone. 2.long bones and mastoid , *Calc. Tiss. Int 46, 367-372.*

**Marcus R (1991)** Understanding osteoporosis. *Western J. of Medicine 155: 53 -60*

**Marieb E.N (1989).** Human anatomy and physiology , *The Benjamin/Cumming Publishing Co.*

**Martens M, Van Audekercke R, Delport P, Demuster P and Muelier J.C (1983).** The mechanical characteristic of cancellous bone upper femoral region , *J. Biomech. 16, 971-983.*

**Martin R.B and Ishida J, (1989).** The relative effects of collagen fiber orientation, porosity, density and mineralization on bone strength , *J. Biomechanics vol 22, 419-426.*

Massie A, Reid D.M and Porter R.W (1993) Screening for osteoporosis: comparison between dual energy x-ray absorptiometry and broadband ultrasound atenuation in 100 perimenopausal women. *Osteo. Int 3: 107 - 110*

Mazess R.B (1990) Bone densitometry for clinical diagnosis and monitoring: Osteoporosis: Physiological basis, assessment and treatment, Deluca HF, Mazess R editors

Mazess R.B (1982) On aging bone loss, *Clin Orthop 165, 239-*

McCloskey E.V, Murray SA, Miller C, Charlesworth D, Tindale W, Doherty O, Bickerstaff R, Hamdy A.T and Kanis J.A (1990a) Broadband ultrasound attenuation in the os calcis: Relationship to bone mineral at other skeletal sites. *Clinical Science 78, 227 - 233*

McCloskey E.V, Murray S.A, Charlesworth D, Miller C, Fordham J, Clifford K, Atkins R and Kanis JA (1990b) Assessment of broadband attenuation in the os calcis in vitro. *Clinical Science; 78: 221 -225*

McElhaney J. H.(1966) . Dynamic response of bone and muscle tissue. *J. Appl. Physiol; 21: 1231-1236.*

McElhaney J.H and Byars E.F (1965). ASME, Publication 65, WA/HUF 9

McElhaney J.H, Alem N.M and Roberts V.L. (1970). A porous block model for cancellous bone, *ASME, Publication 70-WA/BHF 2, 1-9, New York*

McKelvie M.L, Fordham J, Clifford C and Palmer S.W (1989) In vitro comparison of quantitative computer tomography and broadband ultrasonic attenuation of trabecular bone. *Bone; 10 :101 -104*

McKelvie M.L and Palmer S.W (1991). The interaction of Ultrasound with cancellous bone. *Phys Med Biol; 36: 1331-1340*

Melton III JL, O'fallon WM, Rigs BL,(1987) Secular trends in the incidence of hip fractures. *Calcif. Tissue Int.; 41: 57 -64*

Mente J. W and Lewis J.L (1987) Young's modulus of trabecular bone tissue . Transaction of the orthopaedic Society P49

Miller CG, Herd RJM, Ramalingam T, Fogelman I and Blake GM (1993) Ultrasonic velocity measurements through the calcaneus: which velocity should be measured ? *Osteoporosis Int; 3: 31 -35*

Mosekilde Li, Mosekilde Le, Danielsen C C, (1987) Biomechanical competence of vertebral bone in relation to ash density and age in normal individuals. *Bone; 8: 79 - 85*

National Osteoporosis Society (1990). The New Approach to osteoporosis

Neil J.L, Demas T.C, Stone J.L and Hayes W.C (1983). Tensile and compressive properties of vertebral trabecular bone . *Trans. Orthop. Res. Soc. P344*

Newton-John HF, Morgan DB (1970) The loss of bone with age; osteoporosis and fractures. *Clin Orthop; 71: 229 -252*

Nicholson P.H.F, Haddaway M.J and Davie M.W.J (1994).The dependence of ultrasonic properties on orientatiopn in human vertebral bone. *Phys. Med. Biol.; 39: 1013 - 1024*

Njeh CF (1990). Phonophoresis and Erosion of biological tissue by therapeutic ultrasound, *Msc Thesis, Aberdeen University*

**Ostlere SJ and Gold RH (1991)** Osteoporosis and bone density measurement methods. *Clinical Orthopaedics and Related Research; 271: 149 -163*

**Pain H. J (1985)** The Physics of vibrations and waves ( Chichester: Wiley)

**Parfit A.M (1984),** Age related structural changes in trabecular and cortical bone: Cellular mechanisms and biomechanical consequences, *Calcif. Tissue Int. 36* 3123

**Parfit A.M, Mathews H.E, Villanueva A.R, Kleerekoper M, Franne B and Raods (1983).** Relationship between surface vol and thickness of iliac trabecular bone in aging and in osteoporosis. *J. Clin. Invest. 72, 1396-1409*

**Petley G. W, Hames T. K, Cooper C  Langton C. M and Cawley M.D (1987)** A comparison of single photon Absorptiometry and broadband ultrasonic attenuation: past, present and future. Ultrasonics Studies of Bone, IOP Short Meetings no 6, Editors Palmer SB and Langton CM, PP15-21

**Poll V, Cooper C, and  Cawley M .I .D (1986)** Broadband ultrasonic attenuation in the os calcis and single photon absorptiometry in the distal forearm: A comparative study. *Clin Phys Physiol. Meas. 7, 375 - 379*

**Pugh J.W, Rose R.M, and Radin E.L.**   Elastic and viscoelstic properties of trabecular bone, dependence on structure , *J. Biomech. 6, 475-485.*

**Pugh J.W, Rose R.M, and Radin E.L.Reily D.T, Burstein A.H and Frankel V.H, (1974).** The elastic modulus for bone. *J. Biomechanics vol 7, 271-275.*

**Quiblier J (1984).** A new three dimensional modeling technique for studying porous media. *J. Colloid Interface Sci 98, 84 - 102*

**Resch H, Pietschmann P, Bernecker P, Krexner E, Wilvonseda R (1990)** Broadband ultrasound attenuation: A new diagnostic method in osteoporosis. *AJR 155: 825 - 828*

**Rice J. C, Cowin C.S and Bowman A.J (1988).** On the dependence of the elasticity and strength of cancellous bone on apparent density. *J. Biomechanics vol 21, 155-168.*

**Rich C, Klink E, Smith, and Graham B (1966)** Measurement of bone mass from ultrasound transmission time. *Proc Soc. Exp. Biol. Med 123: 282-285*

**Riggs B.L and Melton L.J (1986)** Involutional osteoporsis. *N. Engl. J Med. 314: 1676-1686*

**Ross S.D.K and Sowerby M.R.R, (1985).** The Operative treatment of fractures of the os calcis , *Clinical Orth. and Rel Res. vol 199 132-143*

**Rossman P, Zagzebski J, Mesina C, Sorenson J, and Mazess(1989)** Comparison of speed of sound and ultrasound attenuation in the os calcis to bone density of the radius, femur and lumbar spine . Clin  Physiol. Meas. 10(4), 353 - 360

**Rubin CT, Pratt GW, Porter Al, Lanyon LE and Poss R (1987)** The use of ultrasound in vivo to determine acute change in the mechanical properties of bone following intense physical activity,. *J. Biomechanics, 20(7): 723 -727*

**Runkle J.C and Pugh J.W (1975).** The micromechanics of cancellous bone 2, determination of the elastic modulus of individual trabeculae by buckling analysis.  *Bull Hosp. Jt Dis 36, 2-10.*

**Ryan S.D and Williams J.L (1986)** Tensile testing of individual bovine trabeculae. Proceedings of the 12th annual North East Bioengineering Conference pp35 - 38

Sanie J, Wang T and Bilgutay N (1987) Spectral evaluation of ultrasonic grain signals, *Ultrasonics* pp 1015 - 1020

Schapira D and Schapira C (1992) Osteoporosis: The evolution of scientific term: *Osteo. Int. 2(4) : 164 - 7*

Scheidegger A E (1974) The Physics of flow through porous media. University of Toronto

Sedlin E..D and Hirsch C.(1966). Factors affecting the determination of the physical properties of femoral cortical bone. *Acta. Orthop. Scand. Vol 37, 29-48*

Schoenfeld C.M, Laulenschlager E.P and Meyer, Jim P.R (1974). Mechanical Properties of human cancellous bone in the femoral head. *Med. Biol. Engng , Vol 18, 313 - 317*

Sharp D.J, Tanner K.E and Bonfield W, (1990). Measurement of the density of trabecular bone , *J. Biomechanics, vol 23 853-857*

Siegel IM, Anast GT and Fields T (1958) The determination of fracture healing by measurement of sound velocity across the fracture site. *Surg. Gynecol Obstet. 107: 327-332*

Simkin A and Robin G (1973). The mechanical testing of bone in bending. *J. Biomechanics, vol 6, 31-39*

Singh I, (1978). The architecture of cancellous bone , *J.Anat. 127(2) 305-310.*

Sloten J.V and Van Der Perre G, (1989). Trabecular structure compared to stress trajectories in the proximal femur and the calcaneus , *J. Biomed. Engng 11, 203-208.*

Smith R (1987). Osteoporosis: cause and management, *British medical Journal, vol 294: 329 - 332*

Smith C.B. and Smith D.A (1976). Relations between age, mineral density and mechanical properties of human femoral compacta , *Acta Orthop. Scand. 47, 496-502*

Smith J.W and Walmsley R. (1959). Factors affecting the elasticity of bone, *J. of Anatomy, 93, 503-523*

Smith S. W, Phillps D. J, Von Ramm O T and Thurstone F L (1979). Some advances in acoustic imaging through the skull: Ultrasonic Tissue characterization II, National Bureau of Standard Spec. Publi. 525 ed M Linzer (Washington DC) P 209 -17

Spencer A.P. and Mason E. B. (1979). Human anatomy and Physiology. *The Benjamin/Cumming Publishing Co*

Sprackling M.T. (1985) , Liquids and solids, *Routledge and Kegan Paul*

Stevenson J.C and Whitehead M. I (1982) Postmenopausal osteoporosis . British Medical Journal 285, 585 - 588

Stewart A, Reid D.M and Porter R.W (1994). Brooadband Ultrasound Attenuation and Dual Energy x-ray Absorptiometry in patients with hip fractures: which technique discriminates fracture risk. *Calcif. Tissue Int. 54: 466 - 469*

Stone J.L, Beaupre G and Hayes W.C (1983). Multiaxial strength characteristic of trabecular bone. *J. Biomechanics 16, 743- 752.*

Struhl S, Goldstein SA, Dickie DL, Flynn MJ and Matthews LS (1987). The distribution of mechanical properties of trabecular bone within vertebral bodies and iliac crest: correlation with computed tomography density. *Transaction of the Orthopaedic Research Society P262*

**249**

Swanson S.A.V and Freeman M.A.R (1966). Is bone hydraulically strengthened. *Med. Biol. Engng. 4, 433-438*

Tavakoli MB and Evans JA (1992) The effect of bone structure on ultrasonic attenuation and velocity. *Ultrasonics* 30 : 389-395

Tavakoli M.D amd Evans J.A (1991) Dependence of the velocity and attenuation in bone on the mineral content. *Phys.Med. Biol. 36: 1529 - 1537*

Tothill P (1989), Methods of bone mineral measurements, *Phys. Med. Bol. 34 543- 572*

Townsend P.R, Rose R.M and Radin E.L (1975). Buckling studies of single human trabeculae *J. Biomechanics 8, 199-201*

Turner C. H and  Eich M ( 1991) Ultrasonic velocity as a predictor of strength in bovine cancellous bone  *Calcif Tissue Int 49, 116 - 119*

Vahey J.W and Lewis J.L, (1987). Elastic moduli yield stress and ultimate stress of cancellous bone  in the  canine proximal femur , *J. Biomechanics vol 20, 29-33.*

Vogel J .M, Wasnich R. D and Ross P. D (1988) The clinical relevance of calcaneus bone mineral measuremnets : a review. *Bone and Mineral 5, 35 - 58*

Waterman P. C and Truell R ( 1961) Propagation of ultrasound in a scattering media. *J. Math. Phys. 2:512*

Waud C. E, Lew R, and Baran D. T (1992) The relationship between ultrasound and densitometric measurements of bone mass at the calcaneus in women *Calcif Tissue Int 51, 415 - 418*

Weaver J.K  (1966). The microscopic hardness  of bone, *J. bone  and  Joint Surgery 48A, 273-287*

Weaver J.K and Chalmers J, (1966). Cancellous bone:  its strength and changes with aging and an evaluation  of some  methods for measuring its mineral content , *J. bone and Joint Surgery 48A 289-308*

Wells P.N.T (1977) Biomedical Ultrasonics. *London Academic Press Inc*

Whitehouse W.J, Dyson E.D and Jackson C.K (1971). The scanning electron microscope in studies of trabecular bone from the human vertebral body.  *J. Anat. vol 108, 481-496*

Whitehouse W.J, and Dyson E.D  (1974).  Scanning electron microscope studies of trabecular bone in the proximal end of the human femur. *J. Anat., vol 118, 417-444-*

Whitehouse W. J (1974) The quantitative morphology of anisotropic trabecular bone. *J. Microscopy 101, 153 - 168*

Whitehouse W. J (1975). Scanning electron micrographs of cancellous bone from the human sternum.   *J. Pathol. vol 116,  213-224.*

Whiting JF (1977) Ultrasonics critical angle reflected goniometer for in vivo bone mineral analysis in Ultrasound in Medicine, Engineering Aspects, edited by White D and Brown (Plenum 1629 - 1643

Williams John L (1992) Ultrasonic wave propagation in cancellous and cortical bone. Prediction of some experimental results by Biot's theory *J. Acoust. Soc. Am  91(2), 1106- 1112*

William J.L and Lewis J.L(1982). Properties and an anisotropic model of cancellous bone from the proximal tibial epiphysis. *J. Biomech. Engng, 104, 50-56.*

**Wolff J (1892***) Des gesetz der Transformation der knochen. Hirchwald, Berlin.*

**Woodcock J.P (1979)** Ultrasonics: Medical Physics Handbook (Bristol: Adam Hilger)

**Yoon H.S and Katz J.L (1979)** " Ultrasonic wave propagation in human cortical bone" in Ultrasonic Tissue Characterization II, edited by Linzer (NPS Spec Publ 525) 189 -196

**Zagzebski J, Rossman P, Mesina C, Mezess R, and Madsen E ( 1991).** ULtrasonic transmission measurements through the os calcis. *Calcif. Tissue Int 49:* 107 -111

# Appendix A :

# Experimental Results of the Porous Perspex Study

*Table A.1: The Effect of Increase in Hole Diameter on nBUA for 25 Holes on an Area of 30x30 mm $^2$*

| $\phi$ (mm) | d (mm) | Porosity % $(2.18\phi^2)$ | nBUA (dB/MHz) | Velocity (m.s$^{-1}$) | Atten (0.4MHz) |
|---|---|---|---|---|---|
| 0 | 6 | 0 | 13.9 (4) | 2657 (0.5) | 1.29 (26) |
| 1 | 5 | 2.2 | 15.07 (7) | 2642 (0.6) | 1.82 (36) |
| 1.5 | 4.5 | 4.91 | 26.94 (2.5) | 2639 (0.6) | 3.23 (6) |
| 2 | 4 | 8.7 | 35.57 (1.4) | 2624 (0.6) | 7.72 (3) |
| 2.5 | 3.5 | 13.6 | 40 (2.6) | 2640 (0.6) | 11.61 (5) |
| 3 | 3 | 19.6 | 47.67 (1.7) | 2638 (0.6) | 13.54 (4) |
| 3.5 | 2.5 | 26.7 | 62.99 (1.7) | 2592 (0.7) | 18.66 (3.7) |
| 4 | 2 | 35 | 51.39 (3) | 2592 (0.5) | 20.7 (14) |
| 4.5 | 1.5 | 44.2 | 49.70 (3.3) | 2592 (0.7) | 23.28 (14) |
| 5 | 1 | 55 | 49.19 (3) | 2529 (0.6) | 24.27 (6) |
| 5.5 | 0.5 | 66 | 35.25 (6) | 2413 (0.6) | 37.48 (10) |

*Table A.2:* The Effect of Increase in Hole Diameter on nBUA for 16 holes on an Area of 25x25 mm$^2$

| φ (mm) | d mm | Porosity % $(2.01\phi^2)$ | nBUA (dB.MHz$^{-1}$) | Velocity (m.s$^{-1}$) | Atten (0.4MHz) |
|---|---|---|---|---|---|
| 0 | 6.25 | 0 | 16.94(11) | 2618 (0.5) | 2.4 (7) |
| 1 | 5.25 | 2 | 18.36 (4) | 2633 (0.5) | 4.55 (12) |
| 1.5 | 4.75 | 4.5 | 30.44(5.5) | 2632 (0.6) | 6.58 (13) |
| 2 | 4.25 | 8.04 | 35.14(4) | 2596 (0.5) | 9.12 (7) |
| 2.5 | 3.75 | 12.6 | 38.32(4) | 2596 (0.5) | 15.08 (4) |
| 3 | 3.25 | 18.1 | 57.13(2) | 2574 (0.6) | 25.92 (9) |
| 3.5 | 2.75 | 24.6 | 61.70(4) | 2574 (0.6) | 22.71 (9) |
| 4 | 2.25 | 32.2 | 59.91(2.3) | 2560 (0.7) | 14.44 (3.5) |
| 4.5 | 1.75 | 40.7 | 56.41(3) | 2542 (0.6) | 17.37 (3) |
| 5 | 1.25 | 50 | 50.0(6.3) | 2409 (1.4) | 24.71 (2.5) |
| 5.5 | 0.75 | 61 | 20.03 (7.1) | 2331 (0.7) | 14.1 (3) |

*Table A.3:* The Effect of Increase in Hole Diameter on nBUA and Velocity for 16 Holes on an Area of 34x34 mm $^2$

| φ (mm) | d (mm) | Porosity % $(1.08\phi^2)$ | nBUA (dB.MHz$^{-1}$) | Velocity (m s$^{-1}$) | Atten (0.4MHz) |
|---|---|---|---|---|---|
| 0 | 8.5 | 0 | 14.90 (11) | 2611 (0.5) | 1.48 (4) |
| 1 | 7.5 | 1.1 | 24.87 (4) | 2611 (0.7) | 4.48 (3) |
| 1.5 | 7 | 2.4 | 25.24 (7) | 2588 (0.8) | 6.15 (17) |
| 2 | 6.5 | 4.3 | 38.12 (8) | 2598 (1.3) | 7.0 (9) |
| 2.5 | 6 | 6.8 | 50.24 (5) | 2578 (0.7) | 8.29 (8) |
| 3 | 5.5 | 9.8 | 58.82 (4) | 2565 (0.8) | 12.18 (3.2) |
| 3.5 | 5 | 13.3 | 45.71 (3) | 2569 (0.6) | 25.36 (6) |
| 4 | 4.5 | 17.4 | 28.33 (9) | 2565 (0.5) | 17.03 (4) |
| 4.5 | 4 | 22.0 | 25.21 (7) | 2565 (0.5) | 11.10 (2) |

*Table A.4: The Effect of Varying the Number of Holes and Keeping Hole diameter Fixed at 3 mm with the Exception of Entry Numbers Starting from 16 on nBUA*

| No of Rows | No of Holes | d mm | Direction | nBUA |
|---|---|---|---|---|
| 2 | 4 | 17 | A1 | 21.83 |
| 2 | 6 | 7 | B2 | 45.4 |
| 3 | 6 | 17 | B1 | 15.8 |
| 3 | 8 | 17, 3.7 | C1 | 25.6 |
| 4 | 8 | 7 | C2 | 36.6 |
| 3 | 10 | 17,3.7 | D1 | 31.55 |
| 3 | 10 | 3.7,17 | D3 | 25.8 |
| 4 | 10 | 7 | D2 | 32 |
| 3 | 12 | 3.7 | E1 | 30.06 |
| 4 | 12 | 7 | E2 | 27.3 |
| 4 | 16 | 3 | F2 | 54.5 |
| 4 | 16 | 7,3 | F3 | 53.3 |
| 5 | 16 | 3.7 | F1 | 44.27 |
| 5 | 33 | - | G1 | 39.1 |
| 11 | 33 | - | G2 | 44.3 |
| 4 | 12 (4mm) | 3.75 | H1 | 25.76 |
| 3 | 12 (4mm) | 1.17 | H2 | 57.44 |
| 8 | 56 (1.5mm) | 3 | I1 | 48.61 |
| 7 | 56 (1.5mm) | 2.36 | I2 | * |
| 8 | 56 (2mm) | 2.41 | J1 | 39.27 |
| 7 | 56 (2mm) | 1.79 | J2 | 10.1 |

*Table A.5: nBUA Values for the Same Hole Size (3 mm) and Same Number of Rows (3)*

| No of holes | nBUA |
|---|---|
| 6 | 15.8 |
| 8 | 25.6 |
| 10 | 28.7 |
| 12 | 30.06 |

*Table A.6: The Results of the Random Hole Pattern*

| | nBUA | | | |
|---|---|---|---|---|
| No of holes | X | XX | Y | YY |
| 25 | 38.43 | 41.78 | 66.1 | 66.2 |
| 30 | 50.55 | 52.7 | 40.42 | 39.93 |

For the random hole pattern the directions were labelled as X and XX for opposite direction and Y and YY for the perpendicular directions.

*Table A.7: The Effects of Coupling, Degassing and fluid on BUA and Velocity values*

| nBUA | nnBUA | Coupling | Holes | Velocity |
|---|---|---|---|---|
| 36.62(4) | 8.93(4) | Jelly | Yes-oil(Degassed) | 1999 |
| 28.49(9) | 6.95(9) | Jelly | Yes-water(Degassed) | 1961 |
| 19.92(4) | 4.86(4) | Jelly | Yes-water | 1940 |
| 23.26(4) | 5.67(4) | Water | Yes-Water | 1987 |
| 31.51(6) | 7.68(6) | Water | No | 2657 |
| 30.45(7) | 7.50(7) | Jelly | No | 2643 |

255

**Table A.8:** *Experimental and Theoretical Data for Perspex Models*

| Diameter(mm) | Porosity(%) | Theoretical x$10^{-10}$ | Experimental x$10^{-10}$ |
|---|---|---|---|
| 1.5 | 7.01 | 36.5 | 31.60 |
| 1.75 | 9.54 | 67.63 | 54.35 |
| 2.00 | 12.46 | 115.37 | 84.44 |
| 2.25 | 15.77 | 184.79 | 141.60 |
| 2.50 | 19.46 | 281.66 | 225.90 |
| 2.75 | 23.55 | 412.37 | 329.21 |
| 3.000 | 28.03 | 584.04 | 483.70 |
| 3.25 | 32.89 | 804.44 | 694.50 |
| 3.50 | 38.15 | 1082.01 | 1020.90 |
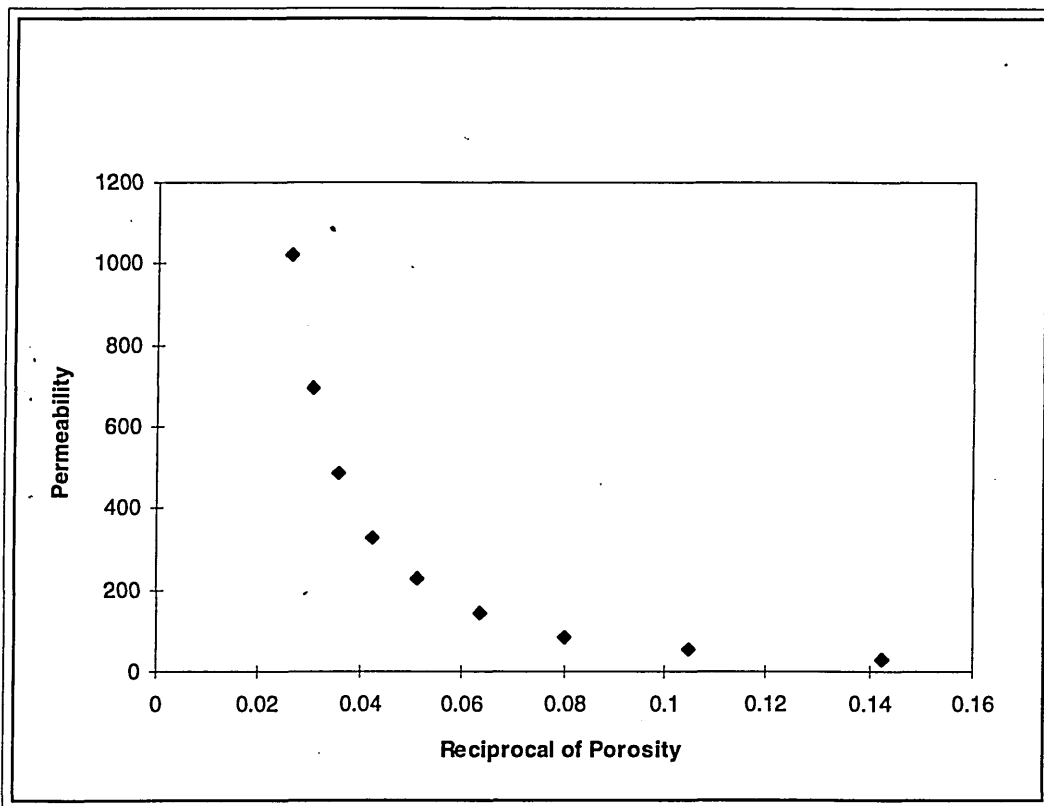


*Figure A-1:* The Relationship Between Permeability and Inverse Porosity

# Appendix B :

# Bovine Mechanical, Ultrasonic and Structural Data

*Table B.1: The Mechanical and Structural Data for Bovine Cancellous Bone*

| Sample | Young's Modulus (MPa) | | | Permeability m³ | | | Strength | Density |
|---|---|---|---|---|---|---|---|---|
| no | P - D | A - P | M - L | P-D | A-P | M-L | (MPa) | (kg/m^3) |
| 1 | 475 | 209 | 475 | 5000 | 6400 | 6411 | 2.9 | 330 |
| 2 | 657 | 187 | 578 | 4323 | 5513 | 4412 | 3.23 | 350 |
| 3 | 579 | 385 | 457 | 3457 | 4410 | 4281 | 4.89 | 365 |
| 4 | 966 | 476 | 485 | 3998 | 5370 | 4865 | 4.14 | 374 |
| 5 | 1334 | 848 | 867 | 1476 | 2214 | 1499 | 9.12 | 515 |
| 6 | 1482 | 1304 | 1408 | 466 | 614 | 568 | 14.77 | 608 |
| 7 | 1884 | 1573 | 1766 | 441 | 616 | 583 | * | 688 |
| 8 | 1993 | 1403 | 1447 | 467 | 941 | 714 | * | 640 |
| 9 | 1493 | 601 | 861 | 550 | 1192 | 770 | 12.39 | 546 |
| 10 | 572 | 362 | 559 | 839 | 2245 | 2236 | 8.41 | 459 |
| 11 | 899 | 807 | 836 | 1809 | 2316 | 2260 | 7.53 | 470 |
| 12 | 1894 | 829 | 1358 | 620 | 2301 | 1419 | 11.52 | 532 |
| 13 | 1687 | 1348 | 1354 | 944 | 1139 | 1064 | * | 607 |
| 14 | 1509 | 1047 | 1058 | 365 | 530 | 401 | 11.14 | 535 |
| 15 | 679 | 595 | 607 | 2400 | 3214 | 3080 | 5.24 | 414 |
| 16 | 429 | 270 | 285 | 4739 | 4998 | 4785 | 4.07 | 309 |
| 17 | 2380 | 1236 | 1908 | 203 | 52 | 203 | 200 | 697 |
| 18 | 599 | 386 | 454 | 615 | 1333 | 1052 | 6.15 | 471 |
| Mean | 1195 | 770 | 931 | 1809 | 2533 | 2256 | 8.05 | 495 |
| stdev | 617 | 453 | 496 | 1712 | 1986 | 1909 | 4.15 | 122.2 |
| CV | 51.6% | 58.9% | 53.3% | 94.6% | 78.4% | 84.6% | 51.6 | 24.6 |

Where * represents specimen with strength above the maximun applied load of the instron

*Table B.2: The Ultrasonic Data for Bovine Cancellous Bone*

| Specimen no | Velocity | | | nnBUA | | |
|---|---|---|---|---|---|---|
| | PD | AP | ML | PD | AP | ML |
| 1 | 2097 | 1848 | 2149 | 24.73 | 34.26 | 57.61 |
| 2 | 2107 | 1814 | 2107 | 58.18 | 28.32 | 64.29 |
| 3 | 2071 | 2005 | 1973 | 43.64 | 40.84 | 32.79 |
| 4 | 2375 | 1963 | 2037 | 65.67 | 39.5 | 48.82 |
| 5 | 2211 | 2241 | 2148 | 44.3 | 36.98 | 31.49 |
| 6 | 2210 | 2347 | 2347 | 26.54 | 28.11 | 30.84 |
| 7 | 2339 | 2354 | 2354 | 24.82 | 23.76 | 29.81 |
| 8 | 2479 | 2142 | 2363 | 27.03 | 24.5 | 30.96 |
| 9 | 2349 | 1984 | 2239 | 33.92 | 28.84 | 36.65 |
| 10 | 2041 | 2026 | 2135 | 54.73 | 32.1 | 61.26 |
| 11 | 2301 | 2185 | 2094 | 55.88 | 38.4 | 37.78 |
| 12 | 2469 | 2124 | 2400 | 33.48 | 44.14 | 33.89 |
| 13 | 2335 | 2172 | 2191 | 32.4 | 28.63 | 31.22 |
| 14 | 2429 | 2216 | 2135 | 33.75 | 30.65 | 38.17 |
| 15 | 2075 | 2050 | 2075 | 44.83 | 36.16 | 53.86 |
| 16 | 2059 | 1948 | 1948 | 70.54 | 50.03 | 59.38 |
| 17 | 2543 | 2222 | 2396 | 28.48 | 29.02 | 27.73 |
| 18 | 2048 | 2048 | 1990 | 55.86 | 38.11 | 43.89 |
| Mean | 2252 | 2094 | 2171 | 42.15 | 34.02 | 41.69 |
| stdev | 170 | 155 | 148 | 14.83 | 7.05 | 12.46 |
| CV | 7.6% | 7.4% | 6.8% | 35.18% | 20.72% | 29.9% |
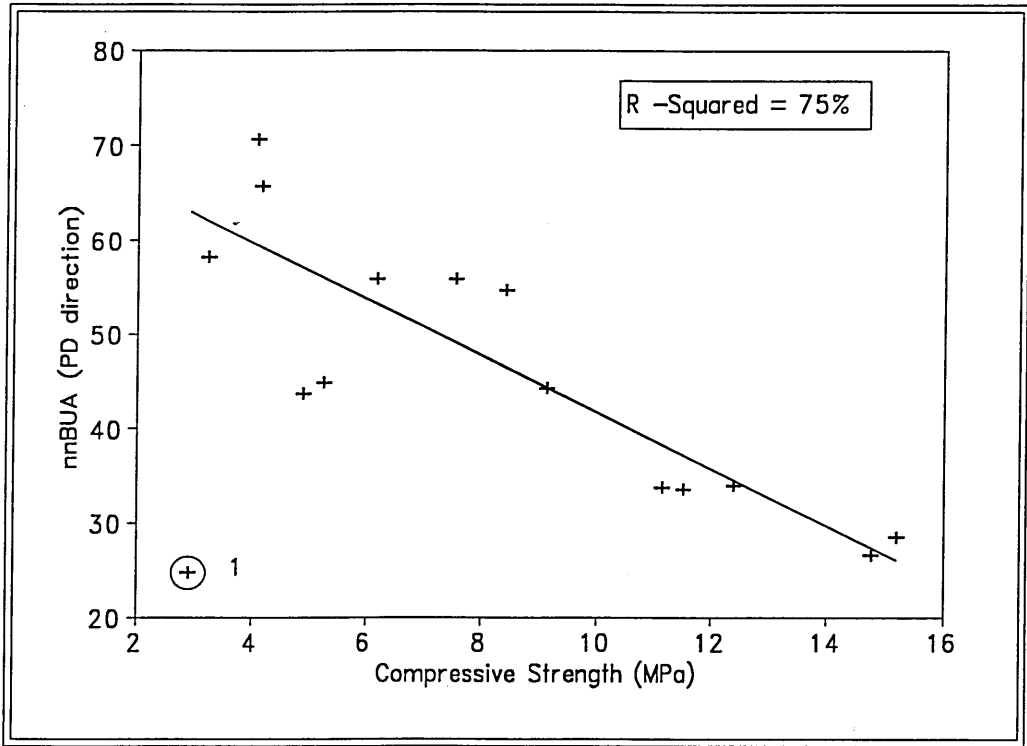
**Figure B-1:** *The Relationship Between BUA and Compressive Strength*
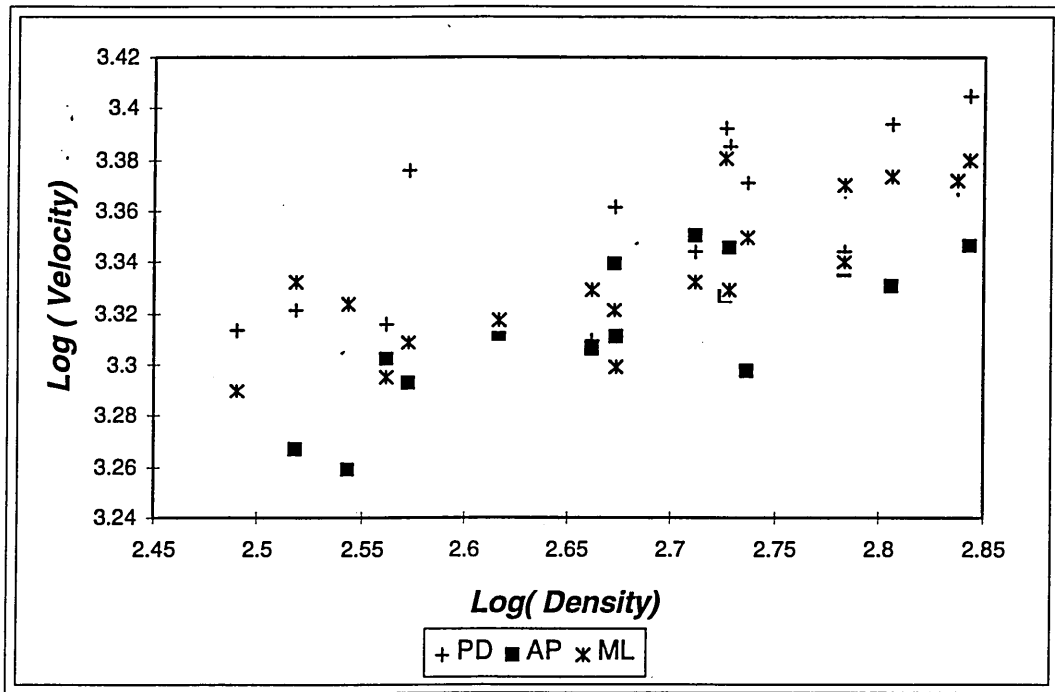


**Figure B-2:** *The Relationship Between Velocity and Density (Bovine)*
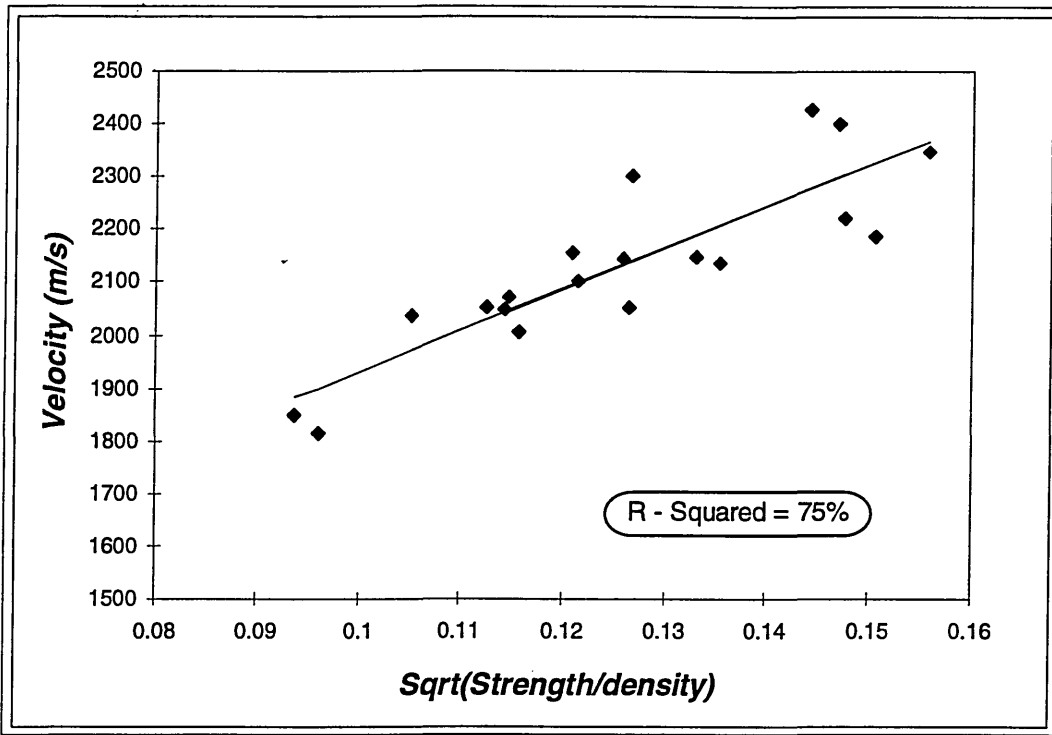
**Figure B-3:** *Relationship Between Velocity, Strength and Density (Bovine)*
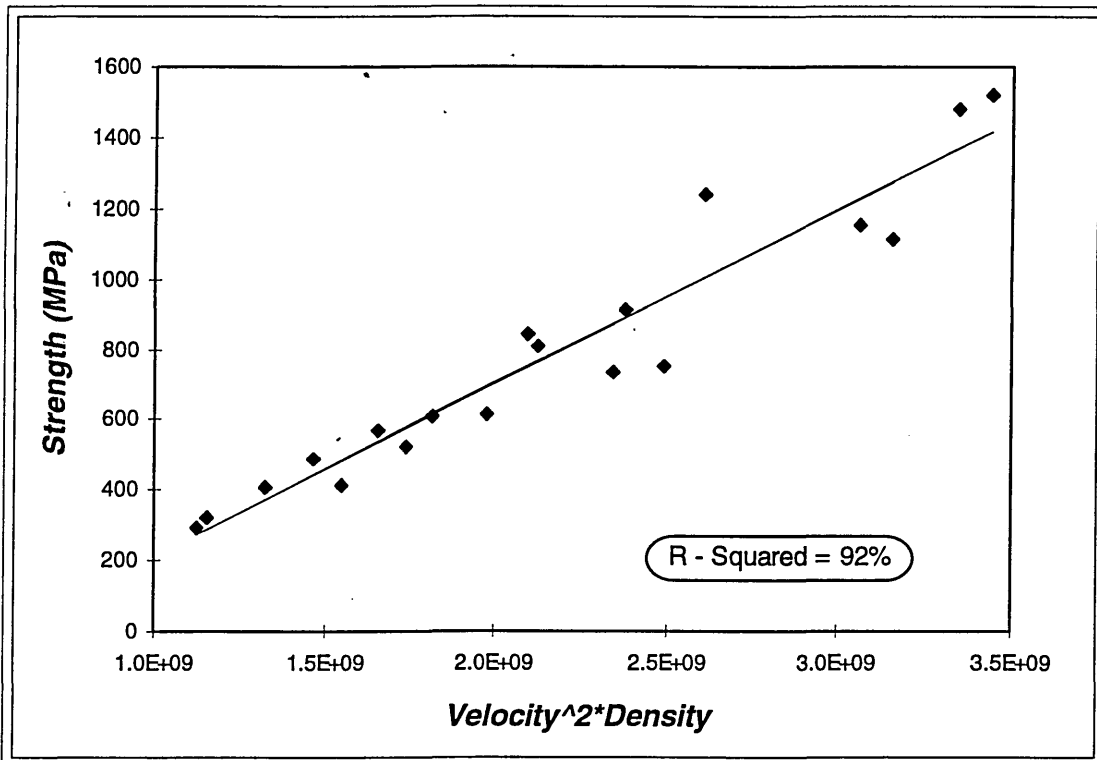


**Figure B-4:** *Strength as a Function of the Product of Velocity Squared and Density*

# Appendix C :

# Relationship Between Longitudinal Wave Velocity and Bar Wave Velocity

As discussed in Chapter 3, many forms of waves velocity can be propagated in a solid depending on the specimen size and wavelength of the wave. The types mostly encountered in the study of cancellous bone are longitudinal wave and bar waves (Equations 3.7 and 3.8 respectively). This theoretical relationship between ultrasound velocity and elasticity was verified by using velocity, elasticity and density data from Kaye and Laby [1986] of metals and alloys. The correlation analysis on the data resulted in the following equations

$$V_{rod} = -46 + 32322\sqrt{E/\rho} \qquad\qquad R^2 = 99\% \qquad (C1)$$

$$V_{long} = 971 + 30567\sqrt{E/\rho} \qquad\qquad R^2 = 94\% \qquad (C2)$$

$$V_{rod} = 1297 + 110456\sqrt{\frac{K + 4/3G}{\rho}} \qquad R^2 = 87\% \qquad (C3)$$

$$V_{long} = -218 + 33021\sqrt{\frac{K + 4/3G}{\rho}} \qquad R^2 = 98\% \qquad (C4)$$

$$V_{bar} = -750 + 0.99 V_{long} \qquad\qquad R^2 = 93\% \qquad (C5)$$

Where $V_{rod}$, $V_{long}$ are in $ms^{-1}$ , K is the bulk modulus, G is shear modulus, E is Young's modulus; K, G, and E are in GPa and $\rho$ the density is in $kgm^{-3}$. A graphical representation of the above equations are given in the following graphs ( Figure C1-C3).
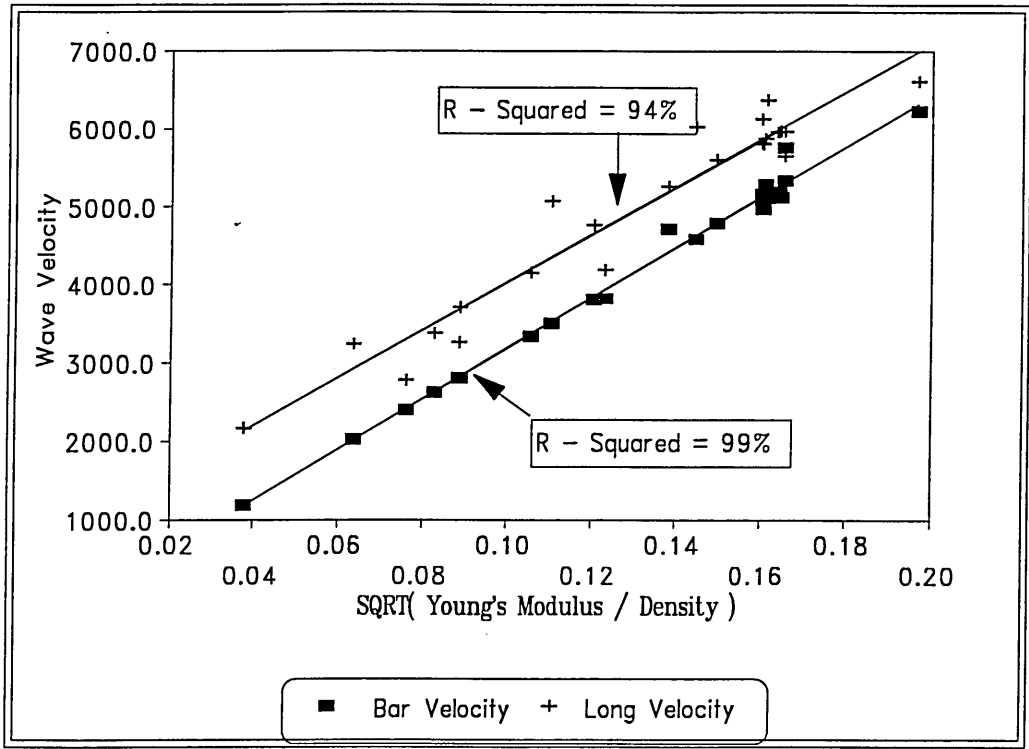
**Figure C-1:** *Bar Velocity and Longitudinal Velocity Plotted against the Square Root of Young's Modulus divided by Density*
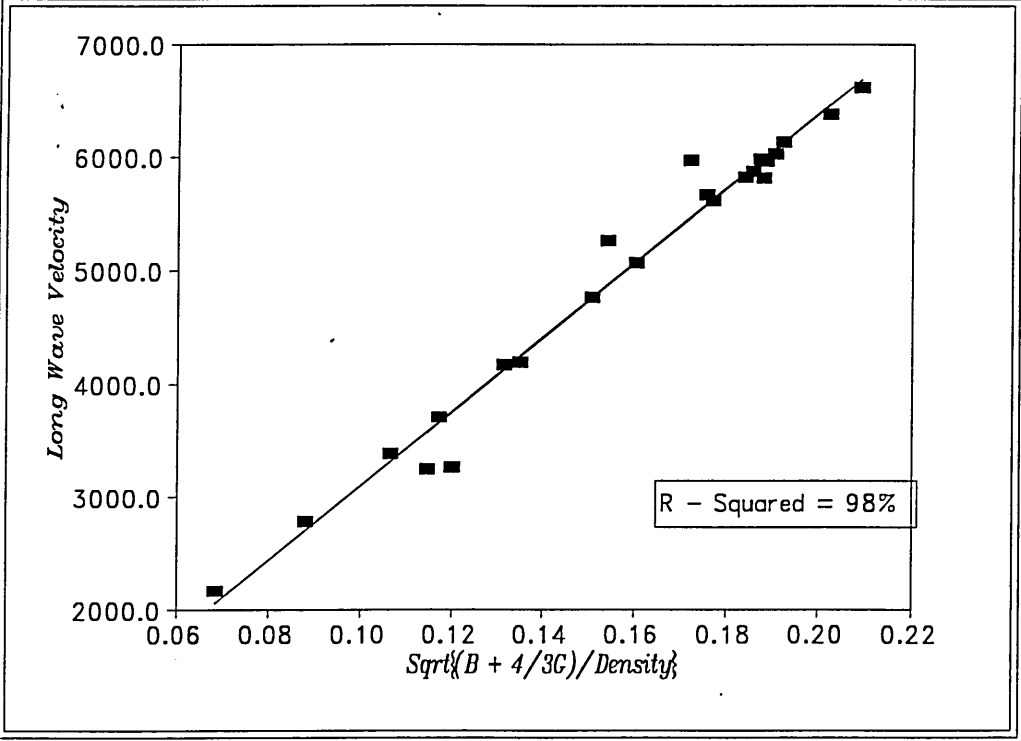


**Figure C-2:** *The Relationship Between Longitudinal Wave Velocity and Elasticity*
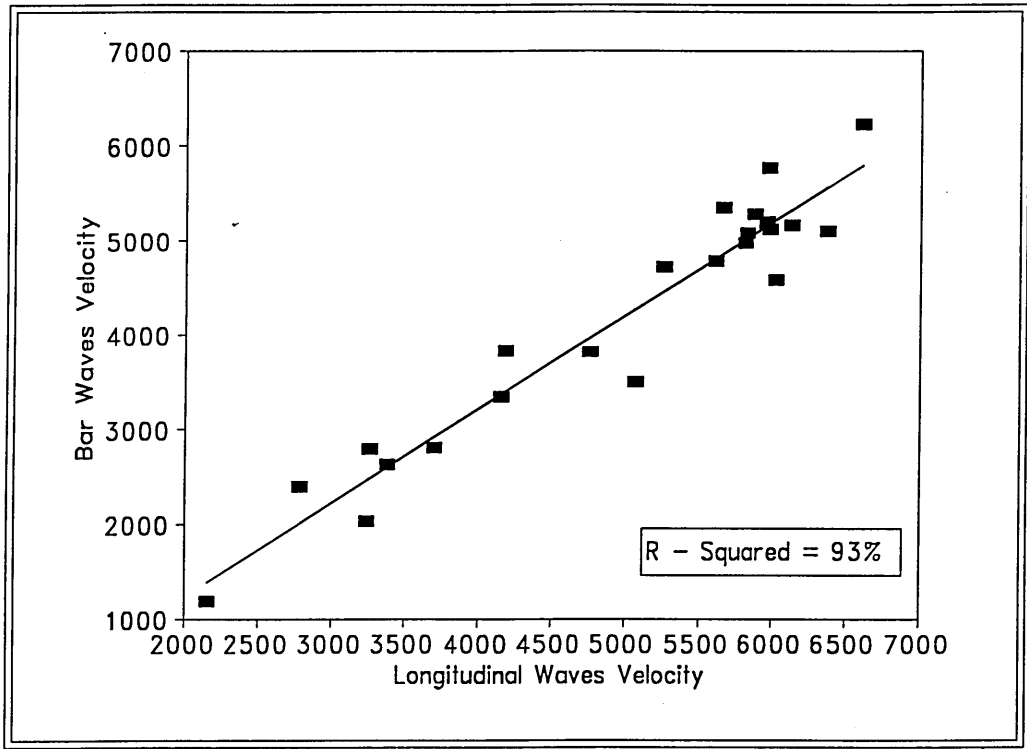
**Figure C-3**: The Relationship Between Bar Wave Velocity and Longitudinal Wave Velocity.

# Appendix D :

# Velocity, nnBUA Values and Some Relationships at the Calcaneus

*Table D.1: Velocity values for the Different Modification at the calcaneus*

| Specimen no | $Vel_{whole}$(m s$^{-1}$) | $Vel_{core}$ (m s$^{-1}$) | $Vel_{can}$(ms$^{-1}$) | $Vel_{defat}$ ms$^{-1}$ |
|---|---|---|---|---|
| 1 | 1601(2.0)* | 1591(2.5) | 1625(3.0) | 1632(1.1) |
| 2 | 1645(2.4) | 1666(3.0) | 1680(1.0) | 1648(1.2) |
| 3 | 1542(1.3) | 1571(1.4) | 1490(0.6) | 1528(1.6) |
| 4 | 1700(1.7) | 1754(2.0) | 1646(1.3) | 1637(1.4) |
| 5 | 1739(2) | 1725(2) | 1728(2) | 1712(1.7) |
| 6 | 1617(0.6) | 1618(1.0) | 1663(2.0) | 1650(1.2) |
| 7 | 1648(2.5) | 1665(2.0) | 1668(1.0) | 1647(1.4) |
| 8 | 1774(2.0) | 1786(1.0) | 1776(1.5) | 1743(1.5) |
| 9 | 1703(1.0) | 1728(1.3) | 1697(0.5) | 1709(0.8) |
| 10 | 1629(3.0) | 1631(1.3) | 1559(1.2) | 1545(0.8) |
| 11 | 1654(2.0) | 1659(1.1) | 1590(0.4) | 1617(1.6) |
| 12 | 1764(1.7) | 1753(1.8) | 1690(0.6) | 1720(2.0) |
| 13 | 1643(1.6) | 1675(1.0) | 1663(1.0) | 1654(2.0) |
| 14 | 1521(1.0) | 1520(1.6) | 1500(1.5) | 1501(0.6) |
| 15 | 1615(2.1) | 1652(1.9) | 1610(1.3) | 1621(0.6) |
| 16 | 1538(2.0) | 1574(0.6) | 1517(0.6) | 1504(1.1) |
| 17 | 1616(2.0) | 1624(1.4) | 1637(0.5) | 1621(1.8) |
| 18 | 1709(3.4) | 1758((2.0) | 1663(2.0) | 1659(1.6) |
| 19 | 1754(0.97) | 1720(1.0) | 1610(0.5) | 1618(1.8) |
| 20 | 1635(2.5) | 1631(1.6) | 1578(1.1) | 1559(0.8) |
| Mean | 1652.3(1.89) | 1665.1(1.58) | 1630(1.18) | 1626(1.33) |
| Stdev | 73.7 | 72.4 | 74.7 | 69.5 |
| CV | 4.46% | 4.35% | 4.58% | 4.27% |

* the values in brackets are the coefficient of variation for that measurement (%)

*Table D.2: Calcaneus BUA Results for the Different Modification (where the values in bracket are coefficients of variation)*

| Specimen no | nnBUA$_{whole}$ dB MHz$^{-1}$cm$^{-1}$ | nnBUA$_{core}$ dB MHz$^{-1}$cm$^{-1}$ | nnBUA$_{can}$ dB MHz$^{-1}$cm$^{-1}$ | nnBUA$_{def}$ dB MHz$^{-1}$cm$^{-1}$ |
|---|---|---|---|---|
| 1 | 26.30(4.5) | 22.75(4.5) | 23.09(4.6) | 21.82(4) |
| 2 | 23.00(5.5) | 17.94(5) | 17.87(4.5) | 16.98(5.4) |
| 3 | 14.96(4.1) | 15.16(6.1) | 14.81(4.4) | 14.38(4.9) |
| 4 | 35.30(3.8) | 33.77(4.7) | 31.29(1.87) | 30.81(1.7) |
| 5 | 32.53(3.7) | 30.26(1.14) | 26.27(1.03) | 23.98(4.4) |
| 6 | 25.13(7) | 20.38(4.6) | 18.10(4.5) | 17.37(1.2) |
| 7 | 26.59(3.3) | 22.42(6.7) | 23.84(3.4) | 24.21(4.8) |
| 8 | 33.35(5.9) | 30.63(4.5) | 30.85(3.37) | 26.72(3.6) |
| 9 | 30.39(2.2) | 25.25(6.1) | 25.26(3.4) | 31.06(5.35) |
| 10 | 16.24(7.8) | 15.76(4.9) | 12.90(3.5) | 12.45(1.1) |
| 11 | 22.17(4.9) | 20.70(3.7) | 15.21(3.2) | 17.76(2.2) |
| 12 | 31.89(2.8) | 28.79(8.9) | 23.19(1.3) | 27.92(4.4) |
| 13 | 19.20(6.1) | 13.38(4.4) | 12.82(3) | 15.85(4.3) |
| 14 | 5.04(4.1) | 4.39(3.7) | 3.66(2.9) | 4.36(6.6) |
| 15 | 23.12(3.5) | 19.82(6.9) | 13.37(1.3) | 13.96(4.9) |
| 16 | 9.28(4.8) | 9.55(5.6) | 6.21(3.4) | 5.56(7.2) |
| 17 | 17.68(4.5) | 18.93(6.7) | 19.02(2.3) | 19(6.1) |
| 18 | 25.60(7.2) | 21.10(6.1) | 16.50(4) | 19.01(4.0) |
| 19 | 27.83(6.9) | 25(3.1) | 20.22(4.3) | 20.29(7.0) |
| 20 | 15.54(4) | 15.82(8) | 11.07(2.9) | 12.29(3.0) |
| Mean | 23.06(4.8) | 20.5(5.3) | 18.28(3.2) | 18.79(4.3) |
| Stdev | 8.15 | 7.28 | 7.40 | 7.37 |
| CV | 35.3% | 35.5% | 40.48% | 39.22% |
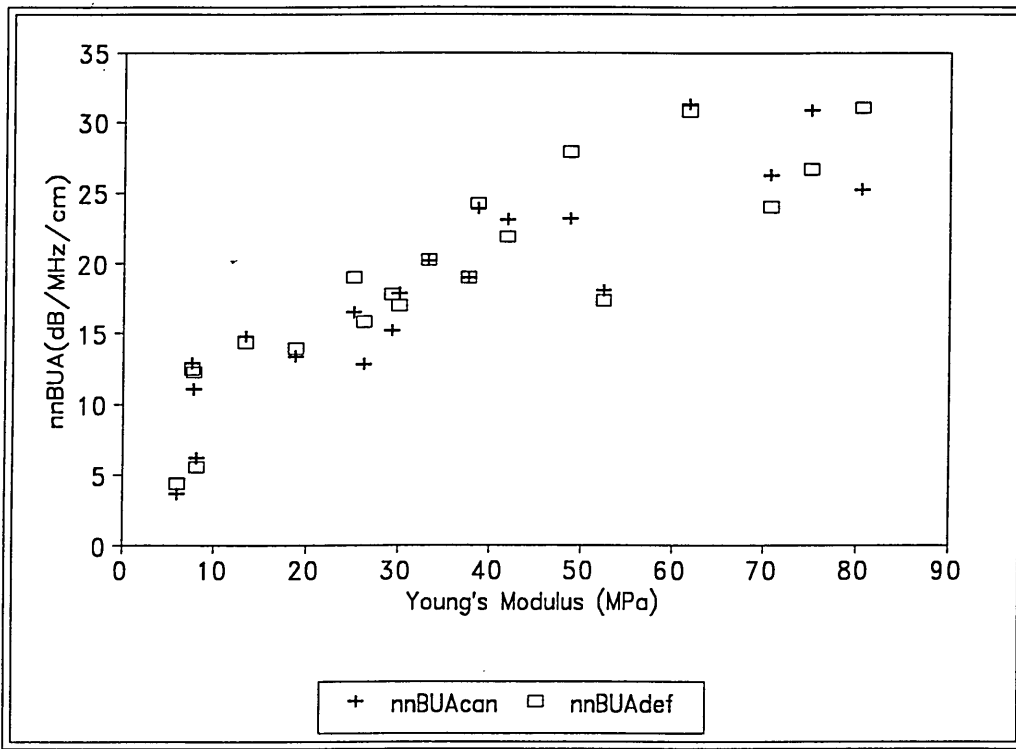
*Figure D-1 : The Relationship Between BUA and Young's Modulus*
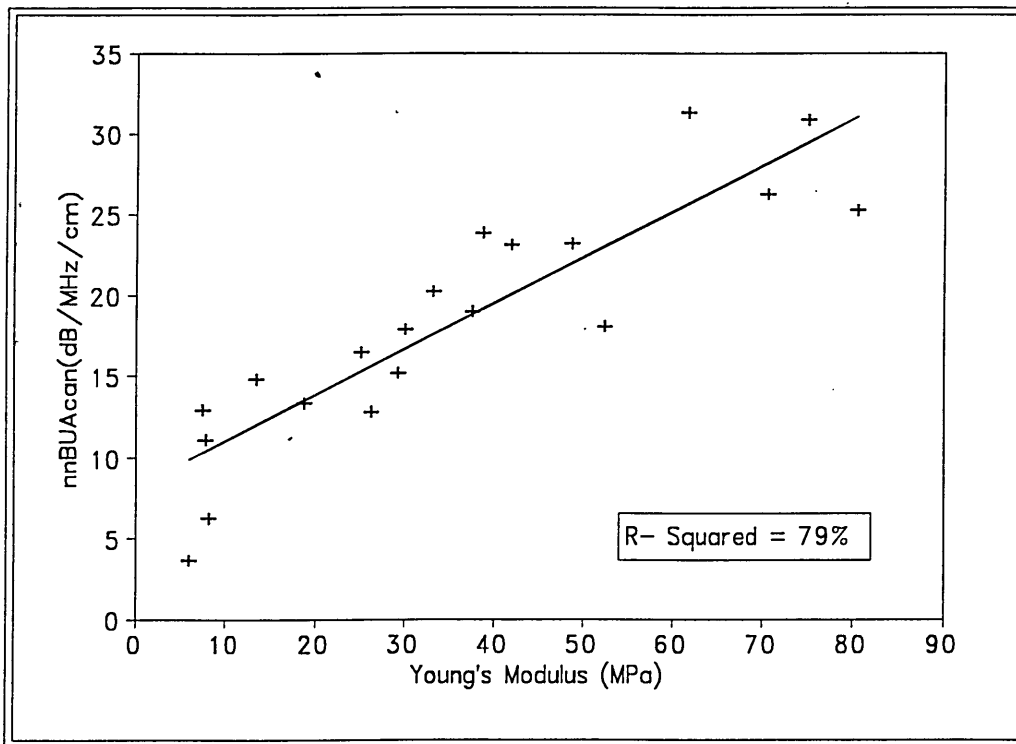


*Figure D-2: A Plot of BUAcan Against Young's Modulus*
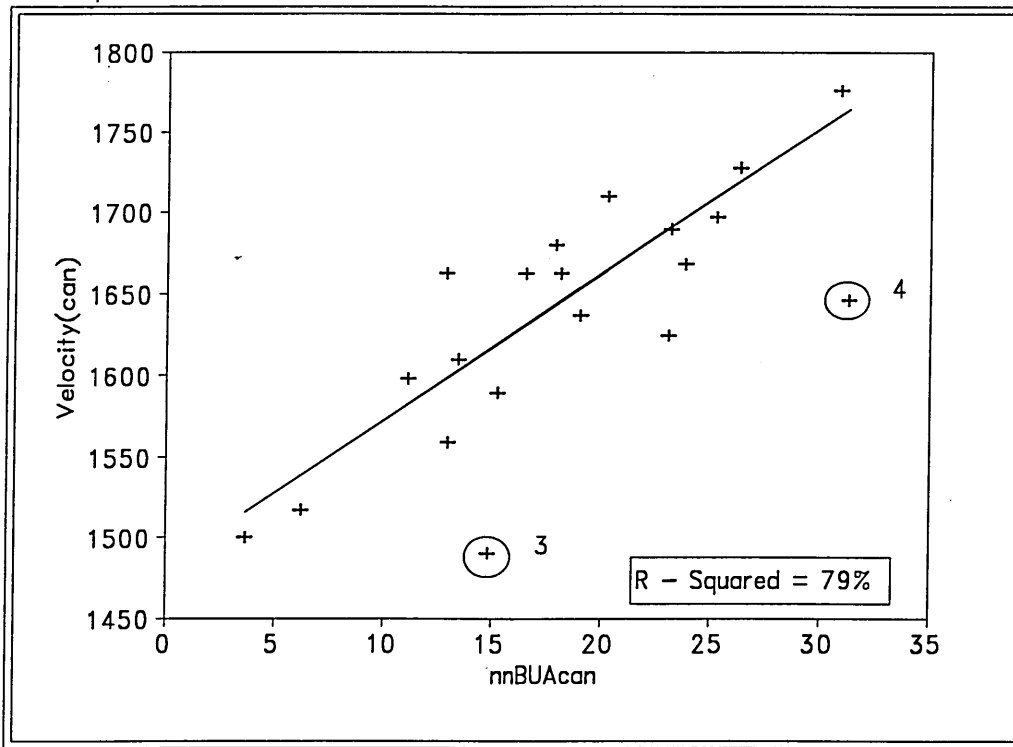
**Figure D-3**: *The Relationship Between Velocity and BUAcan*
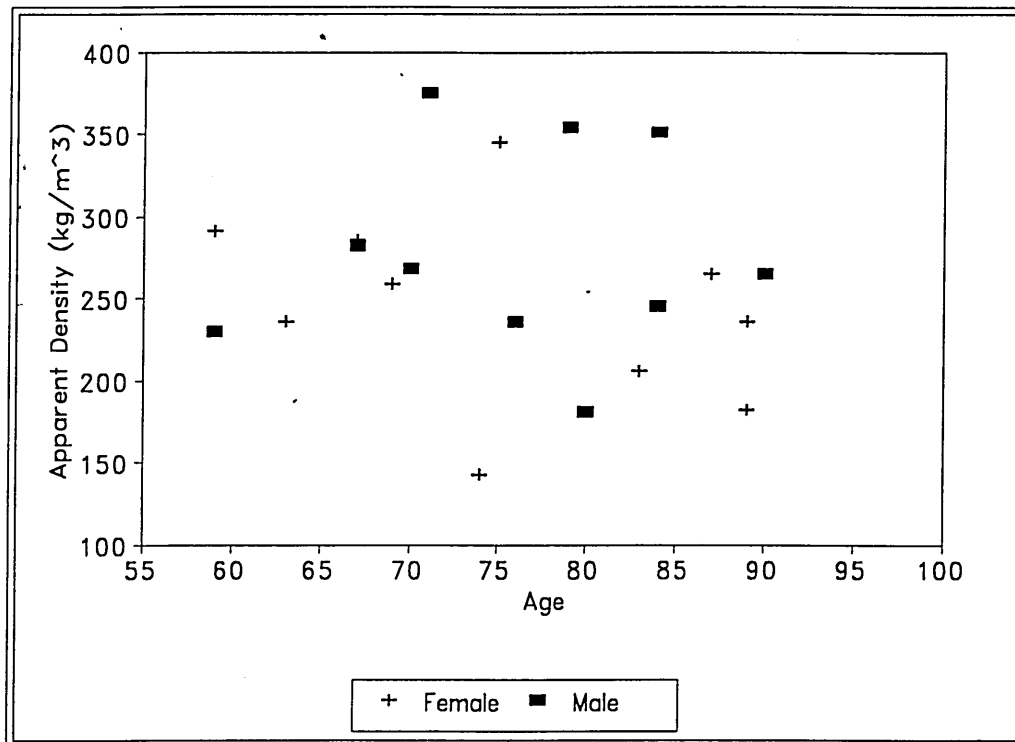


**Figure D-4**: *The Relationship Between Density and Age*
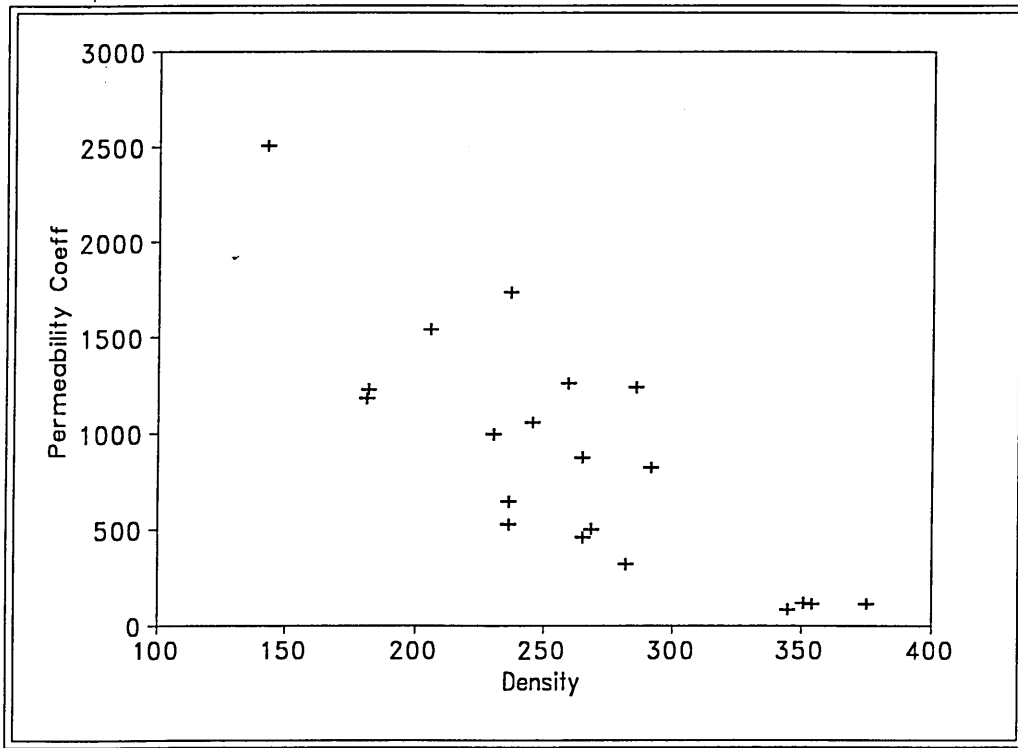
*Figure D-5:* *A Plot of Permeability Against Density for Calceneus*
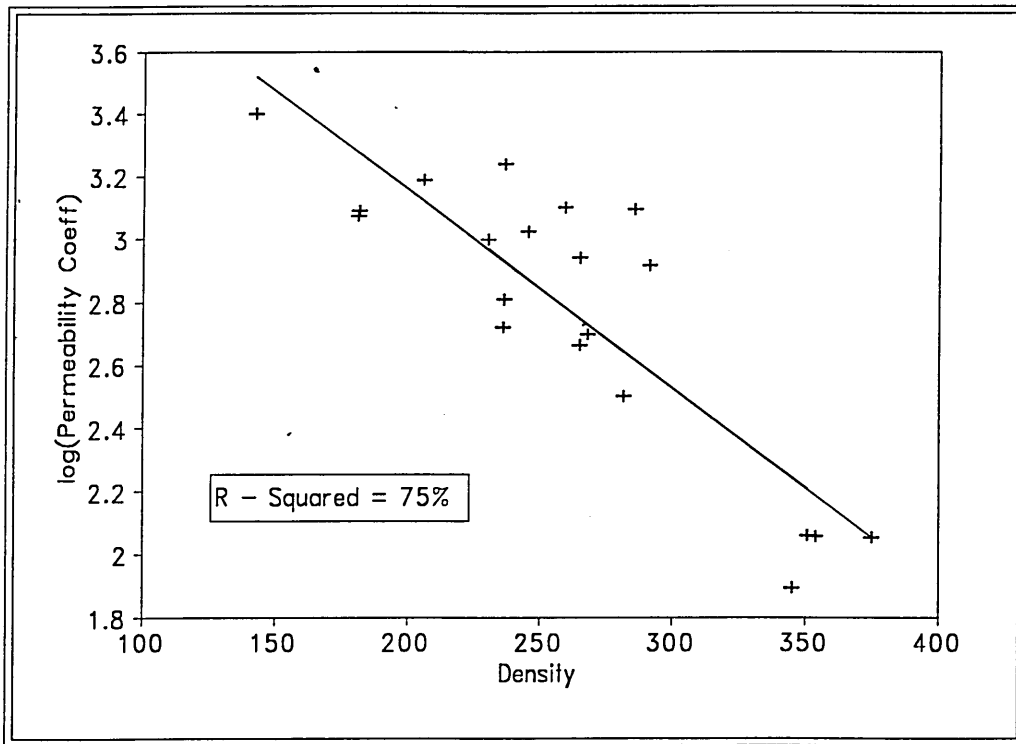


*Figure D-6:* *The Relationship Between log(permeability) and Density*

268
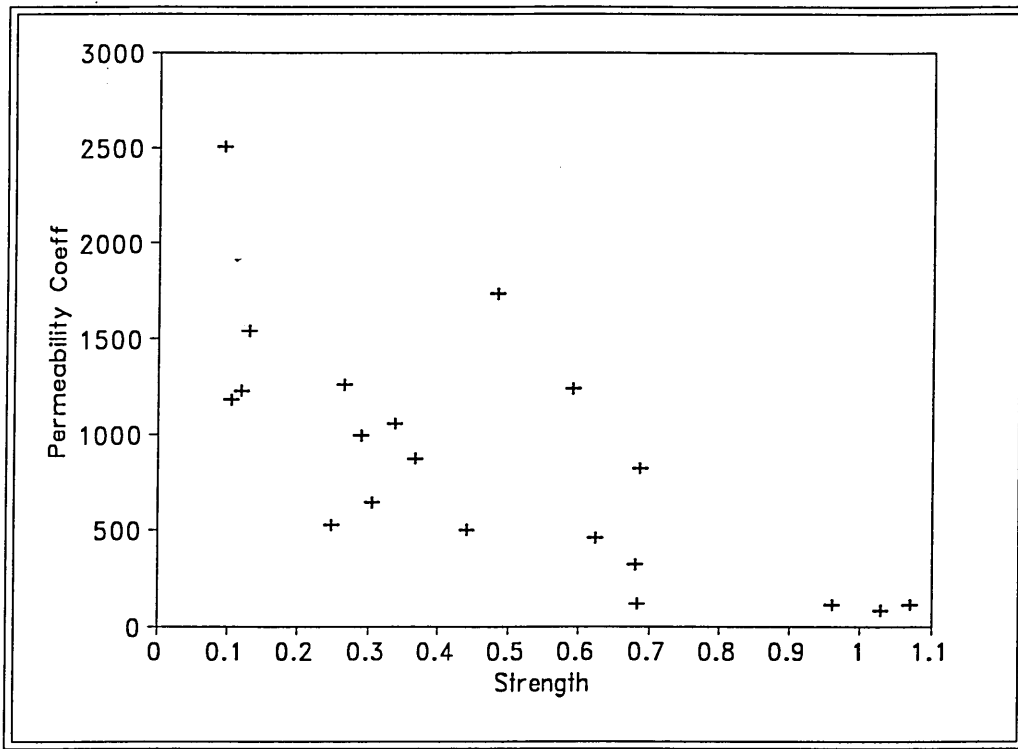
*Figure D-7:* *A Plot of Permeability Against Strength*
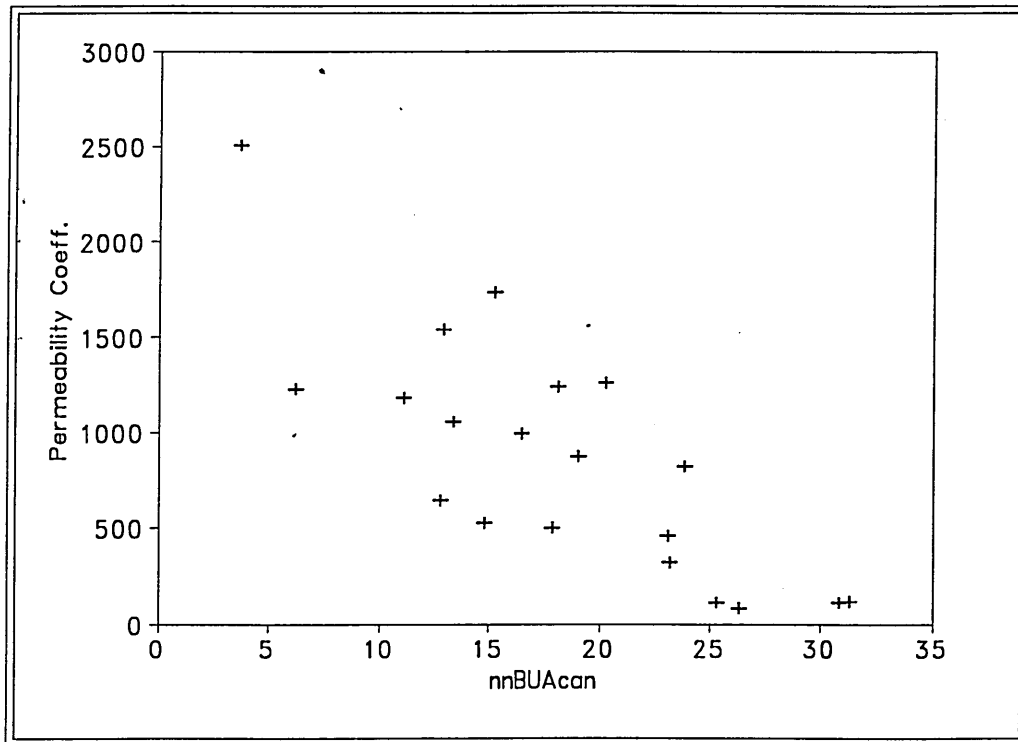


**Figure D-8:** A Plot of Permeability Against nnBUAcan

# Appendix E : Miscellaneous
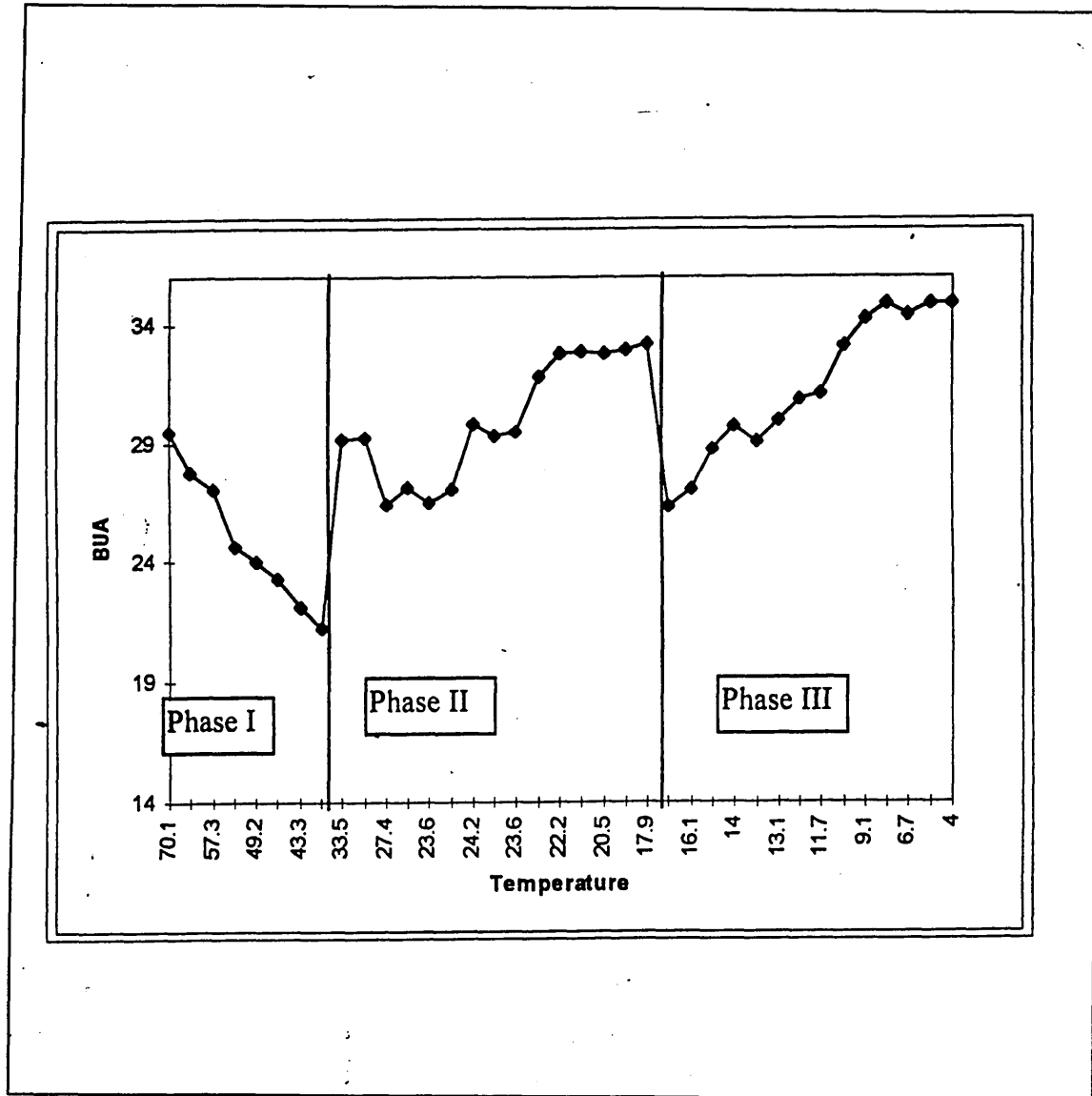


*Figure E-1:* A Line Plot of Change in BUA with Decrease in Temperature
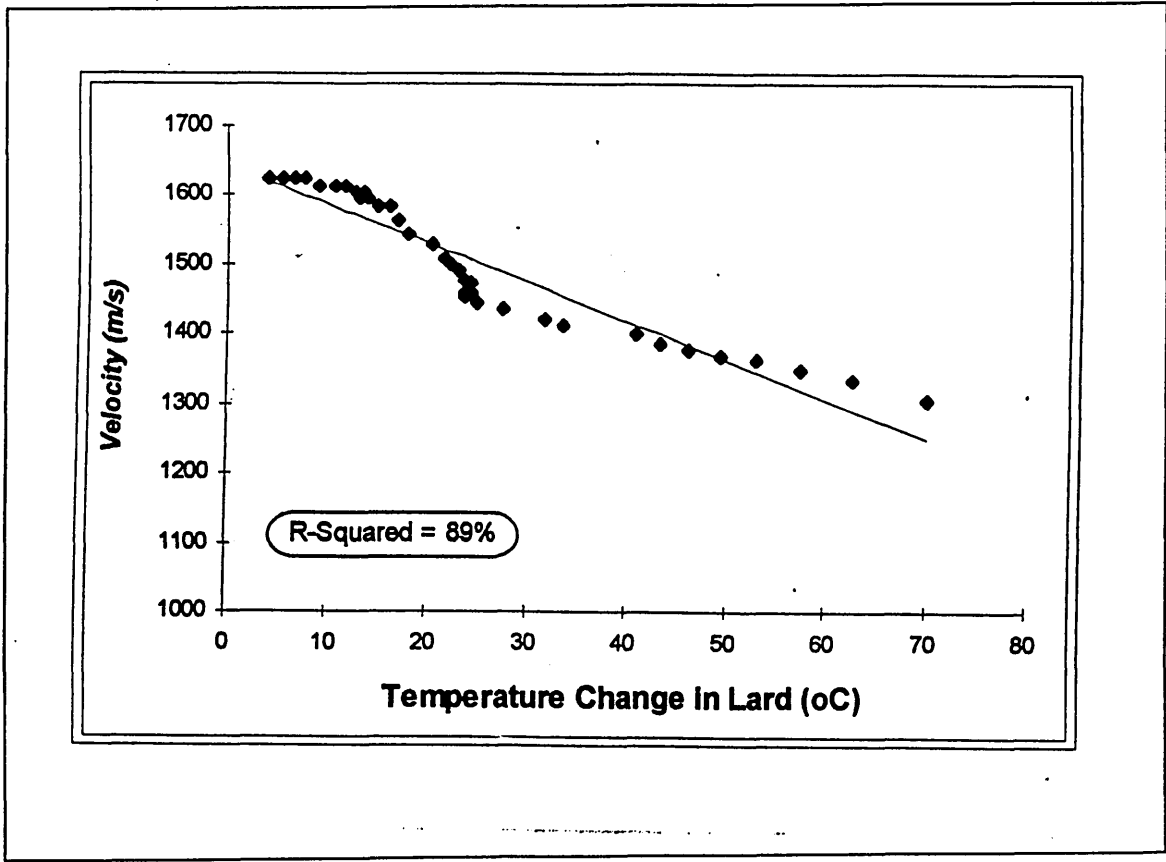
*Figure E-2: Relationship Between Velocity and Changes in Temperature*
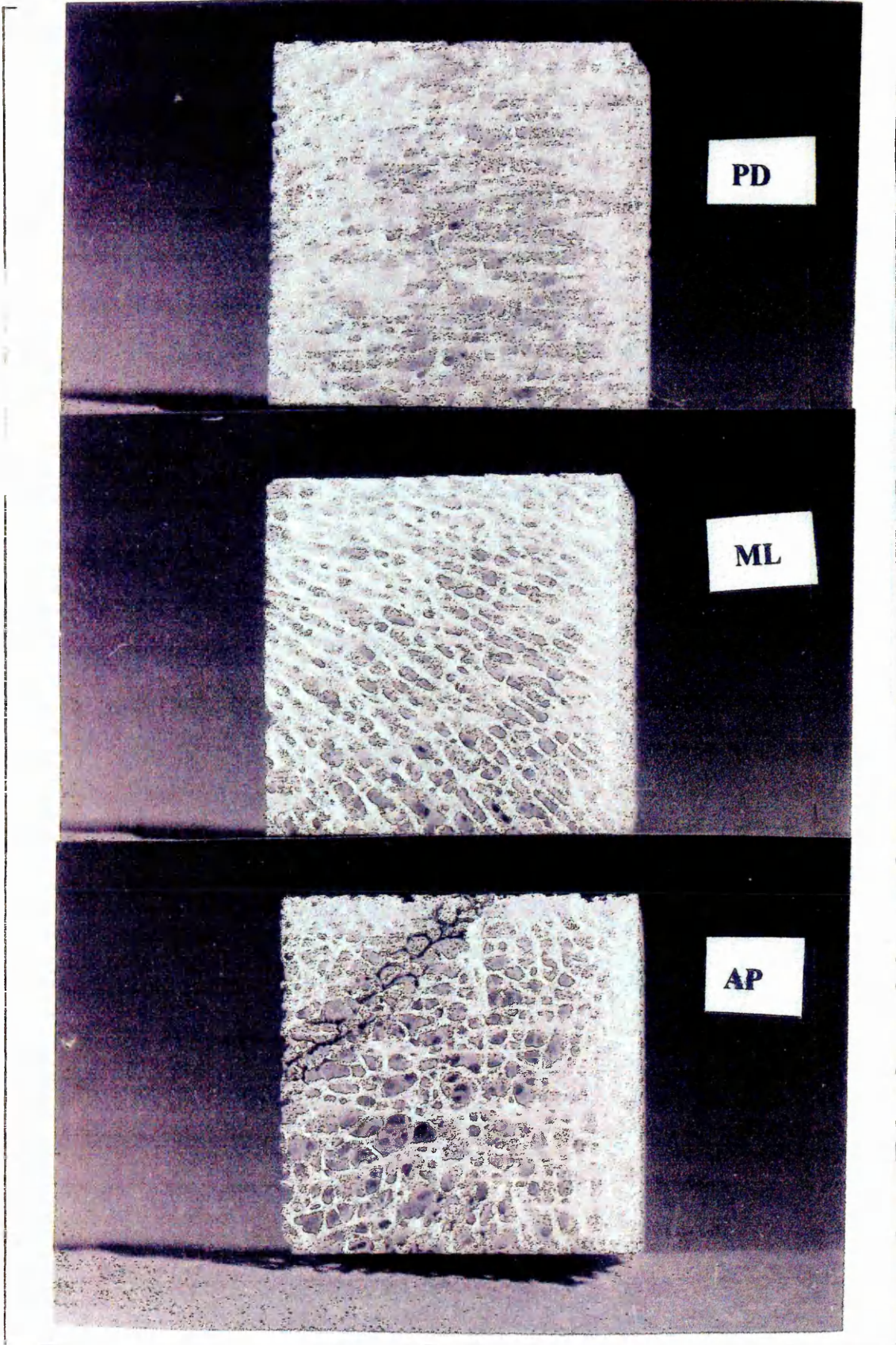
*Figure E-3: Photograh of Bovine Sample(20*20mm) with Density  300Kg/m^3*
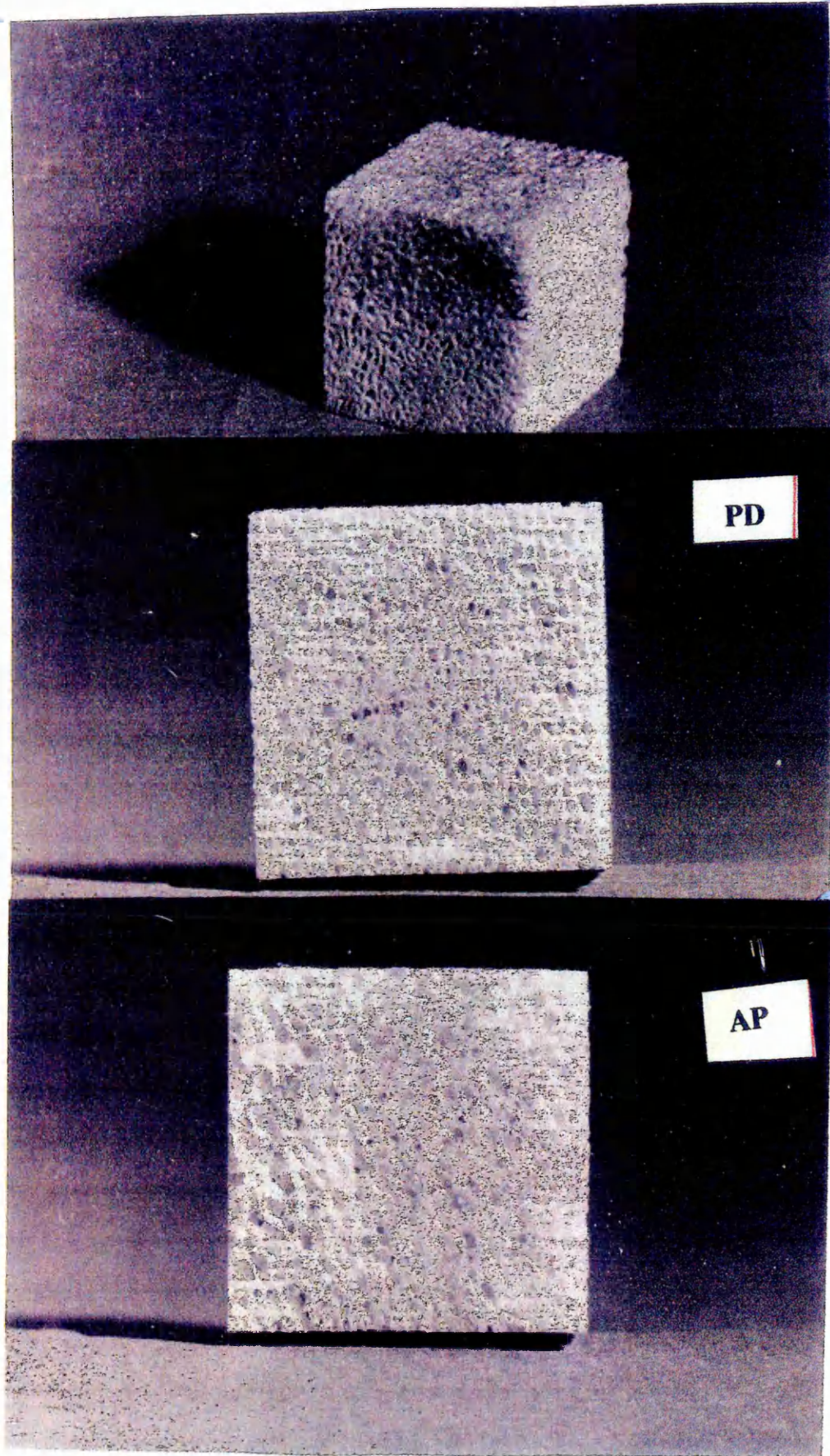
**Figure E-4**: *Photograh of Bovine Sample with Density of 697 Kg/m^3*
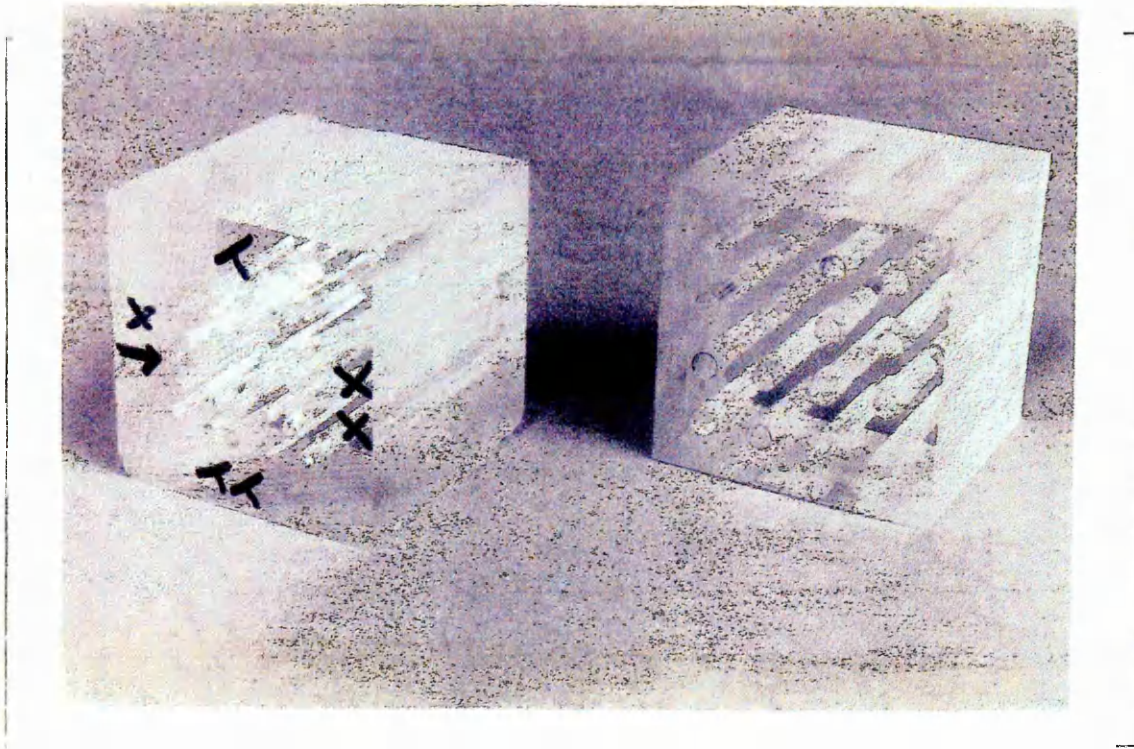
*Figure E-5:* A Photographic Illustration of Perspex Models
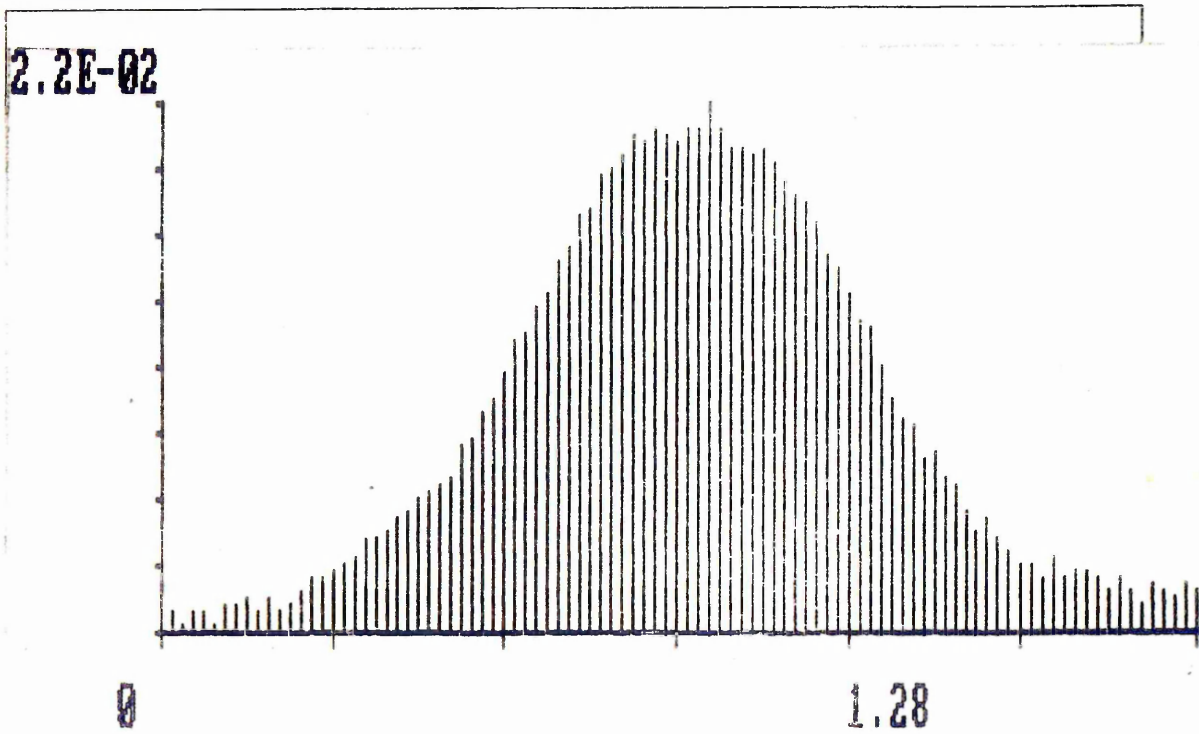


*Figure E-6:* Frequency Spectrum of a 1MHz Broadband Transducer

# Appendix F :

# Quick Basic Program for Permeability

# Measurement

```
DECLARE SUB axis ()
CLS
'    This version uses h as .2, and diameter 21 mm
'     and variable height
'     array dimension

DIM temps (20) AS DOUBLE
DIM velocity (10) AS DOUBLE
DIM SHARED  xstep
'       constants

n = 0
xstep = 50
h = .3
CLS

DO UNTIL work$ = "1" OR work$ = "2"  OR work$ = "3"
LOCATE 5, 10
PRINT  "  Do you want to"
LOCATE  10, 20
PRINT  "  Carry out measurements ----------> 1"
LOCATE  15, 20
PRINT  "  Plot curves from files      ----------> 2"
COLOR 4
LOCATE  20, 20
PRINT  "    EXIT   --------------------> 3"
work$ = INPUT$ (1)
LOOP
IF work$ = "3"  THEN END

CLS

IF work$ = "1" THEN
'  presentation

COLOR 3
LOCATE 2,  26
PRINT  "PERMEABILITY MEASUREMENT

COLOR 7
LOCATE 4
```

```basic
PRINT "                   Press space bar key to start measurements"
PRINT
PRINT "                   then press space bar to carry out a measurement"
PRINT
LOCATE , 23
PRINT "Measurement (no)   Delta (t) in sec.        height (m)"
PRINT

mn = 2
        DO WHILE n < 11              ' 10 measurements to be carried out
              response$ - INKEY$           ' record pressed key

              IF response$ = " " THEN              'if pressed key = space bar
                    temps (n) = TIMER
                     LOCATE , 26: PRINT n,   temps  (n)  -  temps (0), SPC (7) ;
USING "#.#"
                    n = n + 1
                    mn = mn - .2
              END IF
        LOOP

LOCATE 23,  26

COLOR 4
PRINT "    press any key ..."
COLOR 7

P$ = INPUT$ (1)

' velocity calculations

CLS
COLOR 3
LOCATE 2,  30:  PRINT "VELOCITY ARRAY"
COLOR 7

PRIINT  :  PRINT
LOCATE , 20

PRINT "measurement no      velocity in m.s - 1"
PRINT

        FOR t = 0 TO 9
              velocity (t) = h / (temps (t + 1) - temps (t))
              LOCATE , 23:  PRINT t, velocity (t)
        NEXT t

COLOR 4
LOCATE 23,  26
```

276

```
PRINT  " Press any key  ..."
P$ = INPUT$ (1)

END IF

IF work$ = "2" THEN
CLS

FILES  "a:\data\*.dat"
LOCATE 25, 1
INPUT  "Name of the file  "; nom$
 name$ = "a:\data\" + nom$ + ".dat"
  OPEN name$ FOR INPUT AS #2

        FOR index1 = 0 TO 10
              INPUT #2, temps(index1)
        NEXT index1

        FOR INDEX2 = 0 TO 9
            INPUT #2, velocity (INDEX2)
        NEXT INDEX2
    CLOSE #2
END IF

COLOR 7
SCREEN 12   ' graphic mode selection

CALL axis
    fa = (temps(10)  - temps (0)) / 10
    ypas = 22
    FOR jok = 0 TO 10 STEP 1
    ti = 0 + (fa * jok)
      LOCATE ypas, 1: PRINT USING "###.##"; ti
    ypas = ypas -1.8
    NEXT jok
    LOCATE 1, 4:  PRINT "time (s) "

 'plotting of delta time versus height
      X1 = 60
              FOR y = 10 TO 0 STEP -1
              y1 = 300 / (temps (10) - temps (0)) * (temps (y) - temps (0)) +
50

                LINE  (X1 - 5,  y1) - (X1 + 5, y1) , 15
                LINE  (X1 , y1 -  5) - (X1,  y1 + 5) , 15

            X1 = X1 + xstep
          NEXT y
```

```
W$ = INPUT$ (1)

'plotting of velocity = f (time)

CLS
SCREEN 12
   COLOR 15

      CALL axis

      LOCATE 4, 1: PRINT USING "###.##"; velocity (0)
      LOCATE 22, 5: PRINT "0"

      LOCATE 1, 4: PRINT "velocity (m.s-1)"

'  plotting
      X1 = 90
    FOR t = 0 TO 9
      y1 = 350 - 300 / velocity (0) * velocity (t)

      LINE (X1 - 5, yl) - (X1 + 5, yl) , 15
      LINE (X1, yl - 5) - (X1, yl + 5) , 15

      X1 = X1 + xstep .
    NEXT t

      attente$ = INPUT$ (1)
CLS
' constants
   ap = .0012566#      ' m^2
   af. = .001194591# 'm^2 (39mm)
    g = 9.81
   ro = 1000
   Vis = .001         'pá.s
    d = .0305         'm
   SCREEN 0
    'INPUT "Enter area of pipe (m) "; af
   sumh = 0: sumvel = 0: sumh2 = 0: sumvelh = 0:
   h = .2: sumhei = 0 :    sumhei2 = 0 : sumtime = 0: sumheitime = 0

      SCREEN 0
LOCATE 3 , 10
PRINT "Press Any Key for Linear Regression Results"
wait$ = INPUT$ (1)
 FOR t = 0 TO 9
   hi = (2 - (t * .2))
   hei = LOG (hi)
   hei2 = hei ^ 2
```

```
        time  =  temps (t)  -  temps (0)
      heitime  =  hei  *  time

        sumhei  =  sumhei  +  hei
        sumhei2  =  sumhei2  +  hei2
        sumtime  =  sumtime  +  time
        sumheitime  =  sumheitime  +  heitime
  NEXT t

  FOR t  =  0 TO 8
    hi  =  (1.8  -  (t  *  .2))
    h2  =  hi  ^  2

    velocity (t)  =  h  /  (temps (t  +  1)  -  temps (t))
    velh  =  hi  *  velocity (t)

    sumh  =  sumh  +  hi
    sumh2  =  sumh2  +  h2
    sumvel  =  sumvel  +  velocity (t)
  sumvelh  =  sumvelh  +  velh

  NEXT  t
    hn  =  sumh  /  9
    veln  =  sumvel/9
    hn2  =  sumh2  /  9
     velhn  -  sumvelh  / 9
      hn22  -  hn  ^  2
      hein  =  sumhei/10
      hein2  =  sumhei2  /  10
      hein22  -  hein  ^  2
        timen  =  sumtime  /  10
        heitimen  =  sumheitime  /  10
          grad  =  (velhn  -  (hn  *  veln))  /  (hn2  -  hn22)
          grad2  =  (heitimen  -  (hein  *  timen))  /  (hein2  -  hein22))  ^  -1

          SCREEN 0
         LOCATE 10 ,  10
          PRINT  " The gradient using method 1 is";  grad
           LOCATE  13, 10
           PRINT  "The gradient using method 2 is";  grad 2

         attente$  =  INPUT$ (1)
         SCREEN 0
       CLS

     perm1  =  grad  *  (ap  *  Vis  *  d)  /  (af  *  ro  *  g)
     perm2  =  -grad2  *  (ap  *  Vis  *  d)  /  (af  *  ro  *  g)
  LOCATE 8,  24
```

```
        PRINT " Permeability Values "
          LOCATE  12,  16
           PRINT "Method1     ";
           COLOR 12
             PRINT perm1;
             COLOR 2
             PRINT "    m^2  ": Color 7
     LOCATE 16 , 16
             PRINT   " Method 2      ";
             Color 3
             PRINT perm2;
             PRINT "   m^2  ": COLOR 7
                COLOR 12
                LOCATE 21 2
                          PRINT " Press Any Key to Continue "
        attente$ = INPUT$(1)
     IF works = "1" THEN
        SAVE THE VALUES
         LOCATE 25, 1
             PRINT " Do You Want to Save the Results (y/n) ?"
     IF sr$ = INPUT$(1): PRINT
     IF sr$ = "Y" OR sr$ = "y" THEN
             INPUT " Name  of the File  "; nom$
                   name$ = "a:\data\" + nom$ + "; dat"
     OPEN name$ FOR OUTPUT AS #1          OPEN A SEQUENTIAL FILE
             FOR Index1= 0 To 10
                   PRINT #1, temps(index1)
              NEXT index1
              FOR INDEX2 = 0 TO 9
                   PRINT #1, Velocity(Index2)
              NEXT INDEX2
        CLOSE #1
     END IF
     END IF
             work$ = " 0 "
             CLS
     RUN

     SUB axis
             'Drawing of x and y axis
                   LINE (60, 20) - (60, 350)
                   LINE -(600, 350)
                   LINE (595, 345) - (600, 350)
                   LINE -(595,  355)

           For y = 90 to 360 STEP 30
              LINE (53, y - 40) - (60, y - 40)
                   NEXT y
              LINE (55, 30) - (60, 20)
```

280

```
        LINE -(65, 30)

FOR r = 40 TO 560 STEP xstep
   LINE  (r + 20,  350) - ( r + 20, 357)
        NEXT r

LOCATE 26,.35: PRINT  " height    (m)  "
xpas = 70
FOR he = 0  To 2.1   STEP 0.2
        LOCATE 24, xpas:  PRINT USING  "#.#"; he
        xpas = xpas - 6.3
     NEXT he
END SUB
```

# Appendix G :

# Conference Presentation, Paper Publications

# and Posters

## *Conference Presentations*

- Langton CM, Boutinaud RX and **Njeh CF** (1992), Ultrasonic characterisation of porous material. Sheffield City Polytechnic Research seminar.

- **Njeh CF** (1992) Relationship between ultrasound and material properties of cancellous bone. *Expert workshop*, 5 and 6 March, University of Cologne, Germany.

- Langton CM, Boutinaud RX, **Njeh CF**, Naylor K and Bernard O (1992) Recent advances in ultrasonic characterisation of bone. *Ultrasonic Assessment of Bone 2*, 23 June, Bath.

- Boutinaud R, **Njeh CF** and Langton CM (1992), The role of permeability in the ultrasonic assessment of cancellous bone. *Annual Review of Progress in Physical Acoustic and Ultrasonics,* IOP, 22 - 23, September, Oxford.

- Langton C M,  Boutinaud R X, Ducker S and  **Njeh CF** (1993) Theoretical and experimental evaluation of  ultrasound attenuation in solid porous materials. *Internal friction and ultrasound attenuation conference, Rome*

- Boutinaud R, **Njeh CF**,  Hodgskinson R, Whitehead M, Holden G and Langton CM (1994) Ultrasonic prediction of structure and material properties of cancellous bone. *Measurement of the acoustical properties of biological tissue, IOP,15 Feb 1994, London*

- Holden G, **Njeh CF**, Hodgskinson R, Boutinaud R and Langton CM (1994) Ultrasonic prediction of structure and material properties of cancellous bone, *Ultrasonic Assessment of Bone IV, 20 June1994*

- Langton CM, **Njeh CF**, Hodgskinson R, Boutinaud RX, Whitehead MA and Holden GJ (1994), Ultrasonic prediction of structure and material properties of cancellous bone, *Bone and mineral, 25 suppl 2, S24 (10th International Bone Densitometry Workshop, Venezia, Italy April 24- 29)*

- **Njeh C F**(1994) The role of ultrasound in screening for osteoporosis. *East Anglia Regional Annual Physics Meeting , September, Cambridge*

- **Njeh CF**, Hodgskinson R and Langton C M (1994). Determination of bone strength from utrasound velocity and broadband ultrasound Attenuation, *British J Rad 68(811), p789, 1995 (British Medical Ultrasound Society, Annual Meeting, Scarborough, December 14 - 16)*

## PAPERS

- Langton CM, **Njeh CF**, Boutinaud RX, Hodgkinson R, and Currey JD (1994). Ultrasonic prediction of compressive strength in the calcaneus ( in press Bone).

- **Njeh CF**, Hodgskinson and Langton CM (1994). Orientational dependence of ultrasonic and material properties of cancellous bone ( in press Medical Engineering and Physics).

- **Njeh CF**, Hodgskinson R, Boutinaud RX, and Langton CM (1994). The relationship between ultrasonic velocity and material properties in human and bovine cancellous bone. (Under preparation for Ultrasound International)

- **Njeh C F**, Boutinaud RX, Bernard O and Langton C M (1994). The relationship between broadband ultrasound attenuation and porosity of cancellous bone: a comparison of experimental model and *in vitro* samples ( Under preparation for Calcified Tissue International).

- Langton C M, **Njeh C F**, Bernard O and Boutinaud R X. The role of permeability in the ultrasonic assessment of cancellous bone (Under preparation for Physics in Medicine and Biology)

## POSTERS

- Boutinaud R, **Njeh CF** and Langton CM (1993). The role of permeability in the ultrasonic assessment of cancellous bone. *Physics and Technology of Medical ultrasound meeting, York University, April 6-7, p67*

- Nicholson PH, Haddaway MJ, Langton CM, **Njeh C** and Davie MW (1993). Dependence of ultrasonic and mechanical properties of vertebral bone on orientation ( *British Tooth Society Annual Meeting, Birmingham*)